

**Functional and structural characterization of the RTX proteins
MbxA from *Moraxella bovis* and FrpA from *Kingella kingae***

Inaugural-Dissertation

zur Erlangung des Doktorgrades
der Mathematisch-Naturwissenschaftlichen Fakultät
der Heinrich-Heine-Universität Düsseldorf

vorgelegt von

Isabelle Noemi Erenburg

aus Düsseldorf

Düsseldorf, Oktober 2020

aus dem Institut für Biochemie
der Heinrich-Heine-Universität Düsseldorf

Gedruckt mit der Genehmigung
der Mathematisch-Naturwissenschaftlichen Fakultät der
Heinrich-Heine-Universität Düsseldorf

Berichterstatter:

1. Prof. Dr. Lutz Schmitt
2. Prof. Dr. Johannes Hegemann

Tag der mündlichen Prüfung: 16.12.2020

“Above all, don’t fear difficult moments. The best comes from them.”

Rita Levi-Montalcini

Abstract

Repeats in Toxins (RTX) proteins are a large family of proteins secreted by many Gram-negative bacteria and are defined by a conserved Ca^{2+} binding domain. The name of the protein family originates from a repetition of characteristic glycine-rich sequences that coordinate calcium ions and the fact that the first described members were pore-forming toxins. However, members of the RTX protein family not only mediate pathogenicity but are also involved in other aspects of interaction of bacteria with the environment such as adhesion or biofilm formation. Secretion occurs via dedicated type I secretion systems (T1SS) in a one-step mechanism across the inner and the outer membrane of the Gram-negative bacterium. Hemolysin A (HlyA), a pore-forming toxin secreted by uropathogenic *Escherichia coli* (*E. coli*) is not only the first identified RTX protein but also considered a prototype of RTX proteins and type I secretion. Its secretion system consists of the ATP-binding cassette (ABC) transporter hemolysin B, the membrane fusion protein hemolysin D and the outer membrane protein TolC, which when assembled span both membranes of *E. coli*. However, the activity of HlyA beyond pore formation remains elusive as it is known to manipulate host cells functions in various ways. In this thesis, poorly characterized or putative RTX proteins were selected on the basis of a bioinformatic approach for structural and functional characterization. Two candidates, FrpA from the human pathogen *Kingella kingae* and MbxA from the bovine pathogen *Moraxella bovis*, were secreted by the HlyA T1SS when expressed in *E. coli* BL21(DE3). This demonstrates that the HlyA system can serve as an efficient platform for the production of heterologous RTX proteins. Moreover, MbxA was heterologously activated through post-translational acylation, catalyzed by the co-expressed *E. coli* acyltransferase hemolysin C. Subsequently, purification protocols for FrpA and MbxA were developed. Initial structural investigations including small-angle X-ray scattering (SAXS) and cryogenic electron microscopy revealed that HlyA, FrpA and MbxA share a flexible and elongated conformation which is potentially a characteristic of RTX proteins. SAXS analysis yielded a three-dimensional *ab initio* model for HlyA and FrpA in solution. Mass spectrometry and functional studies confirmed that MbxA is a pore-forming toxin that strictly relies on post-translational acylation of internal lysine residues for cytotoxic activity. It was demonstrated that MbxA is a species- and cell type-unspecific protein. MbxA displayed not only hemolysis but was shown to induce membrane lesions in human epithelial cells and T cells. Half maximal cytotoxicity of MbxA against human cells was measured at low nanomolar concentrations. Furthermore, live cell imaging showed an immediate MbxA-induced permeabilization of epithelial cells that lead to rearrangements of the cell membrane resulting in characteristic membrane blebbing.

Zusammenfassung

Repeats in Toxins (RTX)-Proteine stellen eine umfassende Proteinfamilie dar, deren Proteine von vielen Gram-negativen Bakterien sekretiert werden und durch die Anwesenheit einer konservierten Ca^{2+} -Bindedomäne definiert sind. Der Name der Proteinfamilie leitet sich von charakteristischen, sich wiederholenden Glycin-reichen Sequenzen ab, die Calcium-Ionen koordinieren und der Tatsache, dass es sich bei den ersten beschriebenen Vertretern um Poren-bildende Toxine handelte. RTX-Proteine sind allerdings nicht nur für die Pathogenität maßgeblich, sondern auch an der Interaktion der Bakterien mit ihrer Umwelt zum Beispiel im Rahmen der Adhäsion oder Biofilm-Bildung beteiligt. Die Sekretion verläuft über spezialisierte Typ I Sekretionssysteme (T1SS) in einem Ein-Schritt-Mechanismus über die innere und die äußere Membran Gram-negativer Bakterien. Hemolysin A (HlyA), ein Poren-bildendes Protein sekretiert von uropathogenen *Escherichia coli* (*E. coli*) war nicht nur das erste identifizierte RTX-Protein, sondern wird auch als Prototyp der RTX-Proteine und Typ I Sekretion betrachtet. Das Sekretionssystem besteht aus dem *ATP-binding cassette* (ABC)-Transporter Hemolysin B, dem Membranfusionsprotein Hemolysin D und dem äußeren Membranprotein TolC, welche im assemblierten Zustand beide Membranen von *E. coli* überspannen. Jenseits der Porenbildung bleibt die Aktivität von HlyA aber unklar, da bekannt ist, dass HlyA Wirtszellfunktionen auf unterschiedlichen Wegen manipulieren kann.

In dieser Dissertation wurden bisher wenig charakterisierte oder putative RTX-Proteine basierend auf einem bioinformatischen Ansatz für eine strukturelle und funktionelle Charakterisierung ausgesucht. Zwei Kandidaten, FrpA aus dem Humanpathogen *Kingella kingae* und MbxA aus dem bovinen Pathogen *Moraxella bovis*, wurden über das HlyA T1SS sekretiert, wenn sie mit diesem in *E. coli* BL21(DE3) exprimiert wurden. Das zeigt, dass das HlyA Sekretionssystem als effiziente Plattform für die Produktion von heterologen RTX-Proteine genutzt werden kann. Darüber hinaus wurde MbxA mittels posttranslationaler Acylierung, katalysiert durch die co-exprimierte *E. coli* Acyltransferase Hemolysin C, heterolog aktiviert. Anschließend wurden Protokolle zur Reinigung von FrpA und MbxA entwickelt. Initiale Strukturuntersuchungen, unter anderem mittels Kleinwinkel-röntgenstreuung (SAXS) und Kryoelektronenmikroskopie, zeigten, dass HlyA, FrpA und MbxA eine flexible und längliche Konformation gemeinsam haben, welche potentiell ein Charakteristikum von RTX-Proteinen darstellt. Die SAXS-Analyse lieferte dreidimensionale *ab initio* Modelle von HlyA und FrpA. Massenspektrometrie und funktionelle Studien zeigten, dass MbxA ein Poren-bildendes Toxin ist, dessen zytotoxische Aktivität streng von der posttranslationalen Acylierung interner Lysinreste abhängt. Es wurde demonstriert, dass MbxA

ein Spezies- und Zielzell-unabhängiges Protein ist. MbxA wirkt nicht nur hämolytisch sondern verursacht auch Membranläsionen in menschlichen Epithelzellen und T-Zellen. Die halb-maximale Zytotoxizität von MbxA gegenüber menschlichen Zellen wurde bei niedrigen nanomolaren Konzentrationen gemessen. Des Weiteren wurde mithilfe von *Live cell imaging* gezeigt, dass die durch MbxA induzierte Permeabilisierung von Epithelzellen zu Umstrukturierungen der Zellmembran führt, die in der Bildung von charakteristischen Membranbläschen resultiert.

Abbreviations

| | |
|---------------------------------|--|
| <i>A. actinomycetemcomitans</i> | <i>Aggregatibacter (Actinobacillus) actinomycetemcomitans</i> |
| <i>A. pleuropneumoniae</i> | <i>Actinobacillus pleuropneumoniae</i> |
| ABC | ATP-binding cassette |
| AC | adenylate cyclase |
| ACP | acyl carrier protein |
| ATP | adenosine triphosphate |
| <i>B. pertussis</i> | <i>Bordetella pertussis</i> |
| CBB | Coomassie brilliant blue |
| CD | circular dichroism |
| CD18 | β subunit of β_2 integrins |
| CD ₅₀ | cytotoxic dose 50 |
| CDC | cholesterol-dependent cytolysin |
| CLD | C39-like domain |
| cryo-EM | cryogenic electron microscopy |
| CyaA | adenylate cyclase toxin from <i>Bordetella pertussis</i> |
| CyaC | CyaA-activating acyltransferase from <i>Bordetella pertussis</i> |
| <i>E. coli</i> | <i>Escherichia coli</i> |
| FrpA | putative iron-regulated RTX protein from <i>Kingella kingae</i> |
| GG repeats | glycine-rich repeats |
| HlyA | hemolysin A |
| HlyB | hemolysin B |
| HlyC | hemolysin C |
| HlyD | hemolysin D |
| IBK | infectious bovine keratoconjunctivitis |
| IM | inner membrane |
| IMAC | immobilized metal ion affinity chromatography |
| <i>K. kingae</i> | <i>Kingella kingae</i> |
| kDa | kilodalton |
| LDH | lactate dehydrogenase |
| LFA-1 | lymphocyte function-associated antigen 1 |
| LktA | leukotoxin from <i>Mannheimia (Pasteurella) haemolytica</i> |
| LtxA | leukotoxin from <i>A. actinomycetemcomitans</i> |
| <i>M. bovis</i> | <i>Moraxella bovis</i> |

| | |
|------------------------|---|
| <i>M. haemolytica</i> | <i>Mannheimia (Pasteurella) haemolytica</i> |
| <i>M. primoryensis</i> | <i>Marinomonas primoryensis</i> |
| MARTX | Multifunctional-autoprocessing Repeats in Toxins |
| MbxA | RTX protein from <i>Moraxella bovis</i> |
| MbxB | putative ABC transporter of the <i>Moraxella bovis</i> T1SS |
| MbxC | putative MbxA-activating acyltransferase of <i>Moraxella bovis</i> |
| MbxD | putative membrane fusion protein of the <i>Moraxella bovis</i> T1SS |
| MFP | membrane fusion protein |
| mg | milligramm |
| min | minute |
| ml | milliliter |
| mM | millimolar |
| <i>N. meningitidis</i> | <i>Neisseria meningitidis</i> |
| NBD | nucleotide binding domain |
| nM | nanomolar |
| OM | outer membrane |
| OMP | outer membrane protein |
| <i>P. aeruginosa</i> | <i>Pseudomonas aeruginosa</i> |
| <i>P. fluorescens</i> | <i>Pseudomonas fluorescens</i> |
| PDB | Protein Data Bank |
| pI | isoelectric point |
| PMF | proton motive force |
| PP | periplasm |
| PSM | peptide spectrum matches |
| RTX | Repeats in Toxins |
| RtxA | RTX protein from <i>Kingella kingae</i> |
| RtxC | RtxA-activating acyltransferase from <i>Kingella kingae</i> |
| <i>S. marcescens</i> | <i>Serratia marcescens</i> |
| SAXS | small-angle X-ray scattering |
| SDS-PAGE | sodium dodecyl sulfate polyacrylamide gel electrophoresis |
| Sec | general secretion pathway |
| SEC | size exclusion chromatography |
| T1SS | type I secretion system |
| T2SS | type II secretion system |

| | |
|--------------------|------------------------------|
| T3SS | type III secretion system |
| T4SS | type IV secretion system |
| T5SS | type V secretion system |
| T6SS | type VI secretion system |
| Tat | Twin-arginine translocation |
| TMD | transmembrane domain |
| UPEC | uropathogenic <i>E. coli</i> |
| <i>V. cholerae</i> | <i>Vibrio cholerae</i> |
| μl | microliter |
| μm | micrometer |
| μM | micromolar |

| Amino acid | three letter code | one letter code |
|---------------|-------------------|-----------------|
| Alanine | Ala | A |
| Arginine | Arg | R |
| Asparagine | Asn | N |
| Aspartic acid | Asp | D |
| Cysteine | Cys | C |
| Glutamic acid | Glu | E |
| Glutamine | Gln | Q |
| Glycine | Gly | G |
| Histidine | His | H |
| Isoleucine | Ile | I |
| Leucine | Leu | L |
| Lysine | Lys | K |
| Methionine | Met | M |
| Phenylalanine | Phe | F |
| Proline | Pro | P |
| Serine | Ser | S |
| Threonine | Thr | T |
| Tryptophan | Trp | W |
| Tyrosine | Tyr | Y |
| Valine | Val | V |

List of figures

| | |
|---|-----|
| Figure 1: Schematic view of the six main secretion systems found in Gram-negative bacteria. | 2 |
| Figure 2: Schematic representation of exemplary classes of RTX proteins. | 4 |
| Figure 3: Crystal structure of the alkaline protease from <i>P. aeruginosa</i> . | 5 |
| Figure 4: Homology model of HlyB. | 8 |
| Figure 5: Schematic representation of HlyD including the crystal structure of a periplasmic fragment of HlyD. | 9 |
| Figure 6: Crystal structure of TolC. | 10 |
| Figure 7: Postulated secretion mechanism of HlyA. | 12 |
| Figure 8: Schematic view of the domain organization of HlyA. | 13 |
| Figure 9: Structure of the ApxC dimer shown in a surface representation. | 14 |
| Figure 10: Genetic organization of the RTX operons of UPEC and <i>M. bovis</i> . | 16 |
| Figure 11: Schematic view of the HlyA secretion system combined with MbxA as a substrate. | 115 |
| Figure 12: HlyC-mediated acylation of MbxA and HlyA. | 120 |
| Figure 13: Membrane damaging activity of MbxA and potential interaction partners in different cell types. | 126 |

List of tables

| | |
|--|-----|
| Table 1: Selected RTX proteins annotated in genomes of Gram-negative bacteria. | 18 |
| Table 2: Putative cholesterol recognition CRAC and CARC motifs identified in the sequence of MbxA. | 125 |

Table of contents

| | |
|--|-----|
| Abstract | IV |
| Zusammenfassung | V |
| Abbreviations | VII |
| List of figures | X |
| List of tables | X |
| 1. Introduction | 1 |
| 1.1 Protein secretion in bacteria..... | 1 |
| 1.2 The Repeats in Toxins protein family | 2 |
| 1.2.1 The calcium ion-dependent folding of RTX proteins..... | 4 |
| 1.2.2 Hemolysin A, a RTX toxin from uropathogenic <i>E. coli</i> | 6 |
| 1.2.2.1 Pore-forming activity of HlyA | 6 |
| 1.2.2.2 Non-lytic activity of HlyA | 6 |
| 1.2.2.3 The HlyA secretion system | 7 |
| The ABC-transporter HlyB..... | 7 |
| The membrane fusion protein HlyD..... | 8 |
| The outer membrane protein TolC | 10 |
| The secretion mechanism of HlyA..... | 11 |
| 1.2.2.4 Activation of HlyA by Acylation | 12 |
| The acyltransferase HlyC | 13 |
| 1.2.3 MbxA, a RTX toxin from <i>Moraxella bovis</i> | 15 |
| 2. Aims..... | 17 |
| 3. Publications | 19 |
| 3.1 Chapter 1 | 19 |
| 3.2 Chapter 2 | 30 |
| 3.3 Chapter 3 | 40 |
| 3.4 Chapter 4 | 79 |

| | |
|---|-----|
| 4. Discussion | 112 |
| 4.1 The hemolysin T1SS as a production platform for RTX proteins..... | 112 |
| 4.2 Structural insights into HlyA, FrpA and MbxA | 116 |
| 4.3 Heterologous activation of MbxA from <i>M. bovis</i> by the <i>E. coli</i> acyltransferase HlyC | 118 |
| 4.4 The activity of MbxA is acylation-dependent | 121 |
| 4.5 MbxA is a species- and cell type-unspecific pore-forming toxin..... | 122 |
| 4.6 Potential receptors involved in MbxA activity | 123 |
| 4.7 MbxA-induced membrane damage leads to morphological changes in epithelial cells | 127 |
| 5. Bibliography | 129 |
| 6. Curriculum Vitae | 144 |
| 7. Acknowledgments | 147 |
| 8. Declaration | 151 |

1. Introduction

1.1 Protein secretion in bacteria

Bacteria transport numerous proteins across the membrane that separates their cytosol from the extracellular environment. This transport process is known as protein secretion. Secreted proteins interfere with the environment of the bacterium in different ways and aid survival by means of defense, adhesion and pathogenicity. Therefore various secretion machineries have evolved to translocate proteins across the cell envelope. Compared to Gram-positive bacteria where secretion is mediated across the cytoplasmic membrane, in Gram-negative bacteria additionally a second membrane, the outer membrane, needs to be traversed [1, 2]. In Gram-negative bacteria secreted proteins either cross the inner and the outer membrane in a two-step process with a periplasmic intermediate or are transported in a single step by secretion systems that span both membranes bridging the periplasm [3]. Six main types of secretion machineries with different architecture and secretion mechanisms found in Gram-negative bacteria were accordingly named type I-VI secretion systems (T1SS – T6SS) (Fig. 1). Type II and type V rely on substrates that were transported across the inner membrane into the periplasm by the Sec system or by the Twin-arginine translocation (Tat) pathway. Type I, III, IV and type VI function without a periplasmic intermediate and secrete their substrates in a single step. Among these double-membrane spanning systems, type III, IV and VI are even able to cross a third membrane, the membrane of a host cell, and release effector proteins into it [1]. Numerous secreted peptides and proteins target either bacterial or eukaryotic cells. An example from the group of bacteriocins, secreted to kill competing bacteria, is Colicin V. This peptide antibiotic is secreted via a T1SS by some *E. coli* strains and permeabilizes the membrane of other related, sensitive *E. coli* strains [4, 5]. On the other hand, many proteins that are secreted by pathogenic bacteria are virulence factors and play a major role in infection and colonization of the host. For example the cholera toxin from *Vibrio cholerae* (*V. cholerae*) and the related heat-labile enterotoxin of enterotoxigenic *E. coli* are toxins secreted via T2SS and after translocation of a subunit into the host cell upregulate the adenylate cyclase [6-8]. Utilizing two T3SS the pathogen *Salmonella enterica* is able to inject dozens of different effector proteins directly into the cytosol of host cells [9]. However, pore-forming toxins that disrupt host cell membranes are considered to be the largest group of virulence factors [10, 11]. A prominent example is the pore-forming toxin hemolysin A from uropathogenic *E. coli* (UPEC) [12]. Further details on

T1SS will be provided in section 1.2.2.3. Here the hemolysin A T1SS will be discussed in detail.

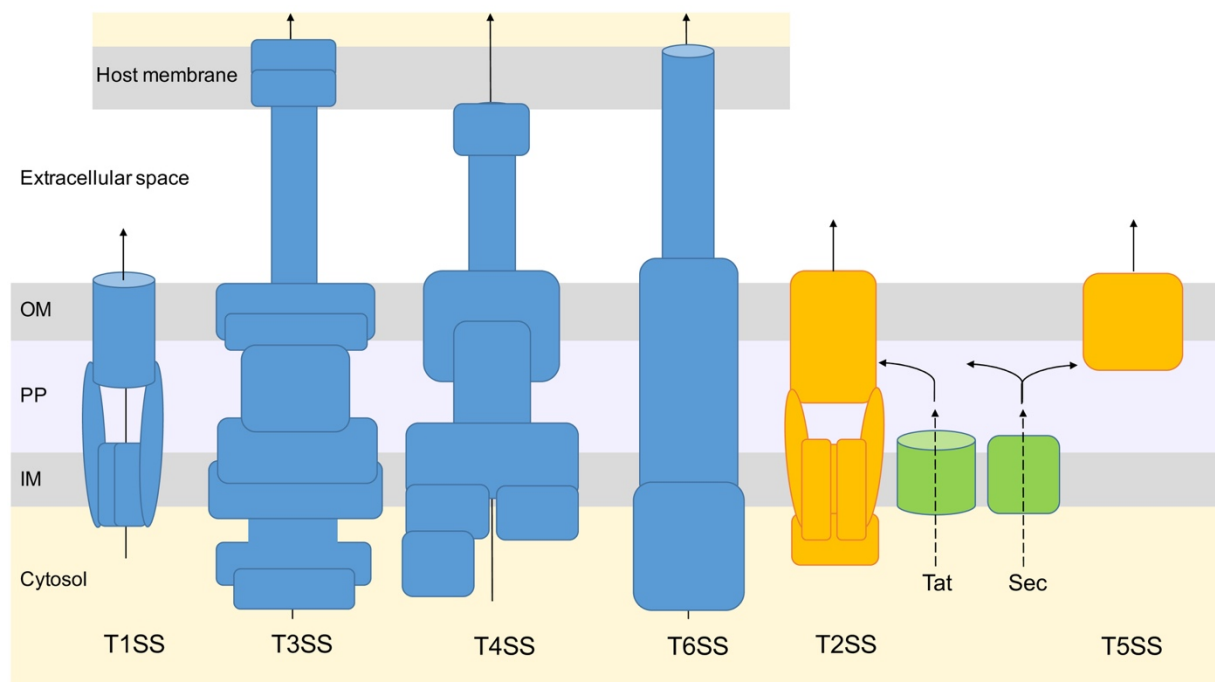


Figure 1: Schematic view of the six main secretion systems found in Gram-negative bacteria. The secretion systems that facilitate transport in a single step across the inner and the outer membrane of the bacterium are shown in blue. T3SS, T4SS and T6SS additionally cross the membranes of host cells to release their substrates. T2SS and T5SS (yellow) mediate secretion across the outer membrane after the substrates are transported into the periplasm via the Sec pathway or in the case of T2SS alternatively via the Tat pathway (green). The simplified figure is based on [1] and [2]. IM: inner membrane, OM: outer membrane, PP: periplasm.

1.2 The Repeats in Toxins protein family

Proteins of the Repeats in Toxins (RTX) family are secreted by various Gram-negative bacteria into their environment via T1SS. This large protein family is named after its characteristic glycine-rich repeats, the GG-repeats, with the common sequence GG-x-G-x-D-x-U-x, in which x stands for any amino acid and U for a large, hydrophobic residue [13-15].

A hemolytically active, pore-forming virulence factor secreted by UPEC, later named hemolysin A (HlyA), was the first RTX protein to be discovered [16, 17]. The identification of the GG-repeats and the elucidation of the single-step secretion process across both the inner and the outer membrane made HlyA the paradigm of RTX proteins [18-20]. Subsequently other pore-forming toxins of other pathogens with hemolytic or leukotoxic activity such as MmxA

from *Morganella morganii* [21], LtxA from *Aggregatibacter* (*Actinobacillus*) *actinomycetemcomitans* (*A. actinomycetemcomitans*) [22] or LktA from *Mannheimia* (*Pasteurella*) *haemolytica* (*M. haemolytica*) [23] were identified. As an exception among the pore-forming RTX cytotoxins the toxin CyaA secreted by *Bordetella pertussis* (*B. pertussis*) harbors not only a pore-forming hemolysin domain but also an adenylate cyclase domain that is translocated into host cell cytosol where it upregulates cAMP levels (Fig. 2) [24, 25]. Besides this class of pore-forming RTX toxins several other functionalities of other members of the RTX family are known. Another group of virulence factors are the large multifunctional-autoprocessing RTX (MARTX) toxins which consist of multiple effector domains with different activities (Fig. 2) [26]. The first identified member was MARTX_{vc} from *V. cholerae*, a protein of 4546 amino acid residues, that undergoes autocatalytic cleavage and translocates its cytotoxic domains into the host cytosol [27-29]. A different group of large, multidomain proteins are the RTX adhesins involved in biofilm formation [30]. Members are for example SiiE from *Salmonella enterica* that promotes adhesion to host cells [31], LapA from *Pseudomonas fluorescens* (*P. fluorescens*) [32] or an ice-binding protein of 1.5 MDa that is produced by *Marinomonas primoryensis* (*M. primoryensis*) [33]. Interestingly, these proteins are not fully secreted but are anchored to the secretion system and released by accessory factors, modulating adherence to other cells and surfaces [34-36] (Fig. 2). Smaller members of the RTX protein family are for examples secreted enzymes such as the alkaline protease of *Pseudomonas aeruginosa* (*P. aeruginosa*) [14] or the serralyisin protease and lipase LipA from *Serratia marcescens* (*S. marcescens*) [37, 38]. The function of other RTX proteins is unknown including the iron-regulated Frp proteins from *Neisseria meningitidis* (*N. meningitidis*) [39]. In one of the RTX proteins, FrpA, a self-processing module was discovered that leads to autocatalytic splicing. Subsequently, the resulting fragment of FrpC can covalently cross-link to lysine residues of other proteins [40]. This protein trans splicing-like activity and the affinity of FrpC for an outer membrane lipoprotein potentially indicate that it is involved in adhesion of the pathogen to host cells [41]. While the functions of different subgroups of RTX toxins vary widely RTX proteins share several characteristics apart of their defining GG-repeats. The variable N-terminal part harbors the different activities whereas the more conserved C-terminus contains the RTX domain formed by a varying number of GG-repeats and a secretion signal [15]. This secretion signal is crucial for the recognition by the designated T1SS and is not cleaved [42]. Located at the extreme C-terminus, the secretion signal does not have a conserved sequence but presumably mediates recognition via a secondary structure element [43]. Other common traits of RTX proteins are a low isoelectric point of 4 to 5 and rare occurrence of

cysteine residues [44]. However, the most prominent common attribute is the formation of calcium binding motifs by the GG-repeats which control the folding of RTX proteins [14, 45, 46].

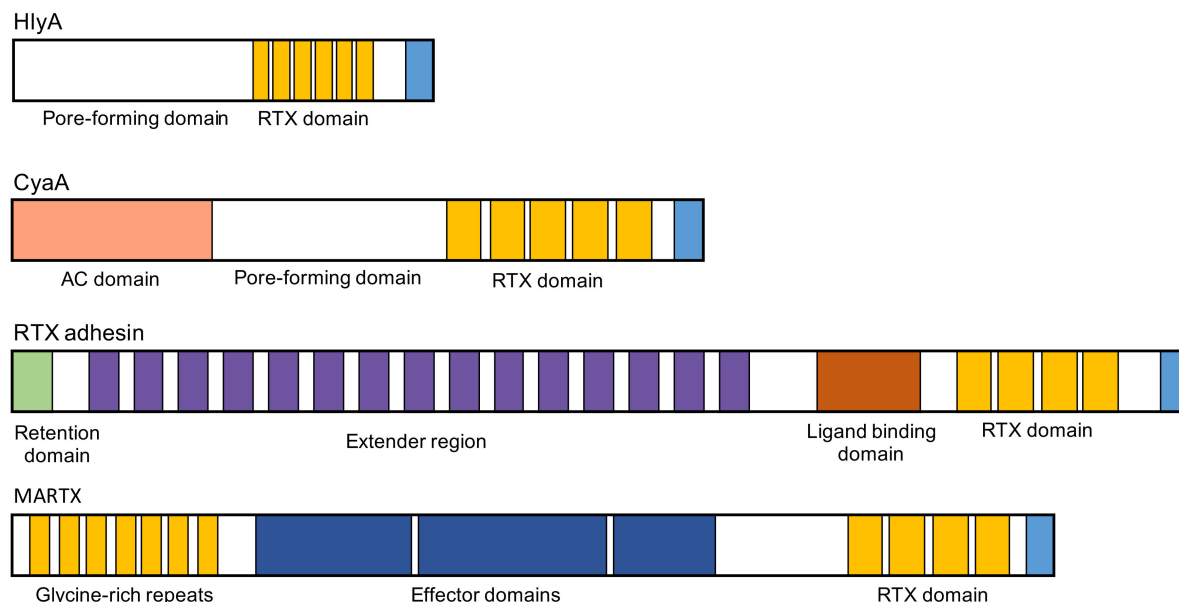


Figure 2: Schematic representation of exemplary classes of RTX proteins. All RTX proteins share a C-terminal secretion signal (light blue) and the characteristic C-terminal RTX domain (yellow). The number of GG-repeats varies in different RTX proteins. As a member of the group of pore-forming RTX proteins, HlyA has a N-terminal pore-forming domain. CyaA from *B. pertussis* harbors not only a pore-forming domain but also a N-terminally located adenylate cyclase (AC) domain that is translocated into host cells. RTX adhesins such as LapA of *P. fluorescens* carry a long extender region that consists of a large number of repetitive motifs. The number and sequence of this repeats varies in different adhesins. Between the extender domain and the RTX repeats a ligand binding domain is found. The N-terminal retention domain tethers the protein to its secretion systems [30, 35]. Additionally to the C-terminal RTX domain MARTX harbor glycine-rich repeats that are located at the N-terminus and have a sequence that differs from the C-terminal GG-repeats. Members of the MARTX subfamily carry different effector domains which are translocated into the host cell [26]. The different RTX proteins are not drawn to scale and the number of repeated domains is exemplary.

1.2.1 The calcium ion-dependent folding of RTX proteins

The number of GG-repeats in RTX proteins ranges from single digit numbers to over 40 but does not strictly correlate with the size of the protein [15]. HlyA from *E. coli*, a 1024 amino acid residue protein, harbors six conserved GGxGxDxUx repeats and including less conserved motifs a total of 13 GG-repeats [44]. The GG-repeats form a calcium ion binding motif by coordinating a Ca^{2+} ion between the first glycine residue and the aspartate residue. In this way

the GG-repeats build turns alternating with β -strand with one calcium ion each between two turns. This results in the characteristic parallel β -roll structure of the RTX domain that was first observed in the crystal structure of the alkaline protease from *P. aeruginosa* (Fig. 3) [14]. In agreement, it was shown that the activity of *E. coli* HlyA depends on calcium ion binding and that HlyA binds Ca^{2+} ions with a K_D of approximately 0.1 mM [47]. Binding of calcium ions does not only dictate the folding of the RTX domain but influences the folding of the complete protein, as shown for HlyA and the alkaline protease [45, 48]. The Ca^{2+} ion dependent folding of RTX proteins is inherently coupled to the secretion process. In bacteria, regulation mechanisms keep the cytosolic Ca^{2+} ion levels at high nanomolar concentrations which is in consequence not sufficient for binding to the RTX domain [49, 50]. Thus, prior to secretion RTX proteins remain in an intrinsically disordered state. This allows secretion of the large, unfolded substrates via the tripartite T1SS. In the extracellular environment, upon Ca^{2+} ion binding, the transition from a loose, disordered state to a functional, compact conformation occurs [46, 48, 51].

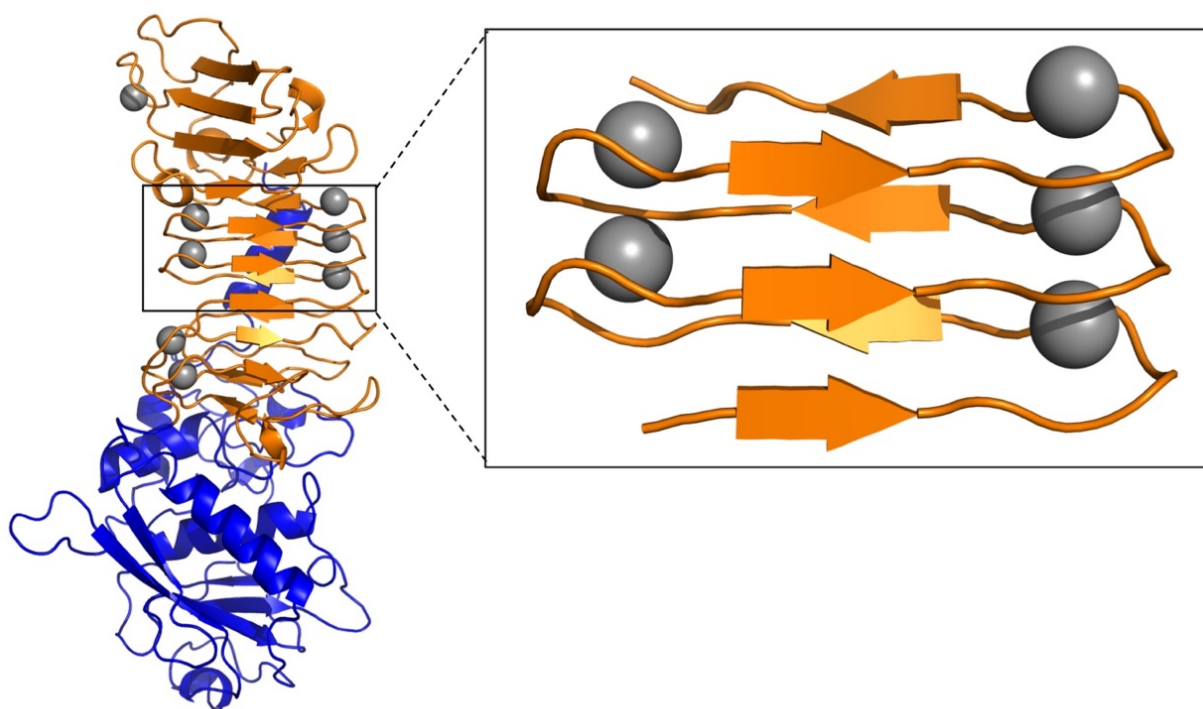


Figure 3: Crystal structure of the alkaline protease from *P. aeruginosa* (PDB entry 1KAP) [14]. The protease domain is shown in blue and the RTX domain is shown in orange. The characteristic β -roll structure where calcium ions, shown as grey spheres, are coordinated between the turns of the GG-repeats is highlighted with a black box and shown magnified on the right.

1.2.2 Hemolysin A, a RTX toxin from uropathogenic *E. coli*

The pore-forming RTX toxin HlyA is produced by large number of UPEC strains, which are the leading cause of urinary tract infections [52, 53]. While the protein was named after its hemolytic activity, it is not only active against erythrocytes but also cytotoxic to a variety of different cell types of different species including monocytes, granulocytes, lymphocytes, endothelial and epithelial cells [12, 54-58]. The activity of HlyA is not only restricted to a pore-forming lytic mode of action but is also associated with a variety of other cellular effects.

1.2.2.1 Pore-forming activity of HlyA

The most prominent function of HlyA is the lysis of host cells, especially erythrocytes. Hemolysis occurs through insertion of HlyA into the erythrocyte membrane and formation of a small hydrophilic transmembrane pore that leads to cell swelling and finally lysis. Across this membrane lesion a potassium ion efflux and calcium ion influx were observed [54]. Using osmotic protectants Bhakdi *et al.* estimated further that the HlyA pore has a size of 3 nm [54]. Pore formation was likewise observed *in vitro* in lipid bilayer experiments [59-61]. HlyA is suggested to adsorb reversibly to the membrane before an irreversible insertion into the membrane occurs [62]. Nonetheless, the insertion of HlyA does not strictly lead to lysis [63]. The domain required for membrane binding and pore formation is localized in the N-terminal part of HlyA [64, 65], but also the C-terminal RTX domain shows interaction with membranes [66]. Still, the stoichiometry and structure of the HlyA pore is unknown as different studies reported both monomeric and oligomeric states involved in membrane permeabilization [59, 60, 67].

1.2.2.2 Non-lytic activity of HlyA

Early on HlyA has been shown to evoke effects in cells treated with low, sublytic concentrations of the toxin [12, 57, 58]. Especially granulocytes appeared to be more susceptible to HlyA than other cell types exhibiting different metabolic responses [12, 68]. Furthermore, the presence of the β_2 integrin LFA-1 expressed in leukocytes increased sensitivity of cells towards HlyA indicating that it represents a receptor for HlyA [69-71]. In different experimental set ups HlyA induced different cell death types such as apoptosis, necrosis and pyroptosis [56, 72-74]. The HlyA-mediated inhibition of the anti-apoptotic regulator Akt in bladder epithelial cell underlines its potential to manipulate host cell signaling, reduce inflammatory responses and

activate cell death pathways [75]. Moreover, UPEC expressing HlyA induce degradation of host proteins involved in signaling and adhesion. This may promote the exfoliation of bladder epithelial cells and aid the dissemination of the pathogen in the host tissue [76]. Another study reported that HlyA induces Ca^{2+} oscillations in rat renal epithelial cells which lead to the production of cytokines and a pro-inflammatory response [77]. In macrophages, the K^{+} efflux caused by HlyA-induced pore formation was shown to be likewise associated with a pro-inflammatory response but also with mitochondrial damage resulting in cell death [78]. Further, Murthy *et al.* reported that UPEC-mediated macrophage killing is tightly bound to HlyA levels and that macrophage cell death is accompanied by inflammasome activation, underlining the potential of HlyA to subvert the host immune response [79].

1.2.2.3 The HlyA secretion system

The dedicated T1SS required for the secretion of HlyA is built of three components that span the inner and outer membrane of *E. coli* [80]. Two of the transporter components, the ATP binding cassette (ABC) transporter hemolysin B (HlyB) and the membrane fusion protein hemolysin D (HlyD) are encoded together with the *hlyA* gene in an operon and are located in the inner membrane [81-84]. The third component, the outer membrane protein (OMP) TolC, is accordingly localized in the outer membrane and encoded separately in the genome of *E. coli* [85].

The ABC-transporter HlyB

The inner membrane localized ABC-transporter HlyB energizes the transport of HlyA by hydrolysis of ATP [86, 87]. As a member of the ABC transporter family HlyB has two nucleotide binding domains (NBDs) facing the cytosol and two transmembrane domains (TMDs) spanning the inner membrane (Fig. 4) [83, 88, 89]. HlyB functions as a dimer, in which one monomer comprises one NBD and one TMD [89-92]. Therefore HlyB is sometimes referred to as a “half-size transporter” [93]. For HlyB, the structure of the NBDs but not of the complete transporter has been solved [90, 94]. The TMDs of ABC-transporters often span the membrane with six transmembrane helices, accordingly for HlyB six but alternatively also eight transmembrane helices were predicted [83, 95]. In contrast to the TMDs that build a pathway for the substrate transport across the membrane and vary among the ABC-transporter family, the NBDs are highly conserved to facilitate binding of ATP and hydrolysis [96, 97]. In HlyB,

ATP induces the dimerization of the two NBDs which then enclose two ATP binding sites between them [90]. The additional coordination of Mg^{2+} ions allows to catalyze the subsequent hydrolysis of ATP, which is the “power stroke” of HlyB for conformational changes and the translocation of the substrate [92]. As the substrate HlyA is a large protein of 1024 amino acids it remains unclear if other factors such as the proton motive force contribute to the energy required for secretion [98, 99]. The NBDs of HlyB not only energize the translocation process but are also thought to be involved in recognition of the C-terminus of the substrate HlyA [100]. Another domain of HlyB that was shown to interact with HlyA is the N-terminal, cytoplasmic C39-like domain (CLD) [101]. Named after the homologous C39 peptidase domain found in bacteriocin transporting ABC transporters, the CLD lacks the conserved cysteine required for peptidase activity [101, 102]. Instead of proteolytic cleavage this domain stabilizes the substrate HlyA and presumably protects it from aggregation [101].

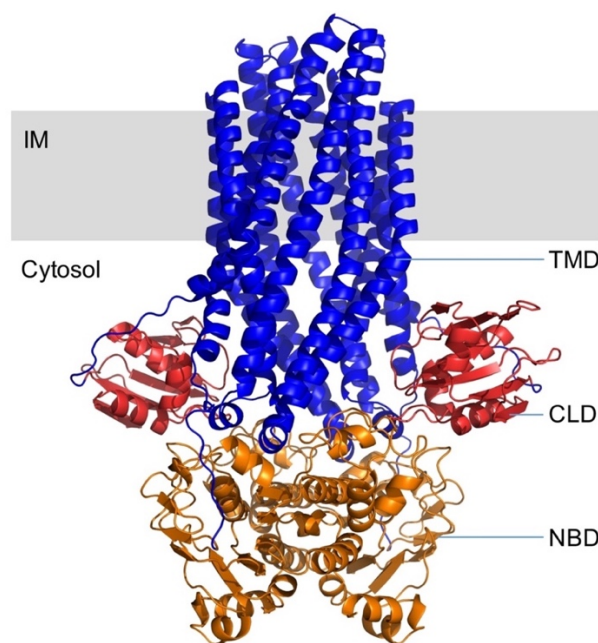


Figure 4: Homology model of HlyB. The structure of HlyB was modelled with Phyre2 [103] based on the crystal structure of the bacteriocin transporting ABC transporter PCAT1 from *Clostridium thermocellum* (PDB entry 4RY2). It is shown as a dimer anchored in the inner membrane (IM), schematically presented in gray. The TMDs of both monomers are colored in blue, the CLDs in red and the cytosolic NBDs are shown in orange.

The membrane fusion protein HlyD

The second component of the HlyA secretion system localized in the inner membrane is HlyD, a protein from the family of membrane fusion proteins. It connects the inner membrane

transporter HlyB with the OMP TolC stabilizing the passage across the periplasm and is therefore sometimes referred to as an “adaptor protein” [104]. The first 59 N-terminal amino acids of the 478 residue protein are predicted to reach into the cytoplasm while an adjacent transmembrane helix anchors HlyD in the inner membrane. The remaining part of HlyD is predicted to form the large periplasmic domain of the protein [105]. A crystal structure of a fragment of this soluble, periplasmic domain covering residue 96-361 was solved and showed an elongated α -helical domain consisting of three α -helices that form a α -helical hairpin structure together with a lipoyl domain (Fig. 5) [106]. The tip of the α -hairpin structure presumably mediates the interaction with TolC [106, 107]. Even in the absence of HlyA, HlyD and the ABC transporter HlyB form the so called inner membrane complex [108]. Cross-linking studies showed that HlyD forms a trimer [108], but more recently solved structures of for example a homologous membrane fusion protein in a multidrug efflux system suggests that HlyD likewise forms hexamers [106, 109]. HlyD not only interacts with the transporter components HlyB and TolC but also with HlyA. The N-terminal, cytosolic domain of HlyD is involved in binding of the substrate and is crucial for the further engagement of TolC for a successful formation of the T1SS [110]. At the same time, the periplasmic domain is suggested to seal the translocation channel and is essential for the transport of HlyA in a secretion and folding competent state [111].

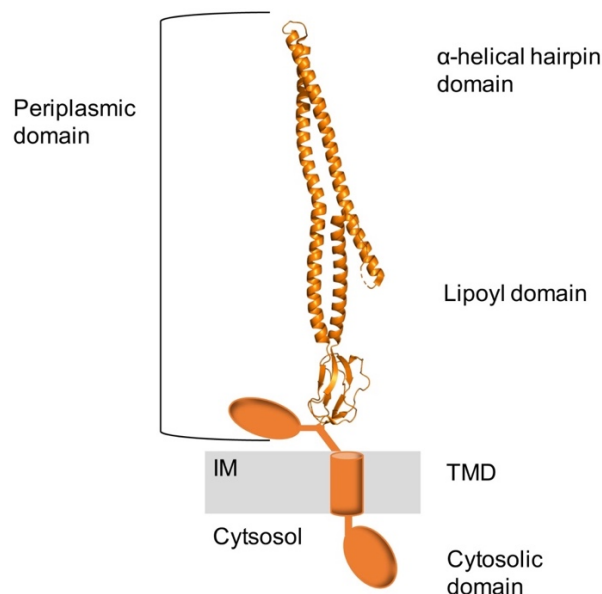


Figure 5: Schematic representation of HlyD including the crystal structure of a periplasmic fragment of HlyD (PDB entry 5C21). Only the structure of a fragment of the periplasmic domain (residue 96-361) containing a coiled coil α -helical domain and lipoyl domain is solved [106]. A monomer of HlyD is shown anchored in the inner membrane with a predicted transmembrane region. Furthermore, a short N-terminal domain located in the cytoplasm is predicted [105].

The outer membrane protein TolC

The OMP TolC completes the HlyA T1SS as it forms a pore in the outer membrane through which HlyA is released into the extracellular environment. However, TolC is also part of other tripartite efflux machineries such as the AcrAB-TolC multidrug efflux pump [109]. TolC is a trimer that forms an open β -barrel in the outer membrane and an α -helical domain with a length of 100 Å that reaches into the periplasm. The 12 α -helices of the trimer build an α -helical barrel, resulting in a tunnel-like overall structure (Fig. 6) [112]. In the crystal structure of TolC described by Koronakis *et al.* [112], the periplasmic opening was closed with a diameter of 3.9 Å in contrast to the open β -barrel anchored in the outer membrane, which has an inner diameter of approximately 20 Å. TolC opens the periplasmic entrance presumably through an iris-like motion of the coiled coils that narrow the periplasmic opening to allow substrate transport [113, 114]. The inner diameter of the TolC channel of approximately 20 Å is indicative of the secretion mechanism of T1SS as it can only support the passage of unfolded proteins [112].

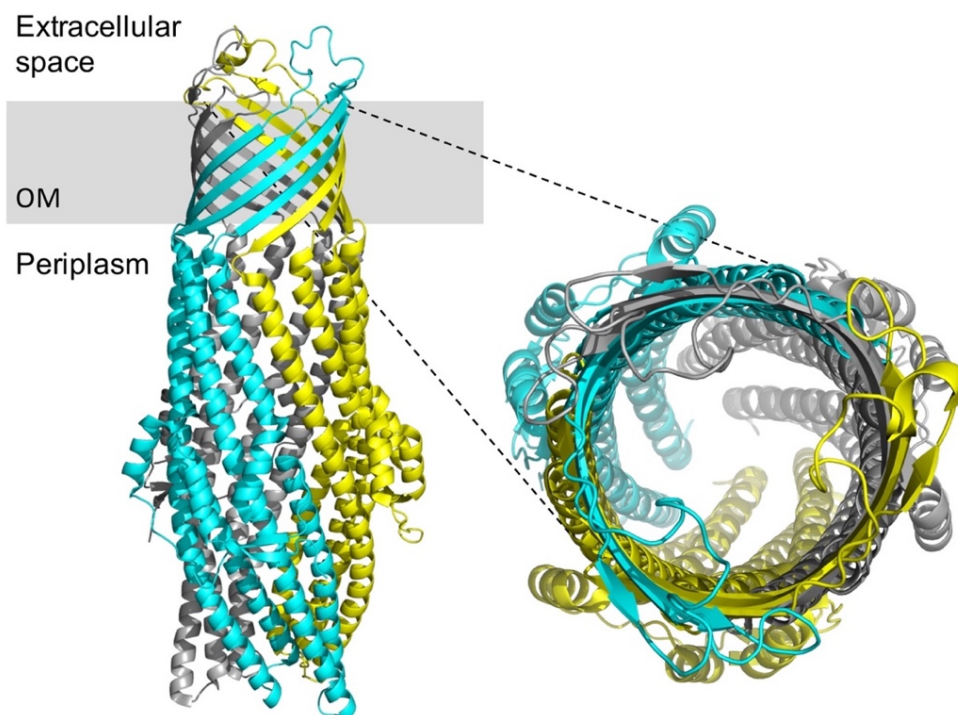


Figure 6: Crystal structure of TolC (PDB entry 1EK9). TolC forms a trimer and is anchored in the outer membrane with an open β -barrel pore. An α -helical barrel reaches into the periplasm. Each monomer forming the tunnel is highlighted in one colour, yellow, grey and cyan. On the right a top view looking from the extracellular space into the β -barrel exit of TolC is shown. The pore is open while the α -helices narrow the periplasmic entrance of TolC [112].

The secretion mechanism of HlyA

In the cytosol of *E. coli* HlyA remains in an unfolded conformation which is the prerequisite for the secretion via its T1SS [112, 115]. The unfolded substrate is not stabilized by the chaperone SecB and no other chaperone involved in secretion of HlyA could be identified [80, 115]. For the secretion the last 50-60 C-terminal amino acid residues of HlyA harboring the secretion signal are essential [19, 20]. HlyA interacts with HlyB as well as HlyD and only after HlyA binds to the inner membrane components TolC is recruited [108]. Therefore the assembly of the full HlyA T1SS is induced by the successful interaction with substrate, which leads to conformational changes in the secretion system [108, 110]. HlyA passes the HlyBD-TolC translocation channel with the C-terminus first [116]. In consequence, the C-terminus and the adjacent RTX domain reach the extracellular space first. In contrast to the bacterial cytosol where Ca^{2+} ion concentrations are kept below the K_D of the GG-repeats of 0.1 mM, the concentration in the extracellular environment is sufficient for binding of Ca^{2+} ions to the RTX domain [47, 49, 51]. This Ca^{2+} binding induces the folding of the secreted protein which at the same time would hinder the moving of the folded molecule back into the confined translocation pore [47, 48, 99]. After secretion is completed, TolC was shown to dissociate from the inner membrane complex (Fig. 7) [108]. The HlyA T1SS secretes its substrate with a secretion rate of 16 amino acid residues per transporter and minute, but it is not known how much ATP is required per secretion cycle [117]. Thus the driving force of secretion is not fully understood. Not only ATP hydrolysis is required already from the start of the secretion process [117], but also the proton motive force (PMF) was shown to be essential in the early stages of transport [98]. The binding of Ca^{2+} is discussed as a further driving force that pulls RTX proteins into the extracellular space, but in the case of HlyA in contrast to CyaA [118] the secretion is independent of the Ca^{2+} concentrations [117]. The concentration gradient for the substrate between the cytosol and the extracellular environment combined with the generally low pI of RTX proteins that results in an overall negative charge could further contribute to energizing the secretion [44, 99].

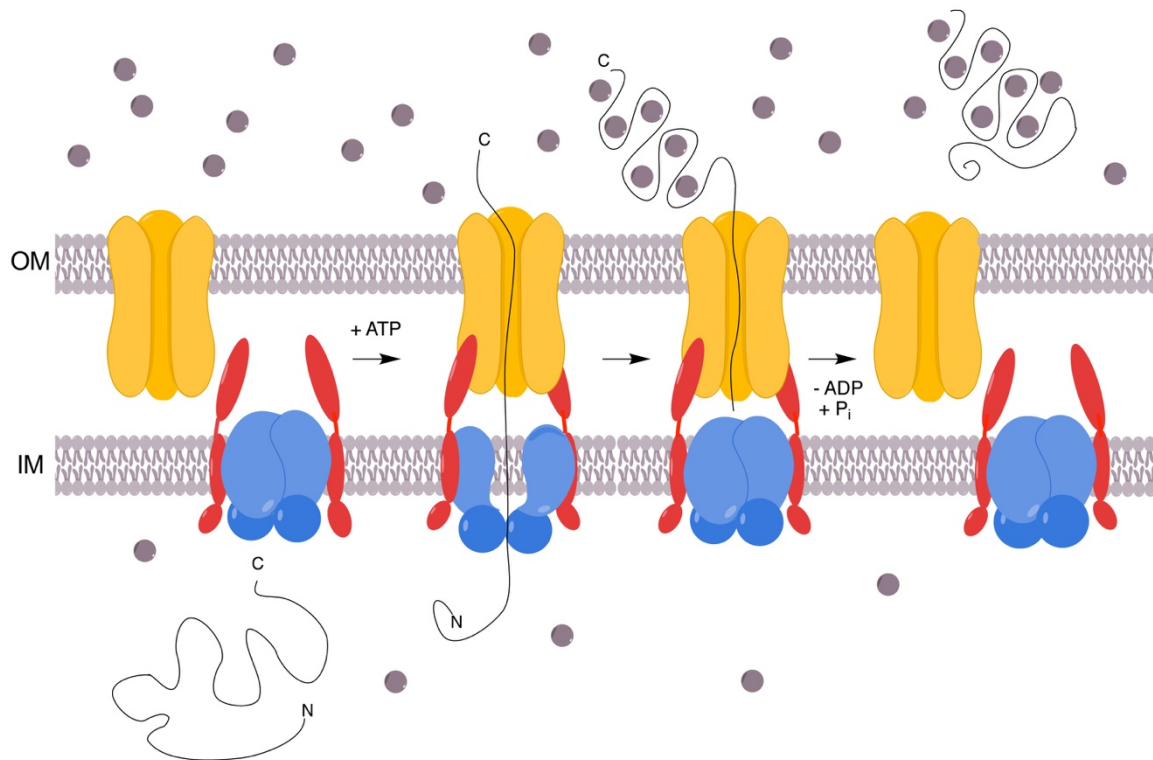


Figure 7: Postulated secretion mechanism of HlyA [99]. The ABC-transporter HlyB (blue), and the MFP HlyD (red) are located in the inner membrane and form the inner membrane complex. In the assembled complex, HlyD is suggested to form a hexamer but for simplicity HlyD is shown as a dimer [106]. In the cytosol, HlyA, indicated in black, remains unfolded due to low calcium ion concentrations (grey spheres) in the bacterial cytosol. Only upon interaction of HlyA with the inner membrane complex, TolC, shown in yellow and located in the outer membrane, is recruited to the complex. Binding and subsequent hydrolysis of ATP by HlyB leads to conformational changes in the transporter and energizes the transport of HlyA. The stoichiometry of ATP hydrolysis per secretion cycle is currently unknown. The C-terminus of HlyA reaches the extracellular space first and subsequently calcium ions bind to the GG-repeats exposed to the Ca^{2+} -rich extracellular environment. This induces folding of the RTX domain and further of the complete protein. The secreted substrate is released into the extracellular space and TolC disengages from the inner membrane complex. Figure based on [99]. OM: outer membrane, IM: inner mebrane.

1.2.2.4 Activation of HlyA by Acylation

Like other members of the subgroup of pore-forming RTX toxins HlyA requires a post-translational modification to display its cytotoxic activity [119-123]. The cytosolic acyltransferase hemolysin C (HlyC) needed for the conversion of the protoxin into the active, acylated HlyA is encoded in the HlyA operon upstream of the *hlyA* gene [119]. Before secretion, HlyC catalyzes the amide-linked acylation of the lysine residues K564 and K690 with fatty acids delivered by an acyl carrier protein (Fig. 8) [120, 124]. Specifically, HlyC

prefers C₁₄ fatty acids for activation but also other fatty acids such as C₁₅, C₁₆ and C₁₇ were reported depending on the study [125, 126]. The acylation of both acylation sites was shown to be essential for activation of proHlyA, but recently Osickova *et al.* suggested that acylation of K690 is sufficient [124, 126]. Only the acylated HlyA exerts lytic activity but unactivated proHlyA was still able to bind to lipid bilayers [127] and form pores in lipid bilayers, albeit the efficiency of pore formation was lower [128]. The acylation of HlyA is suggested to mediate an irreversible insertion into membranes and to be involved in oligomerization of HlyA that further induces lysis [129, 130]. What exact role the acylation status of HlyA plays in the mechanism of cytotoxicity remains unclear, but for CyaA the fatty acids convey effective binding to the host cell receptor [131, 132].

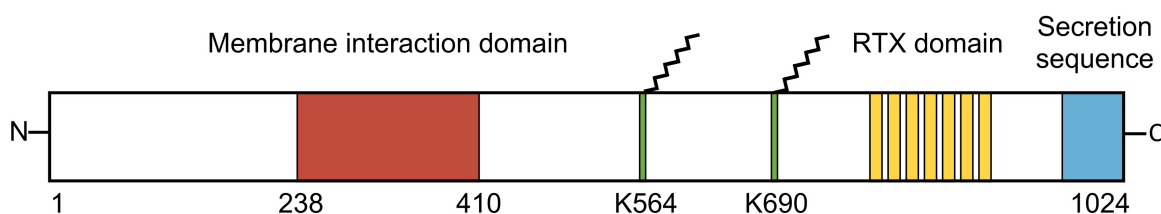


Figure 8: Schematic view of the domain organization of HlyA. The C-terminal part of HlyA carries the RTX domain consisting of six conserved GG-repeats and the secretion sequence comprising the last 50-60 amino acids. Two lysine residues, K564 and K690, are post-translationally acylated and mediate the cytotoxic activity of HlyA. Further a N-terminal hydrophobic domain is required for the pore-forming activity of HlyA [64].

The acyltransferase HlyC

Pore-forming RTX toxins are expressed together with a dedicated acyltransferase necessary for activation of the protoxin. Besides HlyC that post-translationally modifies HlyA several specialized acyltransferases have been shown to activate corresponding RTX proteins such as CyaC from *B. pertussis* or RtxC from *K. kingae* [122, 133]. The N-acylation of the ϵ -amino group of internal conserved lysine residues requires the acyl carrier protein as fatty acid donor [120, 124]. This acylation mechanism is unique among other acyltransferases [134, 135]. HlyC, is a 19.9 kDa cytosolic protein that is active in dimeric form [136]. It recognizes two acylation domains of approximately 50-80 amino acids that contain the conserved lysine residue of HlyA independently from each other [137]. While mutational studies on HlyA lead to the conclusion that the acylation of both sites is required for the cytotoxicity [124], the affinity of HlyC for the

first acylation site was reported to be 4-fold higher than for the second acylation site of HlyA [137]. The structure of HlyC is not solved but a crystal structure of a homologue of HlyC, the acyltransferase ApxC from *Actinobacillus pleuropneumoniae* (*A. pleuropneumoniae*) showed that the so called toxin-activating acyltransferases constitute a subgroup of the Gcn5-like N-acetyl transferase enzyme family [135]. Therefore it was proposed that ApxC and its homologues form a ternary complex with the acyl carrier protein and the substrate protoxin that allows specific fatty acylation [135]. Like HlyC, ApxC forms a dimer in solution in which each monomers is suggested to harbor a substrate-binding grove with an active site (Fig. 9) [135]. HlyC was shown to tolerate a few non-native RTX proteins as substrates for acylation including ApxIA from *A. pleuropneumoniae* [138]. From cross-combination of the RTX proteins HlyA, RtxA and CyaA with the acyltransferases HlyC, RtxC and CyaC, Osickova *et al.* concluded that the choice of fatty acids for modification and whether one or both acylation site are modified depends on the acyltransferase [126].

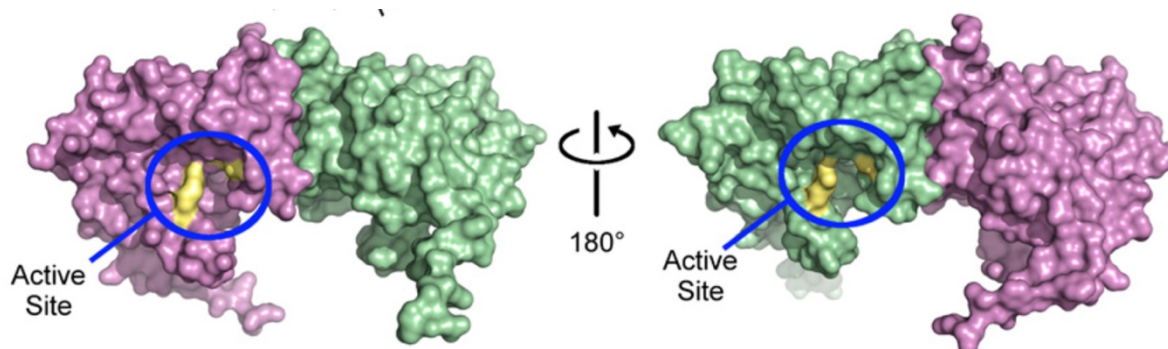


Figure 9: Structure of the ApxC dimer shown in a surface representation [135]. The monomers are highlighted in pink and green, the postulated active site in the binding grove of each monomer is coloured in yellow and highlighted with a blue circle. This figure is taken and modified from [135].

1.2.3 MbxA, a RTX toxin from *Moraxella bovis*

Moraxella bovis (*M. bovis*) is a Gram-negative bacterium and the cause of the infectious bovine keratoconjunctivitis (IBK) [139]. IBK is a highly contagious disease, occurring worldwide and is considered to be the most prevalent ocular disease of cattle. Symptoms include ocular discharge, edema and corneal ulceration, severe cases can lead to blindness [140]. The pathogenicity of *M. bovis* is linked to two major virulence factors, a pilin protein for adhesion and a secreted hemolysin that is only found in hemolytic strains [141-143]. The role of this hemolysin in pathogenicity was deduced from the cytotoxic effects of *M. bovis* culture supernatants on bovine neutrophils, erythrocytes and corneal epithelial cells [144-147]. *M. bovis* cultures showed cytotoxicity towards bovine but not human neutrophils which potentially stemmed from a specificity of the toxin [146]. Due to the reactivity of HlyA antibodies against it, the hemolysin was early on thought to be a member of the RTX protein family [148]. Identification of the gene, named *mbxA*, proved that the cytotoxin harbors GG repeats and indeed is a RTX protein [149]. MbxA is encoded in a classic RTX operon containing all genes necessary for activation and secretion of a pore-forming RTX toxin. Upstream of the *mbxA* gene the putative acyltransferase MbxC is encoded whereas the transporter components MbxB and MbxD are located in 3' direction. Downstream of the RTX operon an ORF homologous to the *tolC* gene is localized [143]. This genomic organization is an exception as typically the OMP gene is not associated with the *rtx* locus such as in the case of HlyA (Fig. 10) [15, 85]. MbxA shares a sequence identity of 42% with the prototype RTX protein HlyA while the activating components MbxC and HlyC are closer relatives with a homology of 55.9%. Comparing the secretion system components of MbxA and HlyA, the ABC transporter MbxB shares the highest sequence identity with HlyB of 67.2%. The putative MFP MbxD is less conserved, with a sequence identity of 40.8% shared with HlyD [143, 150]. The hemolytic activity of MbxA on bovine erythrocytes was reported to be Ca^{2+} dependent and based on pore formation that leads to K^{+} ion efflux, a subsequent colloid osmotic swelling and cell lysis. Using osmotic protection studies the size of the pore was estimated to be 0.9 nm [147]. Lytic activity of MbxA was also observed in neutrophils leading to a release of enzymes which in context of infection could aggravate tissue damage [144].

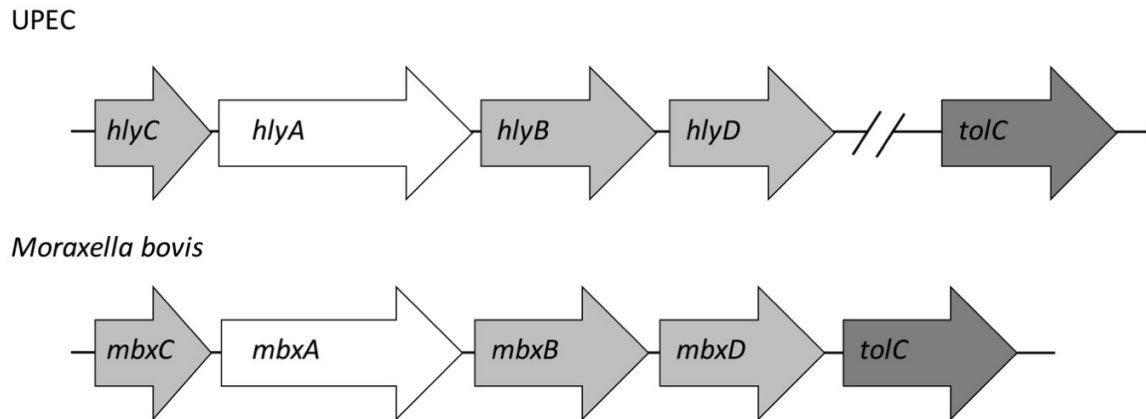


Figure 10: Genetic organization of the RTX operons of UPEC and *M. bovis*. The RTX proteins HlyA and MbxA are encoded in a RTX operon. Upstream of the RTX toxin gene an activating acyltransferase, HlyC or MbxC, are encoded. In both operons the inner membrane components of the T1SS, in *E. coli* HlyB and HlyD and in *M. bovis* accordingly MbxB and MbxD are encoded downstream of the toxin. In contrast to *E. coli* where the outer membrane protein TolC is encoded elsewhere in the genome, in *M. bovis* an open reading frame of a homologue of the *tolC* gene is located downstream of *mbxD*.

2. Aims

Numerous members of the RTX protein family, characterized by Ca^{2+} binding GG-repeats, are major virulence factors of different Gram-negative pathogens. The first to be identified and one of the best characterized RTX proteins is the pore-forming toxin HlyA from UPEC [16]. As a virulence factor, HlyA influences the course of urinary tract infections, which are considered one of the most frequent bacterial infections [73, 79, 151]. Despite being studied for four decades the structure and mechanism of pore formation of HlyA are still unknown and the effect on host cells not fully uncovered. A common characteristic of RTX protein is the secretion into the extracellular environment via T1SS [15]. The secretion system of HlyA consists of the ABC-transporter HlyB, the membrane fusion protein HlyD and the OMP TolC [81, 85]. It facilitates the one-step secretion of HlyA across both the inner and the outer membranes of *E. coli* and has been shown to be suitable for secretion of heterologous proteins [20, 115, 152, 153]. In light of the rapidly growing prevalence of antibiotic resistance in human and animal pathogens, virulence factors gain importance as powerful targets for novel anti-virulence therapies against bacterial infections [154]. Development of anti-virulence strategies relies on the accessibility and thorough understand of virulence factors. At the same time the increasing number of sequenced bacterial genomes allows the identification of yet uncharacterized RTX proteins based on the defining presence of the GG-repeats. This way, in 2010 1024 putative RTX proteins in 251 bacterial species have been identified with a bioinformatic approach [15]. The first aim of this thesis was to identify novel or not fully characterized RTX proteins of different pathogens as potential heterologous substrates for the HlyA secretion system (Tab. 1). The utilization of the HlyA T1SS as a surrogate secretion system opens the possibility to create an efficient production platform for novel RTX proteins. This further allows to avoid the isolation of the toxins directly from the pathogens. Subsequently, the second aim was to gain new structural insights into selected RTX proteins because very few examples of structures of RTX proteins, such as the crystal structure of RTX proteases and lipases, are available [14, 155]. As an essential prerequisite for structural studies purification protocols were developed for chosen RTX proteins. Here, small-angle X-ray scattering (SAXS) and cryogenic electron microscopy (cryo-EM) were applied to study HlyA and other RTX proteins. The third aim of the thesis was to characterize the interaction of RTX proteins with host cells. Studies on the membrane damaging activity were carried out with the RTX protein MbxA from *M. bovis* [149].

| Organism | Annotated protein | Length (amino acids) | Number of GG repeats | HlyA Identity (%) | HlyB Identity (%) | <i>rtx</i> locus structure | GenBank Protein ID |
|---------------------------------|--|----------------------|----------------------|-------------------|-------------------|----------------------------|-------------------------------------|
| <i>Acinetobacter baumannii</i> | Putative Ig domain-containing protein | 2888 | 38 | 43 | 26 | / | WP_002134769.1 |
| <i>Aeromonas diversa</i> | Calcium binding hemolysin | 517 | 7 | 43 | 65 | <i>rtxABD</i> | ENY71443.1 |
| <i>Cardiobacterium valvarum</i> | Type I secretion target GGXGXDXXX-repeat-containing domain protein | 1228 | 14 | 19 | 70 | <i>rtxABD</i> | EHM54655.1, EHM54654.1, EHM54683.1* |
| <i>Kingella kingae</i> | Hemolysin RtxA | 956 | 6 | 43 | 72 | <i>tolC-rtxCA-</i> | EGK07793.1 |
| | Ig-like domain-containing protein | 1113 | 4 | 31 | 72 | / | WP_071461640.1 |
| | Iron regulated protein FrpA | 760 | 4 | 28 | 72 | <i>frpAfrpA2frpC</i> | EGK08641.1 |
| <i>Bibersteinia trehalosi</i> | Leukotoxin LktA | 955 | 6 | 42 | 82 | <i>lktCABD</i> | AAG40310.1 |
| <i>Moraxella bovis</i> | RTX toxin MbxA | 927 | 5 | 42 | 67 | <i>mbxCABD-tolC</i> | AAK84651.1 |

Table 1: Selected RTX proteins annotated in genomes of Gram-negative bacteria.

Annotated proteins chosen within the scope of this thesis are listed with the predicted length of the protein and the number of identified conserved GG repeats. The sequence identity of the RTX proteins shared with HlyA from *E. coli* and the sequence identity of a corresponding ABC transporter identified in the genome of the chosen bacteria shared with HlyB from *E. coli* are given in %. In the case that related genes are found encoded in proximity to the *rtx* gene, the locus structure is given. The GenBank protein ID of the selected protein is listed [156]. In *Cardiobacterium valvarum* three putative RTX protein are annotated but sequencing carried out in this thesis revealed that one fused *rtx* gene comprising the three putative genes is present. Therefore the three separate protein IDs found in the GenBank database are marked with an *.

3. Publications

3.1 Chapter 1

Title: Type I secretion system—it takes three and a substrate

Authors: Kerstin Kanonenberg, Olivia Spitz, Isabelle N. Erenburg,
Tobias Beer, Lutz Schmitt

Published in: *FEMS Microbiology Letters* (2018)
Impact Factor 1.987

Own proportion of this work:
15%
Writing of the manuscript



JOURNALS
investing in science

FEMS Microbiology Letters, 365, 2018, fny094

doi: 10.1093/femsle/fny094

Advance Access Publication Date: 10 April 2018

Minireview

MINIREVIEW – Physiology & Biochemistry

Type I secretion system—it takes three and a substrate

Kerstin Kanonenberg, Olivia Spitz, Isabelle N. Erenburg, Tobias Beer and
Lutz Schmitt*

Institute of Biochemistry, Heinrich Heine University, 40225 Düsseldorf, Germany

*Corresponding author: Institute of Biochemistry, Heinrich Heine University, Düsseldorf, Universitätsstr 1, 40225 Düsseldorf, Germany.

Tel: +49-211-81-10773; Fax: +49-211-81-15310; E-mail: lutz.schmitt@hhu.de

One sentence summary: An overview of type I secretion systems of Gram-negative bacteria and a summary of the recent developments is provided.

Editor: Lily Karamanou

ABSTRACT

Type I secretion systems are widespread in Gram-negative bacteria and mediate the one-step translocation of a large variety of proteins serving for diverse purposes, including nutrient acquisition or bacterial virulence. Common to most substrates of type I secretion systems is the presence of a C-terminal secretion sequence that is not cleaved during or after translocation. Furthermore, these protein secretion nanomachineries are always composed of an ABC transporter, a membrane fusion protein, both located in the inner bacterial membrane, and a protein of the outer membrane. These three membrane proteins transiently form a 'tunnel channel' across the periplasmic space in the presence of the substrate. Here we summarize the recent findings with respect to structure, function and application of type I secretion systems.

Keywords: protein secretion; ABC transporter; secretion sequence; RTX toxin

INTRODUCTION

Bacteria have a need for secreting a variety of proteins and other molecules to the extracellular space, for nutrient acquisition (e.g. iron-scavenger proteins), biofilm formation (adhesins) or host invasion (virulence factors, e.g. exotoxins).

Secretory pathways have been of major research interest over the past decades and depending on the definition applied, a minimum of 15 different secretion systems has been identified so far in Gram-negative bacteria (reviewed in Costa et al. 2015). Here, the outer membrane imposes an additional problem as secreted macromolecules have to cross a second, the outer membrane. These secretion systems are capable of exporting a diverse range of small molecules, DNA and proteins to the extracellular space or even directly into the cytosol of a target cell. They vary greatly in composition and molecular mechanism, but can be easily divided into two major subgroups based on the presence or absence of a periplasmic transport intermediate during the secretion process.

Type I, III and IV secretion systems are double-membrane-spanning export machineries where the substrate is secreted in

one step from the cytosol to the extracellular space (type I). The latter two are even capable of delivering their substrate directly into the cytosol of the target cell, thus traversing three membranes (Fig. 1). Obviously, all these secretion systems require a 'tunnel channel'-like architecture, composed of a minimum of 3 but up to more than 10 membrane-localized proteins (Fig. 1). For further information, the reader is referred to Economou and Dalbey (2014) and Costa et al. (2015) for a review series covering the details of most bacterial secretion systems.

This review highlights the recent advances in research concerning specifically type I secretion systems (T1SS), setting the focus mainly on new structural insights that have been obtained over the last years. T1SS are often referred to as the most 'simple' representative considering that they are composed of only three membrane proteins (also see Delepelaire 2004; Kanonenberg, Schwarz and Schmitt 2013; Thomas, Holland and Schmitt 2014; Holland et al. 2016 for various aspects of T1SS).

Many Gram-negative pathogens make use of T1SS to secrete a great variety of virulence factors. The discovery of the first T1SS substrate dates back to as far as 1979 when the Goebel

Received: 6 February 2018; Accepted: 9 April 2018

© FEMS 2018. All rights reserved. For permissions, please e-mail: journals.permissions@oup.com

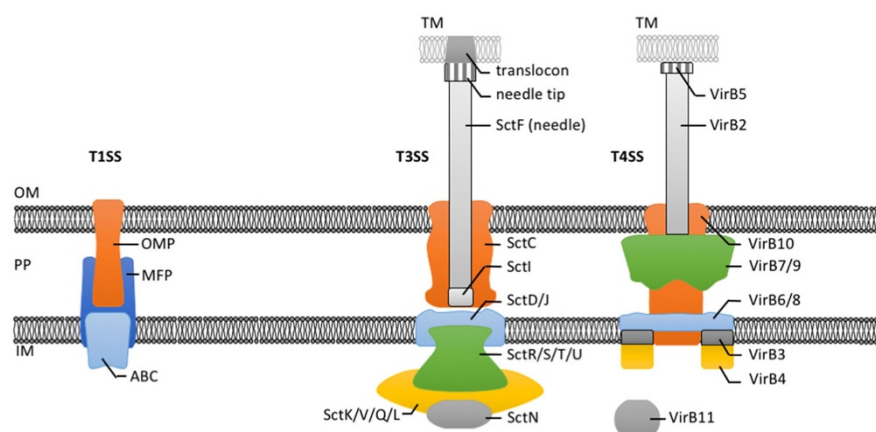


Figure 1. Cartoon of secretion systems from Gram-negative bacteria that translocate their substrates in one step across two (T1SS) or three membranes (T3SS and T4SS). OM: outer membrane, PP: periplasm, IM: inner membrane, OMP: outer membrane protein, MFP: membrane fusion protein, ABC: ABC transporter. Proteins forming the T3SS and T4SS and their putative location are indicated.

laboratory identified hemolysin A (HlyA), named after its ability to lyse erythrocytes from uropathogenic *Escherichia coli* strains (Noegel et al. 1979). Subsequently, the nucleotide sequence of HlyA was determined (Felmlee, Pellett and Welch 1985). Additional studies from the laboratories of Koronakis, Holland and Goebel (Mackman and Holland 1984; Mackman et al. 1985a,b, 1987; Gray et al. 1986, 1989; Felmlee and Welch 1988; Koronakis, Koronakis and Hughes 1989; Gentschev, Hess and Goebel 1990; Chervaux et al. 1995) demonstrated that secretion of HlyA occurred without any periplasmic intermediate and was Sec independent. Moreover, HlyA carried a C-terminal secretion signal indicating an unknown secretion mechanism.

The analysis of the sequence of the *hly* operon (Felmlee, Pellett and Welch 1985) revealed the presence of two additional membrane proteins and a third component in addition to the substrate HlyA. The third component, HlyC, turned out to be essential for the activation of HlyA, but not for secretion per se (Nicaud et al. 1985). HlyC was shown to act as a cytosolic acyltransferase acylating two internal lysine residues of the unfolded HlyA prior to secretion. This required equimolar amounts of the acyl carrier protein (Issartel, Koronakis and Hughes 1991; Stanley, Koronakis and Hughes 1991; Stanley et al. 1994, 1999; Thomas, Smits and Schmitt 2014). Only recently, the crystal structure of an HlyC homolog was reported (Greene et al. 2015) that will open up new approaches to understand the function of this unusual acyltransferase at the molecular level.

HlyD, one of the membrane proteins encoded by the *hly* operon, belongs to the family of bacterial membrane fusion proteins (MFPs) (Symmons, Marshall and Bavro 2015) that is unique to Gram-negative bacteria. The second membrane protein, HlyB, is a member of the ABC transporter family (Davidson et al. 2008), which is found in all kingdoms of life. Since HlyB and HlyD were localized to the inner membrane (Mackman et al. 1985a,b; Wang et al. 1991; Pimenta et al. 1999), the lack of periplasmic intermediates raised an obvious question—How does HlyA reach the extracellular space? This issue was addressed by the Wandersman group, who identified TolC, a ubiquitous and polyvalent outer membrane protein, as the missing, third component of the HlyA-T1SS (Wandersman and Delepelaire 1990). A complex of the two inner membrane proteins and TolC form the ‘tunnel

channel’ that allows the one-step secretion of HlyA. Apart from T1SS, TolC is involved in the extrusion of toxic components (Koronakis, Eswaran and Hughes 2004), for example by being part of tripartite drug efflux systems such as the AcrA-AcrB/TolC complex (Du et al. 2014).

In other T1SS, more than one transport substrate (Letoffe, Delepelaire and Wandersman 1990) or the TolC homolog (Letoffe, Ghigo and Wandersman 1994) can be encoded in the operon. Thus, there are no strict requirements on the genetic level for the operon organization of T1SS, but several lines of evidence suggest that a minimal unit composed of the gene coding for the transport substrate, the ABC transporter and the MFP is present in all operons. In addition, some degree of promiscuity with respect to the transported substrate exists, since the Hly system of *E. coli* was successfully used to secrete, for example, CyaA from *Bordetella pertussis* (Masure et al. 1990; Sebo and Ladant 1993), FrpA from *Neisseria meningitidis* (Thompson and Sparling 1993) or PaxA from *Pasteurella aerogenes* (Kuhnert et al. 2000).

T1SS SUBSTRATES

For the vast majority of T1SS substrates, all the information necessary and sufficient for secretion is encoded in the extreme C-terminus, which is not cleaved during or after translocation. This was recognized early on (Gray et al. 1986) and was one of the first indications that HlyA was secreted independently of the Sec system. However, a small group of substrates (class II microcins) contain an N-terminal propeptide, which is cleaved by a C39 peptidase domain on the ABC transporter prior to secretion (Hwang, Zhong and Tai 1997).

The actual secretion signal of the Hly system was shown to be confined to the last 50 to 60 most extreme C-terminal amino acids (Koronakis, Koronakis and Hughes 1989) but its size and nature varies from system to system. The reader is referred to a review (Holland et al. 2016), which summarizes our current knowledge on T1SS secretion signals, still leaving many unanswered questions that need to be addressed in future research.

Upstream to the secretion sequence of HlyA, aspartate and glycine-rich nonapeptide repeats were identified (Welch 1991).

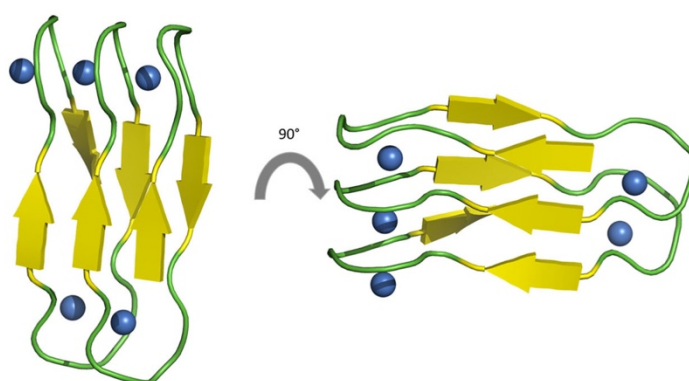


Figure 2. A zoom into the β -roll motif of an alkaline protease (Baumann et al. 1993). Ca^{2+} ions and the Ca^{2+} binding region are shown as blue spheres and in cartoon representation, respectively.

These have the consensus sequence GGXGDXUX (where X can be any amino acid and U is a large hydrophobic amino acid) and the term 'GG repeats' or 'repeats-in-toxins' (RTX) was coined by Rod Welch. These repeats form the hallmark of an entire family of proteins including lipases, proteases, adhesins, S-layer proteins or toxins (reviewed by Linhartova et al. 2010).

Structural studies on the T1SS-secreted alkaline protease from *Pseudomonas aeruginosa* (Baumann et al. 1993) and other substrates (Baumann et al. 1993; Izadi-Pruneyre et al. 1999; Meier et al. 2007; Griessl et al. 2013) revealed that the coordination of one Ca^{2+} by two RTX motifs via the side chains of the aspartate residues and the backbone of the first two glycine residues creates a so-called β -roll or β -helix motif (Fig. 2).

RTX substrates of T1SS bind Ca^{2+} ions in the high micromolar range, for example $\sim 500 \mu\text{M}$ for CyaA from *Bordetella pertussis* (Chenal et al. 2009; Sotomayor Perez et al. 2015) or $\sim 150 \mu\text{M}$ for HlyA from *E. coli* (Ostolaza, Soloaga and Goni 1995; Sanchez-Magraner et al. 2007; Thomas et al. 2014). This binding induces folding of the entire RTX protein. As the concentration of free Ca^{2+} ions in the bacterial cytosol is in the high nanomolar range (Jones et al. 1999), RTX proteins remain unfolded until they reach the extracellular space, where Ca^{2+} concentrations of up to 10 mM result in immediate binding and protein folding.

The N-terminal moiety of T1SS substrates encodes for functionality, i.e. lipolytic, hemolytic, proteolytic, adhesive or any other activity. A recent data mining approach of 840 bacterial genome sequences (Linhartova et al. 2010) identified ~ 1000 RTX proteins, being extremely variable in size (up to 900 kDa, Hinsä et al. 2003) and function, but conforming to the general arrangement of T1SS substrates, functional domain/RTX domain/secretion sequence. The number of RTX domains in an individual RTX-protein scales to some extent with the molecular weight (Linhartova et al. 2010), but the presence of these characteristic motifs is ubiquitous and highlights their functional importance.

The iron siderophore HasA from *Serratia marcescens* represents an exception (Letoffe, Ghigo and Wandersman 1994). With a size of 19 kDa it is the smallest substrate of a T1SS identified so far and interestingly lacks the entire RTX domain, but contains a C-terminal secretion sequence (Izadi-Pruneyre et al. 1999). Interestingly, it is the only T1SS substrate known which requires a chaperone, SecB, for secretion (Sapriel, Wandersman and Delepelaire 2002; Bakkes et al. 2010).

FUNCTIONAL INSIGHTS

Early on, Koronakis and coworkers (Thanabalu et al. 1998; Balakrishnan, Hughes and Koronakis 2001) demonstrated for the HlyA T1SS that upon interaction of the substrate with the inner membrane proteins (HlyB and HlyD), TolC is recruited and a 'channel tunnel' is formed through which HlyA is secreted at the cost of ATP hydrolysis. After substrate translocation is completed, TolC disassembles from the complex, leaving HlyB and HlyD as a stable complex in the inner membrane, ready to start another round of substrate secretion.

Deletion studies proved that the cytosolic domain of HlyD (residues 1–60) forms the hub from which assembly of the secretion complex is initiated (Balakrishnan, Hughes and Koronakis 2001). Complementary data were provided by *in vitro* surface plasmon resonance experiments demonstrating that the isolated nucleotide-binding domain (NBD) of the ABC transporter also interacts with the substrate (Benabdelhak et al. 2003). Interestingly, this interaction was strictly limited to the C-terminal secretion signal.

Indirect (Kenny, Haigh and Holland 1991; Debarbieux and Wandersman 2001) and direct evidence (Bakkes et al. 2010) demonstrated that substrates of T1SS are translocated in an unfolded state. In an elegant set of experiments, Wandersman and colleagues observed that the presence of folded HasA actually inhibited the secretion of newly synthesized HasA (Debarbieux and Wandersman 2001). Subsequently, they addressed the underlying principles of this cis inhibition (Cescau, Debarbieux and Wandersman 2007) and surprisingly, the results of this study demonstrated that the interaction of unfolded HasA with the inner membrane complex also occurs outside the region encoding the secretion sequence, identifying a second, non-overlapping binding site. This interaction resulted in stable recruitment of the outer membrane protein TolC, which could be reversed by adding *in cis* the isolated secretion sequence. This pointed toward an intermolecular activity that triggered complex dissociation (Cescau, Debarbieux and Wandersman 2007).

All structural and functional data obtained for ABC transporters so far indicate that the transport mechanism used by these primary active transporters to shuttle their substrates from one side of the membrane to the other follows the 'alternating two site access model' for membrane transporters (Jardetzky 1966). However, the unfolded state and the mere

physical length (up to 9000 amino acids) of substrates of T1SS make it impossible to apply this generally accepted mechanism also for ABC transporters involved in T1SS. Although some research has been carried out on this issue, there is still very little understanding of the mechanism of secretion through the transenvelope channel.

In contrast to the canonical organization of ABC transporters, HlyB harbors an additional N-terminal domain, a cytosolic appendix (Kanonenberg, Schwarz and Schmitt 2013). Based on the primary structure of HlyB, the first ~130 amino acids belong to the family of C39 peptidases, a subfamily of the papain superfamily of cysteine proteases (Havarstein, Diep and Nes 1995; Wu and Tai 2004). These peptidases are unique to ABC transporters and are only found in bacteriocin exporters (Havarstein, Diep and Nes 1995). In principle, the protein family of bacteriocins is limited to Gram-positive bacteria, but a few members can also be found in Gram-negative strains, e.g. Colicin V in *E. coli*. Using a type I secretion apparatus but retaining the typical N-terminally cleaved propeptide, these peptides form a small yet unique group amongst type I substrates (Hwang, Zhong and Tai 1997).

However, in many T1SS ABC transporters such as HlyB the catalytically active cysteine residue is replaced by a tyrosine, resulting in a corrupted catalytic triad. Lecher *et al.* (2012) therefore established the term 'C39 peptidase-like domain' (CLD). NMR studies revealed an identical tertiary structure compared to C39 peptidase domains (Ishii *et al.* 2010). A conserved interaction of the histidine residue in the corrupted active center with a tryptophan residue was discovered, which is now commonly used to distinguish C39 peptidase domains from CLDs (Lecher *et al.* 2012; Kanonenberg, Schwarz and Schmitt 2013). In a set of *in vitro* functional and structural studies, Lecher *et al.* (2012) confirmed binding of unfolded substrate to the isolated CLD that was independent of the secretion signal. The substrate-binding site was mapped by chemical perturbation experiments and results were subsequently confirmed by mutational studies. These results suggest that the CLD acts as a receptor that grabs unfolded HlyA and positions it for subsequent translocation. It remains speculative whether the CLD also plays a role in preventing folding and degradation of the substrate in the cytosol and further studies are needed to establish its precise function and mechanism of action.

Within the field of study, the question of directionality of type I secretion has long been under debate. The concept of stalling the HlyA T1SS by using substrate N-terminally fused to fast folding enhanced green fluorescent protein (eGFP) (Evdokimov *et al.* 2006) finally answered this question (Lenders *et al.* 2015). Folded eGFP in the cytosol served as a 'plug' while the C-terminal moiety inserted into the channel tunnel and protruded partially into the extracellular space, where it prevented backsliding by adopting its tertiary structure. A combination of fluorescence and super-resolution microscopy exploiting the autofluorescence of eGFP in the cytosol and immunofluorescence-based methods to detect the secreted C-terminus of the substrate demonstrated that the secretion sequence appears first on the external surface of the cell envelope.

QUANTITATIVE ANALYSIS

The concept of stalling a T1SS (as described in section 'Functional insights') not only offered the possibility to address the directionality of transport but was also exploited to determine the secretion rate of the HlyA T1SS (Lenders *et al.* 2016). Importantly,

the fluorescence of Cy3-labeled antibody was first employed to quantify the total number of active HlyA T1SS translocons per cell. Interestingly, the derived number was in good agreement with the absolute number of HlyB dimers present in the membrane, as determined by quantitative western blot analysis, using a standard of purified HlyB (Reimann *et al.* 2016) of known concentrations. By experimentally quantifying the amount of secreted substrate, the secretion rate of the HlyA T1SS was determined to be 16 amino acids per transporter per second. Thus, it requires 90 s to secrete one complete HlyA molecule. This rate is roughly 10-fold lower than the rate of SecA-dependent protein translocation across the inner membrane, which operates at a calculated rate of ~152–228 amino acids per second per transporter (Schiebel *et al.* 1991; Uchida, Mori and Mizushima 1995). Intriguingly, the rate of HlyA secretion is very similar to the rate of bacterial protein synthesis at the ribosome, which was calculated to be 10–20 amino acids per second (Young and Bremer 1976). Whether this similarity is of any relevance and results from some sort of connection still has to be addressed experimentally.

In earlier studies, the proton motive force (pmf) was identified as being essential for substrate secretion (Koronakis, Hughes and Koronakis 1991). In our hands, however, an influence of the pmf on the secretion rate was not observed (unpublished data), supporting recent results on CyaA, an exotoxin from *B. pertussis* (Bumba *et al.* 2016), whose secretion is also independent from the pmf. This seminal study also demonstrated a clear influence of the extracellular Ca^{2+} concentration on the secretion efficiency. Thus, the presence of Ca^{2+} accelerated CyaA secretion by generating intramolecular Brownian ratchets. In other words, this process is passive but involves ratcheted translocation events. Nevertheless, these data do not support the hypothesis that the binding of Ca^{2+} ions to the RTX domains represents a driving force of prime importance for secretion (Chenal *et al.* 2009; Thomas *et al.* 2014). This is in striking contrast to the secretion of HlyA (Lenders *et al.* 2016), where changes in the Ca^{2+} concentration in the medium or even the complete absence of Ca^{2+} did not influence the secretion rate, which remained at 16 amino acids per transporter per second. However, one has to stress that Ca^{2+} is crucial for the functionality of HlyA and that in the absence of Ca^{2+} the pore-forming activity was abolished (Lenders *et al.* 2016). These findings suggest a certain variety in the molecular mechanism of secretion amongst different T1SS, which may be influenced by the size of the substrate or the arrangement of the RTX domains. Thus, it is suggested that a Brownian ratchet mechanism combined with a pulling force is operational in CyaA (Bumba *et al.* 2016), but absent in HlyA (Lenders *et al.* 2016) and further experiments especially involving other T1SS are required to settle this issue.

STRUCTURAL INSIGHTS

Structural elucidation, together with functional characterization, is a powerful tool to investigate the transport mechanisms of membrane proteins. The very first structural information of a T1SS component was derived from two-dimensional crystals of the outer membrane protein TolC from *E. coli*. Even at a resolution of 12 Å, apart from the trimeric β -barrel nature, the presence of a novel periplasmic domain became evident (Koronakis *et al.* 1997). Only a few years later, solving the crystal structure of TolC at 2.1 Å revealed the novel fold of this funnel-like domain (Koronakis *et al.* 2000). This is composed out of 12 α -helices that protrude 100 Å into the periplasmic space. Including the

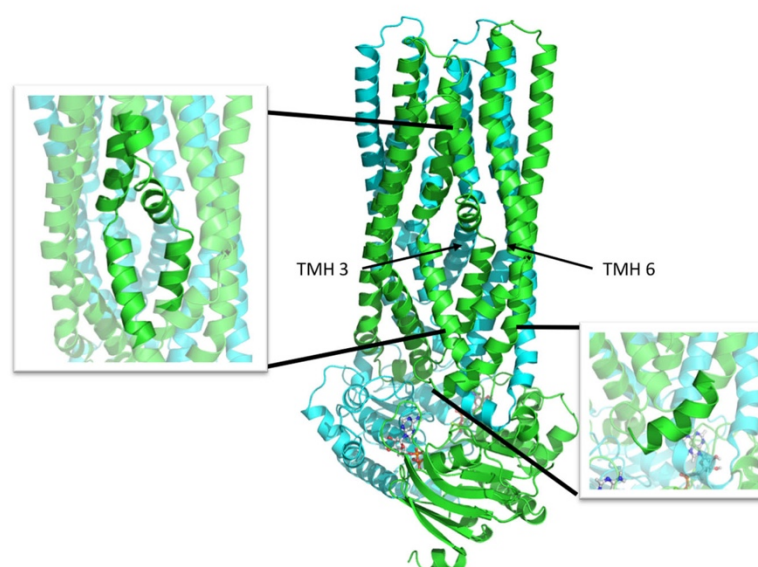


Figure 3. Cartoon representation of AaPrtD (Morgan, Acheson and Zimmer 2017). Monomers are shown in green and cyan. The bound nucleotides are shown in stick representation. The kinked helices 3 and 6 (TMH3 and TMH6) are highlighted for one monomer (left zoom-in). The right zoom-in highlights the coupling helix 1.

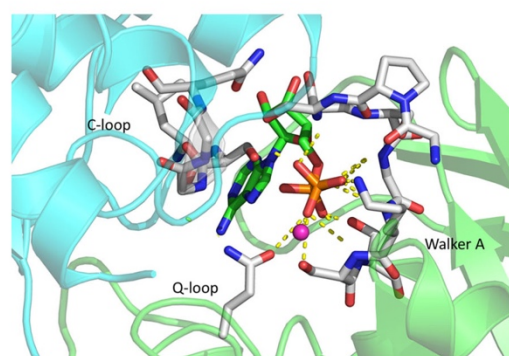


Figure 4. Zoom into the nucleotide-binding site of AaPrtD (Morgan, Acheson and Zimmer 2017) formed by both NBDs colored in green and cyan. ADP is shown in stick representation, the co-factor Mg^{2+} as magenta sphere. The conserved motifs interacting with the bound ADP molecule are labeled and highlighted in stick representation. Interactions are visualized by dashed, yellow lines.

12-stranded β -barrel (3 per monomer) the total length of the protein adds up to 140 Å. The structure was interpreted to represent a closed state as the inner diameter of the water-filled β -barrel of 20 Å narrows to only 3.9 Å at the periplasmic gate of TolC.

Based on this structural information, alanine mutations were placed within the region of the periplasmic gate in order to disrupt the closed state of TolC. Conductivity measurements in black lipid membranes led to a model, in which an 'iris-like' opening of the inner helices opens the periplasmic gate and therefore allows substrate translocation (Andersen et al. 2002a,b). Later on, this model was confirmed by structural information (Bavro et al. 2008; Pei et al. 2011).

Starting in 2003, a series of crystal structures paired with functional analysis on the NBD of the ABC transporter HlyB was

published (Benabdelhak et al. 2003, 2005; Schmitt et al. 2003; Zaitseva et al. 2005a, 2006). These studies offered valuable insights into the motor domain of a T1SS and its detailed molecular mechanism of ATP hydrolysis (Zaitseva et al. 2005b,c; Hanekop et al. 2006; Oswald, Holland and Schmitt 2006).

Additional insights into the structure of T1SS were obtained only recently, when the crystal structure of the ABC transporter of a putative T1SS from the hyperthermophilic Gram-negative bacterium *Aquifex aeolicus* (AaPrtD) was published. It shares a sequence identity of 40% with PrtD from *Dickeya dadantii*, but neither the substrate nor the MFP homolog of AaPrtD was identified (Morgan, Acheson and Zimmer 2017). The structure of the homodimer was determined at a resolution of 3.15 Å and reflected the ADP/ Mg^{2+} -bound state (Fig. 3). The presence of six transmembrane helices (TMH) per monomer and the canonical fold of the NBDs is typical for ABC transporters. Interestingly, the arrangement of the NBDs in the ADP-bound state seems to represent the occluded state (Morgan, Acheson and Zimmer 2017), which contradicts the accepted view that ATP binding induces dimerization of the two NBDs (Locher 2004, 2016; Oswald, Holland and Schmitt 2006).

The ADP molecule is coordinated by residues of the Walker A motif and the glutamine residue of the Q-loop, and also by the serine residue of the C-loop of the opposing NBD resulting in dimerization (Fig. 4). However, a similar architecture has been observed in the crystal structure of Sav1866 from *Staphylococcus aureus* (Dawson and Locher 2006) raising the question of how this architecture fits into the well-established view that only ATP induces formation of the NBD dimer.

The architecture of the TMHs of AaPrtD is distinct from that of other ABC export systems. Generally, ABC transporters contain two coupling helices (CH1 and CH2), which interact with the NBDs. In AaPrtD, the interaction conferred by CH1 is taken over by TMH2, which extends into a loop region that continues without any secondary structure into TMH3.



Figure 5. Crystal structure of a soluble fragment of HlyD from *E. coli* (Kim et al. 2016) that highlights the coiled-coil interaction of the helices. The lipoyl domain is colored in red and blue. N- and C-termini are indicated.

Furthermore, TMH3 and TMH6 are kinked at the approximate position of the lipid head groups, splitting TMH6 into two and TMH3 into three separate helices—a novel architecture—not been observed before (Morgan, Acheson and Zimmer 2017), neither in the bacteriocin transporter McjD (Choudhury et al. 2014) nor in the peptide transporter TAP 1/2 (Oldham, Grigorieff and Chen 2016). The kinks create a restriction within the putative substrate channel. The fact that residues lining this restriction are stabilized by interactions with conserved amino acids emphasizes their functional importance. Although the functionality of AaPrtD has not been demonstrated yet and the identity of the MFP and the transport substrate remain elusive, the structure provided the first glimpse of a T1SS ABC transporter and presents a platform to design new and exciting experiments.

Proteins from the family of MFPs are not only an indispensable part of T1SS but have also been intensively studied in the context of bacterial tripartite drug efflux pumps, such as the AcrB-AcrA-TolC system (Du et al. 2014) or the MacA-MacB-TolC system (Fitzpatrick et al. 2017). Until 2016, structural information was limited to MFPs involved in drug efflux (for a recent review, see Symmons, Marshall and Bavro 2015), while for T1SS MFPs only recently has some limited structural information become available (Kim et al. 2016). In 2016, the crystal structure of a soluble fragment of HlyD, comprising the α -helical domain and lipoyl domain, was published (Kim et al. 2016). However, the construct used for structure determination lacked not only the first 95 N-terminal amino acids, including the cytoplasmic domain (residues 1–59) and the single TMH of HlyD (residues 60–80), but also the last 106 C-terminal residues (residues 373–478), corresponding to the entire membrane proximal domain (Fig. 5).

In contrast to the majority of structurally described MFPs that contain two α -helices, the unusually long (115 Å) α -helical domain of HlyD is built out of three helices, of which helix 3 in-

teracts in an anti-parallel coiled-coil fashion with helix 1 and 2. Based on structural comparison with AcrA (Kim et al. 2010) and sequence conservation analysis, a model was proposed, where the α -helical tip located between helix 2 and 3 forms the interaction site with TolC (Kim et al. 2016). Only recently, in 2017, the crystal structure of the α -helical domain and the lipoyl domain of LipC, the MFP of the lipase secretion system from *Serratia marcescens*, was reported (Murata et al. 2017). Interestingly, the α -helical domain also contained three helices, which might be a common feature of T1SS MFPs.

The AcrA-AcrB-TolC (Du et al. 2014) and the MacA-MacB-TolC (Fitzpatrick et al. 2017) structures revealed a hexameric arrangement of the corresponding MFPs. Contradictory findings provided by cross-linking studies in *E. coli* suggest a trimeric state of HlyD as the functional unit (Thanabalu et al. 1998). Even though in principle a hexameric state seems more likely and is also supported by a model (Kim et al. 2016) based on the available crystal structure of MacA (Yum et al. 2009), the oligomeric state of T1SS MFPs is still under debate and the subject is still in need of further investigation.

BIOTECHNOLOGICAL APPLICATIONS

By achieving the secretion of fusion proteins in high amounts into the extracellular medium, large-scale purification can be significantly simplified, which reflects an attractive approach for biotechnological applications.

The relatively simple nature of T1SS and the C-terminal secretion signal raised interest in their use in biotechnological applications. Two main areas became the focus of intensive research: heterologous protein secretion, in general (Blight and Holland 1994) and antigen production for vaccination (Sebo et al. 1999; Spreng et al. 1999).

Here, we will only focus on the applicability of T1SS for the secretion of heterologous proteins. Based on the T1SS of TliA, a thermostable lipase from *P. fluorescens* (Park et al. 2012), a versatile secretion system was engineered (Ryu et al. 2015). The C-terminal secretion signal of TliA was fused either to GFP or alkaline phosphatase, and both proteins were secreted into the medium. The hydrophobic nature of the secretion signal even allowed subsequent purification via hydrophobic interaction chromatography. Secretion of fusion proteins was further enhanced by engineering a negative net charge by introducing aspartate clusters in the fusion proteins of interest (Byun et al. 2017). These constructs go hand in hand with the direction of the membrane potential, which is positive on the surface of bacteria. This favors the translocation of negatively charged proteins since the directionality of the potential acts electrophoretically (Cao, Kuhn and Dalbey 1995).

The other T1SS that has been extensively studied for the purpose of heterologous protein secretion is the HlyA T1SS from *E. coli*. With the identification of HlyA1 (Nicaud et al. 1986), a 23 kDa, C-terminal fragment of HlyA encouraging the secretion sequence and three of six RTX domains, research efforts were intensified to exploit the system for the secretion of heterologous proteins. The studies of Debarbieux and Wandersman (2001) and Bakkes et al. (2010) stressed the importance of folding rates in the successful secretion of fusion proteins. Remarkably, the natural folding rate of a protein fused to HlyA1 decreased dramatically, which increased the range of possible fusion partners and increased the yields of the proteins of interest (Bakkes et al. 2010).

Only recently, a new expression vector was established that impressively improved secretion efficiencies of various

fusion proteins (Khosa et al. 2018). Here, a 5'-untranslated region (UTR) was identified that increased the amount of secreted HlyA1 several-fold and that, most surprisingly, does contain nucleotides belonging to the coding sequence of HlyC. The region was mapped to an area enriched in adenosine- and uracil nucleotides, located ~36 base pairs upstream from the start codon of HlyA1. Nevertheless, the most striking result to emerge from this data in terms of biotechnological application is that besides boosting the secretion efficiency of HlyA1, the vector enabled the secretion of fast-folding fusion proteins that could not be secreted until then (Khosa et al. 2018). This is likely due to the fact that this 5'-UTR is recognized by ribosomal protein S1 and targeted to the ribosome for faster and more efficient translation. Certainly, these findings could open up new avenues for the exploitation of T1SS and highlights their potential biotechnological and pharmaceutical value. Furthermore, they emphasize the necessity not to limit biotechnological engineering to the mere coding sequence of a protein.

OUTLOOK

Since its discovery nearly 40 years ago, T1SS have been the subject of numerous fruitful studies and the basic outline of the secretion process is by now well established. However, much uncertainty still exists about the detailed mechanism of transport. Ongoing, exciting research should address, for example, additional structural information, the stoichiometry of the T1SS complexes, the nature of the secretion signal and biochemical insights into recognition and processing of the substrate.

ACKNOWLEDGEMENTS

We apologize to all our colleagues whose research could not be appropriately referenced due to space limitation. We thank all current and former members of the Institute of Biochemistry for support and valuable discussion. LS wishes to gratefully acknowledge his long term and highly fruitful collaboration with Prof. I. Barry Holland and his laboratory at the University of Orsay, France.

FUNDING

Research on the hemolysin T1SS is funded by the DFG through CRC 1208 (project A01 to LS) and the Manchot Graduate School Molecules of Infections III (to LS).

Conflict of interest. None declared.

REFERENCES

- Andersen C, Koronakis E, Bokma E et al. Transition to the open state of the TolC periplasmic tunnel entrance. *P Natl Acad Sci USA* 2002a;99:11103–8.
- Andersen C, Koronakis E, Hughes C et al. An aspartate ring at the TolC tunnel entrance determines ion selectivity and presents a target for blocking by large cations. *Mol Microbiol* 2002b;44:1131–9.
- Bakkes PJ, Jenewein S, Smits SH et al. The rate of folding dictates substrate secretion by the *Escherichia coli* hemolysin Type 1 secretion system. *J Biol Chem* 2010;285:40573–80.
- Balakrishnan L, Hughes C, Koronakis V. Substrate-triggered recruitment of the TolC channel-tunnel during type I export of hemolysin by *Escherichia coli*. *J Mol Biol* 2001;313:501–10.
- Baumann U, Wu S, Flaherty KM et al. Three-dimensional structure of the alkaline protease of *Pseudomonas aeruginosa*: a two-domain protein with a calcium binding parallel beta roll motif. *EMBO J* 1993;12:3357–64.
- Bavro VN, Pietras Z, Furnham N et al. Assembly and channel opening in a bacterial drug efflux machine. *Mol Cell* 2008;30:114–21.
- Benabdelhak H, Kiontke S, Horn C et al. A specific interaction between the NBD of the ABC-transporter HlyB and a C-terminal fragment of its transport substrate haemolysin A. *J Mol Biol* 2003;327:1169–79.
- Benabdelhak H, Schmitt L, Horn C et al. Positive cooperative activity and dimerization of the isolated ABC-ATPase domain of HlyB from *E. coli*. *Biochem J* 2005;368:1–7.
- Blight MA, Holland IB. Heterologous protein secretion and the versatile *Escherichia coli* haemolysin translocator. *Trends Biotechnol* 1994;12:450–5.
- Bumba L, Masin J, Macek P et al. Calcium-driven folding of RTX domain beta-Rolls ratchets translocation of RTX proteins through type I secretion ducts. *Mol Cell* 2016;62:47–62.
- Byun H, Park J, Kim SC et al. A lower isoelectric point increases signal sequence-mediated secretion of recombinant proteins through a bacterial ABC transporter. *J Biol Chem* 2017;292:19782–91.
- Cao G, Kuhn A, Dalbey RE. The translocation of negatively charged residues across the membrane is driven by the electrochemical potential: evidence for an electrophoresis-like membrane transfer mechanism. *EMBO J* 1995;14:866–75.
- Cescau S, Debarbieux L, Wandersman C. Probing the in vivo dynamics of type I protein secretion complex association through sensitivity to detergents. *J Bacteriol* 2007;189:1496–504.
- Chenal A, Gujjarro JI, Raynal B et al. RTX calcium binding motifs are intrinsically disordered in the absence of calcium. *J Biol Chem* 2009;284:1781–9.
- Chervaux C, Sauvonnnet N, Le Clainche A et al. Secretion of active beta-lactamase to the medium mediated by the *Escherichia coli* haemolysin transport pathway. *Mol Gen Genet* 1995;249:237–45.
- Choudhury HG, Tong Z, Mathavan I et al. Structure of an antibacterial peptide ATP-binding cassette transporter in a novel outward occluded state. *P Natl Acad Sci USA* 2014;111:9145–50.
- Costa TR, Felisberto-Rodrigues C, Meir A et al. Secretion systems in Gram-negative bacteria: structural and mechanistic insights. *Nat Rev Microbiol* 2015;13:343–59.
- Davidson AL, Dassa E, Orelle C et al. Structure, function, and evolution of bacterial ATP-binding cassette systems. *Microbiol Mol Biol R* 2008;72:317–64, table of contents.
- Dawson RJ, Locher KP. Structure of a bacterial multidrug ABC transporter. *Nature* 2006;443:180–5.
- Debarbieux L, Wandersman C. Folded HasA inhibits its own secretion through its ABC exporter. *EMBO J* 2001;20:4657–63.
- Delepelaire P. Type I secretion in gram-negative bacteria. *BBA-Mol Cell Res* 2004;1694:149–61.
- Du D, Wang Z, James NR et al. Structure of the AcrAB-TolC multidrug efflux pump. *Nature* 2014;509:512–5.
- Economou A, Dalbey RE. Preface to special issue on protein trafficking and secretion in bacteria. *Biochim Biophys Acta* 2014;1843:1427.
- Evdokimov AG, Pokross ME, Egorov NS et al. Structural basis for the fast maturation of Arthropoda green fluorescent protein. *EMBO Rep* 2006;7:1006–12.

- Felmlee T, Pellett S, Welch RA. Nucleotide sequence of an *Escherichia coli* chromosomal hemolysin. *J Bacteriol* 1985;163:94–105.
- Felmlee T, Welch RA. Alterations of amino acid repeats in the *Escherichia coli* hemolysin affect cytolytic activity and secretion. *P Natl Acad Sci USA* 1988;85:5269–73.
- Fitzpatrick AWP, Llabres S, Neuberger A et al. Structure of the MacAB-TolC ABC-type tripartite multidrug efflux pump. *Nat Microbiol* 2017;2:17070.
- Gentschev I, Hess J, Goebel W. Change in the cellular localization of alkaline phosphatase by alteration of its carboxy-terminal sequence. *Mol Gen Genet* 1990;222:211–6.
- Gray L, Baker K, Kenny B et al. A novel C-terminal signal sequence targets *Escherichia coli* haemolysin directly to the medium. *J Cell Sci* 1989;11:45–57.
- Gray L, Mackman N, Nicaud JM et al. The carboxy-terminal region of haemolysin 2001 is required for secretion of the toxin from *Escherichia coli*. *Mol Gen Genet* 1986;205:127–33.
- Greene NP, Crow A, Hughes C et al. Structure of a bacterial toxin-activating acyltransferase. *P Natl Acad Sci USA* 2015;112:E3058–66.
- Griessl MH, Schmid B, Kassler K et al. Structural insight into the giant Ca^{2+} -binding adhesin SiiE: implications for the adhesion of salmonella enterica to polarized epithelial cells. *Structure* 2013;21:741–52.
- Hanekop N, Zaitseva J, Jenewein S et al. Molecular insights into the mechanism of ATP-hydrolysis by the NBD of the ABC-transporter HlyB. *FEBS Lett* 2006;580:1036–41.
- Havarstein LS, Diep DB, Nes IF. A family of bacteriocin ABC transporters carry out proteolytic processing of their substrates concomitant with export. *Mol Microbiol* 1995;16:229–40.
- Hinsa SM, Espinosa-Urgel M, Ramos JL et al. Transition from reversible to irreversible attachment during biofilm formation by *Pseudomonas fluorescens* WCS365 requires an ABC transporter and a large secreted protein. *Mol Microbiol* 2003;49:905–18.
- Holland IB, Peherstorfer S, Kanonenberg K et al. Type I protein secretion-deceptively simple yet with a wide range of mechanistic variability across the family. *EcoSal Plus* 2016;7:1–46.
- Hwang J, Zhong X, Tai PC. Interactions of dedicated export membrane proteins of the colicin V secretion system: CvaA, a member of the membrane fusion protein family, interacts with CvaB and TolC. *J Bacteriol* 1997;179:6264–70.
- Ishii S, Yano T, Ebihara A et al. Crystal structure of the peptidase domain of *Streptococcus* ComA, a Bifunctional ATP-binding cassette transporter involved in the quorum-sensing pathway. *J Biol Chem* 2010;285:10777–85.
- Issartel JP, Koronakis V, Hughes C. Activation of *Escherichia coli* prohaemolysin to the mature toxin by acyl carrier protein-dependent fatty acylation. *Nature* 1991;351:759–61.
- Izadi-Pruneyre N, Wolff N, Redeker V et al. NMR studies of the C-Terminal secretion signal of the haem-binding protein, HasA. *Eur J Biochem* 1999;261:562–8.
- Jardetzky O. Simple allosteric model for membrane pumps. *Nature* 1966;211:969–70.
- Jones HE, Holland IB, Baker HL et al. Slow changes in cytosolic free Ca^{2+} in *Escherichia coli* highlight two putative influx mechanisms in response to changes in extracellular calcium. *Cell Calcium* 1999;25:265–74.
- Kanonenberg K, Schwarz CK, Schmitt L. Type I secretion systems - a story of appendices. *Res Microbiol* 2013;164:596–604.
- Kenny B, Haigh R, Holland IB. Analysis of the haemolysin transport process through the secretion from *Escherichia coli* of PCM, CAT or beta-galactosidase fused to the Hly C-terminal signal domain. *Mol Microbiol* 1991;5:2557–68.
- Khosa S, Scholz R, Schwarz C et al. An A/U-Rich enhancer region is required for high-level protein secretion through the HlyA Type I secretion system. *Appl Environ Microb* 2018;84:e01163–17.
- Kim HM, Xu Y, Lee M et al. Functional relationships between the AcrA hairpin tip region and the TolC aperture tip region for the formation of the bacterial tripartite efflux pump AcrAB-TolC. *J Bacteriol* 2010;192:4498–503.
- Kim JS, Song S, Lee M et al. Crystal structure of a soluble fragment of the membrane fusion protein HlyD in a Type I secretion system of gram-negative bacteria. *Structure* 2016;24:477–85.
- Koronakis V, Eswaran J, Hughes C. Structure and function of TolC: the bacterial exit duct for proteins and drugs. *Annu Rev Biochem* 2004;73:467–89.
- Koronakis V, Hughes C, Koronakis E. Energetically distinct early and late stages of HlyB/HlyD-dependent secretion across both *Escherichia coli* membranes. *EMBO J* 1991;10:3263–72.
- Koronakis V, Koronakis E, Hughes C. Isolation and analysis of the C-terminal signal directing export of *Escherichia coli* hemolysin protein across both bacterial membranes. *EMBO J* 1989;8:595–605.
- Koronakis V, Li J, Koronakis E et al. Structure of TolC, the outer membrane component of the bacterial type I efflux system, derived from two-dimensional crystals. *Mol Microbiol* 1997;23:617–26.
- Koronakis V, Sharff A, Koronakis E et al. Crystal structure of the bacterial membrane protein TolC central to multidrug efflux and protein export. *Nature* 2000;405:914–9.
- Kuhnert P, Heyberger-Meyer B, Nicolet J et al. Characterization of PaxA and its operon: a cohemolytic RTX toxin determinant from pathogenic *Pasteurella aerogenes*. *Infect Immun* 2000;68:6–12.
- Lecher J, Schwarz CK, Stoldt M et al. An RTX transporter tethers its unfolded substrate during secretion via a unique N-terminal domain. *Structure* 2012;20:1778–87.
- Lenders MH, Beer T, Smits SH et al. In vivo quantification of the secretion rates of the hemolysin A Type I secretion system. *Sci Rep* 2016;6:33275.
- Lenders MH, Weidtkamp-Peters S, Kleinschrodt D et al. Directionality of substrate translocation of the hemolysin A Type I secretion system. *Sci Rep* 2015;5:12470.
- Letoffe S, Delepelaire P, Wandersman C. Protease secretion by *Erwinia chrysanthemi*: the specific secretion functions are analogous to those of *Escherichia coli* alpha-haemolysin. *EMBO J* 1990;9:1375–82.
- Letoffe S, Ghigo JM, Wandersman C. Secretion of the *Serratia marcescens* HasA protein by an ABC transporter. *J Bacteriol* 1994;176:5372–7.
- Linhartova I, Bumba L, Masin J et al. RTX proteins: a highly diverse family secreted by a common mechanism. *FEMS Microbiol Rev* 2010;34:1076–112.
- Locher KP. Structure and mechanism of ABC transporters. *Curr Opin Struct Biol* 2004;14:426–31.
- Locher KP. Mechanistic diversity in ATP-binding cassette (ABC) transporters. *Nat Struct Mol Biol* 2016;23:487–93.
- Mackman N, Baker K, Gray L et al. Release of a chimeric protein into the medium from *Escherichia coli* using the C-terminal secretion signal of haemolysin. *EMBO J* 1987;6:2835–41.
- Mackman N, Holland IB. Functional characterization of a cloned haemolysin determinant from *E. coli* of human origin, encoding information for the secretion of a 107K polypeptide. *Mol Gen Genet* 1984;196:129–34.

- Mackman N, Nicaud JM, Gray L et al. Genetical and functional organisation of the *Escherichia coli* haemolysin determinant 2001. *Mol Gen Genet* 1985a;201:282–8.
- Mackman N, Nicaud JM, Gray L et al. Identification of polypeptides required for the export of haemolysin 2001 from *E. coli*. *Mol Gen Genet* 1985b;201:529–36.
- Masure HR, Au DC, Gross MK et al. Secretion of the *Bordetella pertussis* adenylate cyclase from *Escherichia coli* containing the hemolysin operon. *Biochemistry* 1990;29:140–5.
- Meier R, Drepper T, Svensson V et al. A Calcium-gated lid and a large beta-Roll sandwich are revealed by the crystal structure of extracellular lipase from *Serratia marcescens*. *J Biol Chem* 2007;282:31477–83.
- Morgan JL, Acheson JF, Zimmer J. Structure of a Type-1 secretion system ABC transporter. *Structure* 2017;25:522–9.
- Murata D, Okano H, Angkawidjaja C et al. Structural basis for the *Serratia marcescens* lipase secretion system: Crystal structures of the membrane fusion protein and Nucleotide-Binding domain. *Biochemistry* 2017;56:6281–91.
- Nicaud JM, Mackman N, Gray L et al. Regulation of haemolysin synthesis in *E. coli* determined by HLY genes of human origin. *Mol Gen Genet* 1985;199:111–6.
- Nicaud JM, Mackman N, Gray L et al. The C-terminal, 23 kDa peptide of *E. coli* haemolysin 2001 contains all the information necessary for its secretion by the haemolysin (Hly) export machinery. *FEBS Lett* 1986;204:331–5.
- Noegel A, Rdest U, Springer W et al. Plasmid cistrons controlling synthesis and excretion of the exotoxin alpha-haemolysin of *Escherichia coli*. *Mol Gen Genet* 1979;175:343–50.
- Oldham ML, Grigorieff N, Chen J. Structure of the transporter associated with antigen processing trapped by herpes simplex virus. *Elife* 2016;5:e21289.
- Ostolaza H, Soloaga A, Goni FM. The binding of divalent cations to *Escherichia coli* alpha-haemolysin. *Eur J Biochem* 1995;228:39–44.
- Oswald C, Holland IB, Schmitt L. The motor domains of ABC-transporters. *N-S Arch Pharmacol* 2006;372:385–99.
- Park Y, Moon Y, Ryoo J et al. Identification of the minimal region in lipase ABC transporter recognition domain of *Pseudomonas fluorescens* for secretion and fluorescence of green fluorescent protein. *Microb Cell Fact* 2012;11:60.
- Pei XY, Hinchliffe P, Symmons MF et al. Structures of sequential open states in a symmetrical opening transition of the TolC exit duct. *P Natl Acad Sci USA* 2011;108:2112–7.
- Pimenta AL, Young J, Holland IB et al. Antibody analysis of the localisation, expression and stability of HlyD, the MFP component of the *E. coli* haemolysin translocator. *Mol Gen Genet* 1999;261:122–32.
- Reimann S, Poschmann G, Kanonenberg K et al. Interdomain regulation of the ATPase activity of the ABC transporter haemolysin B from *Escherichia coli*. *Biochem J* 2016;473:2471–83.
- Ryu J, Lee U, Park J et al. A vector system for ABC transporter-mediated secretion and purification of recombinant proteins in pseudomonas species. *Appl Environ Microb* 2015;81:1744–53.
- Sanchez-Magraner L, Viguera AR, Garcia-Pacios M et al. The Calcium-binding C-terminal domain of *Escherichia coli* alpha-hemolysin is a major determinant in the surface-active properties of the protein. *J Biol Chem* 2007;282:11827–35.
- Sapriel G, Wandersman C, Delepelaire P. The N terminus of the HasA protein and the SecB chaperone cooperate in the efficient targeting and secretion of HasA via the ATP-binding cassette transporter. *J Biol Chem* 2002;277:6726–32.
- Schiebel E, Driessen AJ, Hartl FU et al. Delta mu H+ and ATP function at different steps of the catalytic cycle of preprotein translocase. *Cell* 1991;64:927–39.
- Schmitt L, Benabdelhak H, Blight MA et al. Crystal structure of the nucleotide-binding domain of the ABC-transporter haemolysin B: identification of a variable region within ABC helical domains. *J Mol Biol* 2003;330:333–42.
- Sebo P, Ladant D. Repeat sequences in the *Bordetella pertussis* adenylate cyclase toxin can be recognized as alternative carboxy-proximal secretion signals by the *Escherichia coli* alpha-haemolysin translocator. *Mol Microbiol* 1993;9:999–1009.
- Sebo P, Moukrim Z, Kalhous M et al. In vivo induction of CTL responses by recombinant adenylate cyclase of *Bordetella Pertussis* carrying multiple copies of a viral CD8(+) T-cell epitope. *FEMS Immunol Med Mic* 1999;26:167–73.
- Sotomayor Perez AC, Karst JC, Davi M et al. Characterization of the regions involved in the calcium-induced folding of the intrinsically disordered RTX motifs from the *Bordetella pertussis* adenylate cyclase toxin. *J Mol Biol* 2015;397:534–49.
- Spreng S, Dietrich G, Goebel W et al. The *Escherichia coli* haemolysin secretion apparatus: a potential universal antigen delivery system in gram-negative bacterial vaccine carriers. *Mol Microbiol* 1999;31:1596–8.
- Stanley P, Hyland C, Koronakis V et al. An ordered reaction mechanism for bacterial toxin acylation by the specialized acyl-transferase HlyC: formation of a ternary complex with acyl-LACP and protoxin substrates. *Mol Microbiol* 1999;34:887–901.
- Stanley P, Koronakis V, Hughes C. Mutational analysis supports a role for multiple structural features in the C-terminal secretion signal of *Escherichia coli* haemolysin. *Mol Microbiol* 1991;5:2391–403.
- Stanley P, Packman LC, Koronakis V et al. Fatty acylation of two internal lysine residues required for the toxic activity of *Escherichia coli* hemolysin. *Science* 1994;266:1992–6.
- Symmons MF, Marshall RL, Bavro VN. Architecture and roles of periplasmic adaptor proteins in tripartite efflux assemblies. *Front Microbiol* 2015;6:513.
- Thanabalu T, Koronakis E, Hughes C et al. Substrate-induced assembly of a contiguous channel for protein export from *E. coli*: reversible bridging of an inner-membrane translocase to an outer membrane exit pore. *EMBO J* 1998;17:6487–96.
- Thomas S, Bakkes PJ, Smits SH et al. Equilibrium folding of pro-HlyA from *Escherichia coli* reveals a stable calcium ion dependent folding intermediate. *BBA-Proteins Proteom* 2014;1844:1500–10.
- Thomas S, Holland IB, Schmitt L. The Type 1 secretion pathway - The hemolysin system and beyond. *Biochim Biophys Acta* 2014;1843:1621–41.
- Thomas S, Smits SH, Schmitt L. A simple in vitro acylation assay based on optimized HlyA and HlyC purification. *Anal Biochem* 2014;464:17–23.
- Thompson SA, Sparling PF. The RTX cytotoxin-related FrpA protein of *Neisseria meningitidis* is secreted extracellularly by meningococci and by HlyBD+ *Escherichia coli*. *Infect Immun* 1993;61:2906–11.
- Uchida K, Mori H, Mizushima S. Stepwise movement of preproteins in the process of translocation across the cytoplasmic membrane of *Escherichia coli*. *J Biol Chem* 1995;270:30862–8.
- Wandersman C, Delepelaire P. TolC, an *Escherichia coli* outer membrane protein required for hemolysin secretion. *P Natl Acad Sci USA* 1990;87:4776–80.
- Wang RC, Seror SJ, Blight M et al. Analysis of the membrane organization of an *Escherichia coli* protein translocator, HlyB, a

- member of a large family of prokaryote and eukaryote surface transport proteins. *J Mol Biol* 1991;**217**:441–54.
- Welch RA. Pore-forming cytolysins of gram-negative bacteria. *Mol Microbiol* 1991;**5**:521–8.
- Wu KH, Tai PC. Cys 32 and His 105 are the critical residues for the calcium-dependent cysteine proteolytic activity of CvaB, an ATP-binding cassette transporter. *J Biol Chem* 2004;**279**:901–9.
- Young R, Bremer H. Polypeptide-chain-elongation rate in *Escherichia coli* B/r as a function of growth rate. *Biochem J* 1976;**160**:185–94.
- Yum S, Xu Y, Piao S *et al*. Crystal structure of the periplasmic component of a tripartite macrolide-specific efflux pump. *J Mol Biol* 2009;**387**:1286–97.
- Zaitseva J, Jenewein S, Jumpertz T *et al*. H662 is the linchpin of ATP hydrolysis in the nucleotide-binding domain of the ABC transporter HlyB. *EMBO J* 2005a;**24**:1901–10.
- Zaitseva J, Jenewein S, Oswald C *et al*. A molecular understanding of the catalytic cycle of the nucleotide-binding domain of the ABC transporter HlyB. *Biochem Soc Trans* 2005b:990–5.
- Zaitseva J, Jenewein S, Wiedenmann A *et al*. Functional characterization and ATP-induced dimerization of the isolated ABC-domain of the haemolysin B transporter. *Biochemistry* 2005c;**44**:9680–90.
- Zaitseva J, Oswald C, Jumpertz T *et al*. A structural analysis of asymmetry required for catalytic activity of an ABC-ATPase domain dimer. *EMBO J* 2006;**25**:3432–43.

3.2 Chapter 2

Title: Type I Secretion Systems — One Mechanism for All?

Authors: Olivia Spitz, Isabelle N. Erenburg, Tobias Beer, Kerstin Kanonenberg,
I. Barry Holland, Lutz Schmitt

Published in: *Microbiology Spectrum* (2019)
Impact Factor 3.88

Own proportion of this work:
20%
Writing of the manuscript

Type I Secretion Systems— One Mechanism for All?

OLIVIA SPITZ,¹ ISABELLE N. ERENBURG,¹ TOBIAS BEER,¹
KERSTIN KANONENBERG,¹ I. BARRY HOLLAND,² and LUTZ SCHMITT¹

¹Institute of Biochemistry, Heinrich Heine University Düsseldorf, Düsseldorf, Germany; ²Institute of Genetics and Microbiology, University of Paris-Sud, Orsay, France

ABSTRACT Type I secretion systems (T1SS) are widespread in Gram-negative bacteria, especially in pathogenic bacteria, and they secrete adhesins, iron-scavenger proteins, lipases, proteases, or pore-forming toxins in the unfolded state in one step across two membranes without any periplasmic intermediate into the extracellular space. The substrates of T1SS are in general characterized by a C-terminal secretion sequence and nonapeptide repeats, so-called GG repeats, located N terminal to the secretion sequence. These GG repeats bind Ca^{2+} ions in the extracellular space, which triggers folding of the entire protein. Here we summarize our current knowledge of how Gram-negative bacteria secrete these substrates, which can possess a molecular mass of up to 1,500 kDa. We also describe recent findings that demonstrate that the absence of periplasmic intermediates, the “classic” mode of action, does not hold true for all T1SS and that we are beginning to realize modifications of a common theme.

INTRODUCTION

Gram-negative bacteria are equipped with at least seven dedicated secretion systems that mediate the export of proteins beyond the outer membrane (1, 2). These are called type 1 to 6 and type 9 secretion systems (T1SS to T6SS and T9SS). Among those, T3SS, T4SS, and T6SS are even capable of delivering their cargo directly into the cytosol of the host cell. In this minireview, we place the major emphasis on the hemolysin A (HlyA) secretion system in *Escherichia coli*. This is by far the most studied and illustrates very well the largely conserved, essential features of T1SS. Interestingly, however, an important mechanistic variation in the translocation of some of the unusually extended giant RTX proteins—adhesins—was discovered recently (3) and is also discussed.

T1SS substrates are usually defined by the presence of several blocks of nonapeptide-binding sequences with the consensus GGxGGDxUx (4, 5), where x can be any amino acid and U is a large hydrophobic amino acid. The exceptions are the SiiE-like adhesins (Fig. 1) (6). These nonapeptides gave rise to the abbreviation RTX (repeats in toxins), the name for the family. These motifs, also called GG repeats, specifically bind Ca^{2+} (see below) and are implicated in posttranslocation folding. The RTX domain (Fig. 1) is located N terminal to the secretion signal at the extreme C terminus.

Like T1SS substrates, the very large and widespread group of peptide bacteriocins in Gram-negative bacteria (7–9) also require an ABC transporter, a membrane fusion protein (MFP), and an outer membrane (OM) protein for secretion. However, these antimicrobials lack RTX repeats, have a cleavable N-terminal secretion sequence instead of the “classical” C-terminal signal, and

Received: 20 August 2018, **Accepted:** 15 January 2019,
Published: 8 March 2019

Editors: Maria Sandkvist, Department of Microbiology and Immunology, University of Michigan, Ann Arbor, Michigan; Eric Cascales, CNRS Aix-Marseille Université, Mediterranean Institute of Microbiology, Marseille, France; Peter J. Christie, Department of Microbiology and Molecular Genetics, McGovern Medical School, Houston, Texas

Citation: Spitz O, Erenburg IN, Beer T, Kanonenberg K, Holland IB, Schmitt L. 2019. Type I secretion systems—one mechanism for all? *Microbiol Spectrum* 7(2):PSIB-0003-2018. doi:10.1128/microbiolspec.PSIB-0003-2018.

Correspondence: Lutz Schmitt, lutz.schmitt@hhu.de

© 2019 American Society for Microbiology. All rights reserved.

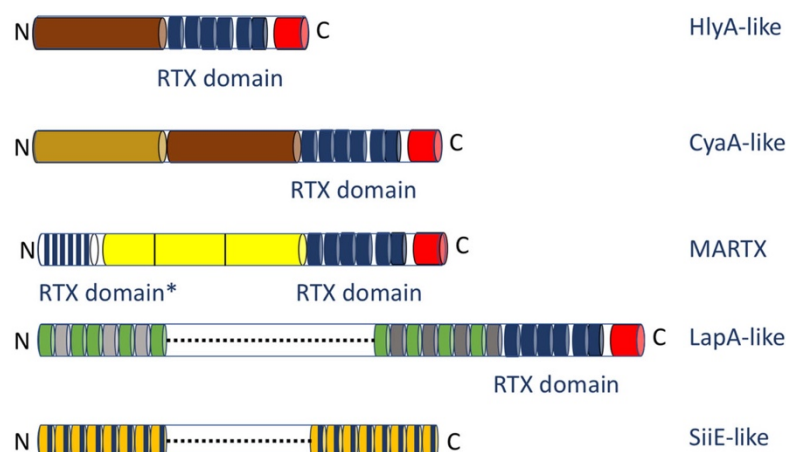


FIGURE 1 Architecture of substrates of T1SS. The primary structure of a canonical substrate of a T1SS is shown as white cylinder with the N and C termini labeled by "N" and "C," respectively. The secretion sequence (approximately 50 to 100 amino acids depending on the substrate) at the C terminus is in red, the GG repeats forming the classic RTX domain are in blue (six GG repeats as in the case of HlyA have been chosen as an example), and the functional, N-terminal domain is in brown. However, the number and types of architectures of this functional domain have increased in recent years. HlyA-like proteins contain only one domain with dedicated activity (pore-forming activity in the case of HlyA), while, for example, CyaA-like proteins contain two domains, which possess an adenylate cyclase (light brown) and a pore-forming (brown) activity in the case of CyaA. A third class are MARTX proteins (exemplified here by a MARTX protein from *V. cholerae*). The effector domains (yellow and separated by black vertical lines) that are autocatalytically excised after secretion are flanked by an N-terminal RTX-like domain (marked as RTX domain*) and a C-terminal RTX domain. The C-terminal domain corresponds to the canonical sequence, while the conserved aspartate is missing in the N-terminal one. Another architecture is present in LapA-like adhesins (or bacterial transglutaminase-like cysteine proteinases) that contain multiple, different domains. In the case of LapA, two different colors indicate two different domains. However, the number of different domains is not restricted to two. Additionally, the double-alanine motif in the N termini of LapA-like RTX adhesins is not shown. Finally, SiiE-like adhesins contain multiple identical domains, such as the 53 copies of the Blg domain in the case of SiiE (6, 71). The vertical blue line indicates that the GG repeats are integrated within the Ig-like domains and do not form a separate RTX domain. Please note that the drawing of the functional domains is not to scale.

have a quite distinctive translocation mechanism (10, 11): alternating access rather than extrusion through an OM "tunnel." In view of these properties, we decided not to include them in this minireview. The interested reader is directed to references 7 to 11.

The first molecular identification of a T1SS, the secretion machinery of the pore-forming toxin HlyA from *E. coli* (12), was made in the 1980s and 1990s (13–15) with the demonstration that two inner membrane proteins, an ABC transporter and an MFP, encoded together with the toxin in the same operon were required for secretion. A fourth gene in the *hly* operon encoded an acyltransferase, HlyC (16), catalyzing the posttranslational modification of two internal lysine residues (17–19). This

modification, with fatty acids ranging from C₁₄ to C₁₇ in length, requires acyl carrier protein (20) and is essential for HlyA to form a pore in the host membrane. Thus, only the acylated, toxic form of hemolysin should be called HlyA, while the nonacylated form should correctly be called pro-HlyA. Such acylation conferring toxicity is observed not only in HlyA but also in other hemolysins, leukotoxins, and cytotoxins that are members of the RTX family (4). The recently published crystal structure of a homologue of the *E. coli* HlyC (21) allows a more detailed understanding of how acylation is installed. Notably, however, acylation is not required for secretion into the extracellular space. On the other hand, the proteins encoded in the *hly* operon are not sufficient for

secretion of (pro-)HlyA. The OM component of the translocon is TolC. The TolC protein is encoded elsewhere in the chromosome and was first described for a related T1SS by Wandersman and Delepelaire (22).

Equally important, the work by the laboratories of Koronakis, Holland, and Goebel demonstrated that substrate secretion by the T1SS is a one-step process, i.e., directly from the cytosol into the extracellular space without any periplasmic intermediate. Furthermore, these data established that the entire process was Sec independent, relying on a novel C-terminal secretion signal (5, 23–31).

However, the view that T1SS is mediated by the one-step translocation of proteins has been challenged. Recently, so-called periplasmic intermediates for a proposed two-step secretion process were described for the adhesins LapA and IBA (3). The exciting results identified a “retention module” (RM) at the N terminus that anchors the adhesion to the cell surface by stalling further translocation. This leaves a stalled short stub in the periplasm, apparently stuck in TolC, and a fully translocated, functional adhesin in the extracellular space. When conditions change, for example, in the case of LapA, to conditions unfavorable for biofilm formation, proteolysis removes the RM and releases the adhesin. Therefore, the secretion of the adhesin, as the authors described it, occurs in two steps. Our interpretation is that this is an exciting and important variation of the T1SS but that translocation is still effectively one step, and therefore, we prefer to call the adhesin-TolC-RM complex a pseudoperiplasmic intermediate.

Here we summarize our current knowledge of the molecular processes that underlie the T1SS and focus on the molecular events that result in secretion of substrates that harbor a C-terminal secretion sequence.

THE SUBSTRATES OF THE T1SS

The N-terminal domain of an RTX protein like HlyA contains one functional domain, the HlyA pore-forming toxin. CyaA from *Bordetella pertussis* (32) harbors an HlyA-like toxin but also an adenylate cyclase that, following translocation into the cytosol of a host cell, manipulates cAMP levels. More complex architectures are present in MARTX (multifunctional autoprocessing repeats in toxins), LapA, and SiiE-like proteins. MARTX proteins are of enormous size (approximately 500 to 900 kDa). This protein family is encoded in a chromosomal island in human pathogens such as *Vibrio cholerae* (33, 34). The extreme N-terminal part of these proteins is composed of an RTX-like domain that, however, lacks

the conserved aspartate residue that normally coordinates the Ca^{2+} ion. Spaced between this domain and the RTX domain near the C terminus are effector proteins that are autoprocessed, posttranslocationally, to release a cocktail of different effectors into a host cell (35). However, little is still known about the mechanism of secretion of MARTX proteins. The RTX adhesins, LapA from *Pseudomonas fluorescens*, and SiiE, the RTX-like protein from *Salmonella*, are even larger, reaching up to 1.5 MDa (3, 36, 37). In LapA (3, 38), the functional domain contains a varying number of domains that mediate adhesion functions. Strikingly, the SiiE-like adhesins deviate from the canonical architecture of RTX proteins, particularly with respect to calcium binding (39). Ca^{2+} binding sites are distributed virtually throughout the entire molecule, which is composed of 53 bacterial immunoglobulin-like (Blg) domains constituting the functional domain—the adhesin (Fig. 1). Ca^{2+} type I sites (three aspartate residues) fulfill the role of RTX repeats in secretion and are positioned at all the interfaces between two Blg domains (6). On the other hand, the translocon is composed of the familiar tripartite complex; translocation depends on a C-terminal secretion sequence (40) inferred to be extruded first (39).

A C-terminal secretion signal remains as a signature characteristic of RTX substrates. Signals appear to be conserved only within groups of related proteins, with no evidence of widespread conservation as far as we are aware. For the hemolysin group, competitive hypotheses have postulated a specific linear code, a structural code, or a combination of the two, but the question remains unresolved (see the extensive discussion in reference 41).

RTX Motifs and Ca^{2+} Promote Extracellular Folding of Substrates

A bioinformational approach based on the presence of the GG repeats revealed more than 1,000 putative RTX proteins in approximately 250 bacterial species (4). Since that study was published in 2010, the number of putative RTX proteins is necessarily much larger today, given the enormous number of genomes now sequenced. However, only the compilation of Linhartová et al. (4) is currently available. The number of identified RTX repeats ranged from below 10 to more than 40, with a slight tendency of the number of repeats to correlate with molecular weight. Additionally, more than 90% of the putative RTX proteins displayed an isoelectric point below 5.0, suggesting that electrophoretic mobility (42) might be important for the secretion process.

Structural studies of the alkaline protease from *Pseudomonas aeruginosa* (43) and other substrates of the

T1SS (6, 44, 45) confirmed that the nonapeptide repeats bind Ca^{2+} ions. Two GG repeats coordinate one Ca^{2+} ion by interaction of the side chain of the aspartate residue and the carbonyl oxygens of the amino acids forming the repeat. This architecture creates a right-handed, so-called β -roll motif (Fig. 2). Functional *in vitro* studies demonstrated that Ca^{2+} ions are a strict requirement for folding. In other words, in the absence of Ca^{2+} ions, substrates, such as HlyA from *E. coli* (46–49) or CyaA from *Bordetella pertussis* (50–52), remain unfolded or in a molten globular state (53). Subsequent studies revealed that the dissociation constant of Ca^{2+} ions from the RTX domain is in the high micromolar range. The concentration of free Ca^{2+} ions in the bacterial cytosol is strictly regulated and remains in the high nanomolar range (100 to 300 nM in *E. coli*) (54). Secretion of RTX proteins therefore presumably occurs in the unfolded state. This hypothesis was indeed experimentally verified by the fusion of maltose binding protein to a C-terminal fragment of HlyA that only harbored the secretion signal and three of the six GG repeats (55). Given that the extracellular con-

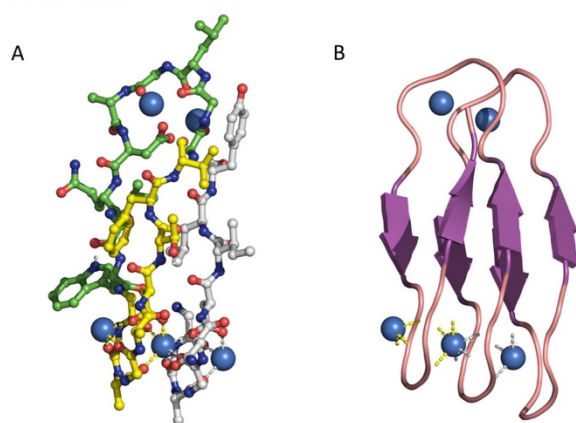
centration of Ca^{2+} ions is normally in the millimolar range (54), this suggests that RTX repeats immediately bind Ca^{2+} upon exit from the bacterium. Elegant *in vitro* studies with CyaA have also demonstrated that binding of Ca^{2+} ions to the RTX domain induces immediate folding of the entire protein (46–48), suggesting that Ca^{2+} ions act as a chemical foldase.

CURRENT WORKING MODEL FOR CLASSIC T1SS

The process of secreting a substrate by a T1SS starts at the ribosome. However, only after the extreme C terminus of the substrate containing the secretion signal (Fig. 1), around 50 to 100 amino acids, has been synthesized will secretion be initiated, since all information necessary and sufficient for secretion is encoded in the secretion signal. Bearing in mind that the sizes of T1SS proteins range from 20 kDa up to 1,500 kDa, two obvious questions arise: why do substrates of T1SS not aggregate and precipitate prior to secretion, and why are these proteins not immediately degraded by cytosolic proteases? Unfortunately, we do not yet have answers to these important questions.

In the second step, the unfolded substrate interacts with both of the two membrane proteins of the inner membrane, the ABC transporter and the MFP (56, 57). Based on cross-linking studies with the HlyA system, these two proteins were shown to form a stable complex in the inner membrane, a dimer of the ABC transporter and a trimer of the MFP (57). However, the remarkable similarity of the T1SS translocon to tripartite drug efflux pumps, such as the AcrB-AcrA-TolC system from *E. coli*, in which there is a 2:6 stoichiometry (ABC:MFP) (58), makes it most likely that the T1SS MFP is also a hexamer. Nevertheless, further research should be undertaken to resolve this obvious discrepancy. Deletion studies by the Koronakis laboratory showed that the cytoplasmic domain of the MFP is required to recruit the OM component, TolC in the case of the HlyA machinery (56). However, the engagement occurred only in the presence of the substrate, indicating that docking of HlyA with the inner membrane complex transmits a signal to the periplasmic domain of HlyD that results in the formation of a transient HlyB-HlyD-TolC complex, a so-called “channel-tunnel” bridging the entire distance from the cytosol to the extracellular space across the periplasm and two membranes. The timing of these events also explains why deletion or inactivation of one of the three translocon components completely abolishes secretion without the appearance of a periplasmic intermediate.

FIGURE 2 Structure of GG repeats of alkaline protease (PDB entry 1KAP) from *P. aeruginosa* in its Ca^{2+} -bound state, resulting in the classic β -roll motif. **(A)** The five Ca^{2+} ions are shown as blue spheres. For simplicity, only the first three GG repeats are shown in ball-and-stick representation. The carbon atoms of GG repeat one are in gray, the carbon atoms of the second GG repeat in green, and the ones of the third repeat in yellow. The interactions of repeat one with the bound Ca^{2+} ion are indicated by gray dashed lines, and the interaction of the third repeat with the bound Ca^{2+} ions is in yellow. As it is evident, one Ca^{2+} ion is coordinated by repeat n and repeat $n + 2$. **(B)** RTX domain of alkaline protease from *P. aeruginosa* in cartoon representation. The orientation is identical to that in panel A, and the gray and yellow dashed lines indicate the interactions.



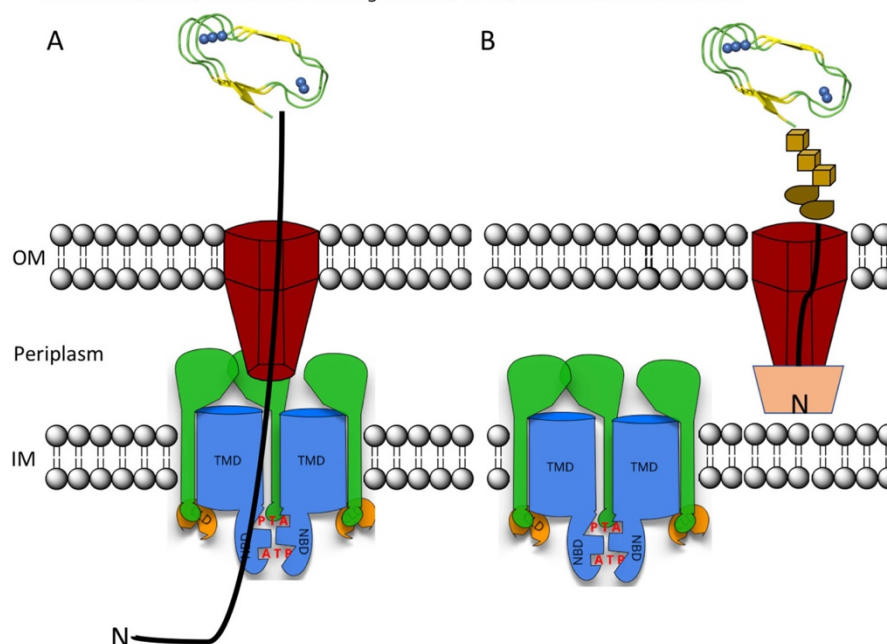
T1SS—One Mechanism for All?

Finally, biophysical studies with the isolated nucleotide binding domain of HlyB, the ABC transporter of the HlyA secretion machinery, demonstrated an interaction with the substrate in the low micromolar range that required the secretion signal (59).

As soon as the outer membrane protein is engaged and a continuous channel tunnel has formed, the substrate enters the translocation pathway (Fig. 3A). For HlyA, it was experimentally demonstrated that secretion is directional, with the C terminus extended first onto the cell surface (60). Furthermore, the entire process proceeds with a secretion rate of 16 amino acids per transporter per second (61). At this stage, Ca^{2+} ions must bind to the

RTX motifs and induce folding as soon as the substrate appears at the cell surface (Fig. 3A). This should prevent backsliding of the entire protein. Interestingly, reducing the external Ca^{2+} concentration below the dissociation constant of the ion from the RTX motif did not reduce the secretion rate in the HlyA system (61). This clearly demonstrates that the secretion rate is independent of Ca^{2+} and that Ca^{2+} -induced folding does not represent a driving force for secretion. A seemingly different scenario was observed for the much larger adenylate cyclase toxin (CyaA) from *B. pertussis* (62). A Ca^{2+} concentration of 2 mM in the media accelerated the efficiency of secretion. However, even when the Ca^{2+} concentration was reduced

FIGURE 3 Schematic summary of the classic T1SS-mediated substrate secretion (A) and the recently discovered secretion mechanism for some RTX adhesins in which secretion stalls just before completion, creating a so-called two-step process with a pseudoperiplasmic intermediate (B). The ABC transporter and the MFP are shown in blue and green, respectively, and the OM protein is in maroon. (A) The unfolded substrate is secreted with its C terminus first. At the cell surface, Ca^{2+} ions (blue spheres) bind to the GG repeats and induce folding, which results in formation of the β -roll (indicated in cartoon representation). (B) In the case of adhesins such as IBA or LapA, the N-terminal domain starts folding prior to or during secretion, which plugs the translocon (indicated by the light brown polygon) and tethers the entire substrate at the cell surface within the OM component of the translocon of the T1SS. The brown cubes and distorted ellipse represent folded domains of the substrate. This scheme clearly demonstrates that the classic T1SS disassembles only after the entire substrate is translocated, while in two-step T1SS disassembly earlier, e.g., when the N-terminal plug domain has not passed the OM. For further details, see the text. IM, inner membrane; NBD, nucleotide binding domain; TMD, transmembrane domain.



to 0.1 mM (which does not allow folding of CyaA), 50% of produced CyaA still reached the cell surface. These differences might be due to the diverging sizes of the two RTX proteins or details of the architecture of the RTX domain. Thus, further experimental approaches and analysis of additional T1SS substrates are required to completely understand the molecular mechanisms of secretion, the influence of Ca^{2+} ion folding and secretion (if any), and the molecular signals that regulate substrate translocation across two membranes in one step for this group of classic T1SS substrates.

RTX ADHESINS—NEW KIDS ON THE BLOCK

RTX proteins include not only toxins but also lipases, S-layer proteins, MARTX, and adhesins, which are extremely large in size. Recently, the structure of an ice-binding adhesin (IBA) of the marine Gram-negative bacterium *Marinomonas primoryensis* (molecular mass, 1.5 MDa) was determined and the putative mechanism of translocation modeled (37). IBA contains the hallmarks of substrates of a T1SS, an RTX domain and a C-terminal secretion sequence. N terminal to the RTX domain, three additional domains are located, namely, peptide-, sugar-, and ice-binding domains. While interactions of the peptide- and sugar-binding domains with surface receptors of other microorganisms allow formation of mixed aggregates of microorganisms, the ice-binding domain anchors *M. primoryensis* to ice in seas, lakes, or rivers. Surprisingly, and in contrast to the classical RTX proteins described earlier that are directly secreted into the extracellular space, IBA is translocated but then retained on the cell surface (Fig. 3B). Guo et al. (37) identified a conserved region (homologous to RM in LapA described above) at the extreme N terminus of IBA that they proposed could plug the channel-tunnel of the T1SS. Based on their structural analysis, Guo et al. proposed that this N-terminal region forms two domains: a proximal sequence that folds and a distal region that is sufficiently unfolded to traverse the TolC homologue into the outer membrane. This prevents further translocation and retains the adhesin at the cell surface. In 2018, exciting new data concerning the LapA adhesin from *Pseudomonas fluorescens* (3; for a summary, see reference 38) provided direct experimental evidence for this model in a comprehensive multidisciplinary study. The 160-residue RM was shown to be essential to tether the adhesin to the translocator and thus to the cell surface (Fig. 3B). Moreover, the RM consists of two domains, folded and unfolded, with the former specifically cleaved by a dedicated protease, LapG, to release the

adhesin. In another exciting twist, LapG is normally inactivated by binding to its membrane receptor, LapD. Binding is controlled by c-di-GMP to favor binding under conditions suitable for biofilm formation (63). Finally, we note that both of these studies (for IBA and LapA) confirm the directionality of translocation, C terminal first, for T1SS secretion.

Finally, it must be stressed that while IBA and LapA are anchored to the surface by stalling translocation, other strategies are used to retain adhesins at the cell surface. SiiE from *Salmonella enterica* contains a putative coiled-coil motif that facilitates immobilization of the entire protein on the surface of the cell envelope, which is controlled by SiiA and SiiB (36). Thus, continued efforts are needed to see whether additional mechanisms and modifications of the classic T1SS exist that are used by Gram-negative bacteria to cope with the demands of their ecological niches.

SUMMARY AND OUTLOOK

An enormous amount of data on T1SS has been gathered since the discovery of the first system. The amount of available structural information on the components of the translocon machinery is increasing constantly. These components include the OM protein TolC (64), a closely related homologue of HlyC (21), isolated domains of the ABC transporter HlyB (65–67) and other ABC transporters (68), a soluble fragment of the MFP HlyD (69), and an entire structure of an ABC transporter (70) of a putative T1SS with unknown substrate from *Aquifex aeolicus*. This article is unable to cover all aspects of type I secretion; however, it provides a broad summary of the accumulating data on functional aspects of the secretion process. The review does not engage with the possibilities of the T1SS in biotechnological applications (for a recent summary, see reference 41) that go well beyond basic research and would allow large-scale protein production and isolation via protein secretion.

However, we are still some distance from a systematic understanding of the T1SS since the nature of molecular signals and intramolecular communication within this nanomachinery remains unclear. In summary, there are still many open questions that have to be addressed and many more fascinating variations and novel insights to be discovered for the T1SS in Gram-negative bacteria.

ACKNOWLEDGMENTS

We apologize to all our colleagues whose work is not cited due to space limitations. We thank all current and former members of the group for fruitful discussions.

Research on hemolysin A and the hemolysin A secretion machinery is funded by the MOI III graduate school under project name Molecules of Infection and the DFG through CRC 1208 under project name Identity and Dynamics of Membrane Systems—From Molecules to Cellular Functions (project A01 to L.S.).

REFERENCES

- Costa TR, Felisberto-Rodrigues C, Meir A, Prevost MS, Redzej A, Trokter M, Waksman G. 2015. Secretion systems in Gram-negative bacteria: structural and mechanistic insights. *Nat Rev Microbiol* 13:343–359. <http://dx.doi.org/10.1038/nrmicro3456>.
- Veith PD, Glew MD, Gorasia DG, Reynolds EC. 2017. Type IX secretion: the generation of bacterial cell surface coatings involved in virulence, gliding motility and the degradation of complex biopolymers. *Mol Microbiol* 106:35–53. <http://dx.doi.org/10.1111/mmi.13752>.
- Smith TJ, Font ME, Kelly CM, Sondermann H, O'Toole GA. 2018. An N-terminal retention module anchors the giant adhesin LapA of *Pseudomonas fluorescens* at the cell surface: a novel sub-family of type I secretion systems. *J Bacteriol* 200:e00734–17. <http://dx.doi.org/10.1128/JB.00734-17>.
- Linhartová I, Bumba L, Mašín J, Basler M, Ošička R, Kamanová J, Procházková K, Adkins I, Hejnová-Holubová J, Sadílková L, Morová J, Sebo P. 2010. RTX proteins: a highly diverse family secreted by a common mechanism. *FEMS Microbiol Rev* 34:1076–1112. <http://dx.doi.org/10.1111/j.1574-6976.2010.00231.x>.
- Felmlee T, Welch RA. 1988. Alterations of amino acid repeats in the *Escherichia coli* hemolysin affect cytolytic activity and secretion. *Proc Natl Acad Sci U S A* 85:5269–5273. <http://dx.doi.org/10.1073/pnas.85.14.5269>.
- Griessl MH, Schmid B, Kassler K, Braunsmann C, Ritter R, Barlag B, Stierhof YD, Sturm KU, Danzer C, Wagner C, Schäffer TE, Sticht H, Hensel M, Müller YA. 2013. Structural insight into the giant Ca^{2+} -binding adhesin SiiE: implications for the adhesion of *Salmonella enterica* to polarized epithelial cells. *Structure* 21:741–752. <http://dx.doi.org/10.1016/j.str.2013.02.020>.
- Hävarstein LS, Diep DB, Nes IF. 1995. A family of bacteriocin ABC transporters carry out proteolytic processing of their substrates concomitant with export. *Mol Microbiol* 16:229–240. <http://dx.doi.org/10.1111/j.1365-2958.1995.tb02295.x>.
- Hävarstein LS, Holo H, Nes IF. 1994. The leader peptide of colicin V shares consensus sequences with leader peptides that are common among peptide bacteriocins produced by gram-positive bacteria. *Microbiology* 140:2383–2389. <http://dx.doi.org/10.1099/13500872-140-9-2383>.
- Michiels J, Dirix G, Vanderleyden J, Xi C. 2001. Processing and export of peptide pheromones and bacteriocins in Gram-negative bacteria. *Trends Microbiol* 9:164–168. [http://dx.doi.org/10.1016/S0966-842X\(01\)01979-5](http://dx.doi.org/10.1016/S0966-842X(01)01979-5).
- Choudhury HG, Tong Z, Mathavan I, Li Y, Iwata S, Zirah S, Rebuffat S, van Veen HW, Beis K. 2014. Structure of an antibacterial peptide ATP-binding cassette transporter in a novel outward occluded state. *Proc Natl Acad Sci U S A* 111:9145–9150. <http://dx.doi.org/10.1073/pnas.1320506111>.
- Husada F, Bountra K, Tassis K, de Boer M, Romano M, Rebuffat S, Beis K, Cordes T. 2018. Conformational dynamics of the ABC transporter McjD seen by single-molecule FRET. *EMBO J* 37:e100056. <http://dx.doi.org/10.15252/embj.2018100056>.
- Felmlee T, Pellett S, Welch RA. 1985. Nucleotide sequence of an *Escherichia coli* chromosomal hemolysin. *J Bacteriol* 163:94–105.
- Härtlein M, Schiessl S, Wagner W, Rdest U, Kreft J, Goebel W. 1983. Transport of hemolysin by *Escherichia coli*. *J Cell Biochem* 22:87–97. <http://dx.doi.org/10.1002/jcb.240220203>.
- Noegel A, Rdest U, Springer W, Goebel W. 1979. Plasmid cistrons controlling synthesis and excretion of the exotoxin alpha-hemolysin of *Escherichia coli*. *Mol Gen Genet* 175:343–350. <http://dx.doi.org/10.1007/BF00397234>.
- Springer W, Goebel W. 1980. Synthesis and secretion of hemolysin by *Escherichia coli*. *J Bacteriol* 144:53–59.
- Nicaud JM, Mackman N, Gray L, Holland IB. 1985. Characterisation of HlyC and mechanism of activation and secretion of haemolysin from *E. coli* 2001. *FEBS Lett* 187:339–344. [http://dx.doi.org/10.1016/0014-5793\(85\)81272-2](http://dx.doi.org/10.1016/0014-5793(85)81272-2).
- Stanley P, Hyland C, Koronakis V, Hughes C. 1999. An ordered reaction mechanism for bacterial toxin acylation by the specialized acyltransferase HlyC: formation of a ternary complex with acylACP and protoxin substrates. *Mol Microbiol* 34:887–901. <http://dx.doi.org/10.1046/j.1365-2958.1999.01648.x>.
- Stanley P, Packman LC, Koronakis V, Hughes C. 1994. Fatty acylation of two internal lysine residues required for the toxic activity of *Escherichia coli* hemolysin. *Science* 266:1992–1996. <http://dx.doi.org/10.1126/science.7801126>.
- Trent MS, Worsham LM, Ernst-Fonberg ML. 1998. The biochemistry of hemolysin toxin activation: characterization of HlyC, an internal protein acyltransferase. *Biochemistry* 37:4644–4652. <http://dx.doi.org/10.1021/bi971588y>.
- Issartel JP, Koronakis V, Hughes C. 1991. Activation of *Escherichia coli* prohaemolysin to the mature toxin by acyl carrier protein-dependent fatty acylation. *Nature* 351:759–761. <http://dx.doi.org/10.1038/351759a0>.
- Greene NP, Crow A, Hughes C, Koronakis V. 2015. Structure of a bacterial toxin-activating acyltransferase. *Proc Natl Acad Sci U S A* 112:E3058–E3066. <http://dx.doi.org/10.1073/pnas.1503832112>.
- Wandersman C, Delepelaire P. 1990. TolC, an *Escherichia coli* outer membrane protein required for hemolysin secretion. *Proc Natl Acad Sci U S A* 87:4776–4780. <http://dx.doi.org/10.1073/pnas.87.12.4776>.
- Chervaux C, Sauvonnnet N, Le Clainche A, Kenny B, Hung AL, Broome-Smith JK, Holland IB. 1995. Secretion of active beta-lactamase to the medium mediated by the *Escherichia coli* haemolysin transport pathway. *Mol Gen Genet* 249:237–245. <http://dx.doi.org/10.1007/BF00290371>.
- Gentschev I, Hess J, Goebel W. 1990. Change in the cellular localization of alkaline phosphatase by alteration of its carboxy-terminal sequence. *Mol Gen Genet* 222:211–216. <http://dx.doi.org/10.1007/BF00633820>.
- Gray L, Baker K, Kenny B, Mackman N, Haigh R, Holland IB. 1989. A novel C-terminal signal sequence targets *Escherichia coli* haemolysin directly to the medium. *J Cell Sci Suppl* 11:45–57. http://dx.doi.org/10.1242/jcs.1989.Supplement_11.4.
- Gray L, Mackman N, Nicaud JM, Holland IB. 1986. The carboxy-terminal region of haemolysin 2001 is required for secretion of the toxin from *Escherichia coli*. *Mol Gen Genet* 205:127–133. <http://dx.doi.org/10.1007/BF02428042>.
- Koronakis V, Koronakis E, Hughes C. 1989. Isolation and analysis of the C-terminal signal directing export of *Escherichia coli* hemolysin protein across both bacterial membranes. *EMBO J* 8:595–605. <http://dx.doi.org/10.1002/j.1460-2075.1989.tb03414.x>.
- Mackman N, Baker K, Gray L, Haigh R, Nicaud JM, Holland IB. 1987. Release of a chimeric protein into the medium from *Escherichia coli* using the C-terminal secretion signal of haemolysin. *EMBO J* 6:2835–2841. <http://dx.doi.org/10.1002/j.1460-2075.1987.tb02580.x>.
- Mackman N, Holland IB. 1984. Functional characterization of a cloned haemolysin determinant from *E. coli* of human origin, encoding information for the secretion of a 107K polypeptide. *Mol Gen Genet* 196:129–134. <http://dx.doi.org/10.1007/BF00334104>.
- Mackman N, Nicaud JM, Gray L, Holland IB. 1985. Genetical and functional organisation of the *Escherichia coli* haemolysin determinant 2001. *Mol Gen Genet* 201:282–288. <http://dx.doi.org/10.1007/BF00425672>.
- Mackman N, Nicaud JM, Gray L, Holland IB. 1985. Identification of polypeptides required for the export of haemolysin 2001 from *E. coli*. *Mol Gen Genet* 201:529–536. <http://dx.doi.org/10.1007/BF00331351>.
- Goyard S, Sebo P, D'Andria O, Ladant D, Ullmann A. 1993. *Bordetella pertussis* adenylate cyclase: a toxin with multiple talents. *Zentralbl Bakteriol* 278:326–333. [http://dx.doi.org/10.1016/S0934-8840\(11\)80849-2](http://dx.doi.org/10.1016/S0934-8840(11)80849-2).

33. Satchell KJ. 2011. Structure and function of MARTX toxins and other large repetitive RTX proteins. *Annu Rev Microbiol* 65:71–90. <http://dx.doi.org/10.1146/annurev-micro-090110-102943>.
34. Satchell KJF. 2015. Multifunctional-autoprocessing repeats-in-toxin (MARTX) toxins of vibrios. *Microbiol Spectr* 3(3):VE-0002-2014. <http://dx.doi.org/10.1128/microbiolspec.VE-0002-2014>.
35. Kim BS, Gavin HE, Satchell KJ. 2015. Distinct roles of the repeat-containing regions and effector domains of the *Vibrio vulnificus* multifunctional-autoprocessing repeats-in-toxin (MARTX) toxin. *mBio* 6:e00324-15. <http://dx.doi.org/10.1128/mBio.00324-15>.
36. Barlag B, Hensel M. 2015. The giant adhesin SiiE of *Salmonella enterica*. *Molecules* 20:1134–1150. <http://dx.doi.org/10.3390/molecules20011134>.
37. Guo S, Stevens CA, Vance TDR, Olijve LLC, Graham LA, Campbell RL, Yazdi SR, Escobedo C, Bar-Dolev M, Yashunsky V, Braslavsky I, Langelaan DN, Smith SP, Allingham JS, Voets IK, Davies PL. 2017. Structure of a 1.5-MDa adhesin that binds its Antarctic bacterium to diatoms and ice. *Sci Adv* 3:e1701440. <http://dx.doi.org/10.1126/sciadv.1701440>.
38. Smith TJ, Sondermann H, O'Toole GA. 2018. Type 1 does the two-step: type 1 secretion substrates with a functional periplasmic intermediate. *J Bacteriol* 200:e00168-18. <http://dx.doi.org/10.1128/JB.00168-18>.
39. Peters B, Stein J, Klingl S, Sander N, Sandmann A, Taccardi N, Sticht H, Gerlach RG, Muller YA, Hensel M. 2017. Structural and functional dissection reveals distinct roles of Ca²⁺-binding sites in the giant adhesin SiiE of *Salmonella enterica*. *PLoS Pathog* 13:e1006418. <http://dx.doi.org/10.1371/journal.ppat.1006418>.
40. Wagner C, Polke M, Gerlach RG, Linke D, Stierhof YD, Schwarz H, Hensel M. 2011. Functional dissection of SiiE, a giant non-fimbrial adhesin of *Salmonella enterica*. *Cell Microbiol* 13:1286–1301. <http://dx.doi.org/10.1111/j.1462-5822.2011.01621.x>.
41. Holland IB, Peherstorfer S, Kanonenberg K, Lenders M, Reimann S, Schmitt L. 2016. Type I protein secretion—deceptively simple yet with a wide range of mechanistic variability across the family. *EcoSal Plus* 7:ESP-0019-2015. <http://dx.doi.org/10.1128/ecosalplus.ESP-0019-2015>.
42. Cao G, Kuhn A, Dalbey RE. 1995. The translocation of negatively charged residues across the membrane is driven by the electrochemical potential: evidence for an electrophoresis-like membrane transfer mechanism. *EMBO J* 14:866–875. <http://dx.doi.org/10.1002/j.1460-2075.1995.tb07068.x>.
43. Baumann U, Wu S, Flaherty KM, McKay DB. 1993. Three-dimensional structure of the alkaline protease of *Pseudomonas aeruginosa*: a two-domain protein with a calcium binding parallel beta roll motif. *EMBO J* 12:3357–3364. <http://dx.doi.org/10.1002/j.1460-2075.1993.tb06009.x>.
44. Baumann U, Bauer M, Létoffé S, Delepelaire P, Wandersman C. 1995. Crystal structure of a complex between *Serratia marcescens* metallo-protease and an inhibitor from *Erwinia chrysanthemi*. *J Mol Biol* 248:653–661. <http://dx.doi.org/10.1006/jmbi.1995.0249>.
45. Meier R, Drepper T, Svensson V, Jaeger KE, Baumann U. 2007. A calcium-gated lid and a large beta-roll sandwich are revealed by the crystal structure of extracellular lipase from *Serratia marcescens*. *J Biol Chem* 282:31477–31483. <http://dx.doi.org/10.1074/jbc.M704942200>.
46. Ostolaza H, Soloaga A, Goñi FM. 1995. The binding of divalent cations to *Escherichia coli* alpha-haemolysin. *Eur J Biochem* 228:39–44.
47. Sánchez-Magraner L, Viguera AR, García-Pacios M, Garcillán MP, Arrondo JL, de la Cruz F, Goñi FM, Ostolaza H. 2007. The calcium-binding C-terminal domain of *Escherichia coli* alpha-hemolysin is a major determinant in the surface-active properties of the protein. *J Biol Chem* 282:11827–11835. <http://dx.doi.org/10.1074/jbc.M700547200>.
48. Soloaga A, Ramírez JM, Goñi FM. 1998. Reversible denaturation, self-aggregation, and membrane activity of *Escherichia coli* alpha-hemolysin, a protein stable in 6 M urea. *Biochemistry* 37:6387–6393. <http://dx.doi.org/10.1021/bi9730994>.
49. Thomas S, Bakkes PJ, Smits SH, Schmitt L. 2014. Equilibrium folding of pro-HlyA from *Escherichia coli* reveals a stable calcium ion dependent folding intermediate. *Biochim Biophys Acta* 1844:1500–1510. <http://dx.doi.org/10.1016/j.bbapap.2014.05.006>.
50. Blenner MA, Shur O, Szilvay GR, Cropek DM, Banta S. 2010. Calcium-induced folding of a beta roll motif requires C-terminal entropic stabilization. *J Mol Biol* 400:244–256. <http://dx.doi.org/10.1016/j.jmb.2010.04.056>.
51. Chenal A, Guijarro JI, Raynal B, Delepierre M, Ladant D. 2009. RTX calcium binding motifs are intrinsically disordered in the absence of calcium: implication for protein secretion. *J Biol Chem* 284:1781–1789. <http://dx.doi.org/10.1074/jbc.M807312200>.
52. Sotomayor Pérez AC, Karst JC, Davi M, Guijarro JI, Ladant D, Chenal A. 2010. Characterization of the regions involved in the calcium-induced folding of the intrinsically disordered RTX motifs from the *Bordetella pertussis* adenylate cyclase toxin. *J Mol Biol* 397:534–549. <http://dx.doi.org/10.1016/j.jmb.2010.01.031>.
53. Zhang L, Conway JF, Thibodeau PH. 2012. Calcium-induced folding and stabilization of the *Pseudomonas aeruginosa* alkaline protease. *J Biol Chem* 287:4311–4322. <http://dx.doi.org/10.1074/jbc.M111.310300>.
54. Jones HE, Holland IB, Baker HL, Campbell AK. 1999. Slow changes in cytosolic free Ca²⁺ in *Escherichia coli* highlight two putative influx mechanisms in response to changes in extracellular calcium. *Cell Calcium* 25:265–274. <http://dx.doi.org/10.1054/ceca.1999.0028>.
55. Bakkes PJ, Jenewein S, Smits SH, Holland IB, Schmitt L. 2010. The rate of folding dictates substrate secretion by the *Escherichia coli* hemolysin type 1 secretion system. *J Biol Chem* 285:40573–40580. <http://dx.doi.org/10.1074/jbc.M110.173658>.
56. Balakrishnan L, Hughes C, Koronakis V. 2001. Substrate-triggered recruitment of the TolC channel-tunnel during type I export of hemolysin by *Escherichia coli*. *J Mol Biol* 313:501–510. <http://dx.doi.org/10.1006/jmbi.2001.5038>.
57. Thanabalu T, Koronakis E, Hughes C, Koronakis V. 1998. Substrate-induced assembly of a contiguous channel for protein export from *E. coli*: reversible bridging of an inner-membrane translocase to an outer membrane exit pore. *EMBO J* 17:6487–6496. <http://dx.doi.org/10.1093/emboj/17.22.6487>.
58. Du D, Wang Z, James NR, Voss JE, Klimont E, Ohene-Agyei T, Venter H, Chiu W, Luisi BF. 2014. Structure of the AcrAB-TolC multidrug efflux pump. *Nature* 509:512–515. <http://dx.doi.org/10.1038/nature13205>.
59. Benabdelhak H, Kiontke S, Horn C, Ernst R, Blight MA, Holland IB, Schmitt L. 2003. A specific interaction between the NBD of the ABC-transporter HlyB and a C-terminal fragment of its transport substrate haemolysin A. *J Mol Biol* 327:1169–1179. [http://dx.doi.org/10.1016/S0022-2836\(03\)00204-3](http://dx.doi.org/10.1016/S0022-2836(03)00204-3).
60. Lenders MHH, Weidtkamp-Peters S, Kleinschrodt D, Jaeger K-E, Smits SHJ, Schmitt L. 2015. Directionality of substrate translocation of the hemolysin A type I secretion system. *Sci Rep* 5:12470. <http://dx.doi.org/10.1038/srep12470>.
61. Lenders MH, Beer T, Smits SH, Schmitt L. 2016. In vivo quantification of the secretion rates of the hemolysin A type I secretion system. *Sci Rep* 6:33275. <http://dx.doi.org/10.1038/srep33275>.
62. Bumba L, Masin J, Macek P, Wald T, Motlova L, Bibova I, Klimova N, Bednarova L, Veverka V, Kachala M, Svergun DI, Barinka C, Sebo P. 2016. Calcium-driven folding of RTX domain β -rolls ratchets translocation of RTX proteins through type I secretion ducts. *Mol Cell* 62:47–62. <http://dx.doi.org/10.1016/j.molcel.2016.03.018>.
63. Monds RD, Newell PD, Gross RH, O'Toole GA. 2007. Phosphate-dependent modulation of c-di-GMP levels regulates *Pseudomonas fluorescens* Pf0-1 biofilm formation by controlling secretion of the adhesin LapA. *Mol Microbiol* 63:656–679. <http://dx.doi.org/10.1111/j.1365-2958.2006.05539.x>.
64. Koronakis V, Sharff A, Koronakis E, Luisi B, Hughes C. 2000. Crystal structure of the bacterial membrane protein TolC central to multidrug efflux and protein export. *Nature* 405:914–919. <http://dx.doi.org/10.1038/35016007>.

T1SS—One Mechanism for All?

65. Lecher J, Schwarz CK, Stoldt M, Smits SH, Willbold D, Schmitt L. 2012. An RTX transporter tethers its unfolded substrate during secretion via a unique N-terminal domain. *Structure* 20:1778–1787. <http://dx.doi.org/10.1016/j.str.2012.08.005>.
66. Zaitseva J, Jenewein S, Jumpertz T, Holland IB, Schmitt L. 2005. H662 is the linchpin of ATP hydrolysis in the nucleotide-binding domain of the ABC transporter HlyB. *EMBO J* 24:1901–1910. <http://dx.doi.org/10.1038/sj.emboj.7600657>.
67. Zaitseva J, Oswald C, Jumpertz T, Jenewein S, Wiedenmann A, Holland IB, Schmitt L. 2006. A structural analysis of asymmetry required for catalytic activity of an ABC-ATPase domain dimer. *EMBO J* 25:3432–3443. <http://dx.doi.org/10.1038/sj.emboj.7601208>.
68. Murata D, Okano H, Angkawidjaja C, Akutsu M, Tanaka SI, Kitahara K, Yoshizawa T, Matsumura H, Kado Y, Mizohata E, Inoue T, Sano S, Koga Y, Kanaya S, Takano K. 2017. Structural basis for the *Serratia marcescens* lipase secretion system: crystal structures of the membrane fusion protein and nucleotide-binding domain. *Biochemistry* 56:6281–6291. <http://dx.doi.org/10.1021/acs.biochem.7b00985>.
69. Kim JS, Song S, Lee M, Lee S, Lee K, Ha NC. 2016. Crystal structure of a soluble fragment of the membrane fusion protein HlyD in a type I secretion system of Gram-negative bacteria. *Structure* 24:477–485. <http://dx.doi.org/10.1016/j.str.2015.12.012>.
70. Morgan JLW, Acheson JF, Zimmer J. 2017. Structure of a type-1 secretion system ABC transporter. *Structure* 25:522–529. <http://dx.doi.org/10.1016/j.str.2017.01.010>.
71. Gerlach RG, Jäckel D, Stecher B, Wagner C, Lupas A, Hardt WD, Hensel M. 2007. *Salmonella* pathogenicity island 4 encodes a giant non-fimbrial adhesin and the cognate type 1 secretion system. *Cell Microbiol* 9:1834–1850. <http://dx.doi.org/10.1111/j.1462-5822.2007.00919.x>.

3.3 Chapter 3

Title: Molecular characterization of the RTX toxin MbxA from *Moraxella bovis* through a heterologous secretion approach

Authors: Isabelle N. Erenburg, Sebastian Wintgens, Sebastian Hänsch, Fabian Stuhldreier, Gereon Poschmann, Olivia Spitz, Kai Stühler, Sebastian Wesselborg, Stefanie Weidtkamp-Peters, Johannes Hegemann, Sander H. J. Smits & Lutz Schmitt

Published in: *to be submitted*

Own proportion of this work:

- 60%
- Bioninformatic analyses
- Cloning of constructs
- Expression and secretion
- Protein purification
- Cytotoxicity assays
- Preparation of the figures
- Writing of the manuscript

Molecular characterization of the RTX toxin MbxA from *Moraxella bovis* through a heterologous secretion approach

Isabelle N. Erenburg¹, Sebastian Wintgens², Sebastian Hänsch³, Fabian Stuhldreier⁴, Gereon Poschmann⁵, Olivia Spitz¹, Kai Stühler^{5,6}, Sebastian Wesselborg⁴, Stefanie Weidtkamp-Peters³, Johannes Hegemann², Sander H. J. Smits¹ & Lutz Schmitt^{1,§}

¹: Institute of Biochemistry, Heinrich Heine University Düsseldorf

²: Institute of Functional Microbial Genomics, Heinrich Heine University Düsseldorf

³: Center for Advanced Imaging, Heinrich Heine University Düsseldorf

⁴: Institute of Molecular Medicine I, Heinrich Heine University Düsseldorf

⁵: Institute of Molecular Medicine, Proteome research, Heinrich Heine University Düsseldorf

⁶: Molecular Proteomics Laboratory, Biomedical Research Centre (BMFZ), Heinrich Heine University Düsseldorf

§Corresponding author: Lutz Schmitt, Institute of Biochemistry, Heinrich Heine University Düsseldorf, Universitätsstr. 1, 40225 Düsseldorf, Germany, E-Mail: lutz.schmitt@hhu.de

Keywords: RTX toxins, acylation, secretion, cell membrane damage, membrane blebbing

Abstract

Many proteins of the Repeats in Toxins (RTX) protein family are toxins of Gram-negative pathogens including hemolysin A (HlyA) of uropathogenic *E. coli*. RTX proteins are secreted via Type I secretion systems (T1SS) and adopt their native conformation in the Ca^{2+} -rich extracellular environment. Here we employed the *E. coli* HlyA T1SS as a heterologous system for the RTX toxin MbxA from the bovine pathogen *Moraxella bovis*. In *E. coli* the HlyA system successfully activates MbxA by acylation and secretes the precursor proMbxA and active MbxA allowing purification of both species. The activating *E. coli* acyltransferase HlyC recognizes the acylation sites in MbxA, but unexpectedly resulting in a different acylation pattern as for its native substrate HlyA. HlyC-activated MbxA shows species-independent activity including toxicity against human lymphocytes and epithelial cells. Using live cell imaging we show an immediate MbxA-mediated permeabilization and a rapidly developing blebbing of the plasma membrane in epithelial cells.

Introduction

In light of a growing frequency of antibiotic resistance observed in human pathogens, characterization of virulence factors is a key factor for the development of novel anti-virulence strategies against bacterial infections. Targeting bacterial toxins is a promising approach for future therapeutics that need to be tailored to specific pathogens and pathogenicity factors [1, 2]. The characterization of toxins relies on their accessibility and therefore requires an efficient bacterial production platform.

Proteins of the Repeats in Toxins (RTX) family are secreted into the extracellular space by a large number of Gram-negative bacteria employing type 1 secretion systems (T1SS). The growing number of sequenced bacterial genomes revealed novel members of this RTX family [3]. Many RTX proteins are virulence factors of important pathogens such as the toxins CyaA from *Bordetella pertussis* or hemolysin A (HlyA) from uropathogenic *E. coli* (UPEC). RTX proteins are characterized by glycine-rich nonapeptide repeats with the consensus sequence GGxGxDxU (x - any amino acid, U - large hydrophobic amino acid,) the so-called GG repeats [3, 4]. Repetitions of this repeat close to the C-terminus form the RTX domain [5], while the variability of the N-terminus between different RTX proteins allows diverse functions (for a review see [3]).

The hemolysin (Hly) secretion system is specific for its sole substrate HlyA and often considered a prototype of T1SS. Transport of HlyA occurs in a one-step mechanism across both membranes of the Gram-negative bacterium [6-8]. It is mediated by two inner membrane components, the ATP-binding cassette (ABC) transporter hemolysin B (HlyB) and the membrane fusion protein hemolysin D (HlyD), together with the outer membrane protein TolC [9-12]. A C-terminal, non-cleavable secretion sequence of 50-60 amino acids conveys specific interaction with the inner membrane components (Fig. 1) [6-8, 13]. Prior to and during transport, HlyA remains unfolded and only achieves its native conformation upon secretion into the extracellular fluid, where binding of Ca^{2+} ions to the RTX domain induces folding of the protein [5, 14-16]. Although RTX proteins lack a conserved secretion sequence the HlyA secretion system was shown to tolerate some non-native RTX toxins as substrates such as for example CyaA from *Bordetella pertussis*, FrpA from *Neisseria meningitidis*, PaxA from *Pasteurella aerogenes* or LktA from *Mannheimia haemolytica* [17-20]. However, the secretion of these non-native RTX protein was not quantified or demonstrated to be efficient. Furthermore, different experiments showed that the HlyA T1SS is able to secrete fusion proteins. The exchange of the HlyA secretion sequence with the C-terminus of LktA still facilitates secretion of HlyA [21]. At the same time non-related, but slow-folding protein carrying the HlyA secretion sequence are recognized and transported [14].

HlyA belongs to the classic pore-forming RTX toxins and is active against a variety of cells including erythrocytes, leukocytes, epithelial and endothelial cells of different species [22-24]. For the cytotoxic activity, but not for secretion, a post-translational fatty acid acylation of two internal lysine residues, catalyzed by the intracellular acyltransferase HlyC, is required (Fig. 1) [25, 26]. Despite being studied for decades the mechanism of pore formation by RTX toxins remains elusive.

The RTX hemolysin MbxA shares a sequence identity of 42% with HlyA and is a key factor in the pathogenicity of *Moraxella bovis* (*M. bovis*) [27, 28]. This animal pathogen is the cause of the most prevalent ocular disease in cattle, the infectious bovine keratoconjunctivitis (IBK) [29, 30]. Studies with supernatants of pathogenic *M. bovis* cultures revealed a cytotoxicity against bovine neutrophils, erythrocytes and corneal epithelial cells attributed to a possibly secreted cytotoxin [31-34]. A classic RTX operon that comprises MbxA together with the putative acyltransferase MbxC along with the transporter components MbxB and MbxD was later found to be present only in pathogenic, hemolytic *M. bovis* strains but not in non-hemolytic strains. In contrast to the *hlyA* operon in UPEC, a TolC homologue is encoded downstream of the *mbx* operon [12, 35]. With a length of 927 amino acids MbxA is approximately 10% smaller than

HlyA. Like in HlyA, sequence alignment and topology predictions revealed two potential acylation sites as well as an ambiguous membrane interaction domain at the N-terminal part of MbxA [27, 36, 37], while the GG repeats are located closer to the C-terminus of MbxA. Altogether MbxA has a putative domain organization that is typical for pore-forming RTX toxins (Fig. 1).

Here we established a complete surrogate T1SS in an *E. coli* lab strain by a combination of the UPEC HlyA T1SS with the heterologous substrate MbxA that secretes active MbxA or its precursor proMbxA. Based on this result, we developed a purification procedure for both MbxA species from the supernatant of secreting *E. coli* cells. Recombinant MbxA was efficiently activated by HlyC, but with an unexpected and different acylation pattern as HlyA. In contrast to the previously shown activity against bovine and ovine cells, we further observed that MbxA displays a target species-independent cytotoxic activity against human epithelial cells and leukocytes. Using live cell imaging, we finally demonstrate a rapid and distinct membrane blebbing phenotype in human epithelial cells in response to permeabilization by MbxA.

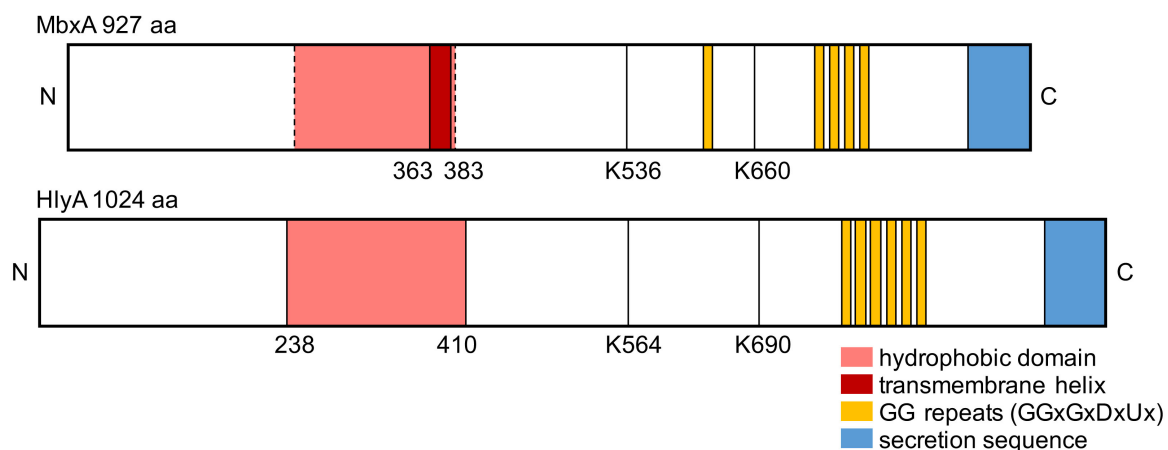


Figure 1: Schematic view of the primary structure of MbxA and HlyA. Five conserved GG repeats with the consensus sequence GGxGxDxUx are present in MbxA (yellow boxes), while HlyA carries six conserved GG repeats (yellow boxes). They form the Ca^{2+} binding RTX domain. As a RTX protein, HlyA characteristically possesses a C-terminal secretion signal of approximately 60 amino acids [6, 8, 13], which is shown in blue. For MbxA the length of the secretion sequence is unknown. In the N-terminal part of HlyA, a hydrophobic domain is involved in pore formation and marked in red [36]. Depending on the prediction algorithm for MbxA either a single membrane spanning helix is predicted from residue 363 to 383 (dark red box) with an additional reentrant helix at residue 215 or a set of transmembrane helices forming an ambiguous hydrophobic domain from residue 210 to 383 or even from residue 120 to 383 (dashed line) are predicted [37]. The position of the acylated lysine residues K564 and K690 of HlyA and the homologous residues predicted to become acylated in MbxA, K536 and K660, are indicated.

Material and Methods

Sequence alignment and topology prediction

Alignment was carried out using EMBOSS Needle pairwise sequence alignment [38]. For the prediction of membrane spanning regions the Constrained Consensus TOPology prediction server (CCTOP) was used [37].

Cloning of the *mbxA* gene

The *mbxA* gene (Uniprot Q93GI2) was amplified from *M. bovis* DSM 6328 genomic DNA with the primer pair *mbxA*-for 5'-AACCTTTTCTAACACAACGAGGAGAGAC-3' and *mbxA*-rev 5'-AAATCACTAAACACTTGGAGCCAAAATTC-3' and cloned into the pJET1.2 vector (Thermo Scientific). Subsequently the *mbxA* gene was cloned into the pSU2726 *hlyA* vector [39] replacing the *hlyA* gene. An N-terminal His₆-Tag site was introduced, resulting in plasmid pSU-6H-*mbxA*. To produce acylated MbxA, 6H-*mbxA* was cloned into the pSU-*hlyC*-6H/*hlyA* plasmid [40] replacing the *hlyA* gene. To restore the *hlyA* enhancer region [41] the His₆-Tag of *hlyC* was deleted, creating pSU-*hlyC*/6H-*mbxA*. In this vector, both genes, *hlyC* and *mbxA*, are under the control of one LacZ promoter [40].

Expression and secretion of proMbxA and MbxA

Secretion of MbxA in *E. coli* BL21(DE3) was facilitated by co-expression of the transporter components HlyB and HlyD of the *E. coli* UIT89 HlyA system. For expression of recombinant proMbxA, ten 300 ml flasks containing 50 ml LB with 100 µg/ml ampicillin and 30 µg/ml kanamycin per flask were inoculated with an *E. coli* BL21(DE3) overnight culture harboring plasmids pK184-*hlyBD* [14] and pSU 6H-*mbxA* to an OD₆₀₀ of 0.05. The culture was grown at 37°C and 180 rpm until OD₆₀₀ reached 0.4-0.6. Subsequently, the culture was supplemented with 10 mM CaCl₂ and expression was induced with 1 mM IPTG. After 5 h of expression at 37°C and 180 rpm the cells were removed by centrifugation at 13500 g for 45 min. The supernatant was filtered with a 0.45 µm filter and stored on ice for purification.

For the secretion of active MbxA, *E. coli* BL21(DE3) transformed with the plasmids pK184-*hlyBD* and pSU-*hlyC*/6H-*mbxA* were grown in 2 L LB medium with 100 µg/ml ampicillin and 30 µg/ml kanamycin in baffled 5 L flasks at 37°C and 160 rpm and induced at the same conditions as pSU-6H-*mbxA*. Secreted MbxA accumulated in the foam of the culture. After 5 h of expression the foam was collected and centrifuged at 4000 g for 10 min. The condensed foam was solubilized in solubilization buffer (6 M urea, 100 mM NaCl, 50 mM TRIS pH 8.0) by

stirring at room temperature overnight. Aggregate was collected by centrifugation at 160.000 g for 30 min and the solubilized protein stored at -80°C.

Purification of MbxA

Solubilized MbxA was refolded by dropwise dilution from 6 M to 400 mM urea with IMAC buffer (50 mM Tris pH 7.8, 400 mM NaCl, 10 mM CaCl₂) with constant stirring at room temperature. All subsequent steps were performed at 4°C. Refolded MbxA was loaded on a 5 ml Ni²⁺ loaded HiTrap IMAC HP column (GE Healthcare) and eluted with a linear 0-75 mM histidine gradient with elution buffer (50 mM Tris pH 7.8, 400 mM NaCl, 10 mM CaCl₂, 75 mM histidine). Elution fractions containing MbxA were pooled and concentrated with Amicon Ultra-15 Centrifugal Filter Units (50 kDa NMWL, Merck Millipore). Histidine was removed with a PD10 desalting column (GE Healthcare) at room temperature and the protein eluted with cold IMAC buffer. Activity of MbxA was tested on Columbia agar with 5% sheep blood (Oxoid).

Purification of proMbxA

The culture supernatant containing proMbxA was concentrated with Amicon Ultra-15 Centrifugal Filter Units (50 kDa NMWL, Merck Millipore) to 1/10 of the starting volume and loaded on a 5 ml Ni²⁺ HiTrap IMAC HP column (GE Healthcare). A linear 0-75 mM histidine gradient with elution buffer was used to elute proMbxA. Elution fractions containing proMbxA were pooled and concentrated. Histidine was removed with a PD10 desalting column (GE Healthcare) and the protein eluted with IMAC buffer.

Size Exclusion Chromatography (SEC) and Multi Angle Light Scattering (MALS)

For SEC, proMbxA or MbxA containing IMAC fractions were pooled, concentrated to 0.5 ml and after centrifugation at 21,700 g for 20 min directly applied to a Superose 6 Increase 10/300 GL column (GE Healthcare) in SEC buffer (50 mM TRIS pH 7.8, 100 mM NaCl, 10 mM CaCl₂). The chromatography was performed on an ÄKTA Purifier system (GE Healthcare). proMbxA peaks resulting from the SEC were pooled separately and stored with 20% glycerol at -80°C. A subsequent SEC-MALS analysis was carried out to investigate the oligomeric state of the proMbxA species. The separated species were concentrated to 1.3- 2.5 mg/ml and 200 µl of each were applied to a Superose 6 Increase 10/300 GL column (GE Healthcare) equilibrated with SEC buffer and connected to a miniDAWN TREOS II triple-angle light scattering detector (Wyatt Technologies) and an Optilab T-rEX differential refractive index detector (Wyatt

Technologies). The set up was performed using an Agilent 1260 HPLC system with a flowrate of 0.6 ml/min and the data was analyzed with the ASTRA 7.1.2.5 software (Wyatt Technologies).

Expression and purification of proHlyA and HlyA

proHlyA was expressed in *E. coli* BL21(DE3) carrying pSU2726-*hlyA* [39] without transporter components to produce inclusion bodies. 2 L of 2xYT medium with 100 µg/ml ampicillin in baffled 5 L flasks were inoculated with an overnight culture to OD₆₀₀ 0.1 and incubated at 37°C and 160 rpm. At OD₆₀₀ 0.6 expression was induced with 1 mM IPTG and expression continued for 4 h at 37°C and 160 rpm. Afterwards cells were collected by centrifugation for 15 min at 13900 g and inclusion bodies purified according to [42]. proHlyA solubilized in 6 M urea was refolded by dropwise dilution to 400 mM urea with 100 mM HEPES pH 8.0, 250 mM NaCl, 10 mM CaCl₂. The refolded protein was concentrated with Amicon Ultra-15 Centrifugal Filter Units (100 kDa NMWL, Merck Millipore) and remaining urea removed with a PD10 desalting column (GE Healthcare). The eluted protein was concentrated and applied to a Superose 6 Increase 10/300 GL column (GE Healthcare) in the same buffer.

Active HlyA was purified from secreting *E. coli* BL21(DE3) harboring pK184-*hlyBD* and pSU-6H-*hlyC/hlyA*. 2 L 2xYT medium with 100 µg/ml ampicillin and 30 µg/ml kanamycin in baffled 5 L flasks were inoculated with an overnight culture to OD₆₀₀ 0.1 and grown at 37°C and 160 rpm. At OD₆₀₀ 0.4-0.6 the culture was supplemented with 10 mM CaCl₂ and expression induced with 1 mM IPTG. After 4 h of expression the foam of the culture was collected, HlyA solubilized in 6 M urea and refolded by dropwise dilution as described for MbxA. Refolded HlyA was concentrated (Amicon Ultra-15 Centrifugal Filter Units, 100 kDa NMWL, Merck Millipore) and remaining urea removed with a PD10 desalting column (GE Healthcare).

MS analysis

MbxA, proMbxA as well as HlyA and proHlyA were separated in a polyacrylamide gel, stained with Coomassie Brilliant Blue (CBB), the corresponding bands of the proteins were cut out from the gel and processed for mass spectrometric analysis as described [43]. Briefly, proteins were reduced with dithiothreitol, alkylated with iodoacetamide and digested with trypsin. Resulting peptides were separated during a 1 h gradient on C18 material using an Ultimate3000 rapid separation liquid chromatography system (Thermo Fisher Scientific) and subsequently injected in an online coupled QExactive plus mass spectrometer (Thermo Fisher Scientific) via a nano-electrospray interface (described in [43]). Briefly, survey scans were recorded at a

resolution of 70,000 and subsequently up to 10 precursors were selected by the build-in quadrupole, fragmented via higher energy collisional dissociation and analyzed at a resolution of 17,500.

Recorded spectra were further analyzed by MaxQuant version 1.6.10.43 (MPI for Biochemistry, Planegg, Germany) using standard parameters if not stated otherwise. Searches for MbxA were carried out in a dataset containing 2734 *Moraxella bovis* sequences as well as an entry for MbxA. For HlyA, a data set was used containing 4156 *E. coli* BL21(DE3) sequences and an additional entry for HlyA. Carbamidomethylation at cysteines was considered as fixed and methionine oxidation, n-terminal acetylation and acylation with C₁₂, C₁₃, C₁₄, C₁₅, C₁₆, C₁₇ and C₁₈ chains at lysines as variable modifications. In a second search, additionally the hydroxylated variants of the acyl chains were considered. The minimal peptide length was set to five, and two variable modifications were allowed per peptide. Identified proteins and peptides were reported at a false discovery rate of 1%.

Cell culture

Human epithelial cells, HEp-2 (epithelial larynx carcinoma, ATCC-CCL-23) were routinely cultured in Dulbecco's modified Eagle's medium (DMEM, Thermo Fisher) and human T lymphocytes, Jurkat J16 (Adult lymphoblastic leukemia ACC-282, DSMZ) were cultured in RPMI-1640 (Thermo Fisher) at 37°C under 5% CO₂. Both media were supplemented with 10% fetal calf serum (FCS), 100 U/ml penicillin, 100 µg/ml streptomycin and 10 mM HEPES.

Lactate dehydrogenase (LDH) release assay

To monitor the cytotoxicity of MbxA the release of cytosolic LDH was measured as an indicator of membrane damage using the LDH Cytotoxicity Assay Kit (Biolegend).

For HEp-2 cells, 10,000 cells per well were seeded in a 96 well plate and grown over night. Prior to the assay, the medium was exchanged to DMEM supplemented with 5% FCS. For Jurkat cells, 100 µl with a density of 6×10⁵ cells/ml in RPMI with 5% FCS were seeded in 96 well plates and for both cell lines all following incubations were carried out in the appropriate cell culture medium supplemented with 5% FCS. HEp-2 cells and Jurkat cells were incubated with a serial dilution of MbxA in DMEM respectively RPMI for 1 h at 37°C under 5% CO₂. To assess if preincubation with proMbxA influences MbxA cytotoxicity purified proMbxA was added to the HEp-2 cells together with fresh DMEM and incubated for 30 min at 37°C under 5% CO₂ before addition of the serial dilution of MbxA. For Jurkat cells proMbxA was added to the cell suspension immediately before seeding and the cells were likewise incubated for

30 min at 37°C under 5% CO₂ before the addition of MbxA. To monitor the basal release and activity of LDH, HEp-2 and Jurkat cells were incubated with cell culture medium with IMAC buffer (basal LDH). Plates were centrifuged (3 min, 1000 g) and supernatants of HEp-2 and Jurkat cells were collected. For the quantification of the LDH release, the assay was carried out according to manufacturer's manual (Biolegend) and absorbance measured at 490 nm. The assay was conducted in biological and technical triplicates. For the calculation of the cytotoxicity absorbance of the background control was subtracted from all other values and the average absorption of triplicates was calculated. The relative cytotoxicity was normalized to the maximal LDH release (maximal absorption after MbxA treatment, Max Abs (MbxA treated)) of each experiment and calculated with the following equation:

Equation 1.

$$\text{Cytotoxicity (\%)} = \frac{\text{Abs (MbxA treated)} - \text{Abs (basal LDH)}}{\text{Max Abs (MbxA treated)} - \text{Abs (basal LDH)}} \times 100$$

The concentration of the half-maximal effect of MbxA (cytotoxic dose 50, CD₅₀) was calculated from three biological replicates with GraphPad Prism 7 with the following equation:

Equation 2.

$$\text{Cytotoxicity (\%)} = \frac{100}{1 + 10^{\log(\text{CD50-conc(MbxA)}) \times \text{Hill slope}}}$$

Live cell imaging

HEp-2 cells were cultivated and passaged in DMEM (Pan Biotech) supplemented with 10% FCS, MEM vitamins, non-essential amino acids, amphotericin B (2.5 µg/ml) and gentamicin (50 µg/ml) (all Thermo Fisher Scientific). One day prior to use, HEp-2 cells were seeded in 2 ml DMEM in 35 mm µ-Dish 1,5H glass bottom dishes and grown overnight at 37 °C under 5 % CO₂. Prior to live cell imaging, cells were washed with DMEM supplemented with 20 mM HEPES as live cell medium (Pan Biotech, Germany) and preincubated with 5 µg/ml Wheat Germ Agglutinin conjugated with Alexa Fluor 488 (WGA-488, Thermo Fisher Scientific) for 10 min at 37 °C. Subsequently, HEp-2 cells were washed twice with live cell buffer and incubated with 1 ml live cell medium with 3.3 nM propidium iodide (PI). Live cell imaging was started after 5 frames, when 1 ml of live cell medium with different concentrations of MbxA (250 nM, 30 nM, 10 nM) or 250 nM of proMbxA were added (resulting in 1.65 nM final concentration of PI during imaging).

Widefield fluorescence imaging was applied at a Nikon Ti-E microscope system (Nikon instruments) equipped with an Apo LWD 40x WI λ S DIC N2 water immersion objective lens with a numerical aperture of 1.15, a C-HGFIE (Precentered Fiber Illuminator, Nikon) as excitation light source for epifluorescence and a Hamamatsu Orca Flash 4.0 (Hamamatsu Photonics) sCMOS camera. To visualize membranous structures with WGA-AF488 a GFP-HQ filter set (Ex 470/40, DM 495, Em 525/50) was utilized. For visualization of PI staining we used a TXRed HYQ filterset (Ex 560/40, DM 595, Em 630/60). Exposure time for the green channel was set to 100 ms and for the red channel to 600 ms, respectively. An additional DIC channel was acquired at 100 ms exposure time, using a standard Halogen lamp (100 W) for illumination. During image acquisition a hardware based autofocus system, the Nikon Perfect Focus System, was used to keep the cells in focus. Linear contrast enhancement for microscopy images was set to the same intensity levels in all figures.

Results

MbxA is secreted and activated by the HlyA system

To produce MbxA employing the HlyA secretion system in *E. coli* BL21(DE3), the *mbxA* gene was introduced into the pSU2726 vector originally used for HlyA expression and secretion resulting in the plasmid pSU-6H-*mbxA*. The HlyA T1SS inner membrane components HlyB and HlyD were expressed from the pK184-*hlyBD* vector, while TolC is chromosomally encoded [14]. In a two-plasmid-system comprised of pK184-*hlyBD* together with pSU-6H-*mbxA* or pSU-*hlyC*/6H-*mbxA*, *mbxA* could either be expressed only in the presence of the transporter components or additionally in the presence of the activating acyltransferase HlyC as a complete T1SS. *E. coli* BL21(DE3) that carry both, pK184-*hlyBD* and pSU-*hlyC*/6H-*mbxA*, showed hemolytic activity when grown on sheep blood agar, while in the absence of HlyC no halo formation occurred. Colonies harboring only pSU-*hlyC*/6H-*mbxA* did not cause hemolysis, which showed that release of cytosolic, activated MbxA from cell lysis did not occur. This indicates that the secretion of active MbxA was indeed mediated by heterologous *E. coli* HlyBD-TolC (Fig. 2). The IPTG-induced expression of HlyBD together with MbxA only or MbxA with HlyC in liquid cultures lead to an accumulation of an approximately 100 kDa protein, proMbxA or MbxA, respectively, in the medium (Fig. 3). In the absence of the HlyC protein, secretion levels of proMbxA were higher during 5 h of expression. While proMbxA was stable in the supernatant, MbxA tended to accumulate in the foam floating on the medium.

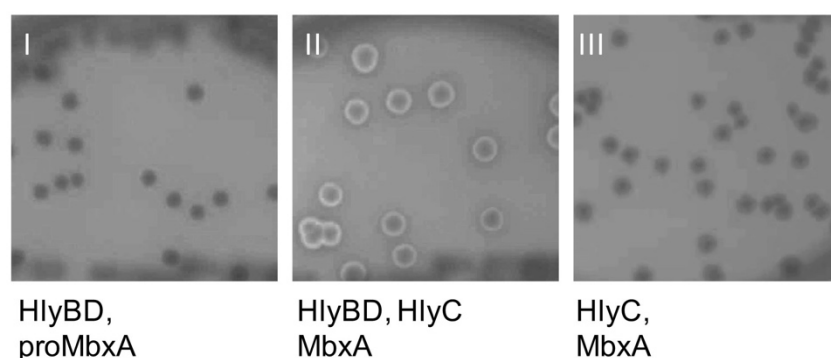


Figure 2: *E. coli* BL21(DE3) grown on Columbia agar with 5% sheep blood harboring the plasmids pK184-*hlyBD* with pSU-6*H-mbxA* (I), pK184-*hlyBD* with pSU-*hlyC/6H-mbxA* (II) or pSU-*hlyC/6H-mbxA* alone (III). Halo formation around colonies that expressed MbxA and HlyC together with the transporter components HlyBD (II) and absence of hemolysis around colonies that express only MbxA and HlyC (III) indicates functional secretion of active and acylated MbxA. Thus MbxA is not released from *E. coli* without additional expression of the Hly secretion system.

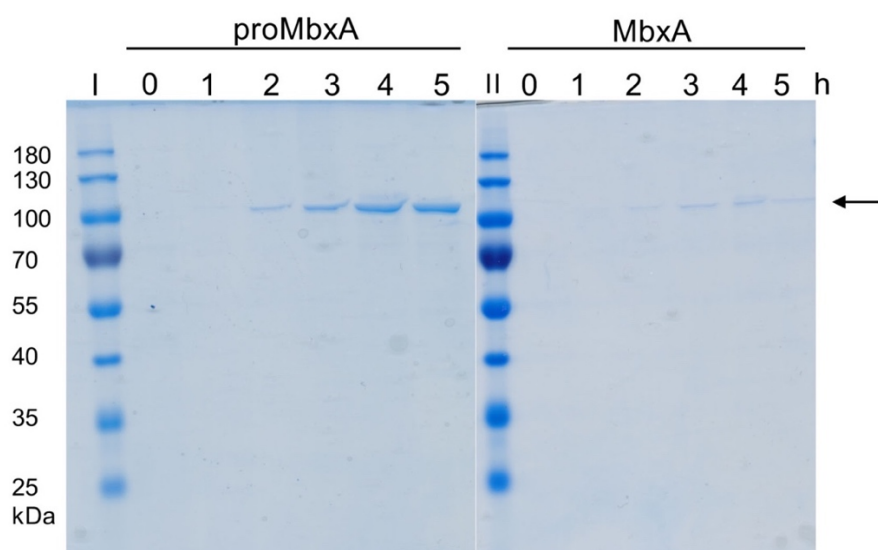


Figure 3: Heterologous secretion of proMbxA and MbxA via the HlyBD system. The Coomassie Brilliant Blue (CBB) SDS-PAGE of culture supernatants of *E. coli* BL21(DE3) co-expressing HlyBD and MbxA or HlyBD, HlyC and MbxA show accumulation of proMbxA or MbxA during a period of 0-5 h of expression (indicated by the numbers above the gel) after induction with IPTG. Molecular weight markers in kDa are shown in lanes I and II. An arrow indicates proMbxA and MbxA.

Purification of proMbxA and MbxA from the supernatants of *E. coli* cultures

From the *E. coli* BL21(DE3) pK184-*hlyBD*, pSU-6*H-mbxA* system approximately 6 mg/L of precursor protein proMbxA was recovered from the supernatant using Ni^{2+} affinity

chromatography. A subsequent size exclusion chromatography (SEC) and SDS-PAGE analysis revealed that two separable species of proMbxA were present (Fig. 4). Determination of the molecular weight (MW) by multi angle light scattering (MALS) analysis confirmed that the first peak with an experimentally determined molecular weight (MW) of 201.5 ± 1.1 kDa corresponded to proMbxA dimers (theoretical MW 201.2 kDa). The second peak contained monomeric MbxA as the determined MW of 93.9 ± 0.3 kDa fitted to the theoretical mass of 100.6 kDa (Fig. 5). Activated MbxA, that was solubilized with 6 M urea from the foam of the expression culture and was afterwards refolded in the presence of Ca^{2+} , was equally purified via IMAC and subsequent SEC. MbxA eluted from the Superose 6 Increase column earlier (elution volume 13.6 ml) and in a broader peak than the proMbxA dimer (elution volume 14.9 ml), which indicates the presence of a higher oligomeric species of MbxA, probably including MbxA dimers and a small fraction of monomers (elution volume 17.1 ml) (Fig. 4). CBB staining confirmed the purity of proMbxA and MbxA already after IMAC (Fig. 4b).

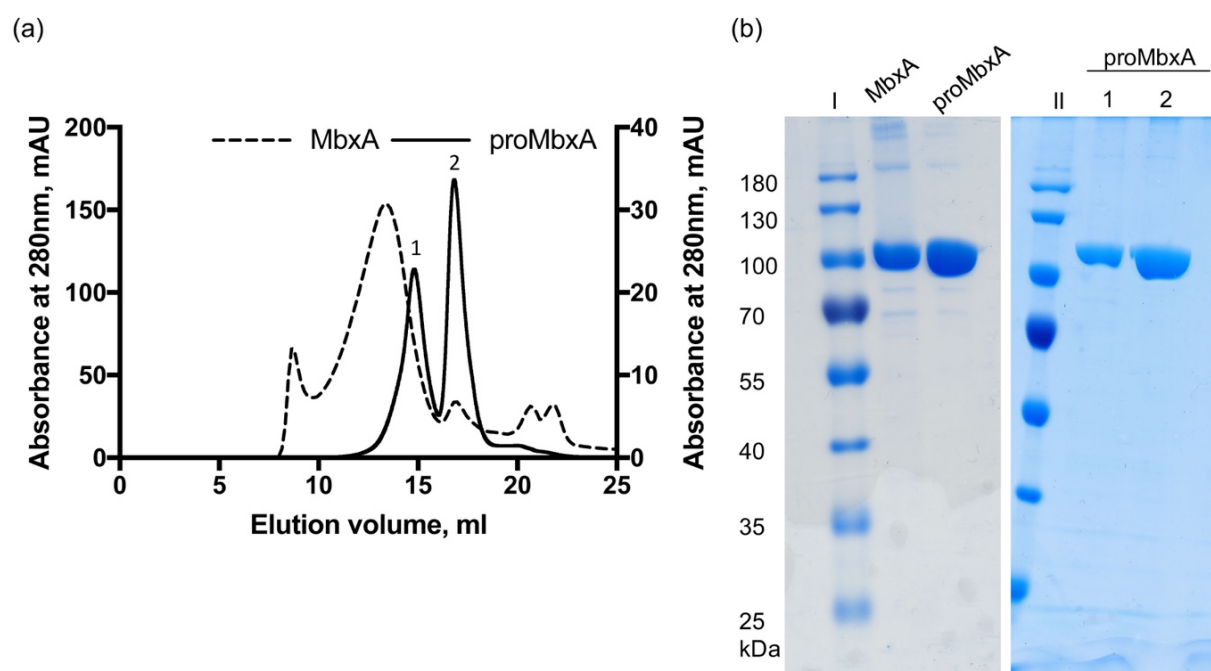


Figure 4: (a) SEC of samples of MbxA (dashed line) and proMbxA (solid line), respectively, applied to a Superose 6 Increase 6/30 column (GE Healthcare). The absorbance at 280 nm of the elution profile of proMbxA is plotted on the left Y axis, the elution profile of MbxA on the right Y axis. proMbxA eluted in two separate peaks, marked 1 and 2 in the chromatogram. (b) CBB stained SDS-PAGE gels of MbxA and proMbxA obtained from IMAC purification and used for SEC (left panel). proMbxA is separated in two species, peak 1 and peak 2, during SEC and evaluated by SDS PAGE (right panel). Molecular weight markers in kDa are shown in lanes I and II.

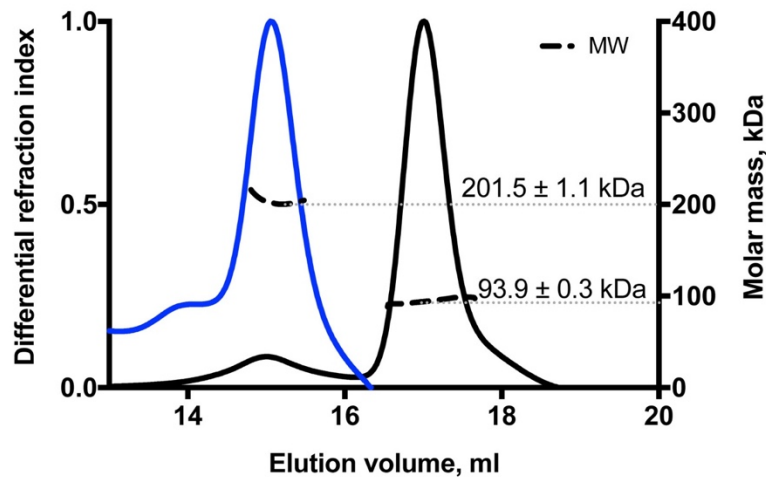


Figure 5: MALS coupled to SEC analysis of the two proMbxA species separated via SEC. The calculated molecular weight (MW) of 201.5 ± 1.1 kDa of the first peak (blue) corresponds to a dimer of MbxA (theoretical MW $(6H\text{-MbxA})_2 = 201.2$ kDa). The molecular weight of 93.9 ± 0.3 kDa of the second peak (black) confirms a monomeric species of proMbxA (theoretical MW $6H\text{-MbxA} = 100.6$ kDa).

Active MbxA is cross-acylated by HlyC at two conserved acylation sites

Besides HlyA, several other pore-forming RTX toxins are known to require a post-translational acylation at two or, as in the example of CyaA, at least one conserved internal lysine residue to confer toxic activity [26, 44-48]. For HlyA acylation of both acylation sites was shown to be required for toxicity [26]. The amide linked fatty-acylation is facilitated by an acyltransferase encoded upstream of the RTX gene and an acyl carrier protein [49]. The presence of the *mbxC* gene in the *M. bovis* operon indicates that MbxA is, when expressed, likely acylated [27]. The lysine residues K536 and K660 of MbxA correspond to the acylation sites at K564 and K690 of HlyA (Fig. S1) [26, 27]. The areas around the two acylation sites, residues H516-G566 and K640-Q680, share a sequence identity of approximately 46% with those of HlyA. This identity is comparable to the overall identity of both proteins. To analyze the acylation status of proMbxA and MbxA co-expressed with HlyC, we used mass spectrometry. Whereas no acylation was detected for proMbxA, MbxA peptides containing acylated lysines were identified at the predicted sites, K536 and K660, respectively. No peptide with non-acylated K536 or K660 was detected in the acylated MbxA variant. A myristoylation (C_{14} acylation) as well as hydroxy myristoylations ($C_{14}\text{-OH}^*$) were determined for all three detected peptides that covered the first acylation site K536 (ERLTNGKYSYINK, LTNGKYSYINK and LTNGKYSYINKLK) (Tab S1) (Considering that the mass shift attributed to hydroxy acylations could potentially originate from tyrosine oxidation hydroxy variants are marked with

an * (Fig. 6, Tab. S1)). Each of those peptides were identified by more than one fragment spectrum recorded by the mass spectrometer resulting in a total of 24 informative spectra for C₁₄ modification with additional five informative spectra for C₁₄-OH* modifications of these three peptides. Those peptide spectrum matches (PSM) can be used as semi-quantitative measure for the occurrence of peptides and peptide modifications. The peptide LTNGKYSYINK was additionally found to be modified with C₁₃, C₁₅ and C₁₆ acylations as well as a C₁₂ hydroxy acylation. These modifications with C₁₃, C₁₅, C₁₆ and C₁₂-OH* fatty acids are probably less frequent as they were detected only with 2, 4, 1 and 1 PSM, respectively. The second acylation site, K660, was only found to be acylated with C₁₄ fatty acids (Fig. 6a). As no other fatty-acylated lysine residues were observed, we conclude that modification of MbxA with the non-native acyltransferase HlyC, here referred to as cross-acylation, targets only the conserved acylation sites (Tab. S1).

To test whether in the *E. coli* BL21(DE3) background HlyC confers the same modifications to MbxA as to HlyA, proHlyA and HlyA were analyzed for their acylation status. For HlyA, peptides acylated at both known acylation sites could be identified [26] (Tab. S1). At K564 peptides modified with C₁₄ acylation and C₁₄-OH* acylation contributed both with 2 PSM. The second acylation site, K690, was predominantly found acylated with C₁₄ fatty acids (48 PSM) but also hydroxy acylated with C₁₄-OH* modifications (8 PSM). In contrast to the second acylation site of MbxA also less frequent modifications, namely C₁₂, C₁₃ and C₁₆ acylations were detected at the K690 acylation site of HlyA with 1, 2 and 1 PSM, respectively. Additionally, unmodified peptides containing K564 and K690 were detected for HlyA (5 and 7 PSM, respectively) (Fig. 6b). Nevertheless, we assume that the vast majority of HlyA proteins are acylated as in proHlyA no acylated peptides were determined, but unmodified peptide variants including K564 and K690 with 114 and 68 PSM, respectively. The *E. coli* BL21(DE3) pK184 *hlyBD* system without co-expression of HlyC secretes approximately 2-3 times more proHlyA than proMbxA which may be due to a generally higher expression of proHlyA. Taking in consideration that likewise in the presence of HlyC the proHlyA levels in the *E. coli* cytosol are probably higher than proMbxA levels it is likely that the relative acylation efficiency is lower for HlyA. This could explain the proportion of unmodified K564 and K690 fragments (Fig. 6b). Interestingly, the ratio of acylation of the two sites is inverses. While in MbxA the first site is more efficiently acylated, the second site showed a more efficient acylation in HlyA, although the same acyltransferase catalyzed the reaction. The presence of peptides resulting from cleavage directly after the less frequently detected second acylation site of MbxA and the

first acylation site of HlyA further indicates that these sites were not fully acylated as a modification would have masked the cleavage site (Tab. S1).

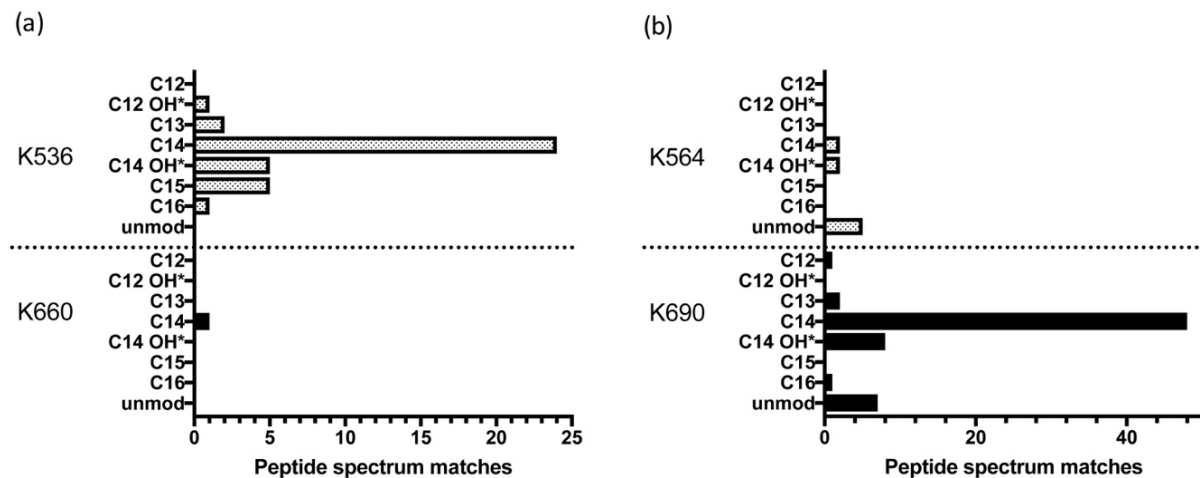


Figure 6: MS analysis of MbxA acylation (a) and HlyA acylation (b). MbxA and HlyA were *in vivo* acylated by co-expressing HlyC [40]. For both acylation sites in MbxA and HlyA, K536 and K660 or K564 and K690 respectively, all detected acyl modifications ranging from C₁₂ to C₁₆ fatty acids including hydroxy fatty acids are shown with the according number of recorded PSM. Mass shifts contributing to hydroxy fatty acids could possibly alternatively originate from the oxidation of tyrosine residues in the peptide fragment and PSM of supposed hydroxy acylations are therefore marked (*). For proMbxA and proHlyA expressed in the absence of HlyC, only unmodified peptides were detected. Acyl modifications were detected only in peptides covering the predicted lysine residues K536 and K660 of MbxA. The PSM of C₁₄ modified sequences suggest that the predominant modification is myristoylation.

The analysis of the *in vivo* acylation of HlyA by HlyC confirms the acylation of the K564 and K690 acylation sites. Similar to MbxA, C₁₄ and C₁₄-OH* acylations account for the majority of PSM of acyl modified peptides in HlyA.

MbxA is cytotoxic to human epithelial cells and T cells

After acylated MbxA displayed hemolytic activity on sheep blood agar, human epithelial cells (HEp-2) and human T cells (Jurkat) were tested for their susceptibility to MbxA with a lactate dehydrogenase (LDH) release assay. Leakage of cytosolic LDH from treated cells into the supernatant serves as an indicator for membrane damage and subsequent cell death. HEp-2 cells and Jurkat cells were incubated with a serial dilution of purified MbxA of 1000 – 0 nM or 500 – 0 nM, respectively, for 1 h. Both cells lines were susceptible to MbxA-induced membrane damage and showed a sigmoidal dose-response curve with increasing MbxA concentrations (Fig. 7). The half maximal effect (cytotoxic dose 50, CD₅₀) of MbxA against

HEp-2 cells occurred at a concentration of 28.1 ± 4.7 nM. For Jurkat cells 50% cytotoxicity were reached at a slightly lower concentration of MbxA resulting in a CD_{50} of 17.7 ± 3.9 nM. proMbxA displayed no cytotoxic effect after 1 h. The calculation of the CD_{50} values was performed under the assumption that the entire pool of MbxA is active. Thus, the values reported likely correspond to CD_{50} values which are too high. This demonstrates that MbxA is toxic to both epithelial and T cells in a similar concentration range, but strictly requires activation by acylation to confer membrane-damaging activity.

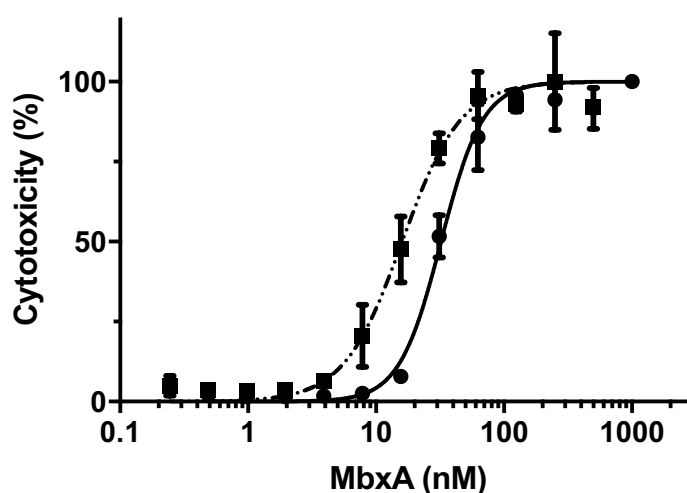


Figure 7: MbxA is cytotoxic to human epithelial cells (HEp-2, ●) and human T cells (Jurkat, ■), respectively. The cytotoxicity mediated by MbxA-induced membrane damage was measured using an LDH release assay. LDH release into the supernatant was measured after 1 h of incubation with MbxA. The cytotoxicity was calculated from the maximal LDH release reached in each measurement. For the CD_{50} determination the MbxA cytotoxicity was plotted against the MbxA concentration and fitted with GraphPad Prism 7 according to equation 2 (see materials and methods). For simplicity, measurements with proMbxA were not included as no LDH release, even at concentrations of 1 μ M, was detected.

proMbxA cannot protect human cells from MbxA-induced membrane damage

As proMbxA did not display any cytotoxicity against epithelial cells or T cells we further proceeded to assess if proMbxA can protect any potential MbxA binding sites on the surface of human cells. Preincubation with 250 nM of proMbxA for 30 min before addition of a serial dilution of active MbxA to HEp-2 cells and Jurkat had no effect on the dose-response curve and the CD_{50} value compared to MbxA alone (Fig. 8). The presence of proMbxA did not decrease the sensitivity of any of the two cell lines. This indicates that proMbxA cannot bind to a putative receptor and fails to prevent the subsequent interaction of MbxA with the cells.

Also, an unspecific shielding can be excluded as a comparison of the calculated surface area covered by all proMbxA molecules with the calculated surface area of the treated HEp-2 cells indicated that the amount of proMbxA is sufficient to cover the entire cell surface.

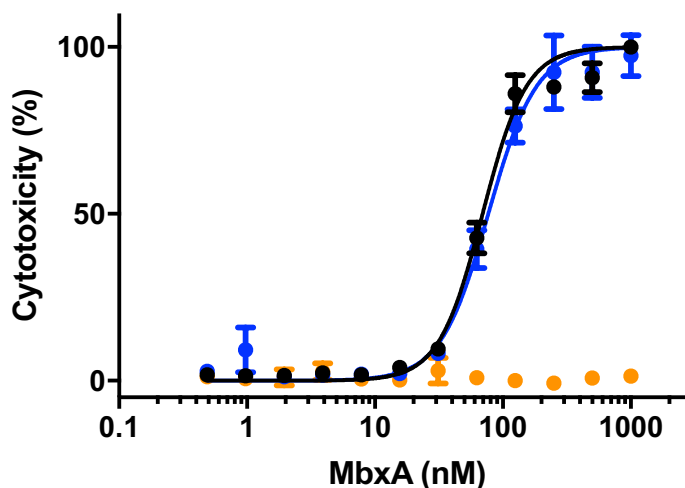


Figure 8: proMbxA does not protect epithelial cells (HEp-2) from MbxA induced membrane damage. Preincubation with 250 nM of proMbxA resulted in a nearly identical dose-response curve to MbxA (blue) compared to treatment with MbxA alone (black). proMbxA was not cytotoxic (orange). The cytotoxicity mediated by MbxA induced membrane damage was measured using an LDH release assay. LDH release into the supernatant was measured after 1 h of incubation with MbxA. The cytotoxicity was calculated from the maximal LDH release reached in each measurement. For the CD_{50} determination the MbxA cytotoxicity was plotted against the MbxA concentration and fitted with GraphPad Prism 7 according to equation 2 (see material and methods).

MbxA induces membrane permeabilization and membrane blebbing in HEp-2 cells

To study the MbxA-induced membrane damage in more detail, we turned to live cell imaging to investigate if changes in the membrane morphology of HEp-2 cells occur. HEp-2 cells were treated with 250 nM of MbxA or proMbxA and images were taken every 10 s over a total time course of 20 min. To visualize changes of the membrane morphology, we applied Wheat Germ Agglutinin conjugated with Alexa Fluor 488 (WGA-488) as a plasma membrane marker. In parallel, propidium iodide (PI) fluorescence was measured to monitor possible permeabilization of the cells. Upon addition of 250 nM MbxA the HEp-2 cell plasma membrane showed changes already during the first minute by forming bulges. These bulges grew until they appeared as spherical bleb-like shapes approximately 4 min after MbxA addition. During 20 min of live-cell imaging the membrane blebs grew in size but remained stable in position and large blebs

did not retract or visibly fuse with other membrane bulges (Fig. S3). Typical blebs reached a size of approximately 10 μm . WGA-488-positive labeling at the spherical protrusions underlined that protrusions were formed by the HEp-2 plasma membrane (Fig. 9). During measurements, the WGA-488 signal of membrane blebs appeared less intense than the original plasma membrane. A possible explanation is a dilution-like effect of WGA-488 labeled glycoconjugates on the expanded membrane. While the membrane is expanding due to blebbing the concentration of glycoconjugates stays the same resulting in much less glycoconjugates per surface area than before. Since glycoconjugates tend to form a network-like structure on the cell surface known as glycocalyx, which is the target of WGA-488 [50], and may be associated with the cortical cytoskeleton [51], a rapid diffusion-like behavior of the WGA-488 signal to the bleb membrane is rather unlikely. Furthermore, the weaker stained membrane blebs observed here are consistent with previously observed staining [52].

The MbxA-induced permeabilization was visualized by influx and accumulation of PI in the nuclei. The initially low intensity of the PI signal in the cytoplasm appeared with a delay compared to membrane blebbing. Plotting the increase of PI fluorescence against the incubation time though revealed an almost linear increase of intensity (Fig. 10). This implies that HEp-2 cells were almost immediately permeable for PI after contact with MbxA and PI influx remained during the entire imaging period. Subsequently, we challenged HEp-2 cells with 30 nM of MbxA, a concentration around the CD_{50} determined by the LDH release assay and 10 nM, a concentration that resulted in minimal effects (Fig. 7). For these concentrations, a prolonged imaging time of 90 min was applied (Fig. S4 and S5). HEp-2 cells treated with 30 nM of MbxA showed a delayed development of the blebbing phenotype, but after 5 min membrane bulges were visible. After 20 min the membrane blebs reached a similar size as in the treatment with 250 nM and continued to expand during 90 min of imaging (Fig. S5). The mean intensity of PI increased continuously during the incubation, but less steep than compared to 250 nM of MbxA (Fig. 7). In the case of 10 nM MbxA, smaller membrane bulges were visible only after 20 min going in hand with a small slope of PI fluorescence increase. After an incubation time of 90 min small bulges as well as large blebs of approximately 10 μm were visible, but the frequency of large spherical blebs compared to treatment with 250 nM or 30 nM was lower. At the end of 90 min of imaging nuclei showed a significant PI staining (Fig. S5). Incubation of HEp-2 cells with proMbxA did not show any visible changes in the membrane morphology over a period of 20 min. Additionally, no increase in PI signal intensity was detected indicating preserved plasma membrane integrity.

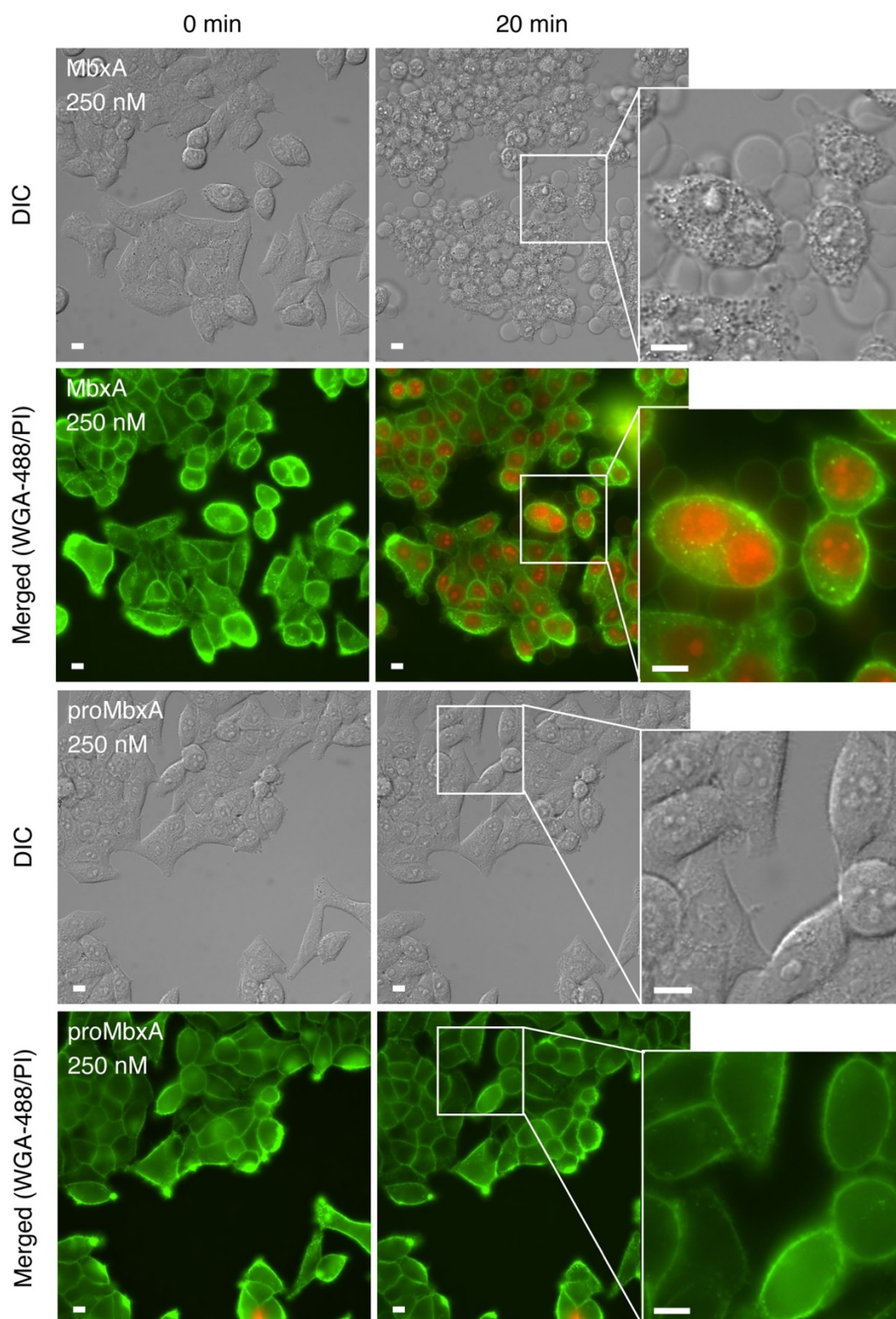


Figure 9: Live cell imaging of MbxA-induced membrane damage in Hep-2 cells. Hep-2 cells were treated with 250 nM MbxA (first and second row) or 250 nM proMbxA (third and fourth row) for 20 min. DIC images display the overall cell morphology. Membranes were stained with WGA-488 and membrane permeability was monitored with PI shown as merged images in the second and fourth row. proMbxA did not induce membrane damage while MbxA induced formation of spherical membrane protrusions and permeabilization, highlighted by the white boxes in the middle row and shown in the insets in the right row, indicated with arrows (Scalebar 10 μ m).

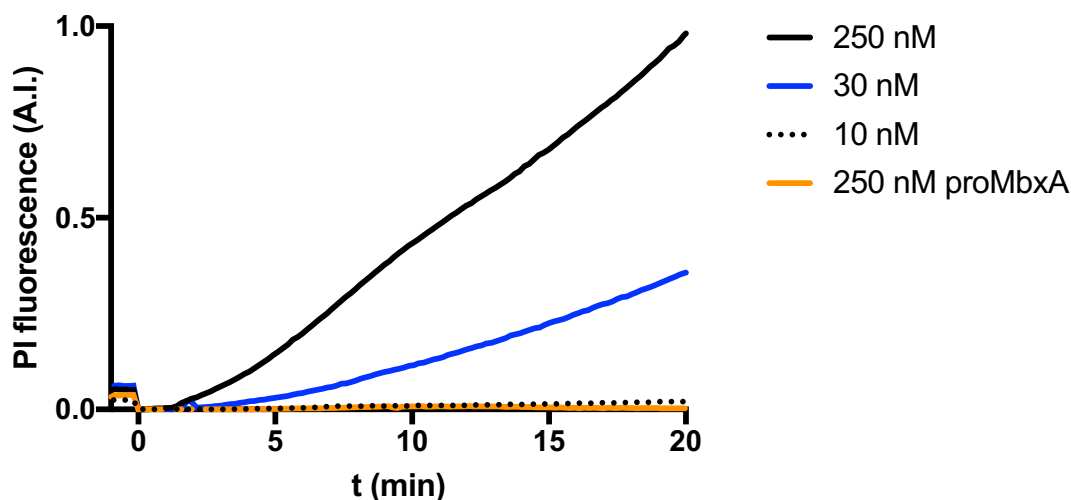


Figure 10: MbxA-induced permeabilization of HEp-2 cells. The relative mean intensity (arbitrary intensity A.I.) of the PI fluorescence was plotted against the time (min) of live cell imaging. Three concentrations of MbxA (250 nM, 30 nM, 10 nM) and 250 nM of proMbxA were tested. One representative measurement of two experiments is shown.

Discussion

MbxA is a cytotoxin of the bovine pathogen *M. bovis* and belongs to the RTX protein family [27]. As an RTX toxin, MbxA is characterized by five conserved Ca^{2+} binding repeats that form the RTX domain and is likely secreted via a cognate T1SS. The necessary tripartite secretion system assumed to secrete MbxA is encoded with an activating acyltransferase and the toxin gene on a pathogenicity island in the *M. bovis* genome [53]. The presence of an intact RTX operon and cytotoxicity of *M. bovis* culture supernatant allows the conclusion that the Mbx secretion system is functional [31, 34, 35].

Here we employed the secretion system of HlyA from the uropathogenic *E. coli* strain UTI89, considered a prototype of RTX proteins, to secrete MbxA, creating a heterologous T1SS with components from two species in *E. coli* BL21(DE3). In our recombinant secretion system the inner membrane components HlyB and HlyD successfully recognize and interact with the secretion signal of MbxA. The C-terminal secretion signals of RTX proteins do not harbor a conserved sequence identifiable by sequence analysis, but are likely recognized by a secondary structure element, presumably an amphipathic helix motif [54]. This suggests that MbxA carries this required information likewise in its C-terminus as it is efficiently transported by the HlyA

system. As a putative pore-forming toxin of the RTX family MbxA requires a post-translational activation by acylation of two internal lysine residues. Therefore, we completed the recombinant secretion system by expression of *E. coli* UTI89 HlyC instead of the putative *M. bovis* acyltransferase MbxC resulting in hemolytically active *E. coli* BL21(DE3) strain (Fig. 2). Both, acylated MbxA and the precursor proMbxA, although in higher amounts, were secreted and facilitated purification from culture supernatants (Fig. 3). This difference in secretion efficiency is similar to proHlyA which is more efficiently secreted than HlyA [16]. Our SEC analysis revealed that for proMbxA a dimer and a monomer are present, while MbxA forms higher oligomeric species, which presumably include dimers (Fig. 4). Similarly, proHlyA forms dimers when purified, but active HlyA is prone to aggregation [16]. On the contrary, for proCyaA acylation favors formation of the active, monomeric CyaA species [55]. Mass spectrometric analysis of cross-acylated MbxA demonstrated that HlyC acylates the predicted lysine residues, K536 and K660, that are homologues to the two acylation sites of HlyA (K564, K690) [26, 27]. HlyC displays a preference for myristic acid as the number of PSM for C₁₄ modified peptides exceeds PSM of C₁₃, C₁₅ or C₁₆ acylated peptides of the first acylation site with 24 PSM compared to 2, 5 or 1 PSM respectively. Additionally potential C₁₂-OH* and C₁₄-OH* hydroxy acylations were detected at the first acylation site with 2 and 1 PSM respectively. The second acylation site is only found to be myristoylated (Fig. 6). We observed a similar preference for myristoylation and a similar variety of fatty acids utilized for modification of HlyA including C₁₂, C₁₃, C₁₄, C₁₄-OH* and C₁₆ acyl chains. In contrast to MbxA, where the first acylation site is modified with different fatty acids, in the case of HlyA variable modifications are detected at the second acylation site. The first lysine residue, K564, is only modified with either C₁₄ or C₁₄-OH* fatty acids. Previous studies already showed that HlyA is predominantly myristoylated but reported a substantial percentage of C₁₅ and C₁₇ modifications of up to 32% [56], which we did not observe. Another recent study underlined the preference of HlyC for C₁₄ and C₁₄-OH fatty acids and reported that the acylation pattern and choice of acylation sites is inherent to the acyltransferase [57]. At the same time, our study shows that the acylation is not solely controlled by the acyltransferase as we observed that HlyC acylates the first acylation site with a variety of fatty acids in MbxA, while for HlyA more variation of the modification is found at the second site. Interestingly, in this report mono-acylation of the second acylation site was also observed for the active species, while our study and the study of Stanley *et al.* [26] demonstrated that the double acylated version represents the active species. Assuming that the relative efficiency of acylation partially depends on the amount of the RTX protein present in the bacterial cytosol prior to secretion, the unmodified fragments of HlyA

detected in our system reflect its higher expression levels compared to MbxA. A very high level expression of the RTX protein that results in inclusion body formation as given in the study of Osickova *et al.* [57] may explain the incomplete modification of the first acylation site. The present acyltransferase possibly does not achieve full acylation of the RTX protein pool. Altogether, the HlyA system can successfully replace the complete T1SS of another RTX substrate and facilitate its recombinant activation and secretion in *E. coli*.

In contrast to previous studies focusing on the activity of MbxA against bovine cells [31-33, 58] we demonstrated cytotoxicity of MbxA outside of its known target species. Besides the hemolytic activity towards sheep erythrocytes, MbxA exhibited cytotoxic activity against human epithelial cells (HEp-2) and human T cells (Jurkat) as we demonstrated using an LDH release assay (Fig. 7). proMbxA did not induce any LDH release indicating that acylation of MbxA was strictly required for its cytotoxicity. Additionally preincubation with unmodified proMbxA was not able to block interaction of MbxA with epithelial cells and T cells or hamper MbxA-induced membrane damage (Fig. 8). This suggests that without the fatty acid-acylation proMbxA cannot successfully bind potential receptors or surface structures on the human cells. For an efficient interaction MbxA depends on the acylation. This confirms that MbxA as a representative of RTX pore-forming toxins relies on post-translational acylation. The necessity of acylation for cytotoxicity was previously shown for different RTX toxins and is linked to oligomerization, irreversible insertion into the membrane or an effective binding to a host cell receptor [26, 46-48, 59-61]. At the same time acylation is not required for binding to and insertion into membranes or pore-formation [39, 62, 63].

The cytotoxicity of MbxA, a toxin from a bovine pathogen, against human epithelial cell or leukocytes was, with a CD_{50} value of 28.1 ± 4.7 nM or 17.7 ± 3.9 nM (Fig. 7), similar to the activity reported for RTX toxins of human pathogens underlining that its activity is not confined to specific structures of bovine cells. HlyA for example is active at CD_{50} values ranging from approximately 0.2 nM to 30 nM depending on the cell line [64]. The pore-forming activity of MbxA was described for bovine erythrocytes, in which MbxA induces leakage of K^+ , cell swelling and finally lysis by forming pores of an estimated size of 0.9 nm [34]. We performed live cell imaging of HEp-2 cells challenged with MbxA and observed a distinct change in the membrane morphology. Besides permeabilization of the membrane, spherical membrane protrusions were induced by MbxA at concentrations ranging from 10 nM to 250 nM, but importantly not by proMbxA (Fig. 9). The formation of these protrusions was reminiscent of membrane blebbing, a phenomenon that is a part of apoptosis and necrosis [65, 66], but is also observed in healthy cells during cell division, spreading and migration [67-69]. Membrane

blebs form either when an increased intracellular pressure leads to tearing of the membrane from the cytoskeleton or when the actin cortex itself breaks and the excess membrane subsequently inflates [70-72]. The lesions induced by MbxA probably might lead to an increase in the cell pressure by influx of medium which then leads to inflation of the excess membrane forming the bleb-like structure. In contrast to blebbing in healthy cells, the blebs observed in this study did not retract and were stable during an imaging time of 90 min (Fig. S5). The nearly linear increase of PI fluorescence upon MbxA treatment was steeper if higher toxin concentrations were applied (Fig. 10). This indicates that the cell membrane is immediately permeabilized after contact with MbxA and the number of pores and possibly also the size of the pores increases with increasing toxin concentrations.

Although membrane blebbing is a hallmark of the execution phase of apoptosis, cell shrinkage and chromatin condensation of the nucleus are observed first. Additionally, the membrane remains intact while membrane blebs form [73, 74]. In apoptotic cells, membrane blebbing ends approximately after an hour leading to fragmentation by formation of apoptotic bodies [75], a process we did not observe in HEp-2 cells. In our case, blebbing is rather an immediate consequence of MbxA-induced damage compared to a programmed process, in which apoptosis is first activated through an apoptotic pathway before changes in the membrane morphology occur. Opposing to a programmed cell death, necrosis involves swelling of the cell and blebbing occurs later than in apoptosis, presumably caused by influx of water and ions [66, 76]. Cholesterol-dependent cytolysins (CDCs), a family of pore-forming toxins, were shown to induce a passive and rapid membrane blebbing in human cells in response to permeabilization. This is not only a sign of membrane damage, but can act as a protection mechanism after membrane permeabilization. The blebbing traps injured regions and thereby reduces efflux of cytosol or even promotes removal of the toxin by shedding of the blebs [77-79]. Regardless of the origin of the blebbing phenotype induced by MbxA, several RTX toxins are reported to induce variants of programmed cell death. For example, LktA from *Mannheimia haemolytica*, CyaA and enterohemorrhagic *E. coli* hemolysin induce apoptosis [80-82], while other studies link HlyA to programmed necrosis, induction of pyroptosis or induction of host cell proteolysis [83-85]. This indicates that MbxA probably harbors underlying cytotoxic functions targeting its host cell.

In summary, we demonstrated that the *M. bovis* cytotoxin MbxA is secreted and acylated by the UPEC HlyA system in an *E. coli* lab strain, which allowed purification of proMbxA and MbxA from *E. coli* culture supernatants. *E. coli* UTI89 HlyC efficiently acylated MbxA at the two predicted lysine residues with predominantly C₁₄ fatty acids. The acylation of MbxA is

necessary for activity against sheep RBC, human epithelial and human T cells as proMbxA did not exert any cytotoxicity. The cytotoxicity studies showed that MbxA is not species- or cell type-specific and active against human cells in a nanomolar range. Live cell imaging revealed an immediate permeabilization and membrane blebbing upon contact with MbxA probably due to its pore-forming activity.

Acknowledgments

We would like to thank Diana Kleinschrodt for valuable support and all members of the Institute of Biochemistry for fruitful discussions. We would also like to thank former students Nicole Jasny and Fabian Adamek. This study was funded by the Jürgen Manchot Graduate School “Molecules of Infection III” (to L.S.) and by the GRK 2158 of the Deutsche Forschungsgemeinschaft (to S.S. and S.W.).

References

1. Rasko, D.A. and Sperandio, V., *Anti-virulence strategies to combat bacteria-mediated disease*. Nat Rev Drug Discov, 2010. **9**(2): p. 117-28.
2. Krueger, E. and Brown, A.C., *Inhibition of bacterial toxin recognition of membrane components as an anti-virulence strategy*. J Biol Eng, 2019. **13**: p. 4.
3. Linhartova, I., Bumba, L., Masin, J., Basler, M., Osicka, R., Kamanova, J., Prochazkova, K., Adkins, I., Hejnova-Holubova, J., Sadilkova, L., Morova, J., and Sebo, P., *RTX proteins: a highly diverse family secreted by a common mechanism*. FEMS Microbiol Rev, 2010. **34**(6): p. 1076-112.
4. Welch, R.A., *Pore-forming cytolytins of Gram-negative bacteria*. Molecular Microbiology, 1991. **5**: p. 521-528.
5. Baumann, U., Wu, S., Flaherty, K.M., and McKay, D.B., *Three-dimensional structure of the alkaline protease of Pseudomonas aeruginosa: a two-domain protein with a calcium binding parallel beta roll motif*. EMBO J, 1993. **12**(9): p. 3357-64.
6. Gray, L., Mackman, N., Nicaud, J.M., and Holland, I.B., *The Carboxy-Terminal Region of Hemolysin 2001 Is Required for Secretion of the Toxin from Escherichia-Coli*. Molecular & General Genetics, 1986. **205**(1): p. 127-133.
7. Felmler, T. and Welch, R.A., *Alterations of amino acid repeats in the Escherichia coli hemolysin affect cytolytic activity and secretion*. Proc Natl Acad Sci U S A, 1988. **85**(14): p. 5269-73.
8. Koronakis, V., Koronakis, E., and Hughes, C., *Isolation and Analysis of the C-Terminal Signal Directing Export of Escherichia-Coli Hemolysin Protein across Both Bacterial-Membranes*. Embo Journal, 1989. **8**(2): p. 595-605.
9. Mackman, N., Nicaud, J.M., Gray, L., and Holland, I.B., *Identification of polypeptides required for the export of haemolysin 2001 from E. coli*. Mol Gen Genet, 1985. **201**(3): p. 529-36.

10. Mackman, N., Nicaud, J.M., Gray, L., and Holland, I.B., *Genetical and functional organisation of the Escherichia coli haemolysin determinant 2001*. Mol Gen Genet, 1985. **201**(2): p. 282-8.
11. Wang, R.C., Seror, S.J., Blight, M., Pratt, J.M., Broome-Smith, J.K., and Holland, I.B., *Analysis of the membrane organization of an Escherichia coli protein translocator, HlyB, a member of a large family of prokaryote and eukaryote surface transport proteins*. J Mol Biol, 1991. **217**(3): p. 441-54.
12. Wandersman, C. and Delepelaire, P., *TolC, an Escherichia coli outer membrane protein required for hemolysin secretion*. Proc Natl Acad Sci U S A, 1990. **87**(12): p. 4776-80.
13. Gray, L., Baker, K., Kenny, B., Mackman, N., Haigh, R., and Holland, J.B., *A Novel C-Terminal Signal Sequence Targets Escherichia-Coli Hemolysin Directly to the Medium*. Journal of Cell Science, 1989: p. 45-57.
14. Bakkes, P.J., Jenewein, S., Smits, S.H.J., Holland, I.B., and Schmitt, L., *The Rate of Folding Dictates Substrate Secretion by the Escherichia coli Hemolysin Type 1 Secretion System*. Journal of Biological Chemistry, 2010. **285**(52): p. 40573-40580.
15. Ostolaza, H., Soloaga, A., and Goni, F.M., *The Binding of Divalent-Cations to Escherichia-Coli Alpha-Hemolysin*. European Journal of Biochemistry, 1995. **228**(1): p. 39-44.
16. Thomas, S., Bakkes, P.J., Smits, S.H., and Schmitt, L., *Equilibrium folding of pro-HlyA from Escherichia coli reveals a stable calcium ion dependent folding intermediate*. Biochim Biophys Acta, 2014. **1844**(9): p. 1500-10.
17. Sebo, P. and Ladant, D., *Repeat sequences in the Bordetella pertussis adenylate cyclase toxin can be recognized as alternative carboxy-proximal secretion signals by the Escherichia coli alpha-haemolysin translocator*. Mol Microbiol, 1993. **9**(5): p. 999-1009.
18. Thompson, S.A. and Sparling, P.F., *The RTX cytotoxin-related FrpA protein of Neisseria meningitidis is secreted extracellularly by meningococci and by HlyBD+ Escherichia coli*. Infect Immun, 1993. **61**(7): p. 2906-11.
19. Kuhnert, P., Heyberger-Meyer, B., Nicolet, J., and Frey, J., *Characterization of PaxA and its operon: a cohemolytic RTX toxin determinant from pathogenic Pasteurella aerogenes*. Infect Immun, 2000. **68**(1): p. 6-12.
20. Highlander, S.K., Engler, M.J., and Weinstock, G.M., *Secretion and expression of the Pasteurella haemolytica Leukotoxin*. J Bacteriol, 1990. **172**(5): p. 2343-50.
21. Zhang, F., Greig, D.I., and Ling, V., *Functional replacement of the hemolysin A transport signal by a different primary sequence*. Proc Natl Acad Sci U S A, 1993. **90**(9): p. 4211-5.
22. Bhakdi, S., Greulich, S., Muhly, M., Eberspacher, B., Becker, H., Thiele, A., and Hugo, F., *Potent leukocidal action of Escherichia coli hemolysin mediated by permeabilization of target cell membranes*. J Exp Med, 1989. **169**(3): p. 737-54.
23. Keane, W.F., Welch, R., Gekker, G., and Peterson, P.K., *Mechanism of Escherichia coli alpha-hemolysin-induced injury to isolated renal tubular cells*. Am J Pathol, 1987. **126**(2): p. 350-7.
24. Suttorp, N., Floer, B., Schnittler, H., Seeger, W., and Bhakdi, S., *Effects of Escherichia coli hemolysin on endothelial cell function*. Infect Immun, 1990. **58**(11): p. 3796-801.

25. Nicaud, J.M., Mackman, N., Gray, L., and Holland, I.B., *Characterisation of HlyC and mechanism of activation and secretion of haemolysin from E. coli 2001*. FEBS Lett, 1985. **187**(2): p. 339-44.
26. Stanley, P., Packman, L.C., Koronakis, V., and Hughes, C., *Fatty acylation of two internal lysine residues required for the toxic activity of Escherichia coli hemolysin*. Science, 1994. **266**(5193): p. 1992-6.
27. Angelos, J.A., Hess, J.F., and George, L.W., *Cloning and characterization of a Moraxella bovis cytotoxin gene*. Am J Vet Res, 2001. **62**(8): p. 1222-8.
28. Beard, M.K. and Moore, L.J., *Reproduction of bovine keratoconjunctivitis with a purified haemolytic and cytotoxic fraction of Moraxella bovis*. Vet Microbiol, 1994. **42**(1): p. 15-33.
29. Henson, J.B. and Grumbles, L.C., *Infectious Bovine Keratoconjunctivitis .1. Etiology*. American Journal of Veterinary Research, 1960. **21**(84): p. 761-766.
30. Baptista, P.J., *Infectious bovine keratoconjunctivitis: a review*. Br Vet J, 1979. **135**(3): p. 225-42.
31. Høien-Dalen, P.S., Rosenbusch, R.F., and Roth, J.A., *Comparative characterization of the leukocidal and hemolytic activity of Moraxella bovis*. Am J Vet Res, 1990. **51**(2): p. 191-6.
32. Kagonyera, G.M., George, L.W., and Munn, R., *Cytopathic effects of Moraxella bovis on cultured bovine neutrophils and corneal epithelial cells*. Am J Vet Res, 1989. **50**(1): p. 10-7.
33. Kagonyera, G.M., George, L., and Miller, M., *Effects of Moraxella bovis and culture filtrates on 51Cr-labeled bovine neutrophils*. Am J Vet Res, 1989. **50**(1): p. 18-21.
34. Clinkenbeard, K.D. and Thiessen, A.E., *Mechanism of action of Moraxella bovis hemolysin*. Infect Immun, 1991. **59**(3): p. 1148-52.
35. Angelos, J.A., Hess, J.F., and George, L.W., *An RTX operon in hemolytic Moraxella bovis is absent from nonhemolytic strains*. Vet Microbiol, 2003. **92**(4): p. 363-77.
36. Ludwig, A., Schmid, A., Benz, R., and Goebel, W., *Mutations affecting pore formation by haemolysin from Escherichia coli*. Mol Gen Genet, 1991. **226**(1-2): p. 198-208.
37. Dobson, L., Remenyi, I., and Tusnady, G.E., *CCTOP: a Consensus Constrained TOPology prediction web server*. Nucleic Acids Res, 2015. **43**(W1): p. W408-12.
38. Madeira, F., Park, Y.M., Lee, J., Buso, N., Gur, T., Madhusoodanan, N., Basutkar, P., Tivey, A.R.N., Potter, S.C., Finn, R.D., and Lopez, R., *The EMBL-EBI search and sequence analysis tools APIs in 2019*. Nucleic Acids Res, 2019. **47**(W1): p. W636-W641.
39. Soloaga, A., Ostolaza, H., Goni, F.M., and de la Cruz, F., *Purification of Escherichia coli pro-haemolysin, and a comparison with the properties of mature alpha-haemolysin*. Eur J Biochem, 1996. **238**(2): p. 418-22.
40. Thomas, S., Smits, S.H.J., and Schmitt, L., *A simple in vitro acylation assay based on optimized HlyA and HlyC purification*. Analytical Biochemistry, 2014. **464**: p. 17-23.
41. Khosa, S., Scholz, R., Schwarz, C., Trilling, M., Hengel, H., Jaeger, K.E., Smits, S.H.J., and Schmitt, L., *An A/U-Rich Enhancer Region Is Required for High-Level Protein Secretion through the HlyA Type I Secretion System*. Appl Environ Microbiol, 2018. **84**(1).

42. Kanonenberg, K., Smits, S.H.J., and Schmitt, L., *Functional Reconstitution of HlyB, a Type I Secretion ABC Transporter, in Saposin-A Nanoparticles*. Sci Rep, 2019. **9**(1): p. 8436.
43. Grube, L., Dellen, R., Kruse, F., Schwender, H., Stuhler, K., and Poschmann, G., *Mining the Secretome of C2C12 Muscle Cells: Data Dependent Experimental Approach To Analyze Protein Secretion Using Label-Free Quantification and Peptide Based Analysis*. J Proteome Res, 2018. **17**(2): p. 879-890.
44. Hormozi, K., Parton, R., and Coote, J., *Target cell specificity of the Pasteurella haemolytica leukotoxin is unaffected by the nature of the fatty-acyl group used to activate the toxin in vitro*. Fems Microbiology Letters, 1998. **169**(1): p. 139-145.
45. Fong, K.P., Tang, H.Y., Brown, A.C., Kieba, I.R., Speicher, D.W., Boesze-Battaglia, K., and Lally, E.T., *Aggregatibacter actinomycetemcomitans leukotoxin is post-translationally modified by addition of either saturated or hydroxylated fatty acyl chains*. Mol Oral Microbiol, 2011. **26**(4): p. 262-76.
46. Osickova, A., Balashova, N., Masin, J., Sulc, M., Roderova, J., Wald, T., Brown, A.C., Koufos, E., Chang, E.H., Giannakakis, A., Lally, E.T., and Osicka, R., *Cytotoxic activity of Kingella kingae RtxA toxin depends on post-translational acylation of lysine residues and cholesterol binding*. Emerg Microbes Infect, 2018. **7**(1): p. 178.
47. Basar, T., Havlicek, V., Bezouskova, S., Hackett, M., and Sebo, P., *Acylation of lysine 983 is sufficient for toxin activity of Bordetella pertussis adenylate cyclase. Substitutions of alanine 140 modulate acylation site selectivity of the toxin acyltransferase CyaC*. J Biol Chem, 2001. **276**(1): p. 348-54.
48. Masin, J., Basler, M., Knapp, O., El-Azami-El-Idrissi, M., Maier, E., Konopasek, I., Benz, R., Leclerc, C., and Sebo, P., *Acylation of lysine 860 allows tight binding and cytotoxicity of Bordetella adenylate cyclase on CD11b-expressing cells*. Biochemistry, 2005. **44**(38): p. 12759-66.
49. Issartel, J.P., Koronakis, V., and Hughes, C., *Activation of Escherichia coli prohaemolysin to the mature toxin by acyl carrier protein-dependent fatty acylation*. Nature, 1991. **351**(6329): p. 759-61.
50. Barker, A.L., Konopatskaya, O., Neal, C.R., Macpherson, J.V., Whatmore, J.L., Winlove, C.P., Unwin, P.R., and Shore, A.C., *Observation and characterisation of the glycocalyx of viable human endothelial cells using confocal laser scanning microscopy*. Physical Chemistry Chemical Physics, 2004. **6**(5): p. 1006-1011.
51. Thi, M.M., Tarbell, J.M., Weinbaum, S., and Spray, D.C., *The role of the glycocalyx in reorganization of the actin cytoskeleton under fluid shear stress: A "bumper-car" model*. Proceedings of the National Academy of Sciences of the United States of America, 2004. **101**(47): p. 16483-16488.
52. Jansen, C., Tobita, C., Umemoto, E.U., Starkus, J., Rysavy, N.M., Shimoda, L.M.N., Sung, C., Stokes, A.J., and Turner, H., *Calcium-dependent, non-apoptotic, large plasma membrane bleb formation in physiologically stimulated mast cells and basophils*. J Extracell Vesicles, 2019. **8**(1): p. 1578589.
53. Hess, J.F. and Angelos, J.A., *The Moraxella bovis RTX toxin locus mbx defines a pathogenicity island*. J Med Microbiol, 2006. **55**(Pt 4): p. 443-9.

-
54. Hui, D., Morden, C., Zhang, F., and Ling, V., *Combinatorial analysis of the structural requirements of the Escherichia coli hemolysin signal sequence*. J Biol Chem, 2000. **275**(4): p. 2713-20.
 55. Karst, J.C., Ntsogo Enguene, V.Y., Cannella, S.E., Subrini, O., Hessel, A., Debard, S., Ladant, D., and Chenal, A., *Calcium, acylation, and molecular confinement favor folding of Bordetella pertussis adenylate cyclase CyaA toxin into a monomeric and cytotoxic form*. J Biol Chem, 2014. **289**(44): p. 30702-16.
 56. Lim, K.B., Walker, C.R., Guo, L., Pellett, S., Shabanowitz, J., Hunt, D.F., Hewlett, E.L., Ludwig, A., Goebel, W., Welch, R.A., and Hackett, M., *Escherichia coli alpha-hemolysin (HlyA) is heterogeneously acylated in vivo with 14-, 15-, and 17-carbon fatty acids*. J Biol Chem, 2000. **275**(47): p. 36698-702.
 57. Osickova, A., Khaliq, H., Masin, J., Jurnecka, D., Sukova, A., Fiser, R., Holubova, J., Stanek, O., Sebo, P., and Osicka, R., *Acyltransferase-mediated selection of the length of the fatty acyl chain and of the acylation site governs activation of bacterial RTX toxins*. J Biol Chem, 2020.
 58. Gray, J.T., Fedorka-Cray, P.J., and Rogers, D.G., *Partial characterization of a Moraxella bovis cytolysin*. Vet Microbiol, 1995. **43**(2-3): p. 183-96.
 59. Herlax, V., Mate, S., Rimoldi, O., and Bakas, L., *Relevance of fatty acid covalently bound to Escherichia coli alpha-hemolysin and membrane microdomains in the oligomerization process*. J Biol Chem, 2009. **284**(37): p. 25199-210.
 60. Herlax, V. and Bakas, L., *Acyl chains are responsible for the irreversibility in the Escherichia coli alpha-hemolysin binding to membranes*. Chem Phys Lipids, 2003. **122**(1-2): p. 185-90.
 61. El-Azami-El-Idrissi, M., Bauche, C., Loucka, J., Osicka, R., Sebo, P., Ladant, D., and Leclerc, C., *Interaction of Bordetella pertussis adenylate cyclase with CD11b/CD18: Role of toxin acylation and identification of the main integrin interaction domain*. J Biol Chem, 2003. **278**(40): p. 38514-21.
 62. Ludwig, A., Garcia, F., Bauer, S., Jarchau, T., Benz, R., Hoppe, J., and Goebel, W., *Analysis of the in vivo activation of hemolysin (HlyA) from Escherichia coli*. J Bacteriol, 1996. **178**(18): p. 5422-30.
 63. Benz, R., Maier, E., Ladant, D., Ullmann, A., and Sebo, P., *Adenylate-Cyclase Toxin (Cyaa) of Bordetella-Pertussis - Evidence for the Formation of Small Ion-Permeable Channels and Comparison with Hlya of Escherichia-Coli*. Journal of Biological Chemistry, 1994. **269**(44): p. 27231-27239.
 64. Ristow, L.C., Tran, V., Schwartz, K.J., Pankratz, L., Mehle, A., Sauer, J.D., and Welch, R.A., *The Extracellular Domain of the beta2 Integrin beta Subunit (CD18) Is Sufficient for Escherichia coli Hemolysin and Aggregatibacter actinomycetemcomitans Leukotoxin Cytotoxic Activity*. MBio, 2019. **10**(4).
 65. Mills, J.C., Stone, N.L., Erhardt, J., and Pittman, R.N., *Apoptotic membrane blebbing is regulated by myosin light chain phosphorylation*. J Cell Biol, 1998. **140**(3): p. 627-36.
 66. Barros, L.F., Kanaseki, T., Sabirov, R., Morishima, S., Castro, J., Bittner, C.X., Maeno, E., Ando-Akatsuka, Y., and Okada, Y., *Apoptotic and necrotic blebs in epithelial cells display similar neck diameters but different kinase dependency*. Cell Death Differ, 2003. **10**(6): p. 687-97.

67. Fishkind, D.J., Cao, L.G., and Wang, Y.L., *Microinjection of the catalytic fragment of myosin light chain kinase into dividing cells: effects on mitosis and cytokinesis*. J Cell Biol, 1991. **114**(5): p. 967-75.
68. Norman, L.L., Bragues, J., Sengupta, K., Sens, P., and Aranda-Espinoza, H., *Cell blebbing and membrane area homeostasis in spreading and retracting cells*. Biophys J, 2010. **99**(6): p. 1726-33.
69. Trinkaus, J.P., *Surface activity and locomotion of Fundulus deep cells during blastula and gastrula stages*. Dev Biol, 1973. **30**(1): p. 69-103.
70. Charras, G.T., Yarrow, J.C., Horton, M.A., Mahadevan, L., and Mitchison, T.J., *Non-equilibration of hydrostatic pressure in blebbing cells*. Nature, 2005. **435**(7040): p. 365-9.
71. Paluch, E., Piel, M., Prost, J., Bornens, M., and Sykes, C., *Cortical actomyosin breakage triggers shape oscillations in cells and cell fragments*. Biophys J, 2005. **89**(1): p. 724-33.
72. Charras, G.T., *A short history of blebbing*. J Microsc, 2008. **231**(3): p. 466-78.
73. Kerr, J.F., Wyllie, A.H., and Currie, A.R., *Apoptosis: a basic biological phenomenon with wide-ranging implications in tissue kinetics*. Br J Cancer, 1972. **26**(4): p. 239-57.
74. Elmore, S., *Apoptosis: a review of programmed cell death*. Toxicol Pathol, 2007. **35**(4): p. 495-516.
75. Mills, J.C., Stone, N.L., and Pittman, R.N., *Extranuclear apoptosis. The role of the cytoplasm in the execution phase*. J Cell Biol, 1999. **146**(4): p. 703-8.
76. Barros, L.F., Hermosilla, T., and Castro, J., *Necrotic volume increase and the early physiology of necrosis*. Comp Biochem Physiol A Mol Integr Physiol, 2001. **130**(3): p. 401-9.
77. Randis, T.M., Zaklama, J., LaRocca, T.J., Los, F.C., Lewis, E.L., Desai, P., Rampersaud, R., Amaral, F.E., and Ratner, A.J., *Vaginolysin drives epithelial ultrastructural responses to Gardnerella vaginalis*. Infect Immun, 2013. **81**(12): p. 4544-50.
78. Babiychuk, E.B., Monastyrskaya, K., Potez, S., and Draeger, A., *Blebbing confers resistance against cell lysis*. Cell Death Differ, 2011. **18**(1): p. 80-9.
79. Keyel, P.A., Loutcheva, L., Roth, R., Salter, R.D., Watkins, S.C., Yokoyama, W.M., and Heuser, J.E., *Streptolysin O clearance through sequestration into blebs that bud passively from the plasma membrane*. J Cell Sci, 2011. **124**(Pt 14): p. 2414-23.
80. Wang, J.F., Kieba, I.R., Korostoff, J., Guo, T.L., Yamaguchi, N., Rozmiarek, H., Billings, P.C., Shenker, B.J., and Lally, E.T., *Molecular and biochemical mechanisms of Pasteurella haemolytica leukotoxin-induced cell death*. Microb Pathog, 1998. **25**(6): p. 317-31.
81. Khelef, N. and Guiso, N., *Induction of macrophage apoptosis by Bordetella pertussis adenylate cyclase-hemolysin*. FEMS Microbiol Lett, 1995. **134**(1): p. 27-32.
82. Bielaszewska, M., Ruter, C., Kunsmann, L., Greune, L., Bauwens, A., Zhang, W., Kuczius, T., Kim, K.S., Mellmann, A., Schmidt, M.A., and Karch, H., *Enterohemorrhagic Escherichia coli hemolysin employs outer membrane vesicles to target mitochondria and cause endothelial and epithelial apoptosis*. PLoS Pathog, 2013. **9**(12): p. e1003797.

83. Lu, Y.N., Rafiq, A., Zhang, Z.G., Aslani, F., Fijak, M., Lei, T., Wang, M., Kumar, S., Klug, J., Bergmann, M., Chakraborty, T., Meinhardt, A., and Bhushan, S., *Uropathogenic Escherichia coli* virulence factor hemolysin A causes programmed cell necrosis by altering mitochondrial dynamics. *Faseb Journal*, 2018. **32**(8): p. 4107-4120.
84. Nagamatsu, K., Hannan, T.J., Guest, R.L., Kostakioti, M., Hadjifrangiskou, M., Binkley, J., Dodson, K., Raivio, T.L., and Hultgren, S.J., *Dysregulation of Escherichia coli* alpha-hemolysin expression alters the course of acute and persistent urinary tract infection. *Proc Natl Acad Sci U S A*, 2015. **112**(8): p. E871-80.
85. Dhakal, B.K. and Mulvey, M.A., *The UPEC pore-forming toxin alpha-hemolysin triggers proteolysis of host proteins to disrupt cell adhesion, inflammatory, and survival pathways*. *Cell Host Microbe*, 2012. **11**(1): p. 58-69.

Supplementary information

Molecular characterization of the RTX toxin MbxA from *Moraxella bovis* through a heterologous secretion approach

Isabelle N. Erenburg¹, Sebastian Wintgens², Sebastian Hänsch³, Fabian Stuhldreier⁴, Gereon Poschmann⁵, Olivia Spitz¹, Kai Stühler^{5,6}, Sebastian Wesselborg⁴, Stefanie Weidtkamp-Peters³, Johannes Hegemann², Sander H. J. Smits¹ & Lutz Schmitt^{1,§}

¹: Institute of Biochemistry, Heinrich Heine University Düsseldorf

²: Institute of Functional Microbial Genomics, Heinrich Heine University Düsseldorf

³: Center for Advanced Imaging, Heinrich Heine University Düsseldorf

⁴: Institute of Molecular Medicine I, Heinrich Heine University Düsseldorf

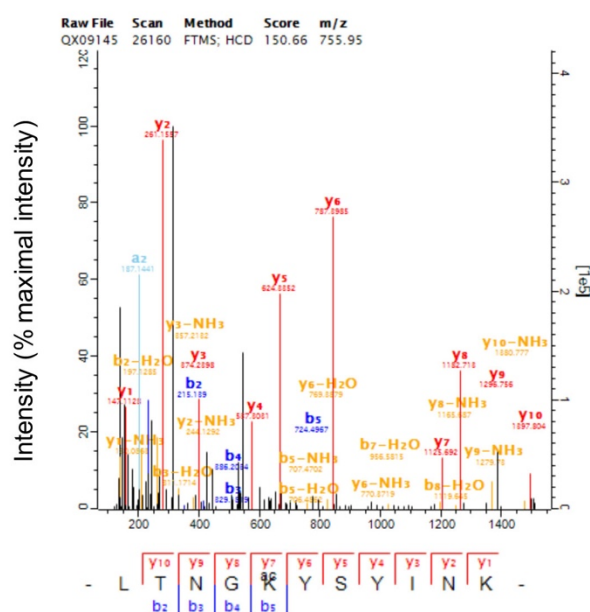
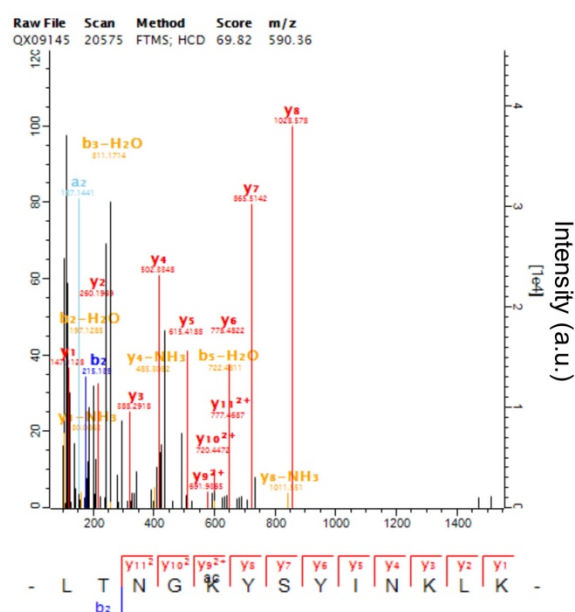
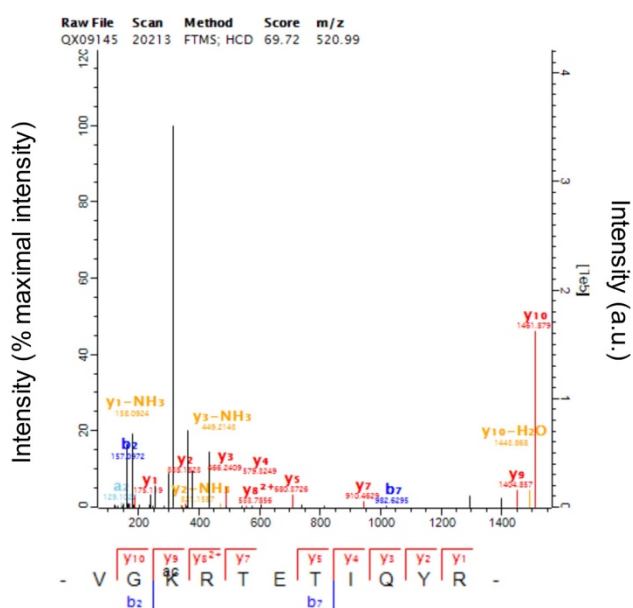
⁵: Institute of Molecular Medicine, Proteome research, Heinrich Heine University Düsseldorf

⁶: Molecular Proteomics Laboratory, Biomedical Research Centre (BMFZ), Heinrich Heine University Düsseldorf

§Corresponding author: Lutz Schmitt, Institute of Biochemistry, Heinrich Heine University Düsseldorf, Universitätsstr. 1, 40225 Düsseldorf, Germany, E-Mail: lutz.schmitt@hhu.de

| | | | | | | | |
|------|-----|----------|---------------|------------------|-----------------------|-----------------------|--------------|
| HlyA | 544 | KFVTPLLT | PGEEIRERRQSG | K Y EYIT | ELLVKGVDKWT | VKGV | 584 |
| | | . | .: | . . | . . | .: | .: |
| MbxA | 516 | HFTSPLL | TAGTESRERLTNG | K YSYINKL | KFGRVKNWQ | VTD- | 555 |
| HlyA | 670 | LG | GDVKVLQ | EVVKEQ | EVSVG | K RTEKTQYRSYEF | THINGKNL 710 |
| | | .. | :.. | . . | . . | . . | .: |
| MbxA | 642 | ARGD-- | IYHEVVKRQ | ETKVG | K RTETIQYRDYEL | RKV-GYGY | 679 |

Figure S1: Sequence alignment of the acylation sites of HlyA sites at lysine residues K564 and K690, which are highlighted in bold. The homologous residues K536 and K660 predicted to be acylated in MbxA are likewise shown in bold.

AK536, C₁₄ acylationK536, C₁₄ hydroxy acylationK660, C₁₄ acylation

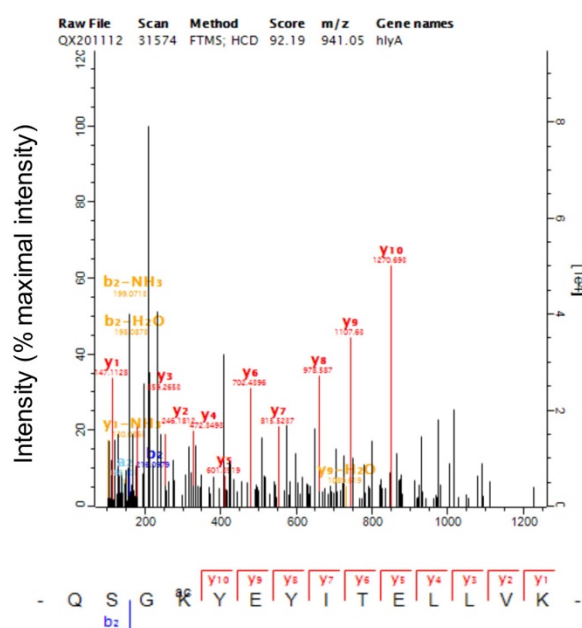
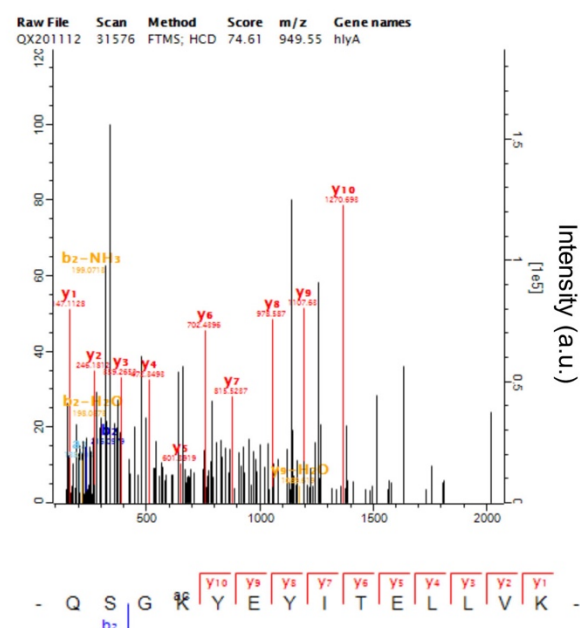
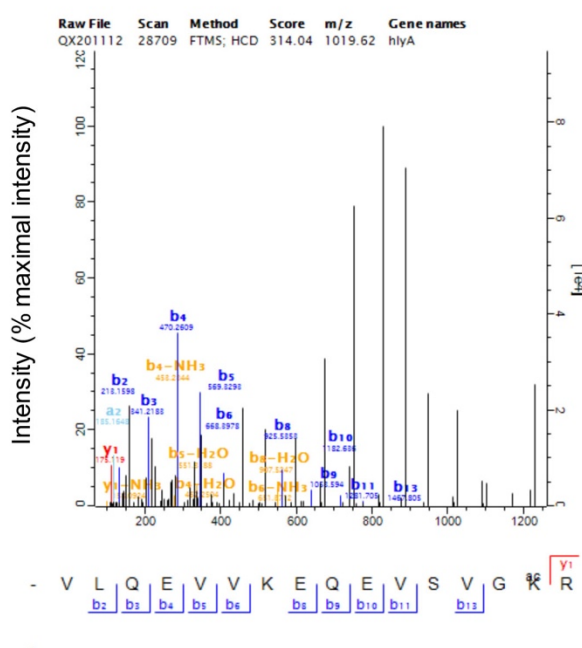
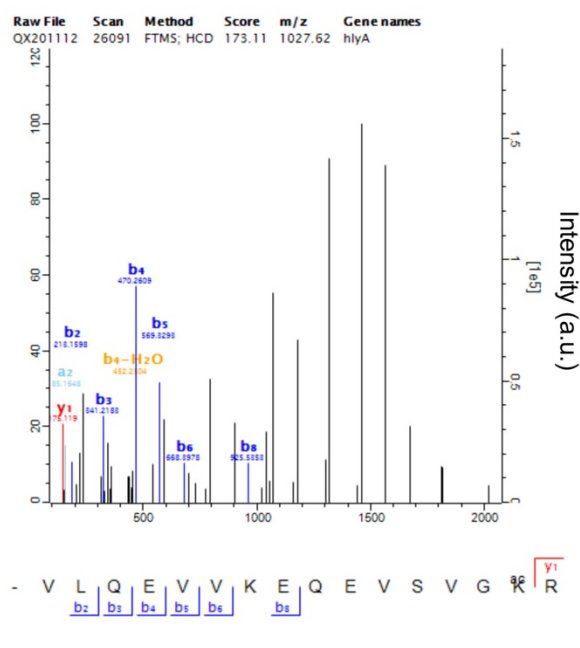
BK564, C₁₄ acylationK564, C₁₄ hydroxy acylationK690, C₁₄ acylationK690, C₁₄ hydroxy acylation

Figure S2: Exemplary MS spectra of the peptides that cover the first, K536, and second acylation site, K660, of MbxA (A) and of the two acylation sites K564 and K690 of HlyA (B) modified with C₁₄ or C₁₄-OH* acylation.

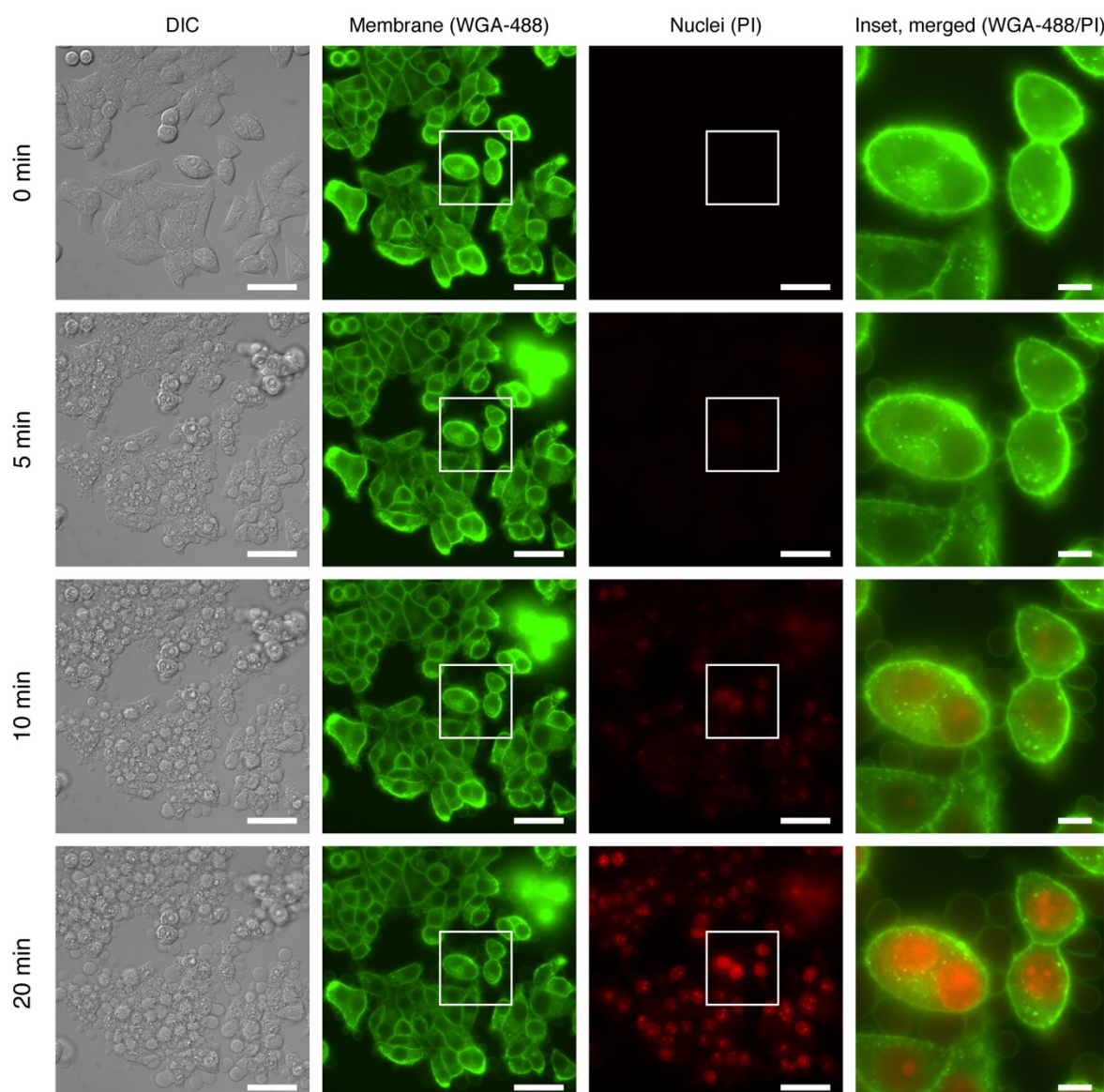


Figure S3: Live cell imaging of HEp-2 cell treated with 250 nM MbxA over a duration of 20 min. MbxA-induced membrane damage is shown after 0 min, 5 min, 10 min and 20 min of treatment with MbxA. DIC images display the overall cell morphology (first row). Membranes were stained with WGA-488 (second row) and membrane permeability was monitored with PI (third row). Growth of spherical membrane protrusions and permeabilization are highlighted by the white boxes in the second and third row and shown in the insets in the right row as a merge of WGA-488 and PI fluorescence.

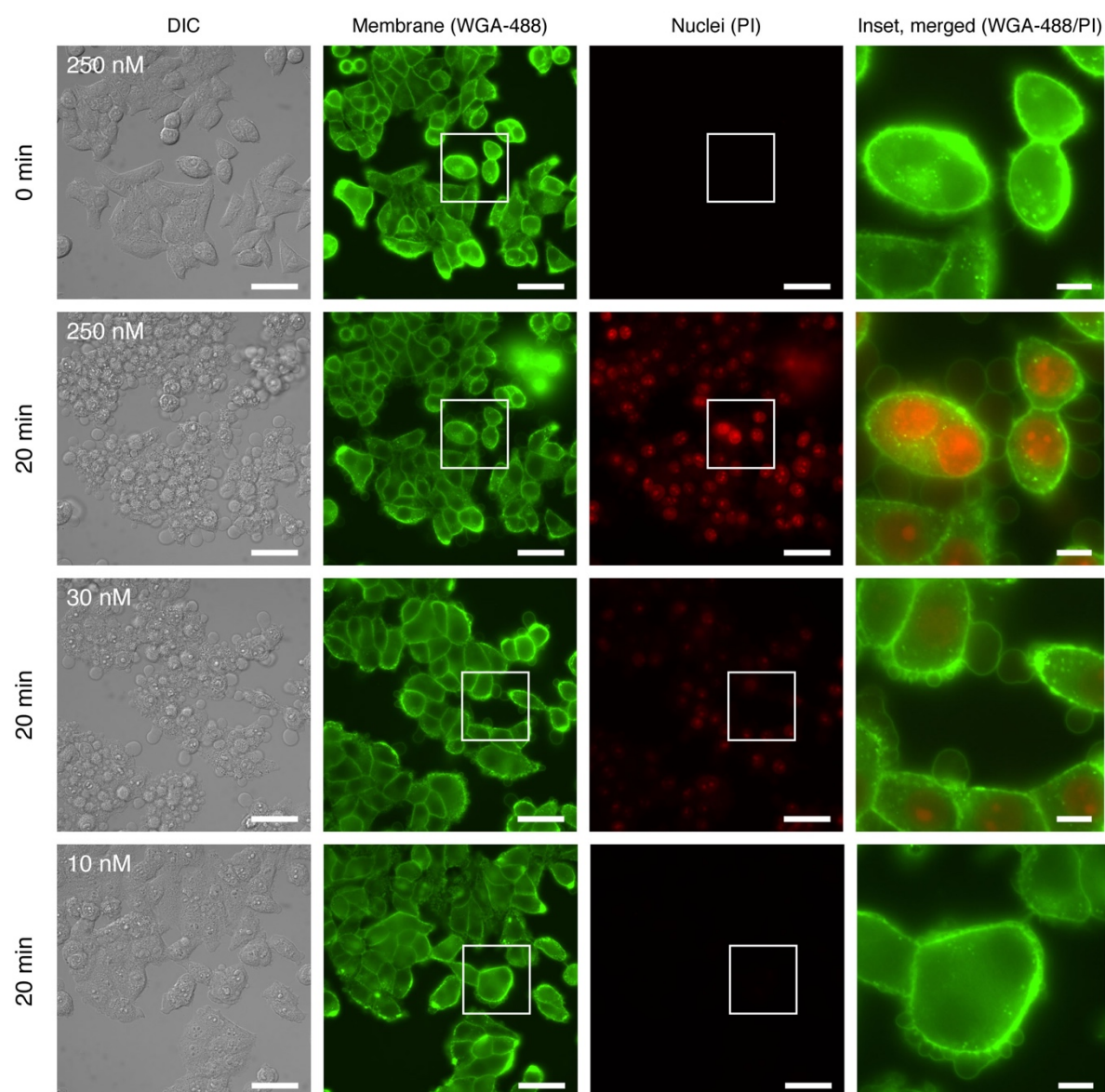


Figure S4: Live cell imaging of HEp-2 cell treated with 250 nM, 30 nM or 10 nM of MbxA over a duration of 20 min. HEp-2 cells exposed to 250 nM of MbxA are shown after 0 min and after 20 min of incubation (first and second row). HEp-2 cells treated with 30 nM and 10 nM are shown after 20 min. Membranes were stained with WGA-488 (second row) and membrane permeability was monitored with PI (third row). Growth of spherical membrane protrusions and permeabilization are highlighted by the white boxes in the second and third row and shown in the insets in the right row as a merge of WGA-488 and PI fluorescence.

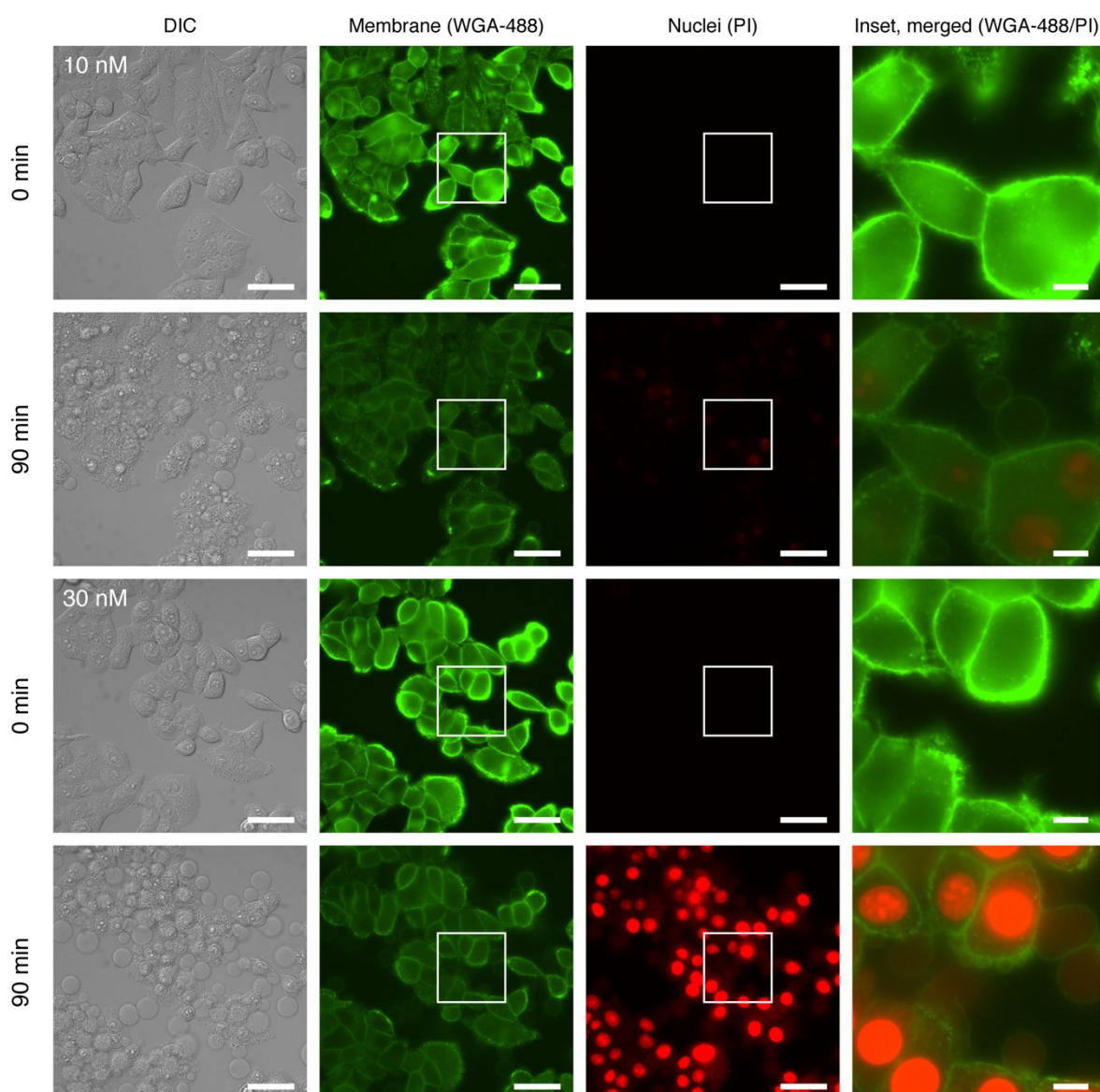


Figure S5: Live cell imaging of HEp-2 cell treated with 10 nM (first and second panel) or 30 nM of MbxA (third and fourth panel) over a duration of 90 min. HEp-2 cells are shown after 0 min and 90 min of incubation. Membranes were stained with WGA-488 (second row) and membrane permeability was monitored with PI (third row). Growth of spherical membrane protrusions and permeabilization are highlighted by the white boxes in the second and third row and shown in the insets in the right row as a merge of WGA-488 and PI fluorescence.

Table S1: MS analysis of MbxA (A) and HlyA (B) acylation. MbxA was *in vivo* cross-acylated by co-expressing HlyC. Modified peptides are listed with their detected fatty acid and hydroxy fatty acid modifications (C₁₂-C₁₆) and the corresponding number of peptide spectrum matches. The acylated lysine residues are shown in bold in row 'Sequence'. Furthermore, the charge states are given with which the respective peptides were detected in the mass spectrometer as well as the score from search engine MaxQuant.

For MbxA acyl modifications were detected only in peptides covering the predicted lysine residues K536 and K660, respectively. Only a low number of PSM were detected for K536 and no K660 lysine containing peptides in proMbxA. This is probably due to a higher specific cleavage of the respective peptides resulting in quite small fragments which have not been considered in the search. Detected fragments resulting from cleavage directly behind a putative acylation site are thus marked with **. Here, the cleavage behind K536 and K660 might not be masked by acylation of the respective residues. The analysis of the *in vivo* acylation of HlyA by HlyC confirms the acylation of the K564 and K690 acylation sites.

A

| Protein | Sequence | Site | Modifications | Charges | Score | PSM |
|----------------|-----------------|------|---------------|---------|--------|-----|
| MbxA | ERLTNGKYSYINK | K536 | C14 | 2 | 209.19 | 5 |
| | ERLTNGKYSYINK | K536 | C14 - OH* | 2 | 103.22 | 2 |
| | ERLTNGKYSYINK | K536 | C15 | 3 | 61.423 | 1 |
| | LTNGKYSYINK | K536 | C12 -OH* | 2 | 50.909 | 1 |
| | LTNGKYSYINK | K536 | C13 | 2 | 93.649 | 2 |
| | LTNGKYSYINK | K536 | C14 | 2 | 150.66 | 17 |
| | LTNGKYSYINK | K536 | C14 - OH* | 2 | 63.159 | 1 |
| | LTNGKYSYINK | K536 | C15 | 2 | 139.98 | 4 |
| | LTNGKYSYINK | K536 | C16 | 2 | 56.258 | 1 |
| | LTNGKYSYINKLK | K536 | C14 | 2 | 146.11 | 2 |
| | LTNGKYSYINKLK | K536 | C14 - OH* | 2;3 | 69.815 | 2 |
| | VGKRTETIQYR | K660 | C14 | 3 | 69.721 | 1 |
| | RTETIQYRDYELR** | K660 | Unmodified | 2;3;4 | 80.522 | 9 |
| | TETIQYRDYELR** | K660 | Unmodified | 2;3;4 | 168.94 | 79 |
| | TETIQYRDYELRK** | K660 | Unmodified | 2;3;4 | 145.46 | 37 |
| proMbxA | LTNGKYSYINKLK | K536 | Unmodified | 2;3;4 | 299.29 | 6 |
| | YSYINKLKFGFR** | K536 | Unmodified | 2;4 | 92.439 | 3 |
| | RTETIQYRDYELR** | K660 | Unmodified | 2;3;4 | 155.48 | 33 |
| | TETIQYRDYELR** | K660 | Unmodified | 2;3;4 | 240.8 | 84 |
| | TETIQYRDYELRK** | K660 | Unmodified | 2;3;4 | 170.89 | 36 |

B

| Protein | Sequence | Site | Modifications | Charges | Score | PSM |
|----------------|------------------------|------|---------------|---------|--------|-----|
| HlyA | QSGKYEYITELLVK | K564 | C14 | 2 | 92.19 | 1 |
| | QSGKYEYITELLVK | K564 | C14 - OH* | 2 | 74.611 | 1 |
| | QSGKYEYITELLVK | K564 | Unmodified | 3 | 83.633 | 4 |
| | RQSGKYEYITELLVK | K564 | C14 | 3 | 90.754 | 1 |
| | RQSGKYEYITELLVK | K564 | C14 - OH* | 3 | 93.909 | 1 |
| | RQSGKYEYITELLVK | K564 | Unmodified | 3 | 71.545 | 1 |
| | YEYITELLVK** | K564 | Unmodified | 2 | 84.615 | 4 |
| | EQEVSVGKR | K690 | C12 | 2 | 49.813 | 1 |
| | EQEVSVGKR | K690 | C14 | 2;3 | 190.08 | 3 |
| | EQEVSVGKR | K690 | C14 - OH* | 2 | 159.04 | 3 |
| | VLQEVVKEQEVSVGKR | K690 | C13 | 3 | 76.85 | 2 |
| | VLQEVVKEQEVSVGKR | K690 | C14 | 2;3 | 314.04 | 45 |
| | VLQEVVKEQEVSVGKR | K690 | C14 - OH* | 2;3 | 173.11 | 5 |
| | VLQEVVKEQEVSVGKR | K690 | C16 | 3 | 97.836 | 1 |
| | VLQEVVKEQEVSVGKR | K690 | Unmodified | 2 | 75.479 | 2 |
| | VLGGDVKVLQEVVKEQEVSVGK | K690 | Unmodified | 3 | 19.975 | 1 |
| | VLQEVVKEQEVSVGK | K690 | Unmodified | 2;3 | 126.83 | 4 |
| proHlyA | QSGKYEYITELLVK | K564 | Unmodified | 2;3 | 287.76 | 36 |
| | RQSGKYEYITELLVK | K564 | Unmodified | 2;3 | 158.11 | 32 |
| | YEYITELLVK** | K564 | Unmodified | 2 | 98.033 | 24 |
| | EQEVSVGKRTEK | K690 | Unmodified | 2;3 | 122.51 | 4 |
| | VLGGDVKVLQEVVKEQEVSVGK | K690 | Unmodified | 2;3;4 | 241.13 | 5 |
| | VLQEVVKEQEVSVGK | K690 | Unmodified | 2;3 | 283.47 | 69 |
| | VLQEVVKEQEVSVGKR | K690 | Unmodified | 2;3;4 | 334.04 | 36 |

3.4 Chapter 4

Title: Structural investigations of the RTX proteins HlyA from *Escherichia coli*, MbxA from *Moraxella bovis* and FrpA from *Kingella kingae*

Authors: Isabelle N. Erenburg, Jens Reiners, Miao Ma, Ben F. Luisi, Sander H. J. Smits, Lutz Schmitt

Published in: *in preparation*

Own proportion of this work:

50%

Bioninformatic analyses

Cloning of constructs

Expression and secretion

Protein purification

Preparation of the figures

Writing of the manuscript

**Structural investigations of the RTX proteins HlyA from
Escherichia coli, MbxA from *Moraxella bovis* and FrpA from
*Kingella kingae***

Isabelle N. Erenburg¹, Jens Reiners², Miao Ma³, Ben F. Luisi³, Sander H. J. Smits^{1,2}, Lutz Schmitt^{1§}

¹: Institute of Biochemistry, Heinrich Heine University Düsseldorf, Universitätsstraße 1, 40225 Düsseldorf, Germany

²: Center for Structural Studies, Heinrich Heine University Düsseldorf, Universitätsstraße 1, 40225 Düsseldorf, Germany

³: Department of Biochemistry, University of Cambridge, Tennis Court Road, Cambridge CB21GA, UK

§Corresponding author: Lutz Schmitt, Institute of Biochemistry, Heinrich Heine University Düsseldorf, Universitätsstr. 1, 40225 Düsseldorf, Germany, E-Mail: lutz.schmitt@hhu.de

Abstract

Repeats in Toxins (RTX) proteins constitute a large protein family that is characterized by conserved glycine-rich repeats that form calcium ion binding domains. They are expressed by Gram-negative bacteria and secreted via Type 1 secretion systems (T1SS) directly from the cytosol into the extracellular space. As a prerequisite for secretion, RTX proteins remain unfolded in the cytosol and adopt their native conformation after secretion mediated by calcium ion binding. Many members of the RTX family are virulence factors of pathogens such as the prototypical pore-forming toxin hemolysin A (HlyA) from uropathogenic *E. coli*. Here we report the heterologous secretion of the RTX proteins MbxA from *Moraxella bovis* and FrpA from *Kingella kingae* via the *E. coli* HlyA secretion system and purification of both proteins. Further structural investigations on HlyA, MbxA and FrpA including single particle cryogenic electron microscopy (cryo-EM) and small-angle X-ray scattering (SAXS) underline the flexibility of these proteins in solution and a common elongated conformation.

Introduction

In Gram-negative bacteria type I secretion system (T1SS) span the inner and the outer membrane and facilitate the transport of proteins into their extracellular environment. The substrates of T1SS have conserved calcium ion binding repeats which lead to the name Repeats in Toxins (RTX) proteins for this protein family. These Ca^{2+} binding nonapeptide repeats share the glycine-rich consensus sequence GGxGxDxUx (x stands for any amino acid, U for a large hydrophobic amino acid) and are therefore referred to as GG-repeats [1, 2]. The first identified RTX protein was the hemolytic virulence factor hemolysin A (HlyA) secreted by uropathogenic *E. coli* [3, 4]. Due to extensive research both on HlyA and its secretion system it soon become a prototype for RTX toxins and T1SS. Several other early identified members of the RTX family were, like HlyA, toxins of Gram-negative pathogens such as CyaA from *Bordetella pertussis* [5] or LktA from *Mannheimia haemolytica* [6]. Besides the classic RTX cytotoxins, the RTX family involves a variety of proteins of different length and functions including proteases [7] and lipases [8] or large multidomain proteins such as the multifunctional-autoprocessing RTX toxins (MARTX) [9, 10] and biofilm-associated adhesins of up to 1.5 MDa [11, 12]. The functional diversity is encoded in the N-terminal part of the protein whereas the GG-repeats are more frequent closer to the C-terminus, which is therefore called the RTX domain [2]. The secretion of RTX toxins via a designated tripartite T1SS in a

single-step process across both membranes of the Gram-negative bacterium has been studied in detail for the prototypical *E. coli* HlyA secretion system [13-16]. An ATP-binding cassette (ABC) transporter, called hemolysin B (HlyB) energizes the transport by hydrolyzing ATP [17, 18]. It is localized in the inner membrane together with the membrane fusion protein HlyD, forming the so-called inner membrane complex [19, 20]. The C-terminus of HlyA carries a non-cleavable secretion signal sequence [21]. Interaction of the C-terminus of HlyA with the inner membrane complex leads to engagement of TolC, an outer membrane protein, that connects the inner membrane components to the outer membrane and allows direct secretion into the extracellular space [20, 22]. The substrate HlyA remains unfolded before and during the secretion process in which the C-terminus reaches the extracellular space first [23, 24]. In the bacterial cytosol calcium ion concentrations are tightly regulated at nanomolar concentrations [25, 26], while the higher concentration found in the extracellular space leads to binding of Ca^{2+} , which induces folding of the RTX domain and subsequently of the complete protein [7, 27, 28]. The cytotoxic activity of pore-forming RTX proteins such as HlyA additionally requires a fatty acid-acylation at two conserved lysine residues [29]. This post-translational modification is mediated by an cytosolic acyltransferase prior to secretion [30, 31]. A homologue of HlyA, the pore-forming RTX toxin MbxA is produced by the bovine pathogen *Moraxella bovis* (*M. bovis*) involved in ocular infection [32, 33]. Like HlyA, it is encoded in an operon together with a corresponding activating acyltransferase and transporter components [34]. The human pathogen *Kingella kingae* (*K. kingae*) secretes a homologous, pore-forming protein, RtxA, as well [35], but also additionally a putative, iron-regulated RTX protein of unknown function, called FrpA, is annotated in the genome. This protein shares 40% sequence identity with a fragment of the iron-regulated protein FrpC from *Neisseria meningitidis*, which undergoes protein *trans*-splicing and interacts with a lipoprotein [36, 37]. FrpC is potentially involved in the adhesion of the pathogen to host cells [37]. However, FrpA from *K. kingae* does not harbor the full self-processing module that mediates protein *trans*-splicing in FrpC [36]. While HlyA and MbxA share a similar predicted domain organization typical for pore-forming RTX proteins, FrpA only harbors the characteristic GG-repeats (Fig. 1) Here, we show that MbxA and FrpA function as heterologous substrates of the HlyA T1SS and can be purified from a heterologous *E. coli* BL21(DE3) system. Further we present structural insights into HlyA, MbxA and FrpA from single particle cryogenic electron microscopy (cryo-EM) and small angle X-ray scattering (SAXS) studies.

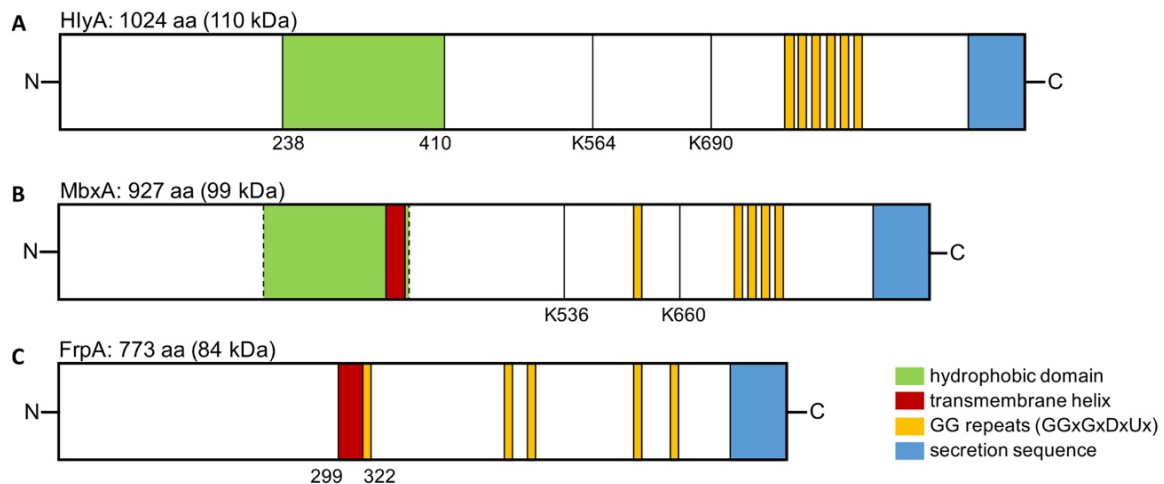


Figure 1: Schematic representation of the RTX proteins HlyA, MbxA and FrpA. The number of amino acid residues and the molecular weight is indicated for the native protein without tags. A) HlyA is considered the prototype of cytolytic RTX toxins. Its characteristic domain organization harbors a C-terminal secretion signal (blue) followed by the Ca^{2+} -binding RTX domain that consists of six conserved GG-repeats (yellow). For the activation of the toxin, two internal lysine residues, K564 and K690, marked in black, undergo covalent fatty-acylation. In the N-terminus a membrane interaction domain is predicted (green). B) MbxA has five GG-repeats located in the C-terminal part of the protein (yellow) likewise forming the RTX domain and two acylation sites (black). Similar to HlyA, for MbxA a hydrophobic domain for membrane interaction is predicted to be localized the N-terminus (green) including a transmembrane helix (red). Due to different prediction algorithms the length of this membrane spanning region is not clearly defined. The length of the secretion sequence is likewise not known. C) FrpA from *K. kingae* is homologous to a central fragment (residue 577-1429) of the 1829 amino acid long FrpC protein from *Neisseria meningitidis*. FrpA does not harbor potential acylation sites that are homologous to HlyA. A transmembrane segment is predicted at residue 299 to 322 for FrpA (red) [38]. The putative secretion signal is highlighted in blue. Figure modified from Chapter 3.3.

Materials and Methods

Expression and purification of secreted proHlyA and proHlyA from inclusion bodies

Pore-forming cytotoxins of the RTX protein family require a post translational acylation at internal lysine residues for activation. In this study *hlyA* was expressed without the activating acyltransferase HlyC and therefore produced as the inactive precursor proHlyA. proHlyA can be isolated from culture supernatants after secretion or expressed without the transporter components HlyB and HlyD which leads to intracellular accumulation of proHlyA and formation of inclusion bodies [39].

For secretion *E. coli* BL21(DE3) was transformed with the two plasmids pK184-*hlyBD* [23] and pSU2726-*hlyA* [41]. An overnight culture was used to inoculate 150 ml 2xYT supplemented with ampicillin (100 µg/ml) and kanamycin (30 µg/ml) in a baffled 300 ml flask to an OD₆₀₀ of 0.05. The culture was incubated at 37°C and 180 rpm shaking until an OD₆₀₀ of 0.4-0.6. The expression of proHlyA was then induced with 1 mM IPTG and the medium was additionally supplemented with 10 mM CaCl₂. After a continuous expression of 4 h at 37°C and 180 rpm the cells were removed by centrifugation for 20 min at 4000 g. The supernatant containing HlyA was stored at -20°C. For purification 450 ml supernatant were thawed on ice and afterwards centrifuged for 30 min at 200,000 g and 4°C. Subsequently, the supernatant was filtered with a 0.45 µm filter and concentrated to 5 ml with Amicon Ultra-15 Centrifugal Filter Units (100 kDa NMWL, Merck Millipore). After centrifugation for 30 min at 100,000 g and 4°C the protein was applied to a Superdex200 16/600 HiLoad column (GE Healthcare) in 50 mM TRIS pH 7.4, 500 mM NaCl and 10 mM CaCl₂ and a flowrate of 0.5 ml/min.

Using *E. coli* BL21(DE3) harboring only pSU2726-*hlyA* proHlyA expressed in absence of the HlyB and HlyD formed inclusion bodies. 2 L 2xYT medium with 100 µg/ml ampicillin in baffled 5 L flasks were inoculated with an overnight culture to an OD₆₀₀ of 0.1. The culture was incubated at 37°C and 160 rpm until it reached an OD₆₀₀ of 0.4-0.6 and was then induced with 1 mM IPTG. proHlyA was expressed for 4 h at the same conditions and cells were afterwards collected by centrifugation for 15 min at 13,900 g and 4°C. The proHlyA inclusion bodies were then purified according to Kanonenberg *et al.* 2019 [40]. The resulting proHlyA was solubilized in 6 M urea and was drop-wise diluted to 400 mM urea with refolding buffer (100 mM HEPES pH 8.0, 250 mM NaCl, 10 mM CaCl₂). After refolding the protein was again concentrated with Amicon Ultra-15 Centrifugal Filter Units (100 kDa NMWL, Merck Millipore). To remove the remaining urea proHlyA was applied to a PD10 desalting column (GE Healthcare) and concentrated for a subsequent SEC. Aggregated protein was collected by centrifugation (20 min, 20,700 g, 4°C) and applied to a Superose 6 10/300 GL column (GE Healthcare) in the same buffer. The column was equilibrated with refolding buffer and the SEC run at a flowrate of 0.5 ml/min.

Cloning of the *frpA* and *mbxA* genes

In the *K. kingae* ATCC 23330/ DSM 7536 genome the *frpA* gene is annotated as a partial, iron-regulated protein (GenBank EGK08641.1). Due to an incomplete sequencing of the genomic fragment an unknown portion of the C-terminus of FrpA is missing and the predicted protein sequence starts with an asparagine residue. Therefore a larger fragment including the potential

C-terminus was amplified from the *K. kingae* genome with the primer pair *frpA* for 5'AGATTTTACGCAAAACATTACAG 3' and *frpA* rev 5'TGTTATTTTAGGATGATA-ATTATGAGTC 3' and cloned into a pJET1.2 vector (Thermo Scientific). This allowed sequencing of the upstream region of the putative *frpA* gene. The first ATG codon localized upstream of the annotated region was assigned as the putative start codon resulting in the additional 5' sequence 5'-ATGGGCGATGTAGAATTTGCTAGCAACAGTTTGTATAG-3' and a total gene length of 2322 bp. Therefore the presumably completed *frpA* gene was amplified with the primer pair pSU-*frpA* for CTGGTTAAG-AGGTAATTAAATGGGCGATGTAGAATTTG and pSU-*frpA* rev GATTGCTATCA-TTTAAATTAATATATTACAGGTTATTTGCAGCG including the restored 5' sequence and inserted into the pSU2726-*hlyA* vector via Gibson assembly [41] replacing the *hlyA* gene. Subsequently an N-terminal His₆-tag was added to the *frpA* gene resulting in the plasmid pSU2726-6H-*frpA*.

To generate a MbxA (Uniprot Q93GI2) expression vector the *mbxA* gene was amplified from the *M. bovis* DSM 6328 genome via PCR using the primer pair *mbxA* for 5'-AACCTTTTCTAACACAACGAGGAGAGAC-3' and *mbxA* rev 5'-AAATCACTAAACACTTGGAGCCAAAATTC-3'. As for *frpA*, after subsequent cloning of the *mbxA* gene into the pJET1.2 vector, *mbxA* was introduced into the pSU2726 vector using Gibson assembly. The plasmid was likewise completed with the addition of an N-terminal His₆-tag to the *mbxA* gene.

Expression and purification of FrpA

E. coli BL21(DE3) were transformed with pSU2726-6H-*frpA* and an overnight culture was grown in 100 ml 2xYT medium with 100 µg/ml ampicillin at 37°C with 180 rpm shaking. 2 L of 2xYT medium supplemented with ampicillin in a 5 L baffled flasks were inoculated with *E. coli* BL21(DE3) pSU2726-*frpA* to a starting OD₆₀₀ of 0.1. The culture was incubated at 37°C with 160 rpm shaking until it reached OD₆₀₀=0.6. The expression was then induced by addition of 1 mM IPTG. For the duration of the expression the temperature was reduced to 25°C and the culture was incubated for 3.5 h at 160 rpm shaking. Afterwards cells were harvested by centrifugation for 20 min at 14,000 g and 4°C and stored at -80°C.

For purification, the *E. coli* BL21(DE2) pSU2726-*frpA* cells were thawed on ice and resuspended in resuspension buffer (50 mM Hepes pH 8, 400 mM NaCl, 10% glycerol). For lysis the resuspended cells were passed through a high-pressure cell disruptor (Microfluidizer M-110L, Microfluidics) at 1500 bar for three times. To remove cell debris, the lysate was

centrifuged for 40 minutes at 200,000 g and 4°C. After addition of 20 mM imidazole the lysate was loaded on a Ni²⁺-loaded ion affinity chromatography (IMAC) column (5 ml HiTrap Chelating HP, GE Healthcare). The column was washed with IMAC buffer (50 mM Hepes pH 8, 400 mM NaCl, 20 mM imidazole) and the protein was eluted with a linear gradient of 0-400 mM imidazole with elution buffer (50 mM HEPES pH 8, 400 mM NaCl, 400 mM imidazole) in 100 min or a step-wise elution with 25%, 50% and 100% elution buffer. For a subsequent SEC, fractions containing FrpA were pooled and concentrated to 8-10 mg/ml with an Amicon Ultra-15 Centrifugal Filter Units (50 kDa NMWL, Merck Millipore). Aggregated protein was removed by centrifugation for 30 min at 20,700 g and 4°C. Depending on the final volume of the sample FrpA was applied to a Superose 6 10/300 GL column (GE Healthcare) or a Superdex200 16/600 HiLoad column (GE Healthcare) equilibrated in SEC buffer (50 mM HEPES pH 8, 400 mM NaCl, 10 mM CaCl₂) with a flow rate of 0.5 ml/min.

Expression and purification of proMbxA

Like HlyA, *mbxA* was expressed in the absence of an acyltransferase as an inactive precursor. To facilitate secretion of proMbxA it was expressed together with the *E. coli* hemolysin secretion system. For this heterologous secretion, *E. coli* BL21(DE3) were transformed with the two plasmids pK184-*hlyBD* and pSU2726-6H-*mbxA*. Harboring both plasmids, an overnight culture was used for inoculation of ten to twelve 300 ml flasks with 50 ml LB medium supplemented with ampicillin (100 µg/ml) and kanamycin (30 µg/ml) to an OD₆₀₀ of 0.1. The culture was incubated at 37°C and 180 rpm shaking. At an OD₆₀₀ of 0.4-0.6, expression was induced by addition of 1 mM IPTG and 10 mM CaCl₂ and incubation was continued for 5 h at 37°C and 180 rpm. After the expression, cells were removed by centrifugation for 45 min at 13,500 g and 4°C and the supernatant was filtered with a 0.45 µm filter. For purification 500-700 ml of supernatant stored on ice were concentrated to a tenth of the starting volume using Amicon Ultra-15 Centrifugal Filter Units (50 kDa NMWL, Merck Millipore). The concentrated supernatant was loaded on a Ni²⁺ loaded IMAC column (5 ml HiTrap IMAC HP, GE Healthcare) and after washing with IMAC buffer (50 mM TRIS pH 7.8, 400 mM NaCl, 10 mM CaCl₂) eluted with elution buffer (50 mM TRIS pH 7.8, 400 mM NaCl, 10 mM CaCl₂, 75 mM histidine) with a linear 0-75 mM histidine gradient. Fractions containing proMbxA were pooled, concentrated and centrifuged for 20 min at 20,700 g at 4°C to collect aggregate. The protein was then applied to a Superose 6 Increase 10/300 GL column (GE Healthcare) in SEC buffer (50 mM TRIS pH 7.8, 100 mM NaCl, 10 mM CaCl₂) and eluted at a flowrate of 0.5 ml/min.

Circular dichroism (CD) spectroscopy

FrpA purified from the *E. coli* BL21(DE3) cytosol and secreted FrpA were tested for their secondary structure content using CD spectroscopy at a concentration of 10 μ M. A CD spectrum from 198 nm to 300 nm was recorded at room temperature with a Jasco J715 spectropolarimeter (JASCO) (Bachelor thesis Nicole Jasny).

Cryogenic electron microscopy (cryo-EM)

Cryo-EM specimen preparation and data collection was carried out at the Department of Biochemistry, University of Cambridge, Cambridge, UK in the laboratory of Prof. Ben Luisi. cryoEM data and images were provided by Dr. Miao Ma. proHlyA was refolded from inclusion bodies and freshly purified via SEC before grid preparation. proMbxA was separated into a monomer and dimer sample via SEC and after storage at -80°C , aggregate was collected by centrifugation at 4°C . For proHlyA, QUANTIFOIL Holey Carbon (Quantifoil Micro Tools GmbH), UltrAuFoil Holey Gold (Quantifoil Micro Tools GmbH) and PEGylated UntrAuFoil grids were tested. The PEGylated gold grids were prepared according to [42]. For proMbxA QUANTIFOIL Holey Carbon and UltrAuFoil Holey Gold (Quantifoil Micro Tools GmbH) were tested. proHlyA was used for specimen preparation at a concentration of 0.2 mg/ml or 0.05 mg/ml and proMbxA at 0.2-0.7 mg/ml combined with varying CaCl_2 concentrations (1-10 mM). Grids were prepared and glow discharged with a Vitrobot IV (FEI) before 3 μ l of proHlyA or proMbxA were applied to the grids with varying blotting time and force as described in Du *et al.* 2014 [43]. Screening of the grids was carried out with a Talos Arctica 200 kV transmission electron microscope (TEM) (Thermo Scientific). Data collection was performed with the best grids, UltrAuFoil Holey Gold grid for proHlyA and QUANTIFOIL Holey Carbon for proMbxA, with a Titan/Krios TEM (Fei, ThermoFisher Scientific) or a Talos Arctica 200 kV TEM (ThermoFisher Scientific), respectively (Tab. 1). Data processing was carried out with RELION-3.0 software [44, 45], motion correction and estimation of the contrast transfer function parameters with Gctf [46] as described in [42].

Table 1: Cryo-EM data collection parameters for proHlyA and proMbxA

| Protein | proHlyA | proMbxA |
|--------------------------------------|-------------------|------------------------------|
| Microscope | Titan Krios | Talos Arctica |
| Detector | Falcon 3 counting | Falcon 3 counting |
| Nominal Magnification, kx | 120 | 120 |
| Pixel Size, Å per pixel | 0.66 | 0.89 |
| Gun Lens/ Spot Size | 4/8 | 4/9 |
| Dose electrons/Å ² /sec | 1.17 | 0.66 |
| Dose electrons/pixel/sec | 0.51 | 0.52 |
| Exposure, sec | 60 | 60 |
| Total Dose, electrons/Å ² | 70.2 | 39.6 |
| Number of Fractions | 70 | 30 |
| Defocus Range | -14.7 | -1.5, -1.8, -2.1, -2.4, -2.7 |
| Autofocus (i.e. every hole) | every 10 µm | every 8 µm |
| Drift Measurement | none | none |
| Delay after stage shift, sec | 10 | 20 |
| Delay after image shift, sec | 5 | 10 |
| Exposures per hole | 1 | 1 |
| Objective Aperture | 100 | 100 |
| C2 aperture | 50 | 50 |

Small-angle X-ray scattering (SAXS)

Directly prior to SAXS data collection, proHlyA and FrpA were subjected to another SEC to ensure homogeneity of the protein. Therefore samples were applied to a Superose 6 Increase 10/300 GL column (GE Healthcare) at a flowrate of 0.5 ml/min in the according SEC buffers. The SAXS experiments were conducted at the European Synchrotron Radiation Facility (ESRF, Grenoble, France) at beamline BM29 [47, 48]. All measurements and analysis were carried out according to [49]. A fixed sample to detector (PILATUS 1 M detector, Dectris) distance of 2.867 m was set for all measurements. With this set up, the achievable s-range was 0.025 - 5 nm⁻¹. The SAXS sample cell was coupled to an on-line SEC (Superose 6 Increase 10/300, GE Healthcare) to allow direct measurement of the eluting protein. For all samples, secreted HlyA, refolded HlyA and FrpA, a 100 µl sample with a concentration of 7.8 mg/ml, 8 mg/ml and 10.9 mg/ml, respectively, was applied at a flow rate of 0.5 ml/min and at 10°C. During the online-SEC-SAXS experiments frames were collected with a exposure time of 2 s. Comparison of the frames allowed to omit possible radiation damage. Data processing and analysis was

based on the SAXS data analysis software suite ATSAS (Version 3.0.2) [50, 51], online available on the EMBL website (<https://www.embl-hamburg.de/biosaxs/software.html>). The programs CHROMIXS and PRIMUS were used for primary data reduction [52, 53]. Further using PRIMUS, the radius of gyration (R_g) and the forward scattering $I(0)$ were determined based on the Guinier approximation [54]. With the program GNOM the pair-distributed function $p(r)$ was determined and used for estimation of the maximum particle dimension D_{\max} [55]. Further, DAMMIF was used for the calculation of low resolution *ab initio* models [56] and DAMAVER and SUPCOMB were used for averaging and superimposition [57, 58]. For calibration, the data was scaled against the absolute intensity of water. For the calculation of the molecular weight of the proteins the MoW2 server and the Volume of correlation (V_c) was used [59, 60].

Results

Secretion and purification of proHlyA, FrpA and proMbxA

RTX proteins are secreted by Gram-negative bacteria into their environment via cognate T1SS. Here, the RTX proteins FrpA from *K. kingae* and MbxA from *M. bovis* were expressed in *E. coli* BL21(DE3). Implementing a two-plasmid system, FrpA or MbxA were combined with the hemolysin T1SS to test whether it can act as a surrogate secretion system for heterologous RTX protein. Expression of pSU-6H-*frpA* or pSU-6H-*mbxA* together with pK184-*hlyBD* encoding the transporter components in *E. coli* BL21(DE3) resulted in accumulation of a single protein species, FrpA or proMbxA, respectively. In contrast to MbxA, which has two acylation sites for post-translational activation homologous to HlyA, FrpA does not harbor these sites. It is not known whether FrpA requires a post-translational modification for its activity. As the activating acyltransferases MbxC was not co-expressed this recombinant system secreted the precursor proMbxA. The CBB stained SDS-PAGE showed that even before induction with IPTG detectable amounts of FrpA were secreted, while secreted proMbxA appeared in the supernatant 1 h after induction. Both FrpA and proMbxA accumulated in the supernatant during the expression period of 5 h, but the secretion levels were lower compared to the native substrate, proHlyA (Fig. 2). The higher concentration of proHlyA could either stem from a more efficient recognition and secretion via the T1SS or from generally higher expression levels.

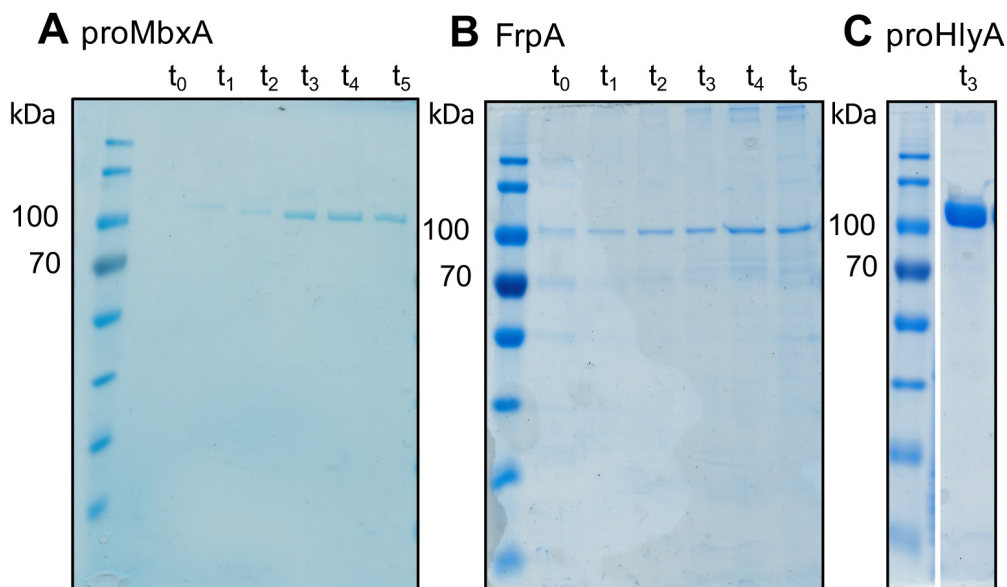


Figure 2: Secretion of proMbxA, FrpA and proHlyA via the hemolysin T1SS. proMbxA, FrpA and proHlyA were co-expressed with the transporter components HlyB and HlyD. The secretion into the culture supernatants was analyzed with CBB stained SDS-PAGE. For proMbxA and FrpA non-concentrated supernatant samples were collected during 5 h of expression (A and B). The non-concentrated supernatant of a proHlyA secreting culture is shown after 3 h of expression (C).

proHlyA carries a C-terminal secretion signal in its last 50-60 amino acids that facilitates interaction with the inner membrane components and is crucial for secretion [13, 15, 16]. Heterologous secretion of proMbxA and FrpA mediated by HlyB and HlyD implies that these RTX proteins possess the information sufficient for successful interaction with the hemolysin translocon. Alignment of the last 60 C-terminal residues of FrpA and MbxA with the HlyA secretion signal did not show an unambiguously conserved sequence (Fig. 3). Earlier studies suggested that the secretion of HlyA is mediated by secondary structure motifs including an amphipathic helix with a linker, located in the extreme C-terminus [61, 62]. Computational prediction of amphipathic helices in the putative secretion signals of FrpA and MbxA revealed three possible amphipathic helices alternating with short linker sequences (Fig. 4.). The predicted middle helix of MbxA and FrpA with 14 or 18 residues respectively could potentially substitute for the first amphipathic helix of HlyA that mediates recognition and secretion [62].

| | | |
|------|---|----|
| HlyA | -----STYGSQDNLNPLINEISKIISAAGNFDVKEERSAASLLQLSGNASDFSYGNSITLTASA | 60 |
| MbxA | ----QELKKLADENKSKLSASDIASSLNKLVGSMALFGTANSVSSNALQPITQPT-QGILAPSV----- | 60 |
| FrpA | GIIPRRIETIQTHD-GSHLD---VSAVQKLQAMASFAPETGSGLVLEQMKEYS-QQVFAANNL----- | 60 |
| | :. *: : . * . * :. : : . . | |

Figure 3: Sequence alignment [63] of the last 60 C-terminal amino acids of proHlyA, MbxA and FrpA. Identical residues are marked with “*”, strongly similar residues with “:” and weakly similar residues with “.”. The three RTX protein do not share a highly conserved primary sequence in their extreme C-terminus. This suggests that the information necessary for the recognition by the transport complex and the secretion is mediated by secondary structure elements.

| | | | | | | | |
|------|-----------------|----------------------|--------------------|--------------|-----------|-----|----|
| | N | 10 | 20 | 30 | 40 | 50 | 60 |
| HlyA | STYGSQDN | LNPLINEISKIISAAGNFDV | KEERSAASLLQL | SGNASDFS | YGRNSITLT | ASA | |
| FrpA | GIIPRRIETIQTHD | GSHLD | VSAVQKLQAMASFAPETG | SGLVLEQMKEYS | QQVFAANNL | | |
| MbxA | QELKKLADENKSKLS | ASDIASSLNKLVGSMAL | FGTANSV | SSNALQPITQPT | QGILAPSV | | |

Figure 4: Prediction of amphipathic helices in the secretion signal of HlyA and the putative secretion signals of MbxA and FrpA [64]. According to the C-terminal secretion signal of proHlyA, the C-terminal fragment of the same length was assumed to mediate secretion of FrpA and MbxA. Residues predicted to form amphipathic helices are highlighted in red.

The heterologous expression of proHlyA in *E. coli* BL21(DE3) offers two possible purification routes. Expressed without its secretion system, proHlyA remains in the cytosol leading to the formation of inclusion bodies, while secreted proHlyA accumulates as an almost pure protein in the culture supernatant. This allows to compare if the structure of proHlyA that was refolded from inclusion bodies adopts the same structure as its secreted counterpart. Secreted proHlyA was isolated from the concentrated culture supernatants directly via SEC and the collected protein applied to a second SEC (Fig. 5 A and B) [39]. proHlyA derived from inclusion bodies was solubilized and refolded in the presence of 10 mM Ca²⁺ according to Kanonenberg *et al.* [40], before it was subjected to a SEC (Fig. 5C).

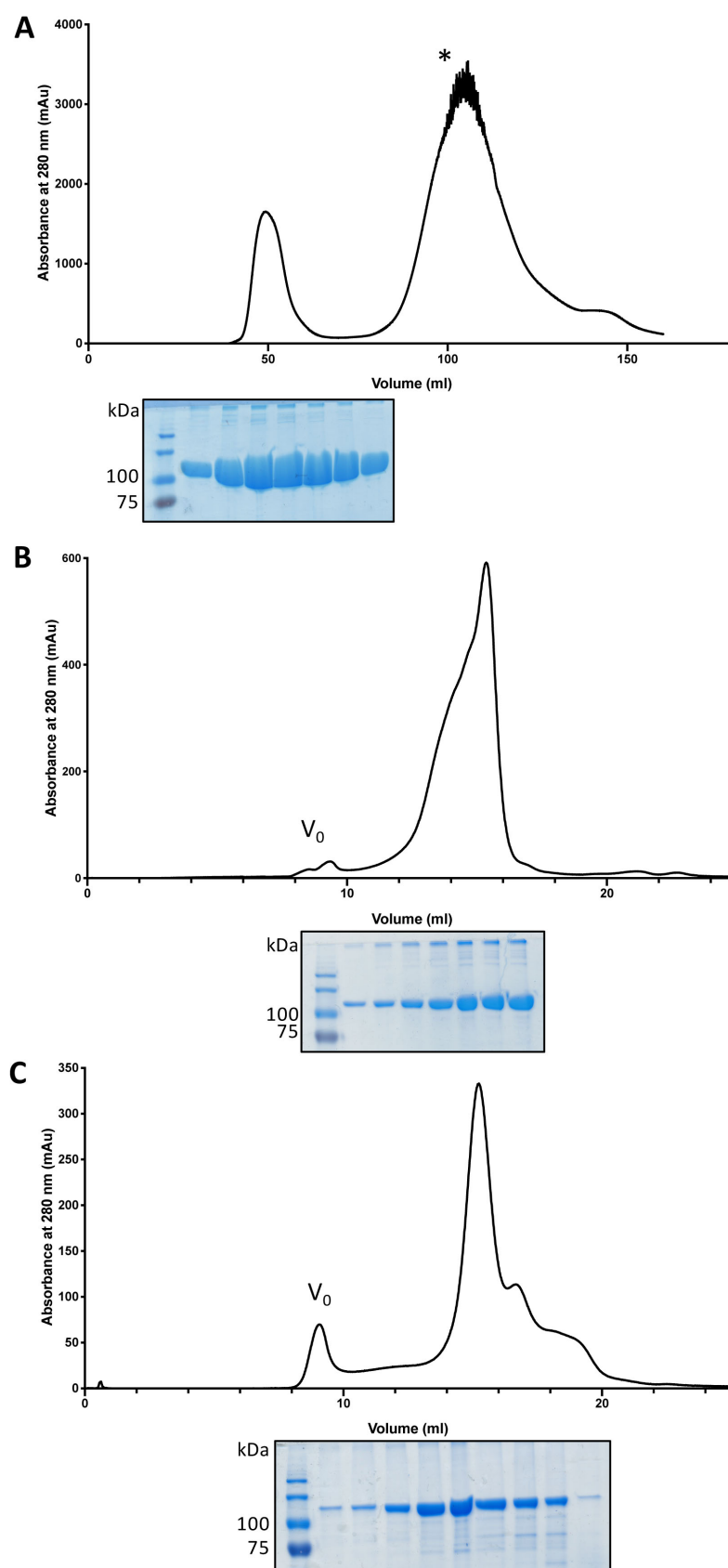


Figure 5: Purification of secreted proHlyA and proHlyA refolded from inclusion bodies. The protein fractions were analyzed with CBB-stained SDS-PAGE which are shown in insets for each protein peak. A) Culture supernatants of *E. coli* BL21(DE3) secreting proHlyA were

concentrated and applied to a Superdex 200 16/60 for a SEC. Secreted proHlyA eluted in peak 1 separated from the elution of the culture media components (*)[39]. B) To evaluate the homogeneity of the secreted protein, peak 1 was pooled and applied to a Superose 6 Increase 10/300 GL column for a second SEC. The purity of the protein was demonstrated via CBB stained SDS-PAGE. C) Alternatively, proHlyA was expressed without its secretion system resulting in formation of inclusion bodies [40]. The refolded protein was subjected to a SEC on a Superose 6 Increase 10/300 GL column.

The heterologous secretion of His-tagged proMbxA mediated by the hemolysin secretion system allowed isolation of proMbxA from the *E. coli* culture supernatant via IMAC. proMbxA eluted from the Ni^{2+} loaded IMAC column was applied to a Superose 6 Increase 10/300 GL column for a subsequent SEC, which separated two distinct proMbxA species (Fig. 6). Multi angle light scattering (MALS) confirmed that the two species were a dimer, eluting at 15 ml and a monomer population of proMbxA, eluting at 17 ml.

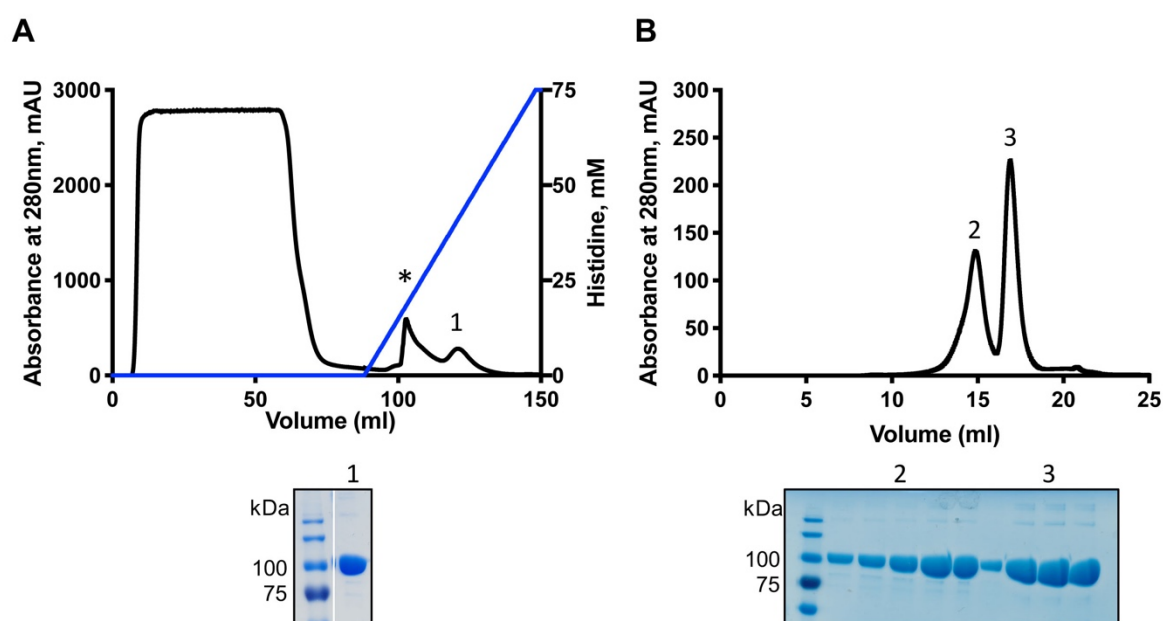


Figure 6: Purification of proMbxA via IMAC and subsequent SEC. A) Concentrated *E. coli* BL21(DE23) supernatant containing His-tagged proMbxA was loaded on a Ni^{2+} IMAC column. With a linear histidine gradient almost pure proMbxA (peak 1) was separated from non-protein impurities (*) and eluted in peak 1. The purity of the pooled elution fractions was demonstrated with a CBB stained SDS-PAGE. B) SEC with a Superose 6 Increase 10/300 GL column separated proMbxA dimers (peak 2) and proMbxA monomers (peak 3). Purity of the fractions of both the dimer and monomer peak are shown in the CBB stained SDS-PAGE.

In contrast to proMbxA, FrpA was purified directly from the cytosol omitting the heterologous secretion. FrpA that was expressed in *E. coli* BL21(DE3) without transporter components, unlike HlyA, did not form inclusion bodies but remained soluble in the cytosol. It was first

isolated from the cytosolic fraction using IMAC and then applied to a Superose 6 Increase 10/300 GL column for SEC. FrpA eluted from the SEC column at a elution volume of 15.6 ml in an almost homogenous peak (Fig. 7).

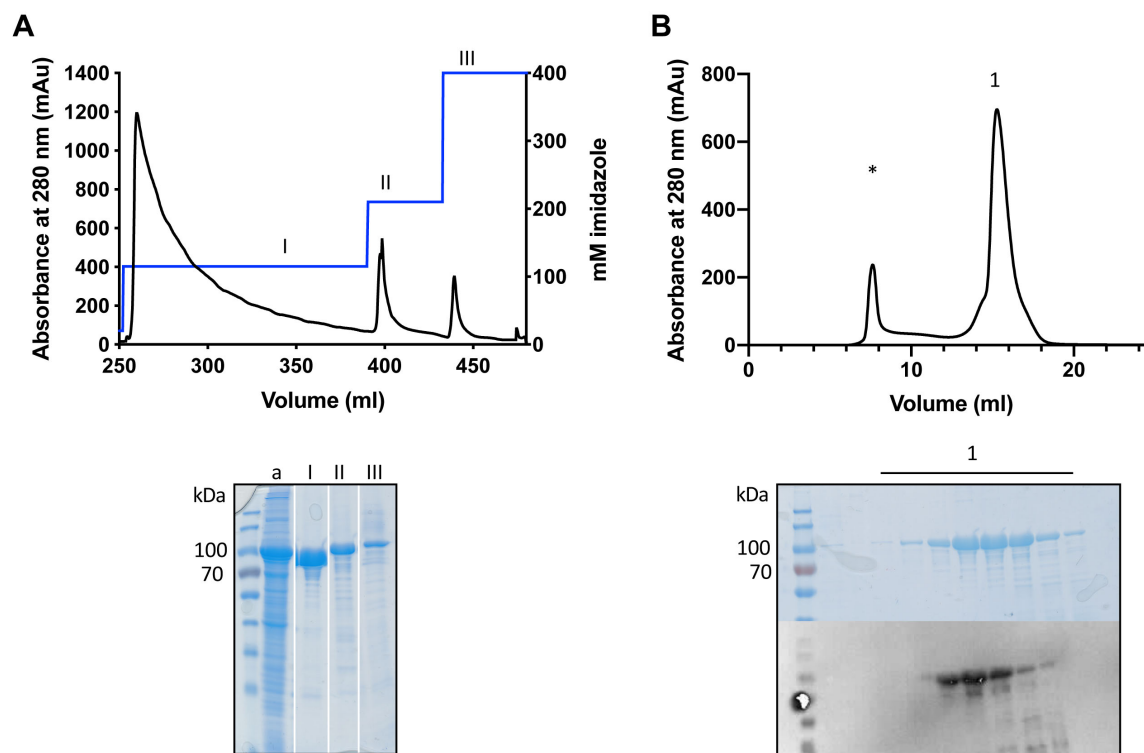


Figure 7: Exemplary purification of FrpA via IMAC and subsequent SEC. FrpA was expressed in *E. coli* BL21(DE3) without a secretion system and purified from the cytosol. A) The cytosolic fraction was loaded on Ni^{2+} IMAC column and FrpA was eluted with imidazole. Proteins present in the loaded cytosolic fraction (a), in the first elution step with 115 mM (I), the second with 240 mM (II) and the third with 400 mM imidazole (III) were analyzed via CBB stained SDS-PAGE. B) For SEC, fractions containing FrpA were pooled and applied to a Superose 6 column. FrpA eluted in a nearly homogenous peak and its purity was checked vis SDS-PAGE and Western Blot with an anti-penta-His antibody. Aggregated protein eluted with the void volume (V_0) of the column.

As FrpA could not only be purified from the cytosol but also as a secreted protein from the *E. coli* culture supernatant, CD spectroscopy was used to evaluate whether both protein variants have a similar content of secondary structure and thus adopt the same conformation (Fig. 8). The CD spectra of secreted and cytosolic FrpA were nearly identical showing a negative maximum in ellipticity at approximately 210 nm to 220 nm indicating the presence of α -helices and β -sheets [65]. Proteins that did not undergo secretion still adopted a similar proportion of secondary structure.

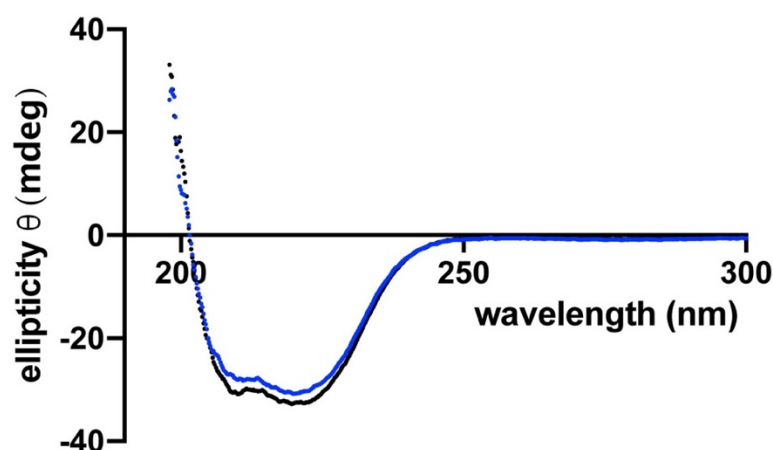


Figure 8: Circular dichroism spectra of cytosolic FrpA (black) and secreted FrpA (blue). The ellipticity is shown in mdeg plotted against the wavelength in nm. The protein concentration for both cytosolic and secreted FrpA was 10 μ M.

Single particle cryo-EM studies of proHlyA and proMbxA

Single particle cryo-EM allows the determination of three dimensional structures of proteins and protein complexes at near atomic resolution in near native conditions. Protein samples are embedded on EM-grids in amorphous ice by rapid freezing [66]. Due to the high flexibility of proHlyA attempts to obtain high resolution structures from X-ray crystallography have not been successful thus far [67]. To overcome the bottleneck of crystallization, cryo-EM was performed on proHlyA and proMbxA in collaborations with Prof. Ben Luisi, Department of Biochemistry, University of Cambridge, Cambridge, UK. Refolded proHlyA from inclusion bodies was used for specimen preparation at a concentration of 0.2 mg/ml or 0.05 mg/ml with 1 mM or 10 mM of CaCl_2 . Three different grid types, UltraFoil gold grids (UltrAuFoil Holey Gold grid R0.6/1.0, 300 mesh, PEGylated UltraFoil gold grids and QUANTIFOIL Holey Carbon (Quantifoil Micro Tools GmbH) with different hole sizes and blotting times were tested. 0.2 mg/ml proHlyA with 1 mM CaCl_2 on a UltrAuFoil grid was chosen for further data collection on a Titan Krios transmission electron microscope (TEM) (Fei, ThermoFisher Scientific) (Fig. 9A). Using a template based auto-picking procedure 17949 particles were picked and used for 2D classification (Fig. 9B). After several rounds of 2D classification good classes were selected as a template for a second auto-picking of particles. With this template based auto-picking 181418 particles were picked for 2D classification. 2D class averaging showed different elongated particles (Fig. 10). For reconstruction of the 3D structure 11 class averages with 9927 particles were chosen, but the quality of the classes did not allow reconstruction of a 3D model.

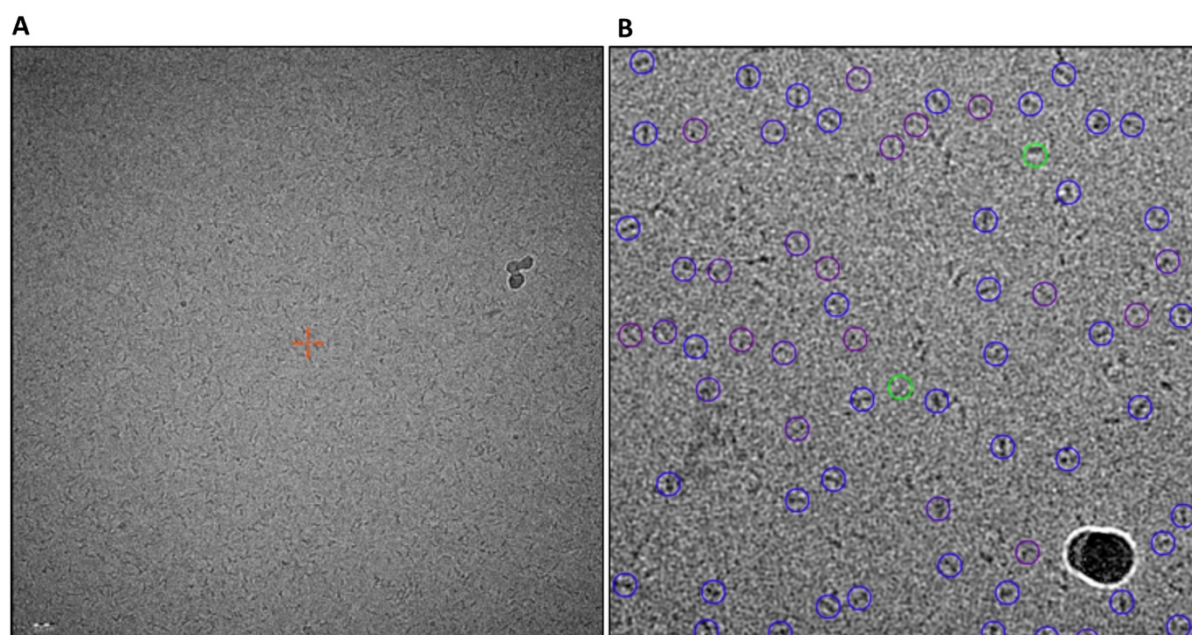


Figure 9: A) Micrograph of 0.2 mg/ml proHlyA on a UltrAuFoil grid. B) Motion corrected micrograph with exemplary auto-picked proHlyA particles circled in blue, purple and green. Images were provided by Dr. Miao Ma.



Figure 10: 2D class averages of proHlyA particles. 11 classes with a total of 9927 particles, highlighted in red, were chosen for an initial 3D model. Image provided by Dr. Miao Ma.

For proMbxA, samples of the monomer and of the dimer species separated by SEC were used for cryo-EM specimen preparation at a concentration of 0.7 mg/ml to 0.2 mg/ml with 3.25 mM to 10 mM of CaCl_2 . The grid screening was performed on a Talos Actrica 200 kV cryo-TEM (ThermoFisher scientific). On the tested grids (QUANTIFOIL Holey Carbon or UltrAuFoil Holey Gold, both 300-mesh R1.2/1.3, Quantifoil Micro Tools GmbH) proMbxA behaved

similarly to proHlyA and no major differences between the monomer and dimer sample was observed (Fig. 11).

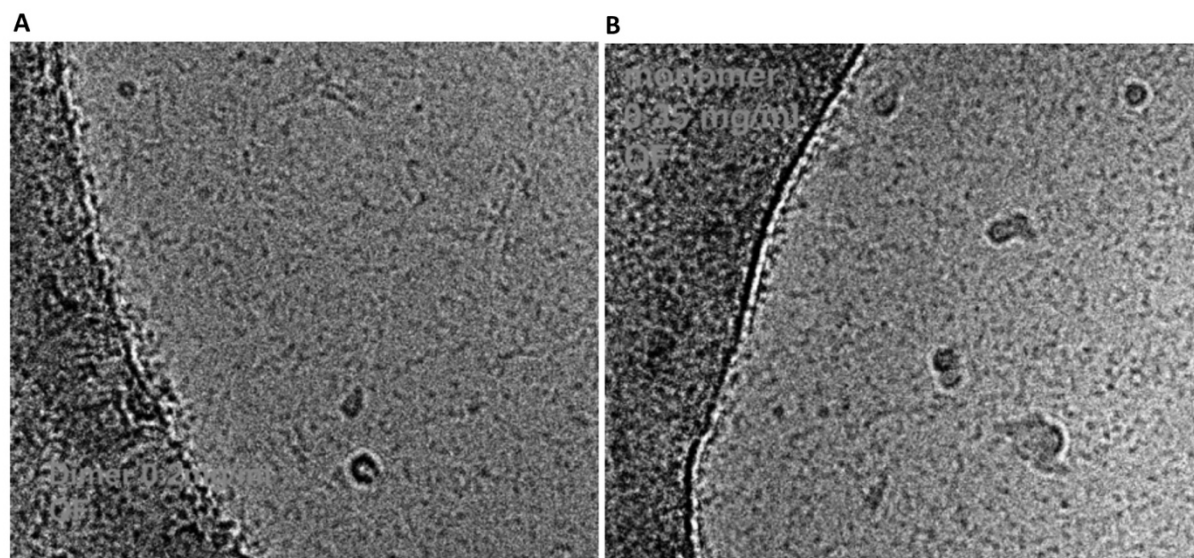


Figure 11: Exemplary, enlarged micrographs of a proMbxA dimer preparation at 0.2 mg/ml (A) and of a proMbxA monomer preparation at 0.35 mg/ml (B) on a QUANTIFOIL Holey Carbon 1.2/1.3 grid. Images provided by Dr. Miao Ma.

The MbxA dimer specimen with a concentration of 0.2 mg/ml and 10 mM CaCl_2 on a QUANTIFOIL Holey Carbon 1.2/1.3 grid was chosen for further data collection on a Talos Actrica 200 kV cryo-TEM (ThermoFisher Scientific). 937 particles were manually picked as a template for 2D classification. Similar to HlyA, the resulting 2D class averages showed elongated but also dot-like particles. Nevertheless, the particles were too heterogenous and the quality of the resulting 2D class averages was too low to continue with a 3D model (Fig. 12)

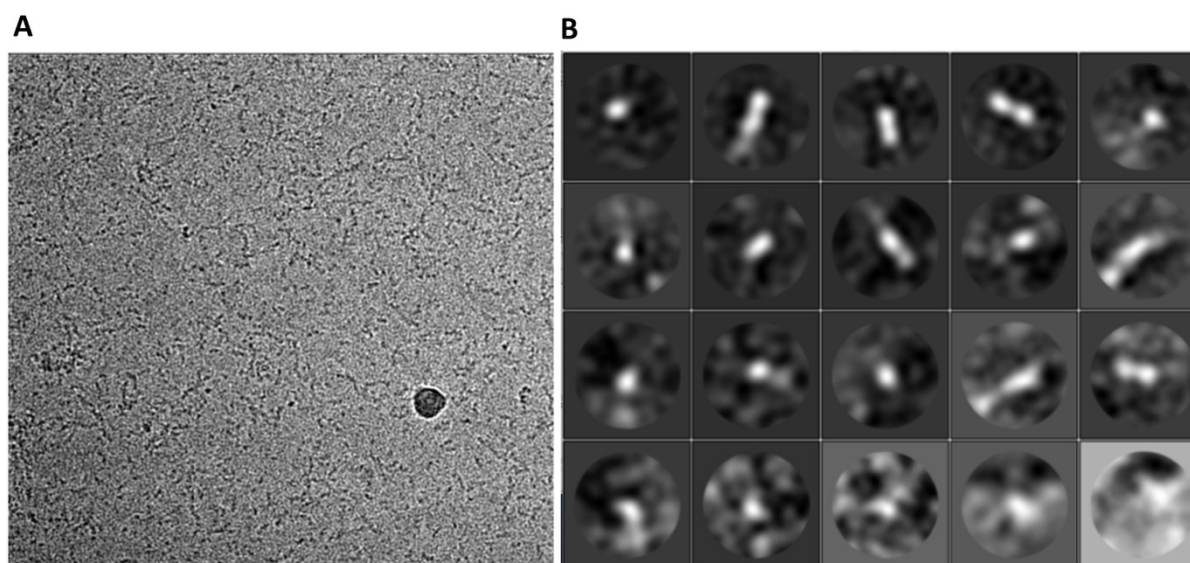


Figure 12: A) Motion corrected micrograph of 0.2 mg/ml proMbxA on a QUANTIFOIL Holey Carbon grid. B) Class averages of manually picked particles of proMbxA. Images provided by Dr. Miao Ma.

Small angle X-ray scattering (SAXS) studies of proHlyA and FrpA

SAXS allows to obtain structural information such as the shape and the oligomeric state from proteins in solution. For proHlyA and FrpA SEC-SAXS data was collected at the BioSAXS Beamline at the ESRF, Grenoble, France. From the resulting scattering curve *ab initio* models were calculated with the program DAMMIF [56] (Fig. 13). The resulting volumetric envelopes for secreted proHlyA and refolded proHlyA show both a similar elongated shape with a kink in the middle. The calculated molecular weight ranges from 165.53 kDa to 183.46 kDa for secreted proHlyA and from 167.71 to 215.49 kDa for refolded proHlyA (Tab. 1). As the monomeric molecular weight of proHlyA is 110.46 kDa this suggest that the scattering fractions contained dimers with a portion of monomers. The larger molecular weight calculated for refolded proHlyA suggest that the fraction of dimers is higher in this species. Nevertheless the overlay of both proHlyA variants shows that the *ab initio* models are similar suggesting that both variants adopt a similar structure (Fig. 14 B). In contrast to HlyA, the calculated molecular weight of FrpA was between 88.20 – 88.75 kDa. This fits with the theoretical monomeric weight of 85.69 kDa, meaning FrpA is a monomer in solution (Tab. 1).

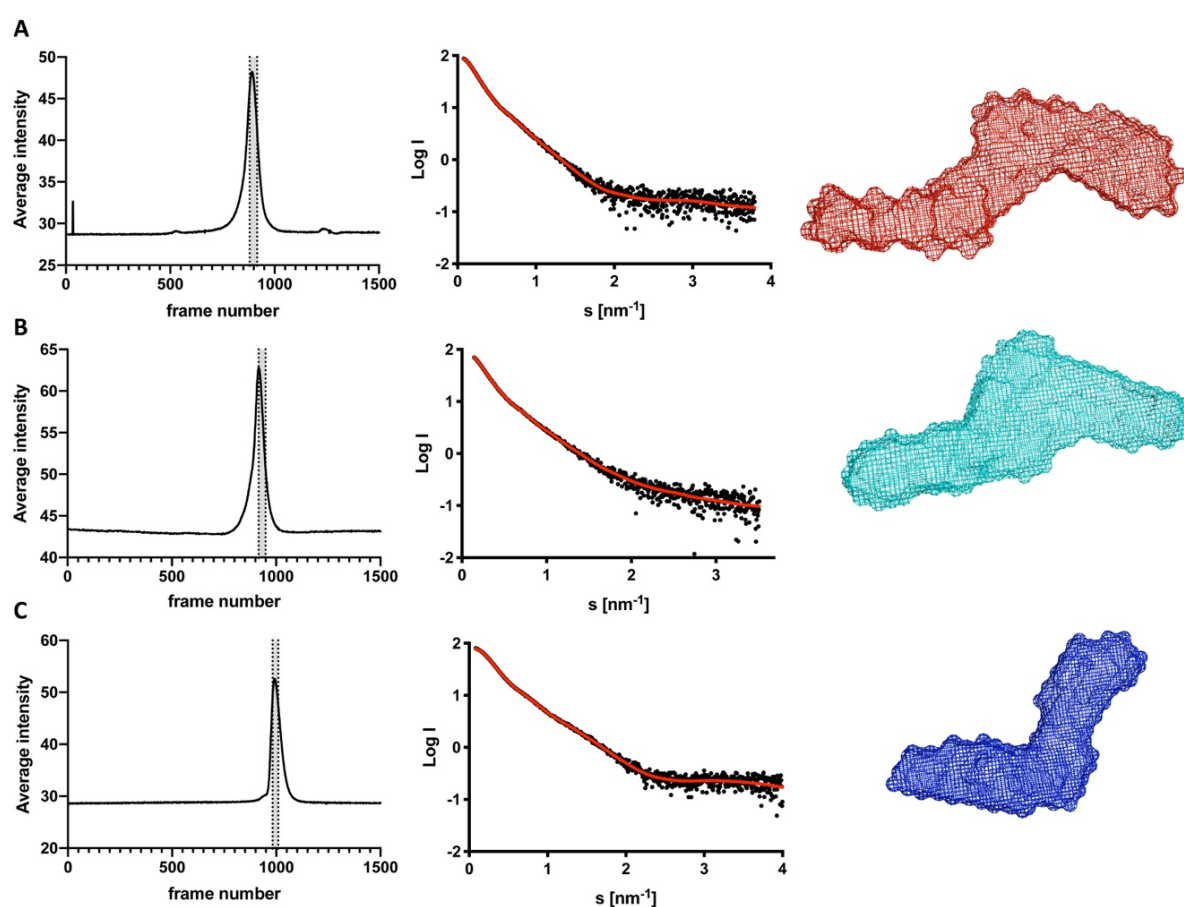


Figure 13: SEC-SAXS analysis of refolded proHlyA (A), secreted proHlyA (B) and FrpA (C). The average intensity recorded during SEC-SAXS is shown in the left row with the fractions chosen for the extraction of the scattering curve and calculation of the *ab initio* model highlighted in grey. The scattering curve is shown in the middle row in black with the theoretical scattering curve calculated with DAMMIF shown in red [56]. The resulting volumetric envelopes of refolded proHlyA, secreted proHlyA and FrpA are shown in the right row.

A homology prediction of the three dimensional structure of HlyA from its sequence using Phyre2 [68] gives only a model for the C-terminus (Fig. 14 A). The resulting model includes as expected for the RTX domain β -roll motifs and short α -helices. As this structure is too small to be docked into the experimentally obtained volumetric envelopes, we used a model from the MbxA sequence as predicted by Phyre2 [68]. The predicted MbxA structure contains again β -roll motifs and an elongated α -helical part. This structure does not fit unambiguously into the *ab initio* model but fills approximately half of its volume, suggesting that the size of a HlyA dimer would go together with the calculated envelope (Fig. 14 C). At the same time docking of the *ab initio* model of FrpA into the *ab initio* model of refolded HlyA shows a similarly twisted elongated shape and could possibly illustrate the position of a HlyA monomer (Fig. 14 D). The Phyre2 predicted homology model of FrpA however contains again β -roll motifs but is not

elongated and does not fit with the volumetric envelope calculate for FrpA (Fig. 14 E). This indicates that FrpA in solution adopts a more flexible conformation. Both for monomeric FrpA and dimeric proHlyA the volumetric envelopes obtained from the SAXS data have stretched shapes with multiple bends. This could possibly represent a common, flexible conformation that RTX protein adopt in solution.

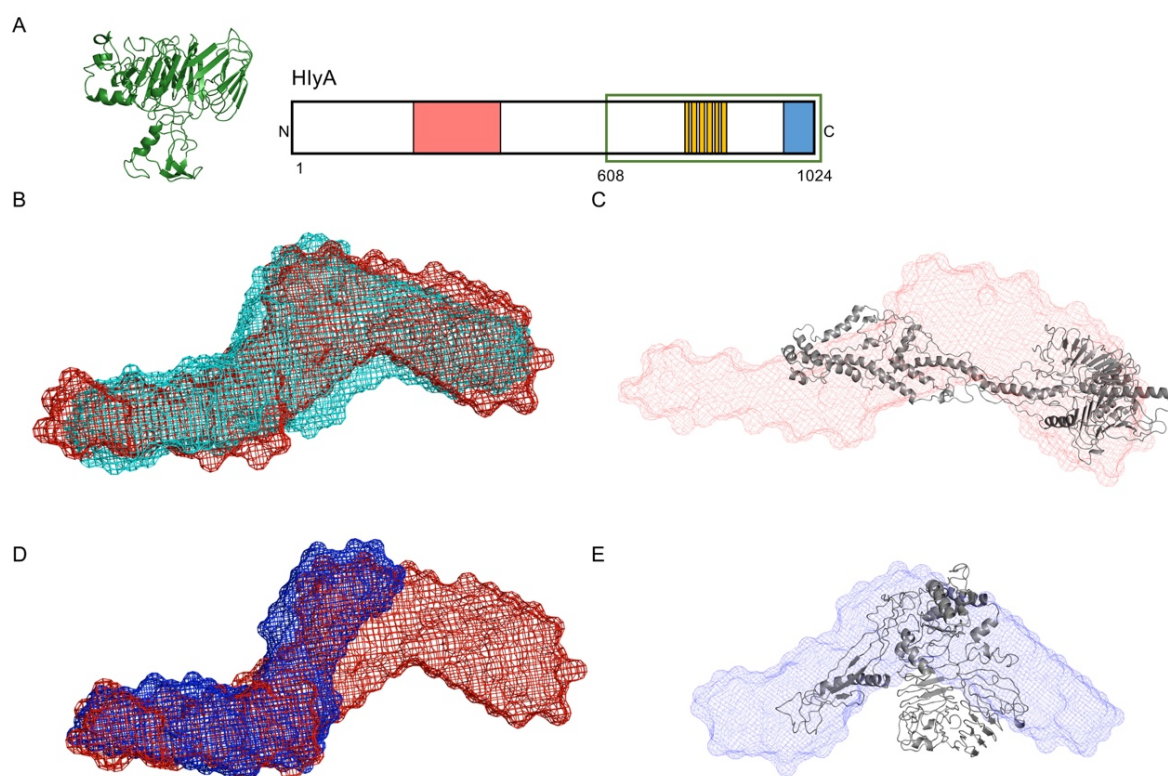


Figure 14: A) A homology model of the C-terminus of HlyA was predicted using Phyre2 [68]. The modelled residues (608-1024) are indicated with a green box in the schematic representation of proHlyA. The N-terminal membrane interaction domain is highlighted in red [69], the GG-repeats in yellow and the secretion signal in blue. B) The volumetric envelope of refolded proHlyA (red) and secreted proHlyA (cyan) are shown as an overlay. C) As no homology prediction of the full-length HlyA protein is calculated with Phyre2 the predicted full length model of monomeric MbxA is shown in the volumetric envelope of refolded proHlyA. D) The *ab initio* model of the FrpA monomer (blue) is docked into the *ab initio* model of refolded proHlyA (red). E) A Phyre2 predicted model of FrpA is shown docked into the volumetric envelope calculated for FrpA.

Table 2: Overall SAXS data for proHlyA, secreted and refolded and for FrpA.

| | | | |
|---|--|----------------------|-------------|
| Beamline | BM29, ESRF Grenoble [47, 48] | | |
| Data collection parameters | | | |
| Detector | PILATUS 1 M | | |
| Detector distance (m) | 2.867 | | |
| Beam size ($\mu\text{m} \times \mu\text{m}$) | 700 x 700 | | |
| Wavelength (nm) | 0.099 | | |
| Sample environment | Quartz glass capillary, 1 mm \varnothing | | |
| s range (nm^{-1}) [‡] | 0.025–5.0 | | |
| Temperature (K) | 277 | | |
| Exposure time per frame (s) | 1 | | |
| Sample | proHlyA secreted | proHlyA, refolded | FrpA |
| Mode of measurement | online SEC-SAXS | | |
| Protein concentration (mg/ml) | 7.8 | 8.0 | 10.9 |
| SEC column | Superose 6 Increase 10/300 | | |
| Injection volume (μl) | 110 | | |
| Structural parameters | | | |
| $I(0)$ from $P(r)$ | 92.55 | 97.36 | 85.28 |
| R_g (real-space from $P(r)$) (nm) | 6.42 | 7.01 | 5.17 |
| $I(0)$ from Guinier fit | 90.84 | 95.91 | 84.81 |
| s -range for Guinier fit (nm^{-1}) | 0.13 – 0.21 | 0.08 – 0.19 | 0.08 – 0.24 |
| R_g (from Guinier fit) (nm) | 6.08 | 6.65 | 5.02 |
| D_{max} (nm) | 20.60 | 23.60 | 17.12 |
| POROD volume estimate (nm^3) | 293.53 | 344.78 | 142.19 |
| Molecular mass (kDa) | | | |
| From $I(0)$ | n.a. | n.a. | n.a. |
| From MoW2 [12] | 165.53 | 167.71 | 88.20 |
| From Vc [13] | 171.58 | 195.50 | 88.79 |
| From POROD | 183.46 | 215.49 | 88.87 |
| From sequence | 110.46 | 110.46 | 85.81 |
| Structure Evaluation | | | |
| Ambimeter score | 2.805 | 2.560 | 2.718 |
| DAMMIF fit χ^2 | 0.702 | 1.151 | 1.102 |
| Software | | | |
| ATSAS Software Version [4] | 3.0.2 | | |
| Primary data reduction | CHROMIXS [52] / PRIMUS [53] | | |
| Data processing | GNOM [55] | | |
| <i>Ab initio</i> modelling | DAMMIF [56] | | |
| Averaging & superimposing | DAMAVAR [58] / SUPCOMB [57] | | |
| Structure evaluation | AMBIMETER [70] | | |
| Model visualization | PyMOL [71] | | |

[‡] $s = 4\pi\sin(\theta)/\lambda$, 2θ – scattering angle, λ – X-ray-wavelength, n.a. not applicable

Discussion

RTX proteins are characterized by conserved Ca^{2+} -binding repeats, referred to as GG-repeats and are secreted via T1SS [1, 2]. Before secretion, in the bacterial cytosol and during the transport through the secretion system, RTX proteins remain unfolded [23, 72]. The folding of the protein is induced when it reaches the extracellular space by subsequent binding of calcium ions to the GG-repeats [7, 27, 39, 73]. The structure of the RTX domain, a characteristic β -roll motif, is formed by binding of calcium ions between the turns of two GGXGXDXUX repeats, coordinated by the glycine and aspartate residues [7]. This motif is known from crystal structures of for example the alkaline protease of *Pseudomonas aeruginosa* [7] or the secreted lipase LipA from *Serratia marcescens* [74]. For cytolytic RTX proteins such as HlyA the three dimensional protein structure still has not been solved. In this study a heterologous secretion approach, single particle cryo-EM and SAXS were implemented to assess structural aspects of the RTX proteins HlyA from *E. coli*, MbxA from *M. bovis* and FrpA from *K. kingae*. While HlyA and MbxA are both classic pore-forming RTX cytotoxins [33, 75, 76] the function of FrpA is unknown. It is homologous to two *Neisseria meningitidis* iron-regulated proteins. The homologues are FrpA and its paralogue the self-processing protein FrpC that interacts with a lipoprotein, but FrpA from *K. kingae* presumably lacks a self-processing domain [37, 77, 78]. In a *E. coli* BL21(DE3) system expressing the hemolysin T1SS components HlyB and HlyD from plasmid pK184-*hlyBD* [23] together with chromosomally encoded TolC both, proMbxA and FrpA, were secreted (Fig. 2). As this heterologous system lacked an activating acyltransferase, MbxA was not acylated, but secreted as the inactive precursor proMbxA. In contrast to pore-forming RTX toxins such as HlyA and MbxA which require acylation at two lysine residues [29], in FrpA these conserved acylation sites were not identified. It is thus not clear if FrpA requires any kind of post-translational acylation for its activity. Nevertheless, the ability of the UPEC hemolysin system to recognize and secrete proMbxA and FrpA mean that these RTX toxins from different species remain in a secretion competent state in the *E. coli* cytosol and further successfully interact with the T1SS. Interestingly, a few other RTX protein previously have been reported to be secretable via HlyBD including the FrpA protein from *Neisseria meningitidis*, CyA from *Bordetella pertussis* and LktA from *Mannheimia haemolytica* [79-81]. The last 50-60 C-terminal amino acids of HlyA have been identified as a non-cleavable secretion signal that interacts with the inner membrane components HlyB and HlyD [13, 15, 21]. As no common, conserved primary sequence is identifiable in the C-termini of RTX proteins a secondary structure motif is suggested to mediate interaction with the translocon [82] (Fig. 3). In HlyA, a helix-linker-helix motif was

shown [61], of which the first of two short amphipathic helices is essential for secretion [62]. With a computational approach three helices connected with short linkers located in the C-terminus were predicted for MbxA and FrpA (Fig. 4). This potential helix-linker motifs could substitute for the recognition motif of HlyA and facilitate heterologous secretion. As HlyA has yet eluded crystallization single particle cryo-EM was the next method of choice for structure determination. Single particle cryo-EM has rapidly gained importance as it yields high resolution structures of dynamic proteins not suitable for crystallization and tolerates more conformational heterogeneity [66]. proHlyA, refolded from inclusion bodies (Fig. 5) as well as proMbxA, purified from *E. coli* secretion supernatants (Fig. 6) were used for cryo-EM specimen preparation with various grids and conditions. proMbxA was beforehand separated in a dimeric and a monomeric species via SEC (Fig. 6B), which were then separately used for grid preparation. For both, proHlyA and proMbxA, the grids were screened for optimal cryo-EM specimen. On the grids suitable for data collection proHlyA and proMbxA behaved similarly and micrographs of both proteins showed prolonged particles (Fig. 9 and 11). Interestingly dimeric and monomeric proMbxA samples did not yield distinguishable different particles on the screened grids (Fig. 11). Data collection and resulting 2D class averages of the picked proHlyA particles showed prolonged particles, partially with broader domains located on one side (Fig. 10). The 2D classification of proMbxA resulted similarly in prolonged, string-like or dot-like particles (Fig. 12). The quality of the 2D classification was not sufficient for a successful reconstruction of a 3D structure. proHlyA and proMbxA both tend to aggregate during grid preparation and form particles that are too heterogeneous for structural analysis. To overcome this problem an optimization of the sample and grid preparation conditions as well as biochemical stabilization such as addition of suitable surfactants or alternatively an analysis of the RTX protein as part of a stalled T1SS yielding larger particles could be considered [24, 83, 84]. A method of structure determination that is applicable to proteins in solution is SAXS. Here, for proHlyA and FrpA SAXS analysis was used to assess the shape and size of these RTX proteins (Fig. 13). Depending on the computation the molecular weight calculated from scattering of refolded proHlyA and of secreted proHlyA was 165.53 kDa to 183.46 kDa or 167.71 to 215.49 kDa, respectively. Previously, proHlyA was shown to form dimers in solution [85]. The masses obtained from SAXS data do not reach the theoretical molecular weight of a dimer of 220 kDa but still indicate that a population of predominantly dimeric molecules is present. Overlay of the *ab initio* models of the two proHlyA species shows that both are similar in shape (Fig. 14 B). Secreted proHlyA appears shorter but both have an twisted, elongated and nearly S-shaped conformation. This shape is formed by two proHlyA monomers but the

arrangement of the monomers cannot be deduced from the volumetric envelope. Nevertheless the SAXS analysis suggests that proHlyA that is refolded with a Ca^{2+} -containing buffer adopts a conformation that is very close to the conformation of secreted proHlyA. Using the protein structure prediction server Phyre2 to build a 3D model of HlyA from its sequence resulted in a model of the C-terminus that covers residue 608-1024 [68]. This model contains the β -roll structure typical for the RTX-domain but fails to predict the N-terminal part of HlyA (Fig. 14 A). This fragment is too short to dock it into the volumetric envelope. Instead a model was predicted from the sequence of MbxA, which shares 42% sequence identity with HlyA. This model contained the expected C-terminal β -roll motif and had an elongated N-terminal domain consisting of α -helices and unstructured loops. This theoretical model is still not able to concisely illustrate the potential position of a proHlyA monomer in the volumetric envelope (Fig. 14 C). With a molecular weight of 88 kDa the FrpA protein is 20% smaller than HlyA. When expressed without the HlyA T1SS the intracellular FrpA does not form inclusion bodies. This suggests that the FrpA is intrinsically stable enough to remain in the *E. coli* cytosol in a soluble state. The CD spectrum of this cytosolic FrpA, isolated from lysed cells and of secreted FrpA is nearly identical which indicates that both adopt a very similar conformation or at least have the same proportion of secondary structure (Fig. 8). It is possible that in directly isolated FrpA the calcium ions present in the buffers during purification induce folding that is close to the conformation that is achieved upon secretion, comparable to the Ca^{2+} -dependent refolding of proHlyA [39]. A more detailed understanding of the FrpA structure was likewise obtained from SAXS analysis. The scattering data of FrpA revealed that it is, in contrast to proHlyA, a monomer and the calculated *ab initio* model showed an elongated, bend shape (Fig. 13). Comparison of this volumetric envelope with a homology model computed from the sequence of FrpA that is more globular indicates that the conformation of soluble FrpA is more relaxed and flexible (Fig 14 E). The volumetric envelope of FrpA can be docked into the proHlyA *ab initio* model and occupies approximately half of the volume therefore potentially illustrating the position of an actual proHlyA monomer (Fig. 14 B). Both the low resolution structure obtained for proHlyA and FrpA revealed prolonged and somehow twisted conformation. This flexible and relaxed, elongated structure could be a common characteristic of secreted RTX proteins in solution. Using among others methods SAXS analysis, the transition of the 701 residue long RTX domain of CyaA from *Bordetella pertussis* from an intrinsically disordered protein before secretion to a folded, more compact functional structure in the presence of Ca^{2+} was shown [28]. Another study presented a similarly elongated and bend SAXS-derived low resolution structure of the RTX domain of CyaA comprising five RTX blocks in Ca^{2+} bound

state [86]. The intrinsically disordered RTX domain itself is suggested to stabilize the unfolded protein in the low Ca^{2+} environment of the bacterial cytosol [72]. This is presumably also applicable to the here presented RTX proteins FrpA, MbxA and HlyA and explains their stability. Nonetheless, currently the elucidation of the structure of a full length RTX proteins remains challenging as the analyzed examples HlyA, MbxA and FrpA keep an inherent degree of flexibility even in presence of calcium ions. Taken together single particle cryo-EM and SAXS both suggest that proHlyA as well proMbxA and FrpA have an elongated and relaxed conformation resulting in structural heterogeneity. This presumably represents a characteristic of not only closely related RTX proteins of the group of cytotoxins such as HlyA and MbxA but also of FrpA, a protein with a different function and different distribution of GG repeats.

Acknowledgments

We would like to thank Dr. Diana Kleinschrodt for her support with cloning of the constructs as well as Nicole Jasny and Dr. Lothar Gremer for CD spectroscopy measurements. We would further like to thank all members of the Institute of Biochemistry for support and valuable discussions. This work was funded by the Jürgen Manchot Graduate School “Molecules of Infection III”.

References

1. Welch, R.A., *Pore-forming cytolysins of Gram-negative bacteria*. Molecular Microbiology, 1991. **5**: p. 521-528.
2. Linhartova, I., Bumba, L., Masin, J., Basler, M., Osicka, R., Kamanova, J., Prochazkova, K., Adkins, I., Hejnova-Holubova, J., Sadilkova, L., Morova, J., and Sebo, P., *RTX proteins: a highly diverse family secreted by a common mechanism*. FEMS Microbiol Rev, 2010. **34**(6): p. 1076-112.
3. Mackman, N. and Holland, I.B., *Secretion of a 107 K dalton polypeptide into the medium from a haemolytic E. coli K12 strain*. Mol Gen Genet, 1984. **193**(2): p. 312-5.
4. Mackman, N., Nicaud, J.M., Gray, L., and Holland, I.B., *Genetical and functional organisation of the Escherichia coli haemolysin determinant 2001*. Mol Gen Genet, 1985. **201**(2): p. 282-8.
5. Glaser, P., Danchin, A., Ladant, D., Barzu, O., and Ullmann, A., *Bordetella pertussis adenylate cyclase: the gene and the protein*. Tokai J Exp Clin Med, 1988. **13 Suppl**: p. 239-52.
6. Lo, R.Y., Strathdee, C.A., and Shewen, P.E., *Nucleotide sequence of the leukotoxin genes of Pasteurella haemolytica A1*. Infect Immun, 1987. **55**(9): p. 1987-96.
7. Baumann, U., Wu, S., Flaherty, K.M., and McKay, D.B., *Three-dimensional structure of the alkaline protease of Pseudomonas aeruginosa: a two-domain protein with a calcium binding parallel beta roll motif*. EMBO J, 1993. **12**(9): p. 3357-64.

8. Duong, F., Soscia, C., Lazdunski, A., and Murgier, M., *The Pseudomonas fluorescens lipase has a C-terminal secretion signal and is secreted by a three-component bacterial ABC-exporter system*. Mol Microbiol, 1994. **11**(6): p. 1117-26.
9. Lin, W., Fullner, K.J., Clayton, R., Sexton, J.A., Rogers, M.B., Calia, K.E., Calderwood, S.B., Fraser, C., and Mekalanos, J.J., *Identification of a vibrio cholerae RTX toxin gene cluster that is tightly linked to the cholera toxin prophage*. Proc Natl Acad Sci U S A, 1999. **96**(3): p. 1071-6.
10. Satchell, K.J., *MARTX, multifunctional autoprocessing repeats-in-toxin toxins*. Infect Immun, 2007. **75**(11): p. 5079-84.
11. Hinsa, S.M., Espinosa-Urgel, M., Ramos, J.L., and O'Toole, G.A., *Transition from reversible to irreversible attachment during biofilm formation by Pseudomonas fluorescens WCS365 requires an ABC transporter and a large secreted protein*. Mol Microbiol, 2003. **49**(4): p. 905-18.
12. Guo, S.Q., Stevens, C.A., Vance, T.D.R., Olijve, L.L.C., Graham, L.A., Campbell, R.L., Yazdi, S.R., Escobedo, C., Bar-Dolev, M., Yashunsky, V., Braslavsky, I., Langelan, D.N., Smith, S.P., Allingham, J.S., Voets, I.K., and Davies, P.L., *Structure of a 1.5-MDa adhesin that binds its Antarctic bacterium to diatoms and ice*. Science Advances, 2017. **3**(8).
13. Gray, L., Mackman, N., Nicaud, J.M., and Holland, I.B., *The Carboxy-Terminal Region of Hemolysin 2001 Is Required for Secretion of the Toxin from Escherichia-Coli*. Molecular & General Genetics, 1986. **205**(1): p. 127-133.
14. Felmler, T. and Welch, R.A., *Alterations of amino acid repeats in the Escherichia coli hemolysin affect cytolytic activity and secretion*. Proc Natl Acad Sci U S A, 1988. **85**(14): p. 5269-73.
15. Koronakis, V., Koronakis, E., and Hughes, C., *Isolation and Analysis of the C-Terminal Signal Directing Export of Escherichia-Coli Hemolysin Protein across Both Bacterial-Membranes*. Embo Journal, 1989. **8**(2): p. 595-605.
16. Gray, L., Baker, K., Kenny, B., Mackman, N., Haigh, R., and Holland, J.B., *A Novel C-Terminal Signal Sequence Targets Escherichia-Coli Hemolysin Directly to the Medium*. Journal of Cell Science, 1989: p. 45-57.
17. Koronakis, V., Koronakis, E., and Hughes, C., *Comparison of the haemolysin secretion protein HlyB from Proteus vulgaris and Escherichia coli; site-directed mutagenesis causing impairment of export function*. Mol Gen Genet, 1988. **213**(2-3): p. 551-5.
18. Wang, R.C., Seror, S.J., Blight, M., Pratt, J.M., Broome-Smith, J.K., and Holland, I.B., *Analysis of the membrane organization of an Escherichia coli protein translocator, HlyB, a member of a large family of prokaryote and eukaryote surface transport proteins*. J Mol Biol, 1991. **217**(3): p. 441-54.
19. Mackman, N., Nicaud, J.M., Gray, L., and Holland, I.B., *Identification of polypeptides required for the export of haemolysin 2001 from E. coli*. Mol Gen Genet, 1985. **201**(3): p. 529-36.
20. Thanabalu, T., Koronakis, E., Hughes, C., and Koronakis, V., *Substrate-induced assembly of a contiguous channel for protein export from E.coli: reversible bridging of an inner-membrane translocase to an outer membrane exit pore*. EMBO J, 1998. **17**(22): p. 6487-96.

21. Felmllee, T., Pellett, S., Lee, E.Y., and Welch, R.A., *Escherichia coli hemolysin is released extracellularly without cleavage of a signal peptide*. J Bacteriol, 1985. **163**(1): p. 88-93.
22. Balakrishnan, L., Hughes, C., and Koronakis, V., *Substrate-triggered recruitment of the TolC channel-tunnel during type I export of hemolysin by Escherichia coli*. J Mol Biol, 2001. **313**(3): p. 501-10.
23. Bakkes, P.J., Jenewein, S., Smits, S.H.J., Holland, I.B., and Schmitt, L., *The Rate of Folding Dictates Substrate Secretion by the Escherichia coli Hemolysin Type 1 Secretion System*. Journal of Biological Chemistry, 2010. **285**(52): p. 40573-40580.
24. Lenders, M.H., Weidtkamp-Peters, S., Kleinschrodt, D., Jaeger, K.E., Smits, S.H., and Schmitt, L., *Directionality of substrate translocation of the hemolysin A Type I secretion system*. Sci Rep, 2015. **5**: p. 12470.
25. Jones, H.E., Holland, I.B., Baker, H.L., and Campbell, A.K., *Slow changes in cytosolic free Ca²⁺ in Escherichia coli highlight two putative influx mechanisms in response to changes in extracellular calcium*. Cell Calcium, 1999. **25**(3): p. 265-74.
26. Jones, H.E., Holland, I.B., and Campbell, A.K., *Direct measurement of free Ca(2+) shows different regulation of Ca(2+) between the periplasm and the cytosol of Escherichia coli*. Cell Calcium, 2002. **32**(4): p. 183-92.
27. Ostolaza, H., Soloaga, A., and Goni, F.M., *The Binding of Divalent-Cations to Escherichia-Coli Alpha-Hemolysin*. European Journal of Biochemistry, 1995. **228**(1): p. 39-44.
28. O'Brien, D.P., Hernandez, B., Durand, D., Hourdel, V., Sotomayor-Perez, A.C., Vachette, P., Ghomi, M., Chamot-Rooke, J., Ladant, D., Brier, S., and Chenal, A., *Structural models of intrinsically disordered and calcium-bound folded states of a protein adapted for secretion*. Sci Rep, 2015. **5**: p. 14223.
29. Stanley, P., Packman, L.C., Koronakis, V., and Hughes, C., *Fatty acylation of two internal lysine residues required for the toxic activity of Escherichia coli hemolysin*. Science, 1994. **266**(5193): p. 1992-6.
30. Nicaud, J.M., Mackman, N., Gray, L., and Holland, I.B., *Characterisation of HlyC and mechanism of activation and secretion of haemolysin from E. coli 2001*. FEBS Lett, 1985. **187**(2): p. 339-44.
31. Hardie, K.R., Issartel, J.P., Koronakis, E., Hughes, C., and Koronakis, V., *In vitro activation of Escherichia coli prohaemolysin to the mature membrane-targeted toxin requires HlyC and a low molecular-weight cytosolic polypeptide*. Mol Microbiol, 1991. **5**(7): p. 1669-79.
32. Clinkenbeard, K.D. and Thiessen, A.E., *Mechanism of action of Moraxella bovis hemolysin*. Infect Immun, 1991. **59**(3): p. 1148-52.
33. Angelos, J.A., Hess, J.F., and George, L.W., *Cloning and characterization of a Moraxella bovis cytotoxin gene*. Am J Vet Res, 2001. **62**(8): p. 1222-8.
34. Angelos, J.A., Hess, J.F., and George, L.W., *An RTX operon in hemolytic Moraxella bovis is absent from nonhemolytic strains*. Vet Microbiol, 2003. **92**(4): p. 363-77.
35. Osickova, A., Balashova, N., Masin, J., Sulc, M., Roderova, J., Wald, T., Brown, A.C., Koufos, E., Chang, E.H., Giannakakis, A., Lally, E.T., and Osicka, R., *Cytotoxic activity of Kingella kingae RtxA toxin depends on post-translational acylation of lysine residues and cholesterol binding*. Emerg Microbes Infect, 2018. **7**(1): p. 178.

-
36. Osicka, R., Prochazkova, K., Sulc, M., Linhartova, I., Havlicek, V., and Sebo, P., *A novel "clip-and-link" activity of repeat in toxin (RTX) proteins from gram-negative pathogens. Covalent protein cross-linking by an Asp-Lys isopeptide bond upon calcium-dependent processing at an Asp-Pro bond*. J Biol Chem, 2004. **279**(24): p. 24944-56.
 37. Sviridova, E., Rezacova, P., Bondar, A., Veverka, V., Novak, P., Schenk, G., Svergun, D.I., Kuta Smatanova, I., and Bumba, L., *Structural basis of the interaction between the putative adhesion-involved and iron-regulated FrpD and FrpC proteins of Neisseria meningitidis*. Sci Rep, 2017. **7**: p. 40408.
 38. Dobson, L., Remenyi, I., and Tusnady, G.E., *CCTOP: a Consensus Constrained TOPology prediction web server*. Nucleic Acids Res, 2015. **43**(W1): p. W408-12.
 39. Thomas, S., Bakkes, P.J., Smits, S.H., and Schmitt, L., *Equilibrium folding of pro-HlyA from Escherichia coli reveals a stable calcium ion dependent folding intermediate*. Biochim Biophys Acta, 2014. **1844**(9): p. 1500-10.
 40. Kanonenberg, K., Smits, S.H.J., and Schmitt, L., *Functional Reconstitution of HlyB, a Type I Secretion ABC Transporter, in Saposin-A Nanoparticles*. Sci Rep, 2019. **9**(1): p. 8436.
 41. Soloaga, A., Ostolaza, H., Goni, F.M., and de la Cruz, F., *Purification of Escherichia coli pro-haemolysin, and a comparison with the properties of mature alpha-haemolysin*. Eur J Biochem, 1996. **238**(2): p. 418-22.
 42. Fitzpatrick, A.W.P., Llabres, S., Neuberger, A., Blaza, J.N., Bai, X.C., Okada, U., Murakami, S., van Veen, H.W., Zachariae, U., Scheres, S.H.W., Luisi, B.F., and Du, D., *Structure of the MacAB-TolC ABC-type tripartite multidrug efflux pump*. Nat Microbiol, 2017. **2**: p. 17070.
 43. Du, D., Wang, Z., James, N.R., Voss, J.E., Klimont, E., Ohene-Agyei, T., Venter, H., Chiu, W., and Luisi, B.F., *Structure of the AcrAB-TolC multidrug efflux pump*. Nature, 2014. **509**(7501): p. 512-5.
 44. Scheres, S.H., *RELION: implementation of a Bayesian approach to cryo-EM structure determination*. J Struct Biol, 2012. **180**(3): p. 519-30.
 45. Zivanov, J., Nakane, T., Forsberg, B.O., Kimanius, D., Hagen, W.J., Lindahl, E., and Scheres, S.H., *New tools for automated high-resolution cryo-EM structure determination in RELION-3*. Elife, 2018. **7**.
 46. Zhang, K., *Gctf: Real-time CTF determination and correction*. J Struct Biol, 2016. **193**(1): p. 1-12.
 47. Pernot, P., Theveneau, P., Giraud, T., Nogueira Fernandes, R., Nurizzo, D., Spruce, D., Surr, J., and McSweeney, S., *New beamline dedicated to solution scattering from biological macromolecules at the ESRF*. Journal of Physics: Conference Series, 2010. **247**(1): p. 012009.
 48. Pernot, P., Round, A., Barrett, R., De Maria Antolinos, A., Gobbo, A., Gordon, E., Huet, J., Kieffer, J., Lentini, M., Mattenet, M., Morawe, C., Mueller-Dieckmann, C., Ohlsson, S., Schmid, W., Surr, J., Theveneau, P., Zerrad, L., and McSweeney, S., *Upgraded ESRF BM29 beamline for SAXS on macromolecules in solution*. J Synchrotron Radiat, 2013. **20**(Pt 4): p. 660-4.
 49. Heilers, J.H., Reiniers, J., Heller, E.M., Golzer, A., Smits, S.H.J., and van der Does, C., *DNA processing by the MOBH family relaxase TraI encoded within the gonococcal genetic island*. Nucleic Acids Res, 2019. **47**(15): p. 8136-8153.

-
50. Petoukhov, M.V., Franke, D., Shkumatov, A.V., Tria, G., Kikhney, A.G., Gajda, M., Gorba, C., Mertens, H.D., Konarev, P.V., and Svergun, D.I., *New developments in the ATSAS program package for small-angle scattering data analysis*. J Appl Crystallogr, 2012. **45**(Pt 2): p. 342-350.
 51. Franke, D., Petoukhov, M.V., Konarev, P.V., Panjkovich, A., Tuukkanen, A., Mertens, H.D.T., Kikhney, A.G., Hajizadeh, N.R., Franklin, J.M., Jeffries, C.M., and Svergun, D.I., *ATSAS 2.8: a comprehensive data analysis suite for small-angle scattering from macromolecular solutions*. J Appl Crystallogr, 2017. **50**(Pt 4): p. 1212-1225.
 52. Panjkovich, A. and Svergun, D.I., *CHROMIXS: automatic and interactive analysis of chromatography-coupled small-angle X-ray scattering data*. Bioinformatics, 2018. **34**(11): p. 1944-1946.
 53. Konarev, P.V., Volkov, V.V., Sokolova, A.V., Koch, M.H.J., and Svergun, D.I., *PRIMUS: a Windows PC-based system for small-angle scattering data analysis*. 2003. **36**(5): p. 1277-1282.
 54. Guinier, A., *La diffraction des rayons X aux très petits angles : application à l'étude de phénomènes ultramicroscopiques*. Annales de Physique, 1939. **11**: p. 161.
 55. Svergun, D., *Determination of the regularization parameter in indirect-transform methods using perceptual criteria*. Journal of Applied Crystallography, 1992. **25**(4): p. 495-503.
 56. Franke, D. and Svergun, D.I., *DAMMIF, a program for rapid ab-initio shape determination in small-angle scattering*. J Appl Crystallogr, 2009. **42**(Pt 2): p. 342-346.
 57. Kozin, M.B. and Svergun, D.I., *Automated matching of high- and low-resolution structural models*. 2001. **34**(1): p. 33-41.
 58. Volkov, V.V. and Svergun, D.I., *Uniqueness of ab initio shape determination in small-angle scattering*. Journal of Applied Crystallography, 2003. **36**(3 Part 1): p. 860-864.
 59. Fischer, H., de Oliveira Neto, M., Napolitano, H.B., Polikarpov, I., and Craievich, A.F., *Determination of the molecular weight of proteins in solution from a single small-angle X-ray scattering measurement on a relative scale*. Journal of Applied Crystallography, 2010. **43**(1): p. 101-109.
 60. Rambo, R.P. and Tainer, J.A., *Accurate assessment of mass, models and resolution by small-angle scattering*. Nature, 2013. **496**(7446): p. 477-81.
 61. Yin, Y., Zhang, F., Ling, V., and Arrowsmith, C.H., *Structural analysis and comparison of the C-terminal transport signal domains of hemolysin A and leukotoxin A*. FEBS Lett, 1995. **366**(1): p. 1-5.
 62. Hui, D., Morden, C., Zhang, F., and Ling, V., *Combinatorial analysis of the structural requirements of the Escherichia coli hemolysin signal sequence*. J Biol Chem, 2000. **275**(4): p. 2713-20.
 63. Madeira, F., Park, Y.M., Lee, J., Buso, N., Gur, T., Madhusoodanan, N., Basutkar, P., Tivey, A.R.N., Potter, S.C., Finn, R.D., and Lopez, R., *The EMBL-EBI search and sequence analysis tools APIs in 2019*. Nucleic Acids Res, 2019. **47**(W1): p. W636-W641.
 64. Sapay, N., Guermeur, Y., and Deleage, G., *Prediction of amphipathic in-plane membrane anchors in monotopic proteins using a SVM classifier*. BMC Bioinformatics, 2006. **7**: p. 255.
 65. Woody, R.W., *Circular dichroism*. Methods Enzymol, 1995. **246**: p. 34-71.

66. Murata, K. and Wolf, M., *Cryo-electron microscopy for structural analysis of dynamic biological macromolecules*. Biochim Biophys Acta Gen Subj, 2018. **1862**(2): p. 324-334.
67. Peherstorfer, S., *Untersuchungen zur Acylierung, Struktur und Glykanbindung des RTX-Toxins Hämolysin A aus Escherichia coli*, 2017, Heinrich-Heine-Universität Düsseldorf: Düsseldorf, Germany.
68. Kelley, L.A., Mezulis, S., Yates, C.M., Wass, M.N., and Sternberg, M.J., *The Phyre2 web portal for protein modeling, prediction and analysis*. Nat Protoc, 2015. **10**(6): p. 845-58.
69. Ludwig, A., Schmid, A., Benz, R., and Goebel, W., *Mutations affecting pore formation by haemolysin from Escherichia coli*. Mol Gen Genet, 1991. **226**(1-2): p. 198-208.
70. Petoukhov, M.V. and Svergun, D.I., *Ambiguity assessment of small-angle scattering curves from monodisperse systems*. Acta Crystallogr D Biol Crystallogr, 2015. **71**(Pt 5): p. 1051-8.
71. PyMOL, *The PyMOL Molecular Graphics System, Version 2.0* Schrödinger, LLC.
72. Chenal, A., Guijarro, J.I., Raynal, B., Delepierre, M., and Ladant, D., *RTX calcium binding motifs are intrinsically disordered in the absence of calcium: implication for protein secretion*. J Biol Chem, 2009. **284**(3): p. 1781-9.
73. Zhang, L., Conway, J.F., and Thibodeau, P.H., *Calcium-induced folding and stabilization of the Pseudomonas aeruginosa alkaline protease*. J Biol Chem, 2012. **287**(6): p. 4311-22.
74. Meier, R., Drepper, T., Svensson, V., Jaeger, K.E., and Baumann, U., *A calcium-gated lid and a large beta-roll sandwich are revealed by the crystal structure of extracellular lipase from Serratia marcescens*. J Biol Chem, 2007. **282**(43): p. 31477-83.
75. Bhakdi, S., Greulich, S., Muhly, M., Eberspacher, B., Becker, H., Thiele, A., and Hugo, F., *Potent leukocidal action of Escherichia coli hemolysin mediated by permeabilization of target cell membranes*. J Exp Med, 1989. **169**(3): p. 737-54.
76. Benz, R., Schmid, A., Wagner, W., and Goebel, W., *Pore Formation by the Escherichia-Coli Hemolysin - Evidence for an Association-Dissociation Equilibrium of the Pore-Forming Aggregates*. Infection and Immunity, 1989. **57**(3): p. 887-895.
77. Thompson, S.A., Wang, L.L., West, A., and Sparling, P.F., *Neisseria meningitidis produces iron-regulated proteins related to the RTX family of exoproteins*. J Bacteriol, 1993. **175**(3): p. 811-8.
78. Kuban, V., Macek, P., Hritz, J., Nechvatalova, K., Nedbalcova, K., Faldyna, M., Sebo, P., Zidek, L., and Bumba, L., *Structural Basis of Ca(2+)-Dependent Self-Processing Activity of Repeat-in-Toxin Proteins*. mBio, 2020. **11**(2).
79. Thompson, S.A. and Sparling, P.F., *The RTX cytotoxin-related FrpA protein of Neisseria meningitidis is secreted extracellularly by meningococci and by HlyBD+ Escherichia coli*. Infect Immun, 1993. **61**(7): p. 2906-11.
80. Sebo, P. and Ladant, D., *Repeat sequences in the Bordetella pertussis adenylate cyclase toxin can be recognized as alternative carboxy-proximal secretion signals by the Escherichia coli alpha-haemolysin translocator*. Mol Microbiol, 1993. **9**(5): p. 999-1009.
81. Highlander, S.K., Engler, M.J., and Weinstock, G.M., *Secretion and expression of the Pasteurella haemolytica Leukotoxin*. J Bacteriol, 1990. **172**(5): p. 2343-50.

-
82. Stanley, P., Koronakis, V., and Hughes, C., *Mutational analysis supports a role for multiple structural features in the C-terminal secretion signal of Escherichia coli haemolysin*. Mol Microbiol, 1991. **5**(10): p. 2391-403.
 83. Glaeser, R.M., Han, B.G., Csencsits, R., Killilea, A., Pulk, A., and Cate, J.H., *Factors that Influence the Formation and Stability of Thin, Cryo-EM Specimens*. Biophys J, 2016. **110**(4): p. 749-55.
 84. Drulyte, I., Johnson, R.M., Hesketh, E.L., Hurdiss, D.L., Scarff, C.A., Porav, S.A., Ranson, N.A., Muench, S.P., and Thompson, R.F., *Approaches to altering particle distributions in cryo-electron microscopy sample preparation*. Acta Crystallogr D Struct Biol, 2018. **74**(Pt 6): p. 560-571.
 85. Thomas, S., Smits, S.H.J., and Schmitt, L., *A simple in vitro acylation assay based on optimized HlyA and HlyC purification*. Analytical Biochemistry, 2014. **464**: p. 17-23.
 86. Bumba, L., Masin, J., Macek, P., Wald, T., Motlova, L., Bibova, I., Klimova, N., Bednarova, L., Veverka, V., Kachala, M., Svergun, D.I., Barinka, C., and Sebo, P., *Calcium-Driven Folding of RTX Domain beta-Rolls Ratchets Translocation of RTX Proteins through Type I Secretion Ducts*. Mol Cell, 2016. **62**(1): p. 47-62.
- .

4. Discussion

This thesis focused on the structural and functional characterization of selected RTX proteins. Members of the RTX protein family vary tremendously in their function, as this protein family comprises for example toxins, enzymes and adhesins, but they share the characteristic calcium ion-binding RTX domain [15]. Moreover, all RTX proteins are extracellular proteins that rely on secretion via T1SS. The prime example of RTX proteins is HlyA secreted by UPEC [17]. Studies on the HlyA secretion system contributed profoundly to the understanding of the mechanism of T1SS [104].

The first aim of this thesis was the identification of RTX proteins that act as heterologous substrates for the *E. coli* HlyA secretion systems. For successful candidates the heterologous expression in *E. coli* was optimized and further purification protocols were developed. The isolation of pure proteins is a principal requirement for biochemical and structural studies, which represent the second aim of this thesis and are addressed in chapter 3.4. For the third aim, the investigation of the effects of RTX proteins on host cells, the RTX protein MbxA from *M. bovis* was chosen. The characterization of MbxA and its cytotoxic activity are presented in chapter 3.3. A view on the current state of the research on T1SS is presented in chapter 3.1 and 3.2.

4.1 The hemolysin T1SS as a production platform for RTX proteins

The presence of the GG repeats allows to easily identify putative substrates of T1SS in sequenced genomes of bacteria [15]. This provides the opportunity to characterize novel RTX proteins and find suitable candidates for structural determination. The heterologous expression of RTX proteins in *E. coli* offers the strong advantage to circumvent cultivation of pathogenic bacteria, as many RTX proteins are virulence factors. *E. coli* is not only an efficient host for the production of recombinant proteins [157], but furthermore offers the opportunity to exploit the HlyA T1SS for the secretion of novel RTX proteins. The HlyA T1SS has early on been considered as a useful biotechnological tool for the secretion of heterologous proteins because it simplifies the isolation of the recombinant protein [152, 153]. As *E. coli* laboratory strains do not secrete other proteins, only the target protein is extruded into the culture medium [153]. The fusion of the C-terminal secretion sequence of HlyA to proteins of interest was shown to direct the heterologous substrate to the T1SS and mediate secretion [153]. Mutational studies on the maltose binding protein additionally showed that slow folding kinetics of the target

protein are essential for a successful transport via the HlyA secretion system [115]. At the same time the HlyA T1SS was shown to secrete several heterologous RTX proteins without the need for a fusion to the C-terminus of HlyA. Examples of non-native RTX substrates of the HlyA secretion system are CyaA from *B. pertussis*, FrpA from *N. meningitidis* and LktA from *M. haemolytica* [158-160]. The initial aim of this thesis was to identify further RTX proteins that can be secreted via a heterologously expressed HlyA secretion system in an *E. coli* BL21(DE3) background. To establish a recombinant T1SS in *E. coli* BL21(DE3) the inner membrane components HlyB and HlyD were expressed from a plasmid. As TolC is chromosomally encoded in *E. coli* BL21(DE3) only an additional plasmid carrying the RTX protein of interest was required to complete the secretion system [115]. This two-plasmid based system was shown to efficiently secrete two RTX proteins of other species, MbxA from *M. bovis* and FrpA from *K. kingae* (Chapter 3.4). MbxA is, as well as HlyA, a pore-forming toxin and therefore requires the post-translational acylation carried out by a specific acyltransferase to display cytotoxic activity [124, 143]. Therefore we additionally introduced the *hlyC* gene to complete the HlyA secretion with the UPEC acyltransferase. Interestingly, the UPEC T1SS including the activating acyltransferase HlyC acted as a fully functional surrogate secretion system for MbxA (Fig. 11). proMbxA was successfully converted into hemolytically active MbxA and secreted into the extracellular space. The secretion of both variants laid the basis for the development of a purification method for proMbxA and MbxA. Both the protoxin and the active protein can be isolated from the culture supernatant and purified via immobilized metal ion affinity chromatography (Chapter 3.3). Consequently, the efficient secretion of proMbxA confirms that like in the case of HlyA the acylation is not required for the secretion process [119].

In contrast to HlyA and MbxA, FrpA is presumably not a pore-forming toxin and no homologous acylation sites were identified. Furthermore, FrpA is homologous to a fragment of the iron-regulated protein FrpC from *N. meningitidis* that potentially mediates adhesion to host cells [41]. Even though HlyA and FrpA are less closely related and share a relatively low sequence identity of 28%, FrpA is recognized by the HlyA T1SS. This underlines that the C-terminal secretion signal of RTX proteins possess common characteristics that allow productive interaction with the inner membrane components of a non-native secretion system. For example, the secretion sequence of HlyA can be replaced with the C-terminus of LktA from *M. haemolytica* and the resulting fusion protein is still secreted by the HlyA system [161]. As no conserved consensus sequence is found in the secretion signals, secondary structure elements, presumably a linker-helix motif are postulated to mediate recognition [43, 162, 163].

Altogether this thesis demonstrates two further examples of non-native RTX proteins, MbxA and FrpA, that are efficiently secreted via the HlyA T1SS. This underlines that in contrast to unrelated heterologous proteins, members of the RTX family do not necessary need to be fused to the HlyA secretion signal but can be recognized with their native C-terminus. Consequently, the HlyA secretion system is an advantageous tool for the production and subsequent purification of uncharacterized RTX proteins.

Other studies rely on the purification of RTX proteins from inclusion bodies as RTX proteins that are expressed in *E. coli* without a secretion system tend to aggregate in the cytosol [164]. Thus, the presented two-plasmid system is a tool to avoid the aggregation of the heterologous RTX protein and preserves their native secretion competent state.

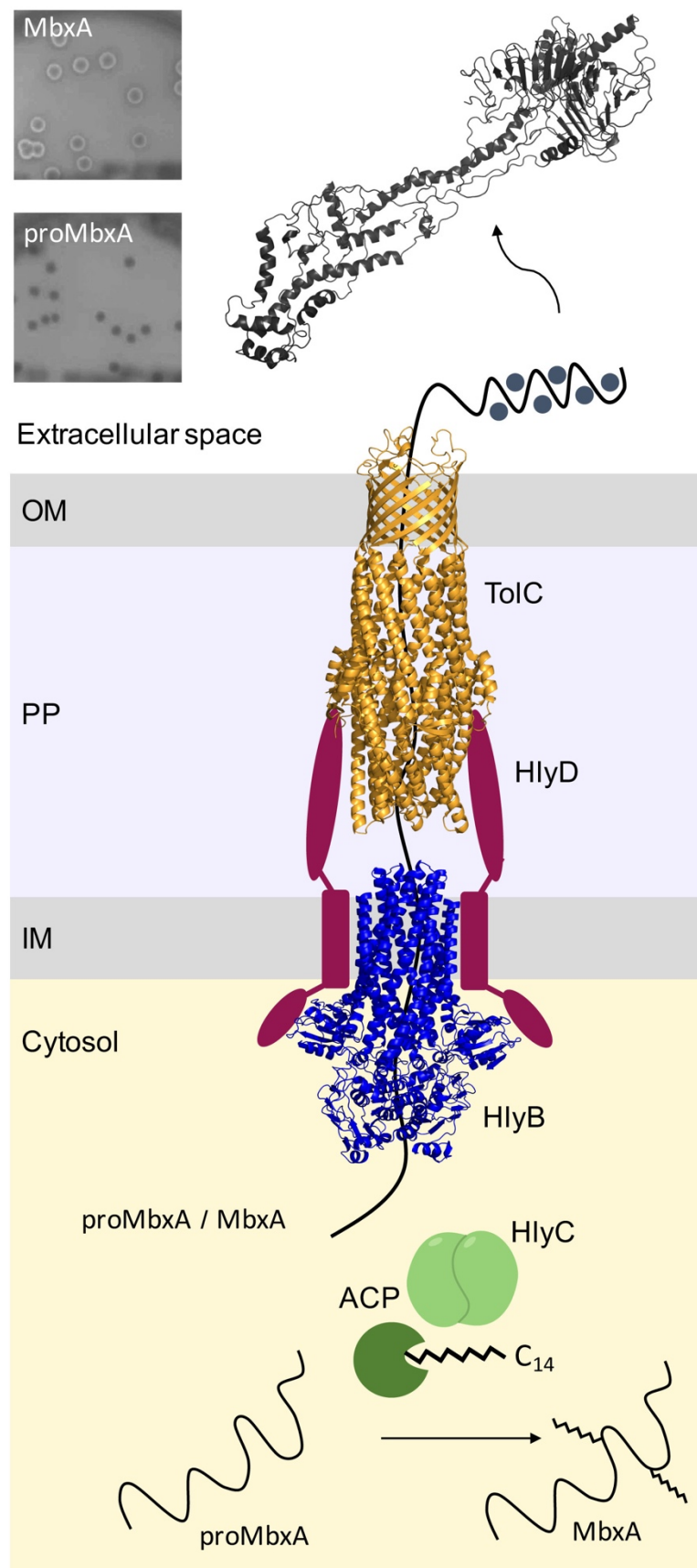


Figure 11: Schematic view of the HlyA secretion system combined with MbxA as a substrate. HlyB (blue) and HlyD (dark red) expressed in *E. coli* BL21(DE3) recognize and

secrete the heterologous substrate MbxA. Interaction of HlyB and HlyD with the substrate induces interaction with the OMP TolC (yellow, PDB entry 1EK9) that completes the T1SS. The activating acyltransferase HlyC (green) mediates heterologous acylation of MbxA with the acyl carrier protein (ACP, dark green) as a donor of predominantly C₁₄ fatty acids. Acylation is necessary for the activity of MbxA but not for secretion. Without co-expression of HlyC the system secretes the non-acylated precursor proMbxA. MbxA (black) is secreted in an unfolded state and adopts its native conformation upon binding of Ca²⁺ (indicated as grey spheres) in the extracellular space. The hemolytic activity of secreted MbxA leads to halo formation around *E. coli* BL21(DE3) colonies grown on blood agar. proMbxA does not induce hemolysis (shown on the left). The structural models of MbxA and HlyB are predicted using Phyre2 [103]. IM: inner membrane, PP: periplasm, OM: outer membrane.

4.2 Structural insights into HlyA, FrpA and MbxA

HlyA, the first identified RTX protein, has up to now eluded crystallization and no crystal structure of a pore-forming RTX toxin is available. The characteristic β -roll structure that the RTX domain adopts upon coordination of calcium is known from the crystal structure of the alkaline protease from *Pseudomonas aeruginosa* [14].

Apart from the solved structures of RTX enzymes such as the aforementioned alkaline protease, the metalloprotease PrtC from *Erwinia chrysanthemi* or the *S. marescens* lipase LipA, structural information on other RTX proteins is scarce [14, 155, 165]. Available structures of for example fragments of the RTX domain of CyaA from *B. pertussis* and fragments of the ice-binding protein from *M. primoryensis* similarly reveal Ca²⁺ binding β -helical domains [118, 166, 167]. In this thesis, single particle cryo-EM and SAXS were applied to study the structure of the RTX proteins HlyA, MbxA and FrpA. As HlyA was shown to be intrinsically too flexible for crystallization [168], both methods, SAXS and cryo-EM, open the opportunity for structure determination in near-native conditions. In the recent years cryo-EM underwent a “resolution revolution” and gained importance as a method that facilitates the three-dimensional determination of protein structures in near-atomic resolution [169]. A major advantage of cryo-EM is that data is collected in a near-native state from different conformations and therefore allows the analysis of dynamic proteins [170]. In chapter 3.4, instead of HlyA and MbxA, the unmodified variants proHlyA and proMbxA were analyzed as the acylated proteins have a higher tendency for aggregation [171]. The analysis of the cryo-specimen of both proHlyA and proMbxA revealed 2D class averages of prolonged particles. Both proteins yielded particles that were too heterogenous to allow a successful reconstruction of a three-dimensional model from the obtained 2D classification. For future attempts the flexibility of proHlyA and

proMbxA needs to be reduced in order to produce more homogenous particles. The specimen preparation could be optimized for example by addition of detergents, as used for membrane proteins, which can stabilize proteins and improve the quality of cryo-EM specimen [172, 173]. In contrast to cryo-EM, SAXS offers the possibility to collect structural data directly from proteins in solution. From the scattering curve of the protein not only structural parameters such as the radius of gyration and the molecular weight can be determined, but also a three dimensional *ab initio* model can be calculated [174]. SAXS is also applicable for the study of dynamic, intrinsically disordered proteins [174, 175]. In chapter 3.4 three dimensional models of FrpA and two variants of proHlyA are presented. The purification protocol established for FrpA in chapter 3.4 is based on an expression in *E. coli* BL21(DE3) without a secretion system. Interestingly, FrpA did not aggregate in the cytosol but remained soluble. Comparison of the CD spectra of FrpA isolated from the cytosol and of secreted FrpA indicated that both have adopted a similar conformation. In contrast to FrpA, proHlyA forms inclusion bodies when it is trapped in the *E. coli* cytosol. This allowed us to compare the structure of proHlyA refolded from inclusion bodies and of secreted proHlyA isolated from the culture supernatant. Both variants formed predominantly dimers and the *ab initio* models of both variants revealed a similar elongated and kinked shape. This underlines that the Ca^{2+} dependent *in vitro* folding of proHlyA that has been reported in previous studies [48] leads to a very similar conformation as the *in vivo* folding dependent on the secretion process. The elongated 3D model of proHlyA obtained from scattering data also confirms the particles observed in the cryo-EM specimen. In contrast to proHlyA, FrpA is monomeric in solution but interestingly the calculated 3D model shows a comparably shaped, elongated and twisted particle. Taken together, cryo-EM and SAXS analysis demonstrate that proHlyA, proMbxA and FrpA adopt a flexible and elongated conformation that is presumably an inherent characteristic of RTX proteins in solution. The relaxed conformation that allows a high degree of flexibility is potentially closely connected to the underlying functions of RTX proteins. RTX proteins generally undergo a transition from a secretion competent, unfolded state to a more compact, folded state that is induced by Ca^{2+} binding upon secretion [46, 51]. Pore-forming toxins such as HlyA and MbxA are thought to need a further transition from a soluble state to a more hydrophobic conformation that allows membrane interaction [176]. The requirement to undergo such a conformational rearrangement potentially explains the inherent flexibility of RTX proteins observed in this study. Altogether, this thesis presents the first cryo-EM images of HlyA and MbxA, as well as the SAXS-derived 3D models of HlyA and FrpA, which contribute to the understanding of the structure of RTX proteins.

4.3 Heterologous activation of MbxA from *M. bovis* by the *E. coli* acyltransferase HlyC

The cytotoxic activity of pore-forming RTX toxins requires the post-translational fatty-acylation of conserved lysine residues [122, 124, 134, 177]. Therefore pore-forming RTX toxins are expressed together with a specialized toxin-activating acyltransferase which catalyzes the unique acylation [119, 135]. This modification happens in the cytosol and relies on the acyl carrier protein as a fatty acid donor [120].

In chapter 3.3, we complemented the two species secretion system consisting of the HlyA secretion components and the *Moraxella bovis* RTX toxin MbxA with the *E. coli* acyltransferase HlyC. With this heterologous combined T1SS *E. coli* BL21(DE3) secreted mature, hemolytically active MbxA. This demonstrated that HlyC not only recognizes its native substrate HlyA [119], but also mediates the acylation of the heterologous substrate MbxA. Subsequent mass spectrometry analysis confirmed that only the two previously predicted lysine residues K536 and K660, that are homologous to the acylation sites K564 and K690 of HlyA, are acylated [124, 149]. The first acylation sites of MbxA and HlyA share the short consensus sequence GKY while the second acylation sites are more conserved harboring the identical sequence VGKRTE (Fig. 12).

Previously, Lim *et al.* [125] showed that HlyC preferentially utilizes saturated C₁₄ fatty acids (myristoylation) for the *in vivo* acylation of HlyA but approximately a third of the modifications constitutes of C₁₅ and C₁₇ fatty acids. In our system, HlyC similarly showed a preference for C₁₄ fatty acids but at the same time C₁₃, C₁₅ and C₁₆ fatty, as well as potential C₁₂ hydroxy (C₁₂-OH) fatty acylation were observed at the first acylation site. However, all mass shifts attributed to hydroxy acylations could potentially stem from tyrosine oxidation of the peptide fragments. The second acylation site was only found to be myristoylated. We also analyzed the native substrate HlyA, produced in the same *E. coli* BL21(DE3) background and likewise confirmed that myristoylation is the predominant modification. Interestingly, also potential hydroxy-myristoylations (C₁₄-OH) were detected at both acylation sites. In contrast to MbxA, the more diverse acylation including C₁₂, C₁₃ and C₁₆ was observed at the second acylation site of HlyA, while only two modification types, C₁₄ and potential C₁₄-OH acylation, were found at the first acylation site of HlyA.

Moreover, the MS analysis indicated that in MbxA the first acylation site is more efficiently acylated than the second one and in HlyA, *vice versa*, the second site more efficiently than the first. This implies that the acyltransferase HlyC modifies two different RTX proteins with a

different acylation pattern and a different preference for the acylation sites (Fig. 12). Osickova *et al* similarly reported that HlyC utilizes mostly C₁₄ fatty acids for HlyA activation but that C₁₄-OH, C₁₂, C₁₂-OH, C₁₆ as well unsaturated C₁₆ modifications occur [126]. The authors combined the acyltransferases HlyC from *E. coli*, RtxC from *K. kingae* and CyaC from *B. pertussis* with each of the RTX toxins HlyA, RtxA and CyaA and showed that the acyltransferases acylated not only the corresponding native substrate but also the other two heterologous RTX proteins. Remarkably, the choice of utilized fatty acids was inherent to the acyltransferase. Combinations of the acyltransferases with a non-native substrate revealed that the second acylation site is preferred and almost no modification of the first acylation site is mediated, further suggesting that the acylation pattern is dependent on the acyltransferase [126]. In contrast, our findings underline that the activity of HlyC towards a non-native substrate, in our system MbxA, is not confined to the second acylation site. The inverse HlyC-mediated acylation pattern at the two acylation sites of the heterologous substrate MbxA and the native substrate HlyA presented in chapter 3.3 suggests that the acylation pattern is not solely influenced by the acyltransferase but also determined by the RTX protein.

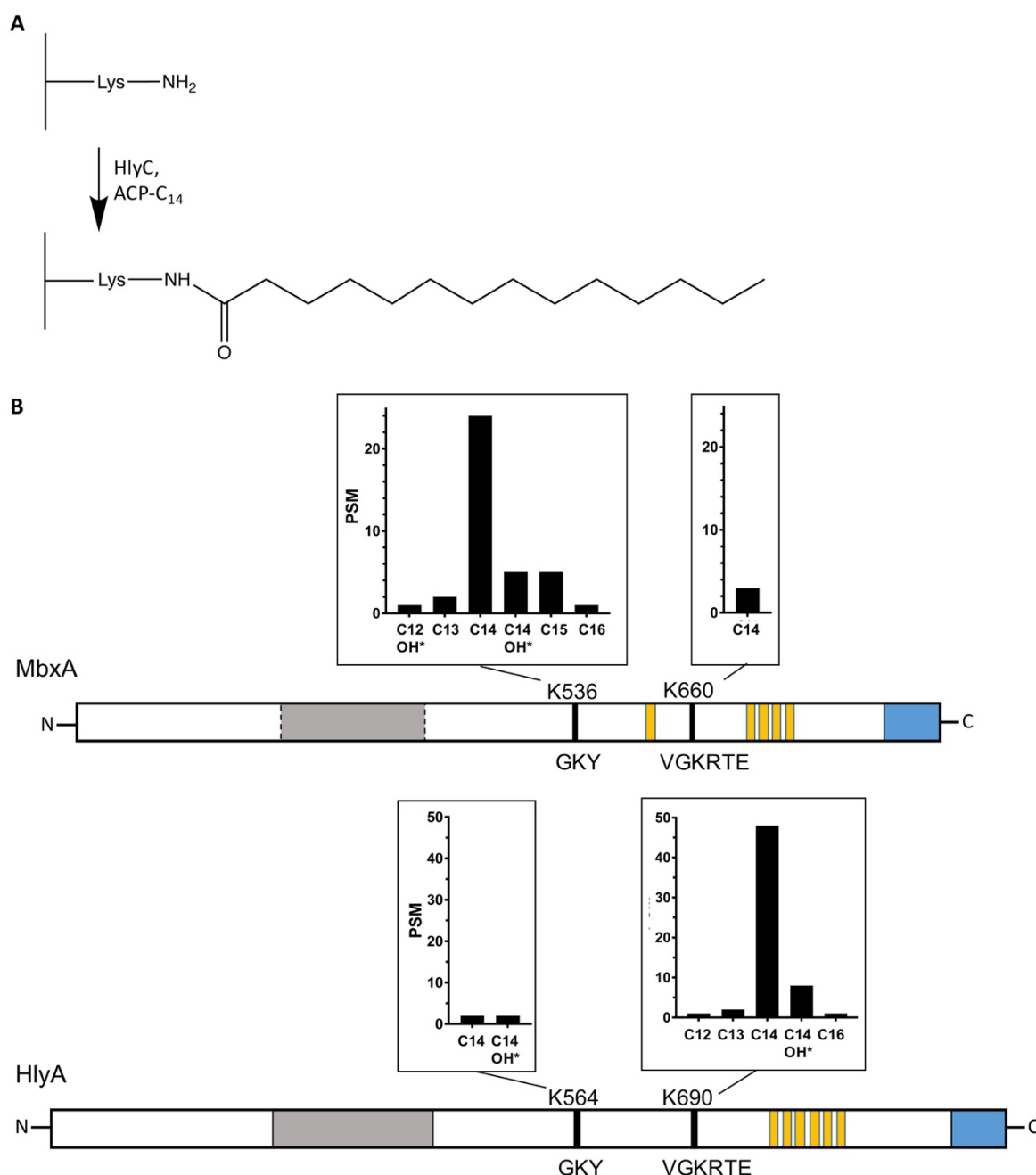


Figure 12: HlyC-mediated acylation of MbxA and HlyA. A) Myristoylation of the ϵ -amino group of a lysine residue. B) The two conserved acylation sites of MbxA and HlyA, K536 and K660 or K564 and K690, respectively are indicated in black in the schematic view of the primary structure together with the acylation pattern at each site. Fatty acid modification were analyzed with mass spectrometry and are indicated with their corresponding carbon chain length ranging from C₁₂ to C₁₆ fatty acids. Each detected fatty acid is given with the corresponding number of peptide spectrum matches (PSM) which are a semi-quantitative measure for the occurrence of peptides and peptide modifications. Potential hydroxy-fatty acid modification are marked with a * as all mass shifts attributed to hydroxy acylations could potentially stem from tyrosine oxidation of the peptide fragments. The putative membrane interaction domains of MbxA and HlyA are indicated in grey, the GG-repeats are indicated in yellow and the secretion sequences are indicated in blue.

4.4 The activity of MbxA is acylation-dependent

The acylation of proHlyA converts the nontoxic precursor into the lytic, mature RTX protein [124, 134]. However, it is not clear what exact role the fatty acid modifications play in the cytotoxic function as the precursor proHlyA was nevertheless shown to bind to membranes and exhibit pore-formation [127, 128]. After HlyC-acylated MbxA was shown to lyse sheep erythrocytes the activity of MbxA was further tested on human cells grown in cell culture. The membrane-damaging activity was assessed based on the release of cytosolic lactate dehydrogenase from MbxA-treated cells. Purified MbxA was cytotoxic against human epithelial cells and human T cells, while proMbxA did not induce any membrane damage, demonstrating that the acylation is strictly required for the membrane damaging activity of MbxA. Live cell imaging of epithelial cells likewise showed that only mature MbxA leads to permeabilization of the cells and to morphological changes in the membrane. This dependence on the acylation is in line with studies on other cytotoxic RTX proteins along with HlyA such as RtxA from *K. kingae* [122, 124]. Interestingly, RtxA is only cytotoxic when modified with C₁₄ fatty acids while CyaA requires an acylation with C₁₆ fatty acids to exert activity. HlyA on the other hand retains activity when modified with both types of fatty acids. This suggests that the acylation shapes the function of RTX proteins and that therefore the dedicated toxin-activating acyltransferases are adapted to the selection of specific fatty acids [126]. The combination of HlyC and MbxA presented in chapter 3.3 resulted in a mature RTX protein that displays membrane-damaging activity against different cell types and different species. Therefore the choice of fatty acids and the HlyC-mediated recognition of the acylation sites of MbxA is suitable to elicit the activity of the pore-forming toxin without the modification machinery of *M. bovis*. LktA from *M. haemolytica* is another example for a RTX protein that is activated by HlyC. Remarkably, both wild type LktA and HlyC-activated LktA show the same specificity towards ruminant leukocytes [178]. This might indicate that the activity of recombinant HlyC-activated MbxA reflects the wild-typic activity of MbxA and that MbxA is inherently a cell type-unspecific RTX toxin.

Incubation of human cells with high concentrations of proMbxA before treatment with active MbxA demonstrated that the precursor fails to protect human cells from MbxA-induced membrane damage. This implies that non-acylated proMbxA is unable to block potential receptors of MbxA on the host cell or to reduce unspecific binding to the membrane (Chapter 3.3). Similarly, proHlyA was reported to bind to red blood cells but no competition between proHlyA and HlyA was observed [179]. Mature HlyA is suggested to displace the precursor

from the membrane [179], which is possibly also true for the binding of proMbxA and MbxA to epithelial cells. The fatty acids presumably contribute to the irreversibility of the insertion of HlyA into host cell membranes [129]. Another suggested explanation is that the fatty acids of RTX proteins mediate oligomerization that is presumably required for pore formation [130, 180]. Moreover, the acylation could contribute to receptor-recognition as, in the case of CyaA, the acylation was shown to promote an effective binding to its receptor, the $\alpha_M\beta_2$ integrin [131, 132].

4.5 MbxA is a species- and cell type-unspecific pore-forming toxin

In this thesis it was demonstrated that MbxA, a toxin from a bovine pathogen, exhibits a species- and target cell-independent membrane-damaging activity. Purified MbxA killed not only sheep erythrocytes but also human epithelial cells (HEp2) and T cells (Jurkat) (Chapter 3.3) (Fig. 13). Earlier studies with *M. bovis* cultures and culture supernatants showed a cytotoxicity against bovine neutrophils, erythrocytes and corneal epithelial cells attributed to the secreted toxin that was later identified as MbxA [144-147, 149]. The activity of MbxA outside its target species is comparable to the wide-range toxicity reported for HlyA targeting erythrocytes, leukocytes, epithelial and endothelial cells of different species [12, 54-58].

Different cell types are not equally sensitive towards HlyA as various studies reported toxic effects mediated by sublytic concentrations of HlyA. This is possibly explained by a receptor-independent toxicity as seen in a wide range of cell types or even as pore formation in lipid bilayers and a receptor-mediated toxicity at sublytic concentrations [12, 57, 59, 60, 69, 71, 181]. In contrast to studies that suggest that HlyA binding is completely independent of a receptor [182, 183] other studies report that the lymphocyte function associated antigen 1 (LFA-1), a heterodimeric β_2 integrin present on leukocytes, represents the receptor of HlyA and other RTX proteins [69]. Transfection of cell lines with the two β_2 integrin genes CD11a and CD18 increased the sensitivity towards HlyA and LtxA from *A. actinomycetemcomitans* [69]. For HlyA, LtxA as well as LktA the receptor has been further narrowed down to the β_2 integrin β subunit (CD18), rendering leukocytes susceptible to the RTX toxins [71, 184, 185]. Moreover, the glycosylation of β_2 integrins was reported to be necessary for the recognition by HlyA, LtxA and CyaA [70].

A measure for the susceptibility of different cell types towards RTX toxins is the concentration of the protein at which the half-maximal toxicity, the cytotoxic dose 50 (CD₅₀), is reached. We

determined that MbxA induces membrane damage and subsequently cell death in human epithelial cells and T cells at low nanomolar concentrations with a CD_{50} of 28.1 ± 4.7 nM and 17.7 ± 3.9 nM, respectively. For HlyA depending on the cell line a CD_{50} of approximately 0.2 nM -30 nM was reported [71]. β_2 integrin expressing cells e. g. T cells are up to 100-fold more sensitive than cell lines devoid of β_2 integrin β subunit expression [71]. The presented CD_{50} of MbxA for human T cells and epithelial cells is therefore very similar to the CD_{50} of HlyA reported for human epithelial cells. This indicates a mechanism of membrane permeabilization that is independent of human β_2 integrin recognition [71]. At this stage we cannot distinguish between a receptor-dependent and -independent action of MbxA. However, the activity of MbxA is not confined to specific structures of bovine cells.

4.6 Potential receptors involved in MbxA activity

Historically pore-forming RTX toxins were divided into non-specific wide-range cytotoxic hemolysins such as HlyA and specific leukotoxins that target only leukocytes such as LktA from *M. haemolytica* [13]. Accordingly MbxA would fit in the first category of unspecific hemolysins. As β_2 integrins on leukocytes act as a receptor for unspecific proteins such as HlyA as well, this could mean that all RTX toxins are more or less specific leukotoxins that kill leukocytes at low concentrations [15]. Consequently in the context of infection, unspecific RTX toxins would at higher concentrations contribute to further local tissue damage by additionally killing other cell types [71]. Even though human T cells did not display an increased sensitivity towards MbxA compared to epithelial cells, this dual mechanism could still be applicable to MbxA as well. The bovine β_2 integrin subunit CD18 is sufficient as a receptor for the leukotoxin LktA from *M. haemolytica* that is species and target specific for ruminant leukocytes [185, 186]. It is possible that this bovine integrin acts as a receptor for MbxA as well (Fig. 13). In line with this interpretation, Kagonyera *et al.* [146] reported that *M. bovis* cultures display cytotoxicity against bovine but not human neutrophils. This could indeed be explained by a higher susceptibility of the bovine immune cells towards MbxA due to the presence of a specific receptor.

Apart from β_2 integrins other target structures facilitating the activity of RTX proteins have been discussed. HlyA was shown to bind glycophorin, a membrane protein found in erythrocytes, at sublytic concentrations and the presence of glycophorin increased the sensitivity of lipid vesicles towards HlyA [187]. As MbxA is a potent hemolysin, glycophorin

could act as a binding partner on erythrocytes as well (Fig. 13). Another discussed recognition motif for RTX toxins is cholesterol (Fig. 13). HlyA, LtxA and RtxA were shown to bind cholesterol in target cells as well as artificial membranes [122, 130, 188, 189]. Cholesterol is suggested to mediate insertion and induce the oligomerization of HlyA in the host membrane [188]. The depletion of cholesterol as well as blocking of cholesterol results in a reduced permeabilization of the membrane [188-190]. The interaction with cholesterol is suggested to be mediated by cholesterol recognition/amino acid consensus (CRAC) sites found in HlyA, LtxA and RtxA [122, 188, 189]. In HlyA, seven putative CRAC sequences and 13 inverse binding motifs, called CARC, were identified [188]. MbxA could potentially likewise rely on interaction with cholesterol for membrane insertion as we identified seven putative variants of the CRAC motif with the consensus sequence L/V-X₁₋₅-Y-X₁₋₅-R/K (in which x is a sequence of one to five residues of any amino acid) and 18 inverted CARC motifs with the consensus sequence R/K-X₁₋₅-Y/F-X₁₋₅-L/V (Tab. 2) [191, 192].

Table 2: Putative cholesterol recognition CRAC and CARC motifs identified in the sequence of MbxA. The motifs were identified with ScanProsite [193]. The presence of such motifs alone does not necessary correspond to a cholesterol binding site [194].

| Predicted cholesterol recognition motifs | | | |
|--|---------------|--------------|---------------|
| CRAC | | CARC | |
| Localization | Sequence | Localization | Sequence |
| 22 – 31 | LAIPKDYDPQK | 202 - 213 | KLQNLNFSKTNL |
| 27-37 | LKNLYLAIPK | 240 - 252 | KVAAGFELSNQV |
| 326 – 332 | LLAEYQR | 258 - 269 | KAISYVLAQRV |
| 532 – 542 | LTNGKYSYINK | 317 - 327 | RKFGYDGDHLL |
| 611 – 615 | VFYSK | 387 - 394 | KQAMFESV |
| 641 - 653 | VARGDIYHEVVKR | 417 - 427 | KGYDSRYAAYL |
| 824 - 831 | LQNYQSNK | 422 - 431 | RYAAYLANNL |
| | | 475 - 487 | KAYADAFEDGKKV |
| | | 511 - 522 | KTQALHFTSPLL |
| | | 531 - 543 | RLTNGKYSYINKL |
| | | 542 - 548 | KLKFGRV |
| | | 561 - 567 | KLDFSKV |
| | | 615 - 624 | KDGGFGNITV |
| | | 643 - 651 | RGDIYHEVV |
| | | 661 - 672 | RTETIQYRDYEL |
| | | 668 - 675 | RDYELRKV |
| | | 673 - 685 | RKVGYGYQSTDNL |
| | | 817 - 824 | RWYITSNL |

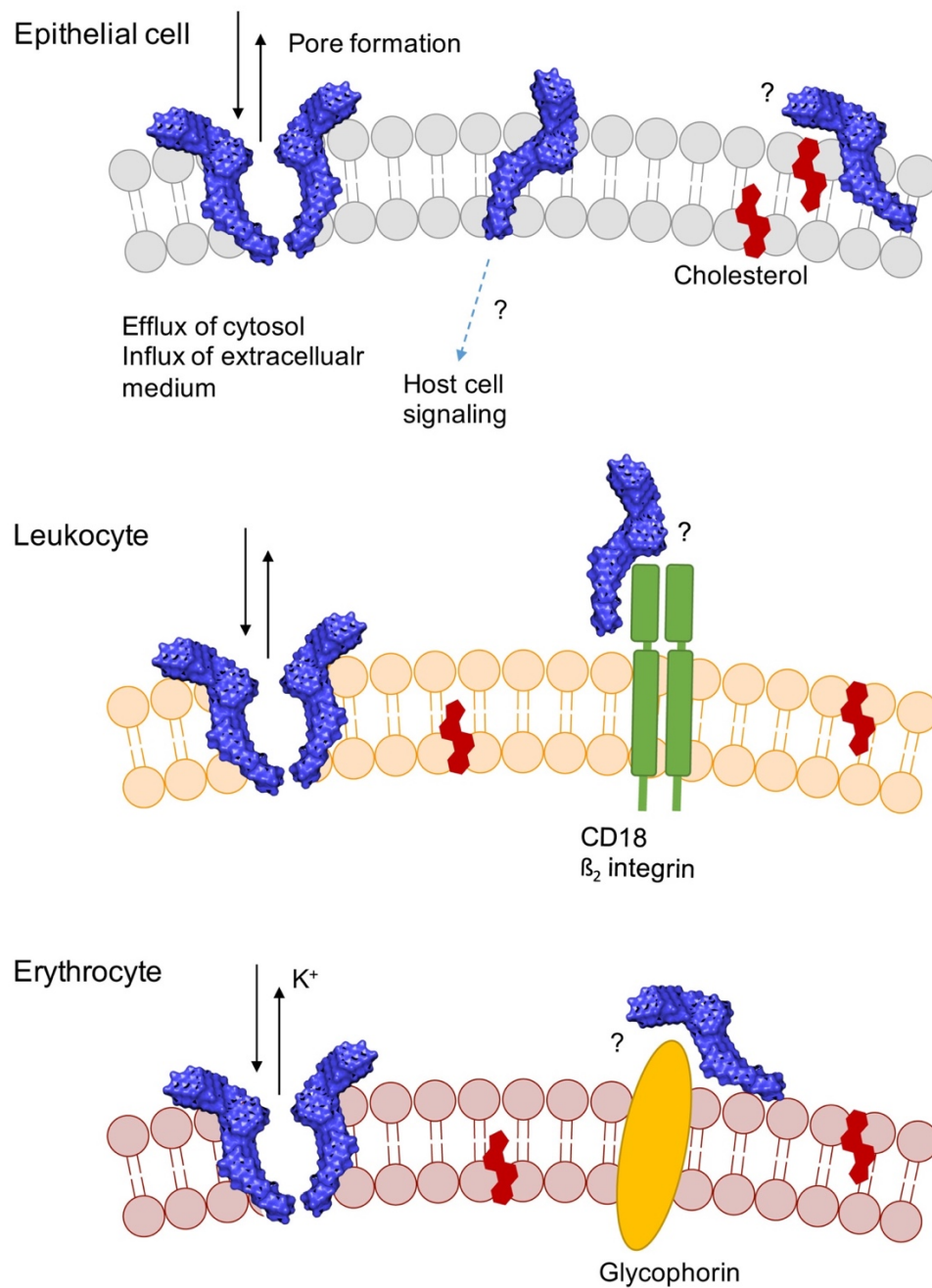


Figure 13: Membrane damaging activity of MbxA and potential interaction partners in different cell types. MbxA (blue) was shown to permeabilize epithelial cells (A), leukocytes (B) and erythrocytes (C). Pore formation leads to efflux of cytosolic and influx of extracellular components. The oligomeric state of MbxA during pore formation is not known and is here depicted as a oligomeric pore for simplicity. Apart from pore formation, MbxA may influence host cell signaling at sublytic concentrations as well. Similar to other RTX proteins MbxA could potentially bind to cholesterol (red) present in the membrane of host cells. β_2 integrins containing the β subunit CD18 (green) expressed by leukocytes represent another potential receptor for MbxA. In erythrocytes MbxA induces efflux of K^+ before cell swelling and subsequent lysis occur [147]. As glycophorin (yellow), found in erythrocyte membranes, was shown to function as a receptor for HlyA [187], it could potentially mediate recognition by MbxA. The SAXS-derived model of HlyA was used to visualize MbxA. The figure is partially based on [195].

4.7 MbxA-induced membrane damage leads to morphological changes in epithelial cells

The MbxA-induced lysis of sheep erythrocytes and the release of cytosolic enzymes from MbxA-treated human cell culture evidently demonstrated a membrane-damaging activity. Live cell imaging of HEp2 cells challenged with purified MbxA additionally revealed that epithelial cells undergo a distinct change in membrane morphology upon permeabilization by the RTX protein. In chapter 3.3 we demonstrate that MbxA immediately creates lesions in the membrane of epithelial cells visualized by the influx of propidium iodide. Moreover, in the course of less than five minutes the membrane responds to the impaired membrane integrity with the formation of blebs. Membrane blebbing occurs usually due to an increased intracellular pressure that results in tearing of the membrane from the cytoskeleton or due to direct rupture of the actin cortex. As a result the excess membrane inflates forming bulges [196-198]. Blebbing also occurs without an influx of water in healthy, intact cells where blebs are usually transient and subsequently regress [196, 199]. The membrane bulges induced by MbxA on the other hand were stable during an imaging time of 90 min. Additionally, the increase of propidium iodide signal in the nuclei during the imaging time suggested that the cells remained permeabilized allowing a continuous influx of extracellular medium. The frequency and size of the protrusions increased with the applied MbxA concentration as well, indicating that the number and potentially the size of the pores is concentration dependent. Upon injury of the membrane integrity blebbing was shown to play a role in the prevention of lysis of the damaged cell [200]. Blebbing occurs in human embryonic kidney cells and various other cell types as a response to influx of extracellular Ca^{2+} through permeabilization by the pore-forming toxin streptolysin O, a cholesterol-dependent cytolysin (CDC) from *Streptococcus pyogenes*. The blebs trap damaged membrane areas preventing efflux of cytosol and further increase of the Ca^{2+} concentration [200]. A similar protective mechanism could underlie the blebbing phenomenon induced by MbxA. For HlyA another protective mechanism associated with membrane rearrangements was reported. Sublytic concentrations of HlyA were shown to induce shedding of microvesicles from erythrocytes which potentially aid removal of the toxin from the membrane [201].

Usually blebbing is associated with cell death as it is a defining feature of the execution phase of apoptosis [202, 203]. However, apoptosis requires the activation of cell death pathways and blebbing is typically preceded by cell shrinkage and chromatin condensation. Moreover, during apoptosis the membrane typically remains intact and blebbing finally results in apoptotic bodies

[203-205]. At the same time blebbing is also typical for necrosis, but compared to apoptosis blebbing develops at later stages of the necrotic process shortly before the lysis of the cell [206]. A large, 501 kDa MARTX toxin from *Vibrio vulnificus* is associated with pore formation, cytoskeletal rearrangements and membrane blebbing, resulting in necrotic cell death [207, 208]. Necrosis is often induced by membrane injury and necrotic blebbing follows after an increase in cell volume due to the influx of water and ions [209]. In contrast to apoptotic blebs, necrotic blebs expand continuously and do not retract which is similar to the MbxA-induced blebbing [206]. Nevertheless, taking in consideration that the blebbing occurs very rapidly after permeabilization by MbxA, it is not unambiguously consistent with the characteristic blebbing observed during apoptotic or necrotic cell death. It is more similar to the membrane blebbing that is induced by another member of the CDC family, the pore-forming toxin vaginolysin. This CDC triggers the rapid formation of membrane protrusions in epithelial cells in the course of minutes. Blebs that have a size of 10 μm or larger, a size that was likewise reached after MbxA-mediated permeabilization, are reported to be stable for hours and are not directly associated with cell death [210]. Randis *et al.* [210] further demonstrated that sublytic concentrations of CDCs are sufficient to cause blebs and that blebbing depends on pore formation. The authors suggest that membrane blebbing may represent a conserved response of epithelial cells to membrane damage induced by pore-forming toxins [210].

However, HlyA and other RTX proteins were shown to induce different cell death pathways. HlyA for example is associated with apoptosis, necrosis as well as pyroptosis [56, 72-74]. The various effects of HlyA on signaling of host cells include Ca^{2+} oscillations, inhibition of anti-apoptotic regulators, mitochondrial damage or inflammasome activation and depend on the cell type [74, 75, 77-79]. Therefore the question arises which intracellular effects apart from pore formation and membrane blebbing are evoked by MbxA. Addressing the signaling of host cells in particular in response to sublytic concentrations of MbxA will aid the understanding of the mechanism of toxicity of RTX proteins.

5. Bibliography

1. Costa, T.R., Felisberto-Rodrigues, C., Meir, A., Prevost, M.S., Redzej, A., Trokter, M., and Waksman, G., *Secretion systems in Gram-negative bacteria: structural and mechanistic insights*. Nat Rev Microbiol, 2015. **13**(6): p. 343-59.
2. Green, E.R. and Mecsas, J., *Bacterial Secretion Systems: An Overview*. Microbiol Spectr, 2016. **4**(1).
3. Rego, A.T., Chandran, V., and Waksman, G., *Two-step and one-step secretion mechanisms in Gram-negative bacteria: contrasting the type IV secretion system and the chaperone-usher pathway of pilus biogenesis*. Biochem J, 2010. **425**(3): p. 475-88.
4. Gilson, L., Mahanty, H.K., and Kolter, R., *Genetic analysis of an MDR-like export system: the secretion of colicin V*. EMBO J, 1990. **9**(12): p. 3875-84.
5. Gerard, F., Pradel, N., and Wu, L.F., *Bactericidal activity of colicin V is mediated by an inner membrane protein, SdaC, of Escherichia coli*. J Bacteriol, 2005. **187**(6): p. 1945-50.
6. Hirst, T.R., Sanchez, J., Kaper, J.B., Hardy, S.J., and Holmgren, J., *Mechanism of toxin secretion by Vibrio cholerae investigated in strains harboring plasmids that encode heat-labile enterotoxins of Escherichia coli*. Proc Natl Acad Sci U S A, 1984. **81**(24): p. 7752-6.
7. Tauschek, M., Gorrell, R.J., Strugnell, R.A., and Robins-Browne, R.M., *Identification of a protein secretory pathway for the secretion of heat-labile enterotoxin by an enterotoxigenic strain of Escherichia coli*. Proc Natl Acad Sci U S A, 2002. **99**(10): p. 7066-71.
8. Spangler, B.D., *Structure and function of cholera toxin and the related Escherichia coli heat-labile enterotoxin*. Microbiol Rev, 1992. **56**(4): p. 622-47.
9. McGhie, E.J., Brawn, L.C., Hume, P.J., Humphreys, D., and Koronakis, V., *Salmonella takes control: effector-driven manipulation of the host*. Current Opinion in Microbiology, 2009. **12**(1): p. 117-124.
10. Los, F.C., Randis, T.M., Aroian, R.V., and Ratner, A.J., *Role of pore-forming toxins in bacterial infectious diseases*. Microbiol Mol Biol Rev, 2013. **77**(2): p. 173-207.
11. Gonzalez, M.R., Bischofberger, M., Pernot, L., van der Goot, F.G., and Freche, B., *Bacterial pore-forming toxins: the (w)hole story?* Cell Mol Life Sci, 2008. **65**(3): p. 493-507.
12. Bhakdi, S., Greulich, S., Muhly, M., Eberspacher, B., Becker, H., Thiele, A., and Hugo, F., *Potent leukocidal action of Escherichia coli hemolysin mediated by permeabilization of target cell membranes*. J Exp Med, 1989. **169**(3): p. 737-54.
13. Welch, R.A., *Pore-forming cytolytins of Gram-negative bacteria*. Molecular Microbiology, 1991. **5**: p. 521-528.
14. Baumann, U., Wu, S., Flaherty, K.M., and McKay, D.B., *Three-dimensional structure of the alkaline protease of Pseudomonas aeruginosa: a two-domain protein with a calcium binding parallel beta roll motif*. EMBO J, 1993. **12**(9): p. 3357-64.
15. Linhartova, I., Bumba, L., Masin, J., Basler, M., Osicka, R., Kamanova, J., Prochazkova, K., Adkins, I., Hejnova-Holubova, J., Sadilkova, L., Morova, J., and Sebo, P., *RTX proteins: a highly diverse family secreted by a common mechanism*. FEMS Microbiol Rev, 2010. **34**(6): p. 1076-112.

16. Noegel, A., Rdest, U., Springer, W., and Goebel, W., *Plasmid cistrons controlling synthesis and excretion of the exotoxin alpha-haemolysin of Escherichia coli*. Mol Gen Genet, 1979. **175**(3): p. 343-50.
17. Felmllee, T., Pellett, S., and Welch, R.A., *Nucleotide sequence of an Escherichia coli chromosomal hemolysin*. J Bacteriol, 1985. **163**(1): p. 94-105.
18. Felmllee, T. and Welch, R.A., *Alterations of amino acid repeats in the Escherichia coli hemolysin affect cytolytic activity and secretion*. Proc Natl Acad Sci U S A, 1988. **85**(14): p. 5269-73.
19. Gray, L., Baker, K., Kenny, B., Mackman, N., Haigh, R., and Holland, J.B., *A Novel C-Terminal Signal Sequence Targets Escherichia-Coli Hemolysin Directly to the Medium*. Journal of Cell Science, 1989: p. 45-57.
20. Koronakis, V., Koronakis, E., and Hughes, C., *Isolation and Analysis of the C-Terminal Signal Directing Export of Escherichia-Coli Hemolysin Protein across Both Bacterial-Membranes*. Embo Journal, 1989. **8**(2): p. 595-605.
21. Koronakis, V., Cross, M., Senior, B., Koronakis, E., and Hughes, C., *The secreted hemolysins of Proteus mirabilis, Proteus vulgaris, and Morganella morganii are genetically related to each other and to the alpha-hemolysin of Escherichia coli*. J Bacteriol, 1987. **169**(4): p. 1509-15.
22. Lally, E.T., Golub, E.E., Kieba, I.R., Taichman, N.S., Rosenbloom, J., Rosenbloom, J.C., Gibson, C.W., and Demuth, D.R., *Analysis of the Actinobacillus actinomycetemcomitans leukotoxin gene. Delineation of unique features and comparison to homologous toxins*. J Biol Chem, 1989. **264**(26): p. 15451-6.
23. Lo, R.Y., Strathdee, C.A., and Shewen, P.E., *Nucleotide sequence of the leukotoxin genes of Pasteurella haemolytica A1*. Infect Immun, 1987. **55**(9): p. 1987-96.
24. Hanski, E., *Invasive adenylate cyclase toxin of Bordetella pertussis*. Trends Biochem Sci, 1989. **14**(11): p. 459-63.
25. Sakamoto, H., Bellalou, J., Sebo, P., and Ladant, D., *Bordetella pertussis adenylate cyclase toxin. Structural and functional independence of the catalytic and hemolytic activities*. J Biol Chem, 1992. **267**(19): p. 13598-602.
26. Satchell, K.J., *MARTX, multifunctional autoprocessing repeats-in-toxin toxins*. Infect Immun, 2007. **75**(11): p. 5079-84.
27. Lin, W., Fullner, K.J., Clayton, R., Sexton, J.A., Rogers, M.B., Calia, K.E., Calderwood, S.B., Fraser, C., and Mekalanos, J.J., *Identification of a vibrio cholerae RTX toxin gene cluster that is tightly linked to the cholera toxin prophage*. Proc Natl Acad Sci U S A, 1999. **96**(3): p. 1071-6.
28. Sheahan, K.L., Cordero, C.L., and Satchell, K.J., *Autoprocessing of the Vibrio cholerae RTX toxin by the cysteine protease domain*. EMBO J, 2007. **26**(10): p. 2552-61.
29. Satchell, K.J.F., *Multifunctional-autoprocessing repeats-in-toxin (MARTX) Toxins of Vibrios*. Microbiol Spectr, 2015. **3**(3).
30. Guo, S., Vance, T.D.R., Stevens, C.A., Voets, I., and Davies, P.L., *RTX Adhesins are Key Bacterial Surface Megaproteins in the Formation of Biofilms*. Trends Microbiol, 2019. **27**(5): p. 453-467.
31. Griessl, M.H., Schmid, B., Kassler, K., Braunsmann, C., Ritter, R., Barlag, B., Stierhof, Y.D., Sturm, K.U., Danzer, C., Wagner, C., Schaffer, T.E., Sticht, H., Hensel, M., and Muller, Y.A., *Structural insight into the giant Ca(2)(+)-binding adhesin SiiE*:

- implications for the adhesion of Salmonella enterica to polarized epithelial cells.* Structure, 2013. **21**(5): p. 741-52.
32. Hinsa, S.M., Espinosa-Urgel, M., Ramos, J.L., and O'Toole, G.A., *Transition from reversible to irreversible attachment during biofilm formation by Pseudomonas fluorescens WCS365 requires an ABC transporter and a large secreted protein.* Mol Microbiol, 2003. **49**(4): p. 905-18.
 33. Guo, S.Q., Stevens, C.A., Vance, T.D.R., Olijve, L.L.C., Graham, L.A., Campbell, R.L., Yazdi, S.R., Escobedo, C., Bar-Dolev, M., Yashunsky, V., Braslavsky, I., Langelaan, D.N., Smith, S.P., Allingham, J.S., Voets, I.K., and Davies, P.L., *Structure of a 1.5-MDa adhesin that binds its Antarctic bacterium to diatoms and ice.* Science Advances, 2017. **3**(8).
 34. Wille, T., Wagner, C., Mittelstadt, W., Blank, K., Sommer, E., Malengo, G., Dohler, D., Lange, A., Sourjik, V., Hensel, M., and Gerlach, R.G., *SiiA and SiiB are novel type I secretion system subunits controlling SPI4-mediated adhesion of Salmonella enterica.* Cell Microbiol, 2014. **16**(2): p. 161-78.
 35. Smith, T.J., Font, M.E., Kelly, C.M., Sondermann, H., and O'Toole, G.A., *An N-Terminal Retention Module Anchors the Giant Adhesin LapA of Pseudomonas fluorescens at the Cell Surface: a Novel Subfamily of Type I Secretion Systems.* J Bacteriol, 2018. **200**(8).
 36. Guo, S., Langelaan, D.N., Phippen, S.W., Smith, S.P., Voets, I.K., and Davies, P.L., *Conserved structural features anchor biofilm-associated RTX-adhesins to the outer membrane of bacteria.* FEBS J, 2018. **285**(10): p. 1812-1826.
 37. Suh, Y. and Benedik, M.J., *Production of active Serratia marcescens metalloprotease from Escherichia coli by alpha-hemolysin HlyB and HlyD.* J Bacteriol, 1992. **174**(7): p. 2361-6.
 38. Akatsuka, H., Kawai, E., Omori, K., Komatsubara, S., Shibatani, T., and Tosa, T., *The lipA gene of Serratia marcescens which encodes an extracellular lipase having no N-terminal signal peptide.* J Bacteriol, 1994. **176**(7): p. 1949-56.
 39. Thompson, S.A., Wang, L.L., West, A., and Sparling, P.F., *Neisseria meningitidis produces iron-regulated proteins related to the RTX family of exoproteins.* J Bacteriol, 1993. **175**(3): p. 811-8.
 40. Osicka, R., Prochazkova, K., Sulc, M., Linhartova, I., Havlicek, V., and Sebo, P., *A novel "clip-and-link" activity of repeat in toxin (RTX) proteins from gram-negative pathogens. Covalent protein cross-linking by an Asp-Lys isopeptide bond upon calcium-dependent processing at an Asp-Pro bond.* J Biol Chem, 2004. **279**(24): p. 24944-56.
 41. Sviridova, E., Rezacova, P., Bondar, A., Veverka, V., Novak, P., Schenk, G., Svergun, D.I., Kuta Smatanova, I., and Bumba, L., *Structural basis of the interaction between the putative adhesion-involved and iron-regulated FrpD and FrpC proteins of Neisseria meningitidis.* Sci Rep, 2017. **7**: p. 40408.
 42. Felmler, T., Pellett, S., Lee, E.Y., and Welch, R.A., *Escherichia coli hemolysin is released extracellularly without cleavage of a signal peptide.* J Bacteriol, 1985. **163**(1): p. 88-93.
 43. Stanley, P., Koronakis, V., and Hughes, C., *Mutational analysis supports a role for multiple structural features in the C-terminal secretion signal of Escherichia coli haemolysin.* Mol Microbiol, 1991. **5**(10): p. 2391-403.

-
44. Delepelaire, P., *Type I secretion in gram-negative bacteria*. Biochim Biophys Acta, 2004. **1694**(1-3): p. 149-61.
 45. Zhang, L., Conway, J.F., and Thibodeau, P.H., *Calcium-induced folding and stabilization of the Pseudomonas aeruginosa alkaline protease*. J Biol Chem, 2012. **287**(6): p. 4311-22.
 46. O'Brien, D.P., Hernandez, B., Durand, D., Hourdel, V., Sotomayor-Perez, A.C., Vachette, P., Ghomi, M., Chamot-Rooke, J., Ladant, D., Brier, S., and Chenal, A., *Structural models of intrinsically disordered and calcium-bound folded states of a protein adapted for secretion*. Sci Rep, 2015. **5**: p. 14223.
 47. Ostolaza, H., Soloaga, A., and Goni, F.M., *The Binding of Divalent-Cations to Escherichia-Coli Alpha-Hemolysin*. European Journal of Biochemistry, 1995. **228**(1): p. 39-44.
 48. Thomas, S., Bakkes, P.J., Smits, S.H., and Schmitt, L., *Equilibrium folding of pro-HlyA from Escherichia coli reveals a stable calcium ion dependent folding intermediate*. Biochim Biophys Acta, 2014. **1844**(9): p. 1500-10.
 49. Jones, H.E., Holland, I.B., Baker, H.L., and Campbell, A.K., *Slow changes in cytosolic free Ca²⁺ in Escherichia coli highlight two putative influx mechanisms in response to changes in extracellular calcium*. Cell Calcium, 1999. **25**(3): p. 265-74.
 50. Jones, H.E., Holland, I.B., and Campbell, A.K., *Direct measurement of free Ca(2+) shows different regulation of Ca(2+) between the periplasm and the cytosol of Escherichia coli*. Cell Calcium, 2002. **32**(4): p. 183-92.
 51. Chenal, A., Guijarro, J.I., Raynal, B., Delepierre, M., and Ladant, D., *RTX calcium binding motifs are intrinsically disordered in the absence of calcium: implication for protein secretion*. J Biol Chem, 2009. **284**(3): p. 1781-9.
 52. Johnson, J.R., *Virulence factors in Escherichia coli urinary tract infection*. Clin Microbiol Rev, 1991. **4**(1): p. 80-128.
 53. Flores-Mireles, A.L., Walker, J.N., Caparon, M., and Hultgren, S.J., *Urinary tract infections: epidemiology, mechanisms of infection and treatment options*. Nat Rev Microbiol, 2015. **13**(5): p. 269-84.
 54. Bhakdi, S., Mackman, N., Nicaud, J.M., and Holland, I.B., *Escherichia coli hemolysin may damage target cell membranes by generating transmembrane pores*. Infect Immun, 1986. **52**(1): p. 63-9.
 55. Gadeberg, O.V., Orskov, I., and Rhodes, J.M., *Cytotoxic effect of an alpha-hemolytic Escherichia coli strain on human blood monocytes and granulocytes in vitro*. Infect Immun, 1983. **41**(1): p. 358-64.
 56. Jonas, D., Schultheis, B., Klas, C., Krammer, P.H., and Bhakdi, S., *Cytocidal effects of Escherichia coli hemolysin on human T lymphocytes*. Infect Immun, 1993. **61**(5): p. 1715-21.
 57. Suttorp, N., Floer, B., Schnittler, H., Seeger, W., and Bhakdi, S., *Effects of Escherichia coli hemolysin on endothelial cell function*. Infect Immun, 1990. **58**(11): p. 3796-801.
 58. Keane, W.F., Welch, R., Gekker, G., and Peterson, P.K., *Mechanism of Escherichia coli alpha-hemolysin-induced injury to isolated renal tubular cells*. Am J Pathol, 1987. **126**(2): p. 350-7.

59. Menestrina, G., Mackman, N., Holland, I.B., and Bhakdi, S., *Escherichia coli haemolysin forms voltage-dependent ion channels in lipid membranes*. Biochim Biophys Acta, 1987. **905**(1): p. 109-17.
60. Benz, R., Schmid, A., Wagner, W., and Goebel, W., *Pore Formation by the Escherichia-Coli Hemolysin - Evidence for an Association-Dissociation Equilibrium of the Pore-Forming Aggregates*. Infection and Immunity, 1989. **57**(3): p. 887-895.
61. Benz, R., Dobereiner, A., Ludwig, A., and Goebel, W., *Haemolysin of Escherichia coli: comparison of pore-forming properties between chromosome and plasmid-encoded haemolysins*. FEMS Microbiol Immunol, 1992. **5**(1-3): p. 55-62.
62. Bakas, L., Ostolaza, H., Vaz, W.L., and Goni, F.M., *Reversible adsorption and nonreversible insertion of Escherichia coli alpha-hemolysin into lipid bilayers*. Biophys J, 1996. **71**(4): p. 1869-76.
63. Sanchez-Magraner, L., Cortajarena, A.L., Goni, F.M., and Ostolaza, H., *Membrane insertion of Escherichia coli alpha-hemolysin is independent from membrane lysis*. J Biol Chem, 2006. **281**(9): p. 5461-7.
64. Ludwig, A., Schmid, A., Benz, R., and Goebel, W., *Mutations affecting pore formation by haemolysin from Escherichia coli*. Mol Gen Genet, 1991. **226**(1-2): p. 198-208.
65. Hyland, C., Vuillard, L., Hughes, C., and Koronakis, V., *Membrane interaction of Escherichia coli hemolysin: flotation and insertion-dependent labeling by phospholipid vesicles*. J Bacteriol, 2001. **183**(18): p. 5364-70.
66. Sanchez-Magraner, L., Viguera, A.R., Garcia-Pacios, M., Garcillan, M.P., Arrondo, J.L., de la Cruz, F., Goni, F.M., and Ostolaza, H., *The calcium-binding C-terminal domain of Escherichia coli alpha-hemolysin is a major determinant in the surface-active properties of the protein*. J Biol Chem, 2007. **282**(16): p. 11827-35.
67. Ludwig, A., Benz, R., and Goebel, W., *Oligomerization of Escherichia coli haemolysin (HlyA) is involved in pore formation*. Mol Gen Genet, 1993. **241**(1-2): p. 89-96.
68. Grimminger, F., Sibelius, U., Bhakdi, S., Suttorp, N., and Seeger, W., *Escherichia coli hemolysin is a potent inductor of phosphoinositide hydrolysis and related metabolic responses in human neutrophils*. J Clin Invest, 1991. **88**(5): p. 1531-9.
69. Lally, E.T., Kieba, I.R., Sato, A., Green, C.L., Rosenbloom, J., Korostoff, J., Wang, J.F., Shenker, B.J., Ortlepp, S., Robinson, M.K., and Billings, P.C., *RTX toxins recognize a beta2 integrin on the surface of human target cells*. J Biol Chem, 1997. **272**(48): p. 30463-9.
70. Morova, J., Osicka, R., Masin, J., and Sebo, P., *RTX cytotoxins recognize beta2 integrin receptors through N-linked oligosaccharides*. Proc Natl Acad Sci U S A, 2008. **105**(14): p. 5355-60.
71. Ristow, L.C., Tran, V., Schwartz, K.J., Pankratz, L., Mehle, A., Sauer, J.D., and Welch, R.A., *The Extracellular Domain of the beta2 Integrin beta Subunit (CD18) Is Sufficient for Escherichia coli Hemolysin and Aggregatibacter actinomycetemcomitans Leukotoxin Cytotoxic Activity*. MBio, 2019. **10**(4).
72. Russo, T.A., Davidson, B.A., Genagon, S.A., Warholic, N.M., Macdonald, U., Pawlicki, P.D., Beanan, J.M., Olson, R., Holm, B.A., and Knight, P.R., 3rd, *E. coli virulence factor hemolysin induces neutrophil apoptosis and necrosis/lysis in vitro and necrosis/lysis and lung injury in a rat pneumonia model*. Am J Physiol Lung Cell Mol Physiol, 2005. **289**(2): p. L207-16.

-
73. Nagamatsu, K., Hannan, T.J., Guest, R.L., Kostakioti, M., Hadjifrangiskou, M., Binkley, J., Dodson, K., Raivio, T.L., and Hultgren, S.J., *Dysregulation of Escherichia coli alpha-hemolysin expression alters the course of acute and persistent urinary tract infection*. Proc Natl Acad Sci U S A, 2015. **112**(8): p. E871-80.
 74. Lu, Y., Rafiq, A., Zhang, Z., Aslani, F., Fijak, M., Lei, T., Wang, M., Kumar, S., Klug, J., Bergmann, M., Chakraborty, T., Meinhardt, A., and Bhushan, S., *Uropathogenic Escherichia coli virulence factor hemolysin A causes programmed cell necrosis by altering mitochondrial dynamics*. FASEB J, 2018. **32**(8): p. 4107-4120.
 75. Wiles, T.J., Dhakal, B.K., Eto, D.S., and Mulvey, M.A., *Inactivation of host Akt/protein kinase B signaling by bacterial pore-forming toxins*. Mol Biol Cell, 2008. **19**(4): p. 1427-38.
 76. Dhakal, B.K. and Mulvey, M.A., *The UPEC pore-forming toxin alpha-hemolysin triggers proteolysis of host proteins to disrupt cell adhesion, inflammatory, and survival pathways*. Cell Host Microbe, 2012. **11**(1): p. 58-69.
 77. Uhlen, P., Laestadius, A., Jahnukainen, T., Soderblom, T., Backhed, F., Celsi, G., Brismar, H., Normark, S., Aperia, A., and Richter-Dahlfors, A., *Alpha-haemolysin of uropathogenic E. coli induces Ca²⁺ oscillations in renal epithelial cells*. Nature, 2000. **405**(6787): p. 694-7.
 78. Verma, V., Kumar, P., Gupta, S., Yadav, S., Dhanda, R.S., Thorlacius, H., and Yadav, M., *alpha-Hemolysin of uropathogenic E. coli regulates NLRP3 inflammasome activation and mitochondrial dysfunction in THP-1 macrophages*. Sci Rep, 2020. **10**(1): p. 12653.
 79. Murthy, A.M.V., Phan, M.D., Peters, K.M., Nhu, N.T.K., Welch, R.A., Ulett, G.C., Schembri, M.A., and Sweet, M.J., *Regulation of hemolysin in uropathogenic Escherichia coli fine-tunes killing of human macrophages*. Virulence, 2018. **9**(1): p. 967-980.
 80. Holland, I.B., Schmitt, L., and Young, J., *Type I protein secretion in bacteria, the ABC-transporter dependent pathway (review)*. Mol Membr Biol, 2005. **22**(1-2): p. 29-39.
 81. Mackman, N., Nicaud, J.M., Gray, L., and Holland, I.B., *Identification of polypeptides required for the export of haemolysin 2001 from E. coli*. Mol Gen Genet, 1985. **201**(3): p. 529-36.
 82. Mackman, N., Nicaud, J.M., Gray, L., and Holland, I.B., *Genetical and functional organisation of the Escherichia coli haemolysin determinant 2001*. Mol Gen Genet, 1985. **201**(2): p. 282-8.
 83. Wang, R.C., Seror, S.J., Blight, M., Pratt, J.M., Broome-Smith, J.K., and Holland, I.B., *Analysis of the membrane organization of an Escherichia coli protein translocator, HlyB, a member of a large family of prokaryote and eukaryote surface transport proteins*. J Mol Biol, 1991. **217**(3): p. 441-54.
 84. Koronakis, V., Koronakis, E., and Hughes, C., *Comparison of the haemolysin secretion protein HlyB from Proteus vulgaris and Escherichia coli; site-directed mutagenesis causing impairment of export function*. Mol Gen Genet, 1988. **213**(2-3): p. 551-5.
 85. Wandersman, C. and Delepelaire, P., *TolC, an Escherichia coli outer membrane protein required for hemolysin secretion*. Proc Natl Acad Sci U S A, 1990. **87**(12): p. 4776-80.

-
86. Holland, I.B. and Blight, M.A., *ABC-ATPases, adaptable energy generators fuelling transmembrane movement of a variety of molecules in organisms from bacteria to humans*. J Mol Biol, 1999. **293**(2): p. 381-99.
 87. Koronakis, E., Hughes, C., Milisav, I., and Koronakis, V., *Protein exporter function and in vitro ATPase activity are correlated in ABC-domain mutants of HlyB*. Mol Microbiol, 1995. **16**(1): p. 87-96.
 88. Higgins, C.F., *ABC transporters: from microorganisms to man*. Annu Rev Cell Biol, 1992. **8**: p. 67-113.
 89. Blight, M.A. and Holland, I.B., *Structure and function of haemolysin B, P-glycoprotein and other members of a novel family of membrane translocators*. Mol Microbiol, 1990. **4**(6): p. 873-80.
 90. Zaitseva, J., Jenewein, S., Jumpertz, T., Holland, I.B., and Schmitt, L., *H662 is the linchpin of ATP hydrolysis in the nucleotide-binding domain of the ABC transporter HlyB*. EMBO J, 2005. **24**(11): p. 1901-10.
 91. Zaitseva, J., Jenewein, S., Wiedenmann, A., Benabdelhak, H., Holland, I.B., and Schmitt, L., *Functional characterization and ATP-induced dimerization of the isolated ABC-domain of the haemolysin B transporter*. Biochemistry, 2005. **44**(28): p. 9680-90.
 92. Zaitseva, J., Oswald, C., Jumpertz, T., Jenewein, S., Wiedenmann, A., Holland, I.B., and Schmitt, L., *A structural analysis of asymmetry required for catalytic activity of an ABC-ATPase domain dimer*. EMBO J, 2006. **25**(14): p. 3432-43.
 93. Biemans-Oldehinkel, E., Doeven, M.K., and Poolman, B., *ABC transporter architecture and regulatory roles of accessory domains*. FEBS Lett, 2006. **580**(4): p. 1023-35.
 94. Schmitt, L., Benabdelhak, H., Blight, M.A., Holland, I.B., and Stubbs, M.T., *Crystal structure of the nucleotide-binding domain of the ABC-transporter haemolysin B: identification of a variable region within ABC helical domains*. J Mol Biol, 2003. **330**(2): p. 333-42.
 95. Gentshev, I. and Goebel, W., *Topological and functional studies on HlyB of Escherichia coli*. Mol Gen Genet, 1992. **232**(1): p. 40-8.
 96. Oswald, C., Holland, I.B., and Schmitt, L., *The motor domains of ABC-transporters. What can structures tell us?* Naunyn Schmiedebergs Arch Pharmacol, 2006. **372**(6): p. 385-99.
 97. Jones, P.M. and George, A.M., *The ABC transporter structure and mechanism: perspectives on recent research*. Cell Mol Life Sci, 2004. **61**(6): p. 682-99.
 98. Koronakis, V., Hughes, C., and Koronakis, E., *Energetically distinct early and late stages of HlyB/HlyD-dependent secretion across both Escherichia coli membranes*. EMBO J, 1991. **10**(11): p. 3263-72.
 99. Lenders, M.H., Reimann, S., Smits, S.H., and Schmitt, L., *Molecular insights into type I secretion systems*. Biol Chem, 2013. **394**(11): p. 1371-84.
 100. Benabdelhak, H., Kiontke, S., Horn, C., Ernst, R., Blight, M.A., Holland, I.B., and Schmitt, L., *A specific interaction between the NBD of the ABC-transporter HlyB and a C-terminal fragment of its transport substrate haemolysin A*. J Mol Biol, 2003. **327**(5): p. 1169-79.

101. Lecher, J., Schwarz, C.K., Stoldt, M., Smits, S.H., Willbold, D., and Schmitt, L., *An RTX transporter tethers its unfolded substrate during secretion via a unique N-terminal domain*. Structure, 2012. **20**(10): p. 1778-87.
102. Ishii, S., Yano, T., Ebihara, A., Okamoto, A., Manzoku, M., and Hayashi, H., *Crystal structure of the peptidase domain of Streptococcus ComA, a bifunctional ATP-binding cassette transporter involved in the quorum-sensing pathway*. J Biol Chem, 2010. **285**(14): p. 10777-85.
103. Kelley, L.A., Mezulis, S., Yates, C.M., Wass, M.N., and Sternberg, M.J., *The Pyre2 web portal for protein modeling, prediction and analysis*. Nat Protoc, 2015. **10**(6): p. 845-58.
104. Holland, I.B., Peherstorfer, S., Kanonenberg, K., Lenders, M., Reimann, S., and Schmitt, L., *Type I Protein Secretion-Deceptively Simple yet with a Wide Range of Mechanistic Variability across the Family*. EcoSal Plus, 2016. **7**(1).
105. Schulein, R., Gentschev, I., Mollenkopf, H.J., and Goebel, W., *A topological model for the haemolysin translocator protein HlyD*. Mol Gen Genet, 1992. **234**(1): p. 155-63.
106. Kim, J.S., Song, S., Lee, M., Lee, S., Lee, K., and Ha, N.C., *Crystal Structure of a Soluble Fragment of the Membrane Fusion Protein HlyD in a Type I Secretion System of Gram-Negative Bacteria*. Structure, 2016. **24**(3): p. 477-85.
107. Lee, M., Jun, S.Y., Yoon, B.Y., Song, S., Lee, K., and Ha, N.C., *Membrane fusion proteins of type I secretion system and tripartite efflux pumps share a binding motif for TolC in gram-negative bacteria*. PLoS One, 2012. **7**(7): p. e40460.
108. Thanabalu, T., Koronakis, E., Hughes, C., and Koronakis, V., *Substrate-induced assembly of a contiguous channel for protein export from E.coli: reversible bridging of an inner-membrane translocase to an outer membrane exit pore*. EMBO J, 1998. **17**(22): p. 6487-96.
109. Du, D., Wang, Z., James, N.R., Voss, J.E., Klimont, E., Ohene-Agyei, T., Venter, H., Chiu, W., and Luisi, B.F., *Structure of the AcrAB-TolC multidrug efflux pump*. Nature, 2014. **509**(7501): p. 512-5.
110. Balakrishnan, L., Hughes, C., and Koronakis, V., *Substrate-triggered recruitment of the TolC channel-tunnel during type I export of hemolysin by Escherichia coli*. J Mol Biol, 2001. **313**(3): p. 501-10.
111. Pimenta, A.L., Racher, K., Jamieson, L., Blight, M.A., and Holland, I.B., *Mutations in HlyD, part of the type I translocator for hemolysin secretion, affect the folding of the secreted toxin*. J Bacteriol, 2005. **187**(21): p. 7471-80.
112. Koronakis, V., Sharff, A., Koronakis, E., Luisi, B., and Hughes, C., *Crystal structure of the bacterial membrane protein TolC central to multidrug efflux and protein export*. Nature, 2000. **405**(6789): p. 914-9.
113. Eswaran, J., Hughes, C., and Koronakis, V., *Locking TolC entrance helices to prevent protein translocation by the bacterial type I export apparatus*. J Mol Biol, 2003. **327**(2): p. 309-15.
114. Andersen, C., Koronakis, E., Bokma, E., Eswaran, J., Humphreys, D., Hughes, C., and Koronakis, V., *Transition to the open state of the TolC periplasmic tunnel entrance*. Proc Natl Acad Sci U S A, 2002. **99**(17): p. 11103-8.

115. Bakkes, P.J., Jenewein, S., Smits, S.H.J., Holland, I.B., and Schmitt, L., *The Rate of Folding Dictates Substrate Secretion by the Escherichia coli Hemolysin Type I Secretion System*. Journal of Biological Chemistry, 2010. **285**(52): p. 40573-40580.
116. Lenders, M.H., Weidtkamp-Peters, S., Kleinschrodt, D., Jaeger, K.E., Smits, S.H., and Schmitt, L., *Directionality of substrate translocation of the hemolysin A Type I secretion system*. Sci Rep, 2015. **5**: p. 12470.
117. Lenders, M.H., Beer, T., Smits, S.H., and Schmitt, L., *In vivo quantification of the secretion rates of the hemolysin A Type I secretion system*. Sci Rep, 2016. **6**: p. 33275.
118. Bumba, L., Masin, J., Macek, P., Wald, T., Motlova, L., Bibova, I., Klimova, N., Bednarova, L., Veverka, V., Kachala, M., Svergun, D.I., Barinka, C., and Sebo, P., *Calcium-Driven Folding of RTX Domain beta-Rolls Ratchets Translocation of RTX Proteins through Type I Secretion Ducts*. Mol Cell, 2016. **62**(1): p. 47-62.
119. Nicaud, J.M., Mackman, N., Gray, L., and Holland, I.B., *Characterisation of HlyC and mechanism of activation and secretion of haemolysin from E. coli 2001*. FEBS Lett, 1985. **187**(2): p. 339-44.
120. Issartel, J.P., Koronakis, V., and Hughes, C., *Activation of Escherichia coli prohaemolysin to the mature toxin by acyl carrier protein-dependent fatty acylation*. Nature, 1991. **351**(6329): p. 759-61.
121. Fong, K.P., Tang, H.Y., Brown, A.C., Kieba, I.R., Speicher, D.W., Boesze-Battaglia, K., and Lally, E.T., *Aggregatibacter actinomycetemcomitans leukotoxin is post-translationally modified by addition of either saturated or hydroxylated fatty acyl chains*. Mol Oral Microbiol, 2011. **26**(4): p. 262-76.
122. Osickova, A., Balashova, N., Masin, J., Sulc, M., Roderova, J., Wald, T., Brown, A.C., Koufos, E., Chang, E.H., Giannakakis, A., Lally, E.T., and Osicka, R., *Cytotoxic activity of Kingella kingae RtxA toxin depends on post-translational acylation of lysine residues and cholesterol binding*. Emerg Microbes Infect, 2018. **7**(1): p. 178.
123. Basar, T., Havlicek, V., Bezouskova, S., Hackett, M., and Sebo, P., *Acylation of lysine 983 is sufficient for toxin activity of Bordetella pertussis adenylate cyclase. Substitutions of alanine 140 modulate acylation site selectivity of the toxin acyltransferase CyaC*. J Biol Chem, 2001. **276**(1): p. 348-54.
124. Stanley, P., Packman, L.C., Koronakis, V., and Hughes, C., *Fatty acylation of two internal lysine residues required for the toxic activity of Escherichia coli hemolysin*. Science, 1994. **266**(5193): p. 1992-6.
125. Lim, K.B., Walker, C.R., Guo, L., Pellett, S., Shabanowitz, J., Hunt, D.F., Hewlett, E.L., Ludwig, A., Goebel, W., Welch, R.A., and Hackett, M., *Escherichia coli alpha-hemolysin (HlyA) is heterogeneously acylated in vivo with 14-, 15-, and 17-carbon fatty acids*. J Biol Chem, 2000. **275**(47): p. 36698-702.
126. Osickova, A., Khaliq, H., Masin, J., Jurnecka, D., Sukova, A., Fiser, R., Holubova, J., Stanek, O., Sebo, P., and Osicka, R., *Acyltransferase-mediated selection of the length of the fatty acyl chain and of the acylation site governs activation of bacterial RTX toxins*. J Biol Chem, 2020.
127. Soloaga, A., Ostolaza, H., Goni, F.M., and de la Cruz, F., *Purification of Escherichia coli pro-haemolysin, and a comparison with the properties of mature alpha-haemolysin*. Eur J Biochem, 1996. **238**(2): p. 418-22.

128. Ludwig, A., Garcia, F., Bauer, S., Jarchau, T., Benz, R., Hoppe, J., and Goebel, W., *Analysis of the in vivo activation of hemolysin (HlyA) from Escherichia coli*. J Bacteriol, 1996. **178**(18): p. 5422-30.
129. Herlax, V. and Bakas, L., *Acyl chains are responsible for the irreversibility in the Escherichia coli alpha-hemolysin binding to membranes*. Chem Phys Lipids, 2003. **122**(1-2): p. 185-90.
130. Herlax, V., Mate, S., Rimoldi, O., and Bakas, L., *Relevance of fatty acid covalently bound to Escherichia coli alpha-hemolysin and membrane microdomains in the oligomerization process*. J Biol Chem, 2009. **284**(37): p. 25199-210.
131. El-Azami-El-Idrissi, M., Bauche, C., Loucka, J., Osicka, R., Sebo, P., Ladant, D., and Leclerc, C., *Interaction of Bordetella pertussis adenylate cyclase with CD11b/CD18: Role of toxin acylation and identification of the main integrin interaction domain*. J Biol Chem, 2003. **278**(40): p. 38514-21.
132. Masin, J., Basler, M., Knapp, O., El-Azami-El-Idrissi, M., Maier, E., Konopasek, I., Benz, R., Leclerc, C., and Sebo, P., *Acylation of lysine 860 allows tight binding and cytotoxicity of Bordetella adenylate cyclase on CD11b-expressing cells*. Biochemistry, 2005. **44**(38): p. 12759-66.
133. Sebo, P., Glaser, P., Sakamoto, H., and Ullmann, A., *High-level synthesis of active adenylate cyclase toxin of Bordetella pertussis in a reconstructed Escherichia coli system*. Gene, 1991. **104**(1): p. 19-24.
134. Stanley, P., Koronakis, V., and Hughes, C., *Acylation of Escherichia coli hemolysin: a unique protein lipidation mechanism underlying toxin function*. Microbiol Mol Biol Rev, 1998. **62**(2): p. 309-33.
135. Greene, N.P., Crow, A., Hughes, C., and Koronakis, V., *Structure of a bacterial toxin-activating acyltransferase*. Proc Natl Acad Sci U S A, 2015. **112**(23): p. E3058-66.
136. Hardie, K.R., Issartel, J.P., Koronakis, E., Hughes, C., and Koronakis, V., *In vitro activation of Escherichia coli prohaemolysin to the mature membrane-targeted toxin requires HlyC and a low molecular-weight cytosolic polypeptide*. Mol Microbiol, 1991. **5**(7): p. 1669-79.
137. Stanley, P., Koronakis, V., Hardie, K., and Hughes, C., *Independent interaction of the acyltransferase HlyC with two maturation domains of the Escherichia coli toxin HlyA*. Mol Microbiol, 1996. **20**(4): p. 813-22.
138. Gygi, D., Nicolet, J., Frey, J., Cross, M., Koronakis, V., and Hughes, C., *Isolation of the Actinobacillus pleuropneumoniae haemolysin gene and the activation and secretion of the prohaemolysin by the HlyC, HlyB and HlyD proteins of Escherichia coli*. Mol Microbiol, 1990. **4**(1): p. 123-8.
139. Henson, J.B. and Grumbles, L.C., *Infectious Bovine Keratoconjunctivitis .1. Etiology*. American Journal of Veterinary Research, 1960. **21**(84): p. 761-766.
140. Baptista, P.J., *Infectious bovine keratoconjunctivitis: a review*. Br Vet J, 1979. **135**(3): p. 225-42.
141. Ruehl, W.W., Marrs, C.F., George, L., Banks, S.J., and Schoolnik, G.K., *Infection rates, disease frequency, pilin gene rearrangement, and pilin expression in calves inoculated with Moraxella bovis pilin-specific isogenic variants*. Am J Vet Res, 1993. **54**(2): p. 248-53.

-
142. Beard, M.K. and Moore, L.J., *Reproduction of bovine keratoconjunctivitis with a purified haemolytic and cytotoxic fraction of Moraxella bovis*. Vet Microbiol, 1994. **42**(1): p. 15-33.
143. Angelos, J.A., Hess, J.F., and George, L.W., *An RTX operon in hemolytic Moraxella bovis is absent from nonhemolytic strains*. Vet Microbiol, 2003. **92**(4): p. 363-77.
144. Høien-Dalen, P.S., Rosenbusch, R.F., and Roth, J.A., *Comparative characterization of the leukocidal and hemolytic activity of Moraxella bovis*. Am J Vet Res, 1990. **51**(2): p. 191-6.
145. Kagonyera, G.M., George, L.W., and Munn, R., *Cytopathic effects of Moraxella bovis on cultured bovine neutrophils and corneal epithelial cells*. Am J Vet Res, 1989. **50**(1): p. 10-7.
146. Kagonyera, G.M., George, L., and Miller, M., *Effects of Moraxella bovis and culture filtrates on ⁵¹Cr-labeled bovine neutrophils*. Am J Vet Res, 1989. **50**(1): p. 18-21.
147. Clinkenbeard, K.D. and Thiessen, A.E., *Mechanism of action of Moraxella bovis hemolysin*. Infect Immun, 1991. **59**(3): p. 1148-52.
148. Gray, J.T., Fedorka-Cray, P.J., and Rogers, D.G., *Partial characterization of a Moraxella bovis cytotoxin*. Vet Microbiol, 1995. **43**(2-3): p. 183-96.
149. Angelos, J.A., Hess, J.F., and George, L.W., *Cloning and characterization of a Moraxella bovis cytotoxin gene*. Am J Vet Res, 2001. **62**(8): p. 1222-8.
150. Madeira, F., Park, Y.M., Lee, J., Buso, N., Gur, T., Madhusoodanan, N., Basutkar, P., Tivey, A.R.N., Potter, S.C., Finn, R.D., and Lopez, R., *The EMBL-EBI search and sequence analysis tools APIs in 2019*. Nucleic Acids Res, 2019. **47**(W1): p. W636-W641.
151. Stamm, W.E. and Norrby, S.R., *Urinary tract infections: disease panorama and challenges*. J Infect Dis, 2001. **183** Suppl 1: p. S1-4.
152. Holland, I.B., Kenny, B., Steipe, B., and Pluckthun, A., *Secretion of heterologous proteins in Escherichia coli*. Methods Enzymol, 1990. **182**: p. 132-43.
153. Blight, M.A. and Holland, I.B., *Heterologous protein secretion and the versatile Escherichia coli haemolysin translocator*. Trends Biotechnol, 1994. **12**(11): p. 450-5.
154. Rasko, D.A. and Sperandio, V., *Anti-virulence strategies to combat bacteria-mediated disease*. Nat Rev Drug Discov, 2010. **9**(2): p. 117-28.
155. Meier, R., Drepper, T., Svensson, V., Jaeger, K.E., and Baumann, U., *A calcium-gated lid and a large beta-roll sandwich are revealed by the crystal structure of extracellular lipase from Serratia marcescens*. J Biol Chem, 2007. **282**(43): p. 31477-83.
156. Benson, D.A., Cavanaugh, M., Clark, K., Karsch-Mizrachi, I., Lipman, D.J., Ostell, J., and Sayers, E.W., *GenBank*. Nucleic Acids Res, 2013. **41**(Database issue): p. D36-42.
157. Rosano, G.L. and Ceccarelli, E.A., *Recombinant protein expression in Escherichia coli: advances and challenges*. Front Microbiol, 2014. **5**: p. 172.
158. Sebo, P. and Ladant, D., *Repeat sequences in the Bordetella pertussis adenylate cyclase toxin can be recognized as alternative carboxy-proximal secretion signals by the Escherichia coli alpha-haemolysin translocator*. Mol Microbiol, 1993. **9**(5): p. 999-1009.
159. Thompson, S.A. and Sparling, P.F., *The RTX cytotoxin-related FrpA protein of Neisseria meningitidis is secreted extracellularly by meningococci and by HlyBD+ Escherichia coli*. Infect Immun, 1993. **61**(7): p. 2906-11.

160. Highlander, S.K., Engler, M.J., and Weinstock, G.M., *Secretion and expression of the Pasteurella haemolytica Leukotoxin*. J Bacteriol, 1990. **172**(5): p. 2343-50.
161. Zhang, F., Greig, D.I., and Ling, V., *Functional replacement of the hemolysin A transport signal by a different primary sequence*. Proc Natl Acad Sci U S A, 1993. **90**(9): p. 4211-5.
162. Yin, Y., Zhang, F., Ling, V., and Arrowsmith, C.H., *Structural analysis and comparison of the C-terminal transport signal domains of hemolysin A and leukotoxin A*. FEBS Lett, 1995. **366**(1): p. 1-5.
163. Hui, D., Morden, C., Zhang, F., and Ling, V., *Combinatorial analysis of the structural requirements of the Escherichia coli hemolysin signal sequence*. J Biol Chem, 2000. **275**(4): p. 2713-20.
164. Stanek, O., Masin, J., Osicka, R., Jurnecka, D., Osickova, A., and Sebo, P., *Rapid Purification of Endotoxin-Free RTX Toxins*. Toxins (Basel), 2019. **11**(6).
165. Hege, T. and Baumann, U., *Protease C of Erwinia chrysanthemi: The crystal structure and role of amino acids Y228 and E189*. Journal of Molecular Biology, 2001. **314**(2): p. 187-193.
166. Garnham, C.P., Campbell, R.L., and Davies, P.L., *Anchored clathrate waters bind antifreeze proteins to ice*. Proceedings of the National Academy of Sciences of the United States of America, 2011. **108**(18): p. 7363-7367.
167. Motlova, L., Klimova, N., Fiser, R., Sebo, P., and Bumba, L., *Continuous Assembly of beta-Roll Structures Is Implicated in the Type I-Dependent Secretion of Large Repeat-in-Toxins (RTX) Proteins*. J Mol Biol, 2020. **432**(20): p. 5696-5710.
168. Peherstorfer, S., *Untersuchungen zur Acylierung, Struktur und Glykanbindung des RTX-Toxins Hämolysin A aus Escherichia coli*, 2017, Heinrich-Heine-Universität Düsseldorf: Düsseldorf, Germany.
169. Kühlbrandt, W., *The Resolution Revolution*. Science, 2014. **343**(6178): p. 1443-1444.
170. Murata, K. and Wolf, M., *Cryo-electron microscopy for structural analysis of dynamic biological macromolecules*. Biochim Biophys Acta Gen Subj, 2018. **1862**(2): p. 324-334.
171. Thomas, S., Smits, S.H.J., and Schmitt, L., *A simple in vitro acylation assay based on optimized HlyA and HlyC purification*. Analytical Biochemistry, 2014. **464**: p. 17-23.
172. Glaeser, R.M., Han, B.G., Csencsits, R., Killilea, A., Pulk, A., and Cate, J.H., *Factors that Influence the Formation and Stability of Thin, Cryo-EM Specimens*. Biophys J, 2016. **110**(4): p. 749-55.
173. Drulyte, I., Johnson, R.M., Hesketh, E.L., Hurdiss, D.L., Scarff, C.A., Porav, S.A., Ranson, N.A., Muench, S.P., and Thompson, R.F., *Approaches to altering particle distributions in cryo-electron microscopy sample preparation*. Acta Crystallogr D Struct Biol, 2018. **74**(Pt 6): p. 560-571.
174. Lipfert, J. and Doniach, S., *Small-angle X-ray scattering from RNA, proteins, and protein complexes*. Annual Review of Biophysics and Biomolecular Structure, 2007. **36**: p. 307-327.
175. Kikhney, A.G. and Svergun, D.I., *A practical guide to small angle X-ray scattering (SAXS) of flexible and intrinsically disordered proteins*. FEBS Lett, 2015. **589**(19 Pt A): p. 2570-7.

176. Lally, E.T., Hill, R.B., Kieba, L.R., and Korostoff, J., *The interaction between RTX toxins and target cells*. Trends in Microbiology, 1999. **7**(9): p. 356-361.
177. Hackett, M., Guo, L., Shabanowitz, J., Hunt, D.F., and Hewlett, E.L., *Internal lysine palmitoylation in adenylate cyclase toxin from Bordetella pertussis*. Science, 1994. **266**(5184): p. 433-5.
178. Forestier, C. and Welch, R.A., *Nonreciprocal complementation of the hlyC and lktC genes of the Escherichia coli hemolysin and Pasteurella haemolytica leukotoxin determinants*. Infect Immun, 1990. **58**(3): p. 828-32.
179. Bauer, M.E. and Welch, R.A., *Association of RTX toxins with erythrocytes*. Infect Immun, 1996. **64**(11): p. 4665-72.
180. Hackett, M., Walker, C.B., Guo, L., Gray, M.C., Van Cuyk, S., Ullmann, A., Shabanowitz, J., Hunt, D.F., Hewlett, E.L., and Sebo, P., *Hemolytic, but not cell-invasive activity, of adenylate cyclase toxin is selectively affected by differential fatty-acylation in Escherichia coli*. J Biol Chem, 1995. **270**(35): p. 20250-3.
181. Cavalieri, S.J. and Snyder, I.S., *Cytotoxic activity of partially purified Escherichia coli alpha haemolysin*. J Med Microbiol, 1982. **15**(1): p. 11-21.
182. Ostolaza, H., Bartolome, B., Ortiz de Zarate, I., de la Cruz, F., and Goni, F.M., *Release of lipid vesicle contents by the bacterial protein toxin alpha-haemolysin*. Biochim Biophys Acta, 1993. **1147**(1): p. 81-8.
183. Valeva, A., Walev, I., Kemmer, H., Weis, S., Siegel, I., Boukhallouk, F., Wassenaar, T.M., Chavakis, T., and Bhakdi, S., *Binding of Escherichia coli hemolysin and activation of the target cells is not receptor-dependent*. J Biol Chem, 2005. **280**(44): p. 36657-63.
184. Dileepan, T., Kachlany, S.C., Balashova, N.V., Patel, J., and Maheswaran, S.K., *Human CD18 is the functional receptor for Aggregatibacter actinomycetemcomitans leukotoxin*. Infect Immun, 2007. **75**(10): p. 4851-6.
185. Li, J., Clinkenbeard, K.D., and Ritchey, J.W., *Bovine CD18 identified as a species specific receptor for Pasteurella haemolytica leukotoxin*. Vet Microbiol, 1999. **67**(2): p. 91-7.
186. Deshpande, M.S., Ambagala, T.C., Ambagala, A.P., Kehrli, M.E., Jr., and Srikumaran, S., *Bovine CD18 is necessary and sufficient to mediate Mannheimia (Pasteurella) haemolytica leukotoxin-induced cytolysis*. Infect Immun, 2002. **70**(9): p. 5058-64.
187. Cortajarena, A.L., Goni, F.M., and Ostolaza, H., *Glycophorin as a receptor for Escherichia coli alpha-hemolysin in erythrocytes*. J Biol Chem, 2001. **276**(16): p. 12513-9.
188. Vazquez, R.F., Mate, S.M., Bakas, L.S., Fernandez, M.M., Malchiodi, E.L., and Herlax, V.S., *Novel evidence for the specific interaction between cholesterol and alpha-haemolysin of Escherichia coli*. Biochem J, 2014. **458**(3): p. 481-9.
189. Brown, A.C., Balashova, N.V., Epand, R.M., Epand, R.F., Bragin, A., Kachlany, S.C., Walters, M.J., Du, Y.R., Boesze-Battaglia, K., and Lally, E.T., *Aggregatibacter actinomycetemcomitans Leukotoxin Utilizes a Cholesterol Recognition/Amino Acid Consensus Site for Membrane Association*. Journal of Biological Chemistry, 2013. **288**(32): p. 23607-23621.

190. Brown, A.C., Koufos, E., Balashova, N.V., Boesze-Battaglia, K., and Lally, E.T., *Inhibition of LtxA toxicity by blocking cholesterol binding with peptides*. Molecular Oral Microbiology, 2016. **31**(1): p. 94-105.
191. Li, H. and Papadopoulos, V., *Peripheral-type benzodiazepine receptor function in cholesterol transport. Identification of a putative cholesterol recognition/interaction amino acid sequence and consensus patterns*. Endocrinology, 1998. **139**(12): p. 4991-4997.
192. Baier, C.J., Fantini, J., and Barrantes, F.J., *Disclosure of cholesterol recognition motifs in transmembrane domains of the human nicotinic acetylcholine receptor*. Sci Rep, 2011. **1**: p. 69.
193. de Castro, E., Sigrist, C.J., Gattiker, A., Bulliard, V., Langendijk-Genevaux, P.S., Gasteiger, E., Bairoch, A., and Hulo, N., *ScanProsite: detection of PROSITE signature matches and ProRule-associated functional and structural residues in proteins*. Nucleic Acids Res, 2006. **34**(Web Server issue): p. W362-5.
194. Epand, R.M., *Proteins and cholesterol-rich domains*. Biochim Biophys Acta, 2008. **1778**(7-8): p. 1576-82.
195. Ristow, L.C. and Welch, R.A., *Hemolysin of uropathogenic Escherichia coli: A cloak or a dagger?* Biochim Biophys Acta, 2016. **1858**(3): p. 538-45.
196. Charras, G.T., Yarrow, J.C., Horton, M.A., Mahadevan, L., and Mitchison, T.J., *Non-equilibration of hydrostatic pressure in blebbing cells*. Nature, 2005. **435**(7040): p. 365-9.
197. Paluch, E., Piel, M., Prost, J., Bornens, M., and Sykes, C., *Cortical actomyosin breakage triggers shape oscillations in cells and cell fragments*. Biophys J, 2005. **89**(1): p. 724-33.
198. Charras, G.T., *A short history of blebbing*. J Microsc, 2008. **231**(3): p. 466-78.
199. Charras, G.T., Coughlin, M., Mitchison, T.J., and Mahadevan, L., *Life and times of a cellular bleb*. Biophys J, 2008. **94**(5): p. 1836-53.
200. Babiychuk, E.B., Monastyrskaya, K., Potez, S., and Draeger, A., *Blebbing confers resistance against cell lysis*. Cell Death Differ, 2011. **18**(1): p. 80-9.
201. Strack, K., Lauri, N., Mate, S.M., Saralegui, A., Munoz-Garay, C., Schwarzbaum, P.J., and Herlax, V., *Induction of erythrocyte microvesicles by Escherichia Coli Alpha hemolysin*. Biochem J, 2019. **476**(22): p. 3455-3473.
202. Mills, J.C., Stone, N.L., Erhardt, J., and Pittman, R.N., *Apoptotic membrane blebbing is regulated by myosin light chain phosphorylation*. J Cell Biol, 1998. **140**(3): p. 627-36.
203. Mills, J.C., Stone, N.L., and Pittman, R.N., *Extranuclear apoptosis. The role of the cytoplasm in the execution phase*. J Cell Biol, 1999. **146**(4): p. 703-8.
204. Kerr, J.F., Wyllie, A.H., and Currie, A.R., *Apoptosis: a basic biological phenomenon with wide-ranging implications in tissue kinetics*. Br J Cancer, 1972. **26**(4): p. 239-57.
205. Elmore, S., *Apoptosis: a review of programmed cell death*. Toxicol Pathol, 2007. **35**(4): p. 495-516.
206. Barros, L.F., Kanaseki, T., Sabirov, R., Morishima, S., Castro, J., Bittner, C.X., Maeno, E., Ando-Akatsuka, Y., and Okada, Y., *Apoptotic and necrotic blebs in epithelial cells display similar neck diameters but different kinase dependency*. Cell Death Differ, 2003. **10**(6): p. 687-97.

- 207. Kim, Y.R., Lee, S.E., Kook, H., Yeom, J.A., Na, H.S., Kim, S.Y., Chung, S.S., Choy, H.E., and Rhee, J.H., *Vibrio vulnificus RTX toxin kills host cells only after contact of the bacteria with host cells*. Cell Microbiol, 2008. **10**(4): p. 848-62.
- 208. Kim, Y.R., Lee, S.E., Kang, I.C., Nam, K.I., Choy, H.E., and Rhee, J.H., *A Bacterial RTX Toxin Causes Programmed Necrotic Cell Death Through Calcium-Mediated Mitochondrial Dysfunction*. Journal of Infectious Diseases, 2013. **207**(9): p. 1406-1415.
- 209. Barros, L.F., Hermosilla, T., and Castro, J., *Necrotic volume increase and the early physiology of necrosis*. Comp Biochem Physiol A Mol Integr Physiol, 2001. **130**(3): p. 401-9.
- 210. Randis, T.M., Zaklama, J., LaRocca, T.J., Los, F.C., Lewis, E.L., Desai, P., Rampersaud, R., Amaral, F.E., and Ratner, A.J., *Vaginolysin drives epithelial ultrastructural responses to Gardnerella vaginalis*. Infect Immun, 2013. **81**(12): p. 4544-50.

6. Curriculum Vitae

Personal Data

| | |
|----------------|-------------------------|
| Name | Isabelle Noemi Erenburg |
| Date of birth | 16.01.1992 |
| Place of birth | Düsseldorf, Germany |

University Education

| | |
|-------------------|---|
| since Jan 2017 | Doctorate Heinrich-Heine-Universität Düsseldorf Institute of Biochemistry Supervisor Prof. Dr. Lutz Schmitt <i>Functional and structural characterization of the RTX proteins MbxA from Moraxella bovis and FrpA from Kingella kingae</i> |
| Oct 2014-Sep 2016 | Master of Science (M.Sc.), Biochemistry (grade 1.2) Heinrich-Heine-Universität Düsseldorf Institute of Biochemistry Prof. Dr. Lutz Schmitt Thesis: <i>Stabilität und Integrität eines Typ I Sekretionssystems (Stability and Integrity of a Type I Secretion System)</i> |
| Dec 2015-Feb 2016 | Internship at the Weizmann Institute of Science, Department of Biomolecular Sciences, Rehovot, Israel |
| Oct 2011-Aug 2014 | Bachelor of Science (B.Sc.), Biochemistry (grade 1.2) Heinrich-Heine-Universität Düsseldorf Institute of Biochemistry Prof. Dr. Vlada B. Urlacher Thesis: <i>Selektive Oxidation von Oktan zu 2-(S)-Oktanol im Ganzzellsystem (Selective oxidation of octane to 2-(S)-octanol in a whole cell system)</i> |

Professional experience

Oct 2016-Dec 2016 Internship at QIAGEN GmbH, Hilden, Germany

School Education

2002-2011 General qualification for university entrance (Abitur) grade 1.4
Gymnasium am Neandertal, Erkrath, Germany

Scholarships

since Jan 2017 Scholarship from the Manchot Graduate School “Molecules of
Infection III”
Dec 2015-Feb 2016 PROMOS scholarship from the German Academic Exchange
Service
Oct 2014-Sep 2016 Deutschlandstipendium scholarship

Conferences and symposia attended

Feb 2020 3rd Molecules of Infection III Symposium, Bergisch-Gladbach, Germany (Oral
presentation)
Jun 2019 European Workshop on Bacterial Protein Toxins ETOX19, Davos, Switzerland
(Poster presentation)
Mar 2019 2nd Molecules of Infection III Symposium, Düsseldorf, Germany (Oral and
poster presentation)
Mar 2019 Dynamics of Membrane Systems; CRC 1208 2nd International Conference,
Düsseldorf, Germany
Jul 2018 Gordon Research Conference and Seminar on Microbial Toxins and
Pathogenicity, Waterville Valley, NH, USA (Poster presentation)
Feb 2018 1st Molecules of Infection III Symposium, Bergisch-Gladbach, Germany (Oral
presentation)
Sep 2017 Dynamics of Membrane Systems; CRC 1208 1st International Conference,
Düsseldorf, Germany

Publications

- 2019 Spitz, O., **Erenburg, I.N.**, Beer, T., Kanonenberg, K., Holland, I.B., and Schmitt L., Type I Secretion Systems-One Mechanism for All? Microbiology Spectrum, 2019. 7(2).
- 2018 Kanonenberg, K., Spitz, O., **Erenburg, I.N.**, Beer, T., and Schmitt, L., Type I secretion system-it takes three and a substrate. FEMS Microbiology Letters, 2018. 365(11).
- 2016 Tieves, F., **Erenburg, I.N.**, Mahmoud, O., and Urlacher, V.B., Synthesis of chiral 2-alkanols from n-alkanes by a *P. putida* whole-cell biocatalyst. Biotechnology and Bioengineering, 2016. 113(9): p. 1845-52.

7. Acknowledgments

An dieser Stelle möchte ich mich bei allen Menschen bedanken, die mich auf diesem Weg unterstützt und begleitet haben.

Zuallererst gilt mein Dank Prof. Dr. Lutz Schmitt. Vielen Dank für dieses spannende Projekt und die Möglichkeit zu promovieren. Danke für deine Ideen, deinen Enthusiasmus und für den Freiraum, den du gegeben hast. Genauso möchte ich für deine Unterstützung in allen Situationen danken und dass du nicht nur immer eine offene Tür für uns hattest, sondern auch immer offen für neue Ideen warst. Ein großes Dankeschön möchte ich auch für die Möglichkeit aussprechen an den ganzen spannenden Konferenzen und Kooperationen teilzunehmen. Ich habe in dieser Zeit wirklich unheimlich viel gelernt und mich entwickelt.

Prof. Johannes Hegemann möchte ich für die Übernahme des Korreferats danken und für das stete Interesse an meiner Arbeit, sowie die wertvollen Diskussionen und Anregungen, die ich immer bekommen habe. Ich danke auch dafür, dass ich für die Durchführung von Experimenten in seinem Institut willkommen war.

Dr. Sander Smits, danke dir für deinen Optimismus, die Diskussionen und die Motivation, die du gegeben hast. Danke für deine Ideen und dein kritisches Hinterfragen. Von deiner ideenreiche Herangehensweise an alle Fragestellungen habe ich wirklich viel gelernt. Ein großes Dankeschön natürlich auch für die Hilfe bei der Korrektur dieser Arbeit.

PD Dr. Ulrich Schulte möchte ich dafür danken, dass er seit Beginn des Studiums ein toller Wegweiser und Betreuer war, der bei jeder Frage mit Rat zur Seite stand. Auch für die Organisation der Praktika möchte ich mich bedanken.

Bei Dr. Gereon Poschmann möchte ich mich für die massenspektrometrischen Analysen bedanken.

Prof. Dr. Sebastian Wesselborg möchte ich für die Möglichkeit danken Experimente bei ihm im Institut durchzuführen. Ein großes Dankeschön an dieser Stelle auch an Fabian Stuhldreier für die Hilfe beim Thema Zellkultur und der Planung der Versuche.

Bei Dr. Stefanie Weidtkamp-Peters sowie Dr. Sebastian Hänsch möchte ich mich für das Live cell imaging und die damit zusammenhängende Unterstützung bedanken.

Prof. Dr. Ben Luisi und Dr. Miao Ma danke ich für die Kooperation und ihre Gastfreundschaft, sowie die tolle Gelegenheit ihre Forschung und Cambridge kennenzulernen.

Der Jürgen Manchot Stiftung und der MOI Graduiertenschule möchte ich für die finanzielle Unterstützung und für das vielseitige Programm danken. Ein großes Dankeschön geht auch an Dr. Inge Krümpelbeck, Dr. Stephanie Spelberg und Dr. Sabrina Zander für die Koordination, Organisation und Hilfe bei allen Fragen.

Danke auch an meine MOI Mitstreiter, es war toll euch kennen zu lernen und wir hatten einige tolle (Symposiums-)Abende. Ein besonderes Dankeschön gilt Sebastian Wintgens, für deine Hilfe mit der Zellkultur, für die Zeit, die du dir dafür genommen hast und für die Planung unserer Versuche.

Dr. Diana Kleinschrodt, danke für deine Unterstützung bei meinem Start in die Klonierung, du hast mir den Einstieg in mein Projekt sehr erleichtert und ich konnte vieles von dir lernen. Danke, dass du dein Klonierungs-Wissen geteilt hast.

Tobias, in Lab 29 und mit dir als Masterbetreuer hat doch irgendwie alles angefangen. Auch als ich von Masterstudentin zur Labornachbarin wurde hast du immer deine Ideen, dein Wissen und deine Geschichten geteilt hast und mit nach Lösungen gesucht hast. Danke für die Donnerstagspost und dafür, dass du vom Türrahmen aus als Biene sorgsam auf uns aufgepasst hast. Von dir kann man immer etwas Neues lernen, es war eine tolle Zeit.

Marcel, auch du hast mich in Lab 29 willkommen geheißen. Danke für deine hilfreichen Tipps, Ideen und dein Interesse. Du kennst dich einfach mit allem aus, was einem im Labor begegnen kann. Danke auch für die kunsthistorischen Katzenpostkarten auf meiner Bench. Ob sie nun von dir oder von Tobi kamen weiß man nicht, aber ich habe mich immer gefreut.

Julia, was für ein Glück, dass ich dich die meiste Zeit über als Büronachbarin haben durfte. Danke für das Zuhören, Mitdenken und Durchsprechen aller wissenschaftlichen und unwissenschaftlichen Fragestellungen, du hast mir damit immer wieder sehr geholfen. Deine kreativen Ansätze für alle möglichen Experimente sind bewundernswert. Danke für die gute Laune und die passenden Hintergrundmusik für jede Situation.

Oli, du warst von Anfang an mein Homologie-Gegenstück. Danke für all die Kaffeegespräche, deine Hilfsbereitschaft und deine Ideen. Danke auch für die kreativen Bastelsessions, es hat unglaublich Spaß gemacht.

Rebecca und Katja, die anderen Zwei, die die Kaffeerrunde erst komplett machen. Danke, dass ihr mich im Büro und beim Kaffee aufgenommen habt. Ein großes Dankeschön an euch für die tolle Zeit und die gute Laune.

Martin, du hast es zu guter Letzt irgendwie geschafft unser Büro zu vervollständigen. Danke für die Diskussionen, Denkanstöße und deine ehrliche Meinung. Acceptable oder unacceptable conditions, es war immer wieder hilfreich und lustig.

Jens, vielen Dank für deine unglaubliche Hilfsbereitschaft und Unterstützung in allen Situationen, von ÄKTA bis SAXS. Du hast immer einen Rat und ich konnte vieles von dir lernen. Die Grenoble-Trips werden einfach in Erinnerung bleiben.

Tim, danke für die witzigen Gespräche und deine Unterstützung bei unseren Cell disruptor Aufgaben und Pflichten. Sogar dabei konntest du deine gute Laune bewahren.

Florestan und Manuel, schön, dass ihr unser T1SS-Team bereichert habt. Danke für eure Hilfsbereitschaft, eure Zuverlässigkeit und eure Ideen. Es hat echt Spaß gemacht mit euch, ich wünsche euch weiterhin viel Erfolg mit euren Projekten.

Zohreh, thank you for your help, sharing your experiences and also bringing fresh ideas to the T1SS group. I wish you the best of luck on your journey!

Auch Neuzugang Eymen wünsche ich viel Erfolg für seine Arbeit.

Vivien, Steffi, Alex und Julia, euch möchte ich auch danken dafür, dass ihr das Institut mit Hilfsbereitschaft, guten Ratschlägen, spannenden Gesprächen zu euren Projekten und anderen Themen, sowie Humor und guter Laune so bereichert habt. Viel Erfolg und Durchhaltevermögen wünsche ich euch!

Bedanken möchte ich mich auch ganz herzlich bei Martina. Du bist immer ansprechbar und hast mir im Laufe der Zeit so viele Fragen beantwortet und mir mit deinem Erfahrungsschatz so oft helfen können. Genauso möchte ich auch Silke danken, auf eure Organisation und Hilfe war immer Verlass.

Jun.-Prof. Dr. Alexej Kedrov, Maryna, Athanasios und Michael, danke für den frischen Wind den ihr mit der Synthetic Membrane Systems Group in das Institut gebracht habt. Danke für euren Input und für spannende Gespräche. Sie haben mir so einige neue Herangehensweisen und neue Blickwinkel auf wissenschaftliche Fragen gezeigt.

Frau Platz und Frau Blum möchte für die unkomplizierte Hilfe bei allen Organisations- und Verwaltungsangelegenheiten ein großes Dankeschön aussprechen

Bei Astrid und Stefanie möchte ich mich für die Kristallisationsversuche bedanken.

Bedanken möchte ich mich auch bei meinen Studenten Nicole und Fabian für die Begeisterung, die sie für das Thema aufgebracht haben, ihren Fleiß und ihre Kreativität.

Den Ehemaligen, die ich noch nicht erwähnt habe Manuel, Katharina, Kalpana, Kerstin, Sandra, Sven, Michael, Sakshi euch möchte ich natürlich auch danken für die tolle Zeit danken, für die Erfahrungen, die ihr geteilt habt und das Wissen, das ihr weiter gegeben habt.

Meinen Freunden möchte ich danken für ihre Unterstützung, für ihr Verständnis, für das Zuhören, aber auch für die Ablenkung. Danke, dass ihr immer für mich da seid.

Ein ganz besonderer Dank gilt meiner Familie. Ihr habt mich immer begleitet und bedingungslos unterstützt, eurer Rückhalt hat mir Kraft gegeben. Ihr hattet immer Verständnis, habt mir Mut zugesprochen, euch für alles interessiert. Danke, dass ihr immer unerschütterlich an mich glaubt. Ohne euch wäre das alles nicht möglich gewesen.

Genauso möchte ich meinem Freund Tobias danken. Danke für dein Verständnis, deine Rückhalt und dass du immer an mich glaubst immer. Darüber hinaus du hast dich auch bis ins Detail für meine Arbeit interessiert und meine Begeisterung geteilt. Danke für deine ganze Unterstützung und deine Zuversicht, mit dir bin ich mutiger.

8. Declaration

Ich versichere an Eides statt, dass die vorliegende Dissertation von mir selbstständig und ohne unzulässige fremde Hilfe unter Beachtung der „Grundsätze zur Sicherung guter wissenschaftlicher Praxis an der Heinrich-Heine-Universität Düsseldorf“ erstellt worden ist. Diese Dissertation wurde in der vorgelegten oder in ähnlicher Form noch bei keiner anderen Institution eingereicht. Ich habe bisher keine erfolglosen oder erfolgreichen Promotionsversuche unternommen.

(Ort, Datum)

Isabelle Noemi Erenburg